GEORGE C. MARSHALL SPACE FLIGHT CENTER,

HUNTSVILLE, ALABAMA

PROGRESS REPORT NO. 4 [20 Dec. 1962 - 18 Jul. 1963]
ON STUDIES IN THE FIELDS OF SPACE FLIGHT AND GUIDANCE THEORY

NATIONAL AERONAUTICS AND SPACE ADMINISTRATION

GEORGE C. MARSHALL SPACE FLIGHT CENTER

MTP-AERO-63-65

PROGRESS REPORT NO. 4

on Studies in the Fields of

SPACE FLIGHT AND GUIDANCE THEORY

Sponsored by Aero-Astrodynamics Laboratory of

Marshall Space Flight Center

ABSTRACT

12102

This paper contains progress reports of NASA-sponsored studies in the areas of space flight and guidance theory. The studies are carried on by several universities and industrial companies. This progress report covers the period from December 20, 1962. to July 18, 1963. The technical supervisor of the contracts is W. E. Miner, Deputy Chief of the Future Projects Branch of Aeroballistics Division, George C. Marshall Space Flight Center.

AUTHOR

GEORGE C. MARSHALL SPACE FLIGHT CENTER

MTP-AERO-63-65

September 19, 1963

PROGRESS REPORT NO. 4
on Studies in the Fields of
SPACE FLIGHT AND GUIDANCE THEORY

Sponsored by Aero-Astrodynamics Laboratory of
Marshall Space Flight Center

TABLE OF CONTENTS

TABLE OF CONTENTS (CONT'D)

GEORGE C. MARSHALL SPACE FLIGHT CENTER

MTP-AERO-63-65

PROGRESS REPORT NO. 4
on Studies in the Fields of
SPACE FLIGHT AND GUIDANCE THEORY
Sponsored by Aero-Astrodynamics Laboratory of
Marshall Space Flight Center

SUMMARY

This paper contains progress reports of NASA-sponsored studies in the areas of space flight and guidance theory. The studies are carried on by several universities and industrial companies. This progress report covers the period from December 20, 1962 to July 18, 1963. The technical supervisor of the contracts is W. E. Miner, Deputy Chief of the Future Projects Branch, Aeroballistics Division, George C. Marshall Space Flight Center.

INTRODUCTION

This report contains thirteen papers, the subject matter of which lies in the areas of guidance and space flight theory. These papers were written by investigators employed at agencies under contract to MSFC.

This report is the fourth of the "Progress Reports" and covers the period from December 20, 1962 to July 18, 1963. This progress report will hereinafter be referred to as "the report." Information given in Progress Reports 1, 2, and 3 will not be repeated here.

The agencies contributing and their fields of major interest are:

Field of Interest	Agency
Calculus of Variations	Grumman Aircraft Engineering Corp. Republic Aviation Corporation Auburn University Aeronutronics (Ford) Analytical Mechanics Associates, Inc.
Impulse Orbit Transfer	North American Aviation, Inc.
Celestial Mechanics	Republic Aviation Corporation University of Kentucky
Large Computer Exploitation	Haynes International Corporation University of North Carolina

The objective of this introduction is to review and summarize the contribution of each agency.

The first paper, written by Hans K. Hinz of Grumman Aircraft, extends the work reported on in Progress Report No. 2. Primarily, it presents the results of earth-to-moon trajectory computations (done by direct methods of calculus of variations) for the years 1965 to 1973.

The second paper, written by H. Gardner Moyer of Grumman Aircraft Engineering Corporation, presents two methods of treating a class of discontinuities in state and control variables. The first method, called the wavelet-wavefront method, adds to the classical results in allowing a jump discontinuity in a state variable at a known value. The statement is made that this method can be gradually extended until the multistage rocket problem is included, but this is not done. Instead, the second method based on the work of Cicala is extended to care for certain special problems of multistage rockets.

The third paper, written by George N. Nomicos of Republic Aviation Corporation, extends the work reported on in Progress Report No. 3 by Jack Richman of the same company. A differential correction scheme, developed for improving the initial values of the adjoint variables (direction numbers and their derivations of the thrust vector), is extended to include the discontinuities in thrust and variations in cutoff time. It is recommended that the parameters of conics be used for calculating purposes. The use of these parameters has the effect of changing the variable end-condition problem into

a fixed end-point problem for many applications, but is limited in that transformations would be required to develop the desired information for hardware use.

The fourth paper, written by Douglas Raney at Auburn University, develops a computational procedure for obtaining extremal reentry trajectories. The vehicle considered has an offset center of gravity. The forces acting on the vehicle are lift, drag, gravity, and roll control jets. The integral over time of the square of the total aerodynamic force is minimized, and the magnitude of the roll control force is used as the control variable. The classical calculus of variation approach is used to establish computational procedures for reentry trajectories.

The fifth paper, by Richard R. Auelmann of Aeronutronic (Ford), should not of its own right be classified under calculus of variations. However, the purpose of the paper was to establish a method of computing trajectories with the force normal to the velocity vector. A solution of this problem hopefully would give a basis for a perturbation theory in computing low thrust trajectories. The problem was solved to the point of reducing the solution to that of quadrature. The resulting integrals appear to have little chance of solution; therefore, this procedure offers little as a basis for a perturbation theory. A solution of either the circumferential or tangential force direction problems appears to offer a better base when combined with the radial solution. The result is interesting but of small engineering value.

The sixth paper, written by Gary A. McCue of North American Aviation, Inc., presents a method of developing an "impulse function space," a four dimensional space (φ_i - the angle from the line of nodes of the initial orbit and the final desired orbit to the line of nodes of the initial orbit and the transfer orbit measured in the plane i where i=1 is the initial orbit plane, and i=2 is the final orbit plane; p is the semi-latus rectum of the transfer orbit; and Δv is the total cost in velocity of the orbit transfer). Contour lines of equal velocity are presented on a ϕ_1 vs ϕ_2 graph with p used as a parameter. The "impulse function space" presented in the graphical form described above gives a method for visual inspection to determine optimum two-impulse orbit transfer and to determine the sensitivity of the parameters (ϕ_1, ϕ_2, p) in the neighborhood of such optima. Notice that the cost of presenting graphically such a picture for study is less than one minute of IBM 7090 time.

The seventh paper, written by Gentry Lee, also of North American Aviation, Inc., presents an eighth order polynomial expression. The real roots of this polynomial may refer to extrema in the "impulse function space." Two test functions are developed that define regions in which all extrema must lie. These regions identify those roots that correspond to extrema in the impulse function and those that are extraneous. The analysis shows that there are cases in which transfers between elliptical orbits contain hyperbolic trajectories for a minimum transfer.

These seven papers are in some manner related to optimizing trajectories. The next two papers concern special solutions or approximations of solutions in the field of celestial mechanics.

The first (eighth paper) of these papers, written by Mary Payne of Republic Aviation Corp., follows work done on the restricted three body problem reported on in Progress Reports no. 2 and 3. This paper introduces four new parameters into the Hamiltonian. The non-integrable terms in the perturbation equations are minimized with respect to these four parameters. A method for determining these four parameters is presented and is applied to several special cases or arcs and the errors checked. The paper reports in its conclusions the following:

> "None of the numerical results obtained can be regarded as satisfactory, or, in fact, as fulfilling the expectations that one might have for the theory. Nevertheless, there are a number of reasons for expecting that further development of the theory should lead to useful and interesting results."

Based on this statement, we may conclude that this is an unfinished problem.

The ninth paper, written by the University of Kentucky team, presents development of the convergence of the series used in Hill's solution of the three body problem. An interval in which the series is convergent was established. Future work will attempt to enlarge the estimates of this interval and to develop some transformations which permit comparison with known results.

The last two papers on celestial mechanics were attempts to find improved estimates to the restricted three body problem. Work will continue on both approaches until it becomes evident that no further advance can be made.

The next two papers on exploitation of large computers deal with statistical methods of developing steering equations for the adaptive guidance mode.

The first (tenth) of these papers, by R. E. Wheeler of Hayes International Corporation, presents a mathematical model for fitting the steering function for a simplified problem. The solution presents a ratio of polynomials based on the necessary condition of Euler and the first integral of the system of differential equations. The solution gives $\tan \chi$ (χ-the steering angle) as a function of time and state variables along the trajectory. This function evaluated $t = t_o$ should be the desired "steering function" as normally developed. No end-conditions are considered. It is proposed that they are to be obtained by the curve fitting of the constants of integration.

The eleventh paper, written by Shigemichi Suzuki of the University of North Carolina, deals with the application of linear programming techniques to the determination of the steering and time to cutoff functions. Two problems are discussed. In the first problem, the ratio of linear combinations of known functions is fixed in form, and coefficients are sought such that the Tchebycheff criterion of minimizing the maximum deviation over a finite point set is satisfied. The second problem is to find the "simplest" function from the given class of ratios of linear combinations of known functions where deviation over a finite point set is held less than a preassigned value. The criterion for "simplicity" is either (1) the minimization of the number of non-zero terms in the approximation, or (2) the minimization of the sum of the orders of the highest order non-zero terms in the numerator and the denominator. Work has been initiated at MSFC to check the feasibility of the methods on problems of fitting steering and time to cutoff functions.

The last two papers of this report deal with special cases in the theory of calculus of variations. They are by Henry J. Kelley of Analytical Mechanics Associates, Inc.

The first of these papers is on the singular extremals in Lawden's problem of optimal rocket flight. The analysis presents an alternate method for the derivation of Lawden's intermediate thrust solution. This is done by a transforming to a new set of coordinates and a redevelopment of the problem in these coordinates.

The last paper of this report deals with the same problem as the preceding paper where the differential equations are linear in a single control variable. The paper proposes a transformation that reduces the dimension in the state space.

One paper prepared by Harry Passmore, III of Hayes International Corporation, proposing to uncouple the equations of motion is not included. The variables are separated by a long and laborious procedure of repeated messy operations. A copy of this report will be furnished to interested persons.

RESEARCH DEPARTMENT

GRUMMAN AIRCRAFT ENGINEERING CORPORATION

OPTIMUM EARTH-TO-MARS TRAJECTORIES FOR LOW-THRUST VEHICLES

by

Hans K. Hinz

BETHPAGE, NEW YORK

RESEARCH DEPARTMENT

GRUMMAN AIRCRAFT ENGINEERING CORPORATION
BETHPAGE, NEW YORK

OPTIMUM EARTH-TO-MARS TRAJECTORIES FOR LOW-THRUST VEHICLES

by

Hans K. Hinz

Summary

Optimum trajectories and thrust steering programs for thrust-limited propulsion systems are determined for Earth-to-Mars missions in the time period from 1965 to 1973. Vehicle performance is evaluated for thrust/initial weight ratios from 8×10^{-5} to 10^{-3}. Optimum launch dates occur once every synodic period (780 days), with the best departures taking place in 1971, the "vintage" year for low-thrust trajectories.

INTRODUCTION

In "Progress Report Nos. 1 and 2 On Studies in the Fields of Space Flight and Guidance Theory" (Refs. 1 and 2) an account is given of the theoretical development of several successive approximation techniques for optimizing rocket trajectories involving terminal (equality) con-

straints and control variable (inequality) constraints. These reports also contain descriptions of the two computer programs for determining optimum, three dimensional, low-thrust interplanetary trajectories. One program is specialized to treat constant, continuous thrust rockets; the other deals with variable, but limited thrust engines. The propulsion system for both programs is assumed to have constant specific impulse and only one maximum value of thrust.

For the system model and equations of motion, it is assumed that the entire flight is under the effects of solar gravity only. The orbits of the planets of departure and destination are taken as elliptic and noncoplanar. For each trajectory to be optimized, the planetary orbital elements are computed for the date of departure, using ephemeris information, and taken as constant throughout the flight. Although the computer programs are capable of dealing with missions initiated from any position in the solar system, it is usually assumed that the vehicle has been launched from some planet of departure and boosted to a velocity sufficient for escape from that planet. Thus, the initial components of position and velocity of the vehicle with respect to the heliocentric-inertial system are taken to be identical with those of the planet of departure. By appropriate selection of the penalty constants which govern convergence to the desired terminal conditions, it is possible to study missions such as orbital transfer, rendezvous, intercept, and others.

Optimization is achieved by determining the time varying control functions which minimize the final value of time. These functions consist of the two thrust steering angles and the thrust magnitude within limits from zero to some maximum value. For the constant thrust application, the fuel expended is not limited, and minimizing time is equivalent to minimizing fuel. For the variable thrust case, the total propellant allocated is less than that required for the corresponding constant thrust example, and as a consequence one will obtain coasting arcs or thrust magnitudes less than maximum.

COMPUTATIONAL RESULTS

Optimum Earth-to-Mars rendezvous trajectories have been computed for departure dates from January 1965 to September 1973, covering a range of four synodic periods of Mars. For this phase of the numerical studies, the thrust magnitude is constant and continuous. Comparison with previous circle-to-circle coplanar studies indicates that there are no distinct or highly significant differences between two-and three-dimensional optimum trajectories. This is due to the small inclination of Mars' orbit (1.85°). The differences that do exist appear to be associated mainly with the eccentricity of the orbits of the two planets. A portion of these results, for a thrust/initial weight ratio, T/W_o, of 8.47×10^{-5} and a specific impulse of 5685 seconds, is shown in Fig. 1.

Examination of the trajectories indicates that there are three types of optimum rendezvous trajectories, as shown in Fig. 2. For one type, the vehicle's trajectory is entirely within the orbits of Earth and Mars. Because the planets are in a more favorable position, this class of transfers includes the "minimum minimorum" of the minimum time rendezvous trajectories. At progressively later launch dates, Mars falls behind the Earth, resulting in a second type of transfer for which the vehicle flies out past the Martian orbit and "waits" for the planet to overtake it. At still later launch dates, Mars is so far behind the Earth that the vehicle "decides" that rather than wait for Mars it is more "profitable" in terms of time and fuel to increase its angular velocity, passing closer to the Sun than the planet Mercury, and eventually catching up with Mars. Although this maneuver requires an additional revolution about the Sun, the transfer time is less. At the point of transition between the second and third type, two optimum solutions exist, each with the same values of transfer time, departure date, and time of arrival, but each having an entirely different trajectory and thrust steering program. Two such transition points are shown in the upper part of Fig. 1 where the curves intersect.

In order to appreciate the performance capability of low-thrust propulsion systems, a limited vehicle parameter variation was carried out. For this phase of the study four values of T/W_o were selected, and the specific impulse of the rocket engine kept fixed at 5685 seconds. Optimum rendezvous trajectories were computed for values of launch date in the vicinity of time when the planets are in the most favorable position. The results for 1971 are shown in Fig. 3. From this figure, and from similar plots for other favorable time periods, the minimum transfer times have been determined and are summarized in the table below.

T/W_o	Jan.-Feb. 1967	Mar.-Apr. 1969	May-July 1971	Aug.-Sept. 1973
8.467×10^{-5}	204	186	166	180
2×10^{-4}	132	120	108	116
5×10^{-4}	80	72	$66\frac{1}{2}$	72
1×10^{-3}	-	-	$45\frac{1}{4}$	47

The findings clearly indicate that 1971 is the "vintage" year for low-thrust trajectories. These results are plotted in Fig. 4 on a log-log scale and exhibit almost a linear variation.

The minimum-time optimum trajectories for the results tabulated above are shown in Figs. 5 to 8. Examination of the trajectories reveals that rendezvous for the superior 1971 launch dates occurs when Mars is near, and preferably just past, the perihelion of its orbit.

The component of the thrust steering angle in the plane of the ecliptic generally displays the same characteristic motion (Figs. 9 and 10). Early in flight this vector component points generally in the direction of motion and away from the sun. About half-way in flight it rotates almost

abruptly from a position pointing away from the sun to a position pointing toward the sun. Thereafter the vector is generally in the direction of motion and toward the sun. This steering program is remarkably similar to the one derived in the linearized near-circular orbital transfer studies (Ref. 3). A comparison of the two programs is shown in Fig. 11. The component of the thrust normal to the plane of the ecliptic is generally quite small ($\pm 5°$). This may be expected since it is this control component which must change the small inclination of the vehicle's orbital plane by 1.85 degrees without duly penalizing the in-plane energy-producing component of the thrust vector.

In addition to the variation in T/W_o, the effect of changing the specific impulse, I_s, was also briefly examined. For values of I_s 100% larger, the transfer time increased only slightly by 2-3%. The real significance of the more efficient engines, of course, is in the greater payloads delivered.

Optimum Earth-to-Mars intercept trajectories were also computed for vehicles with constant continuous thrust engines. Because of the removal of constraints upon the terminal values of the velocity components, there is an appreciable savings in transfer time — as much as 40%. Whether or not there is a proportional savings in fuel consumed for the corresponding fly-by-and-return mission, could be determined only by detailed analysis of the round-trip case.

Optimum Earth-to-Mars variable thrust rendezvous trajectories were determined for several launch dates in the vicinity of January 1967 and May 1971. These dates correspond to times when the planets are in very favorable positions. As in the previous circle-to-circle coplanar studies, the thrust magnitude programs have a bang-bang throttle characteristic, the transfers consisting of an initial full throttle period, a coasting period, and a final full throttle period. The significant feature of these variable thrust-limited vehicles is that a considerable reduction in fuel requirements may be achieved if the transfer time is permitted to be slightly longer. For example, the results

of the January 1967 launch indicate that a 5% sacrifice in time yields a 30% savings in fuel. The ratio, however, does not remain constant, i.e., if the time is permitted to increase 15% the savings in fuel is 50%.

REFERENCES

1. Kelley, H.J., Hinz, H.K., Pinkham, G., and Moyer, H.G., Low-Thrust Trajectory Optimization, "Progress Report No. 1 On Studies in the Fields of Space Flight and Guidance Theory," NASA-MSFC Report MTP-AERO-61-91, December 18, 1961.

2. Hinz, H.K., and Moyer, H.G., Three-Dimensional Low-Thrust Interplanetary Trajectory Optimization, "Progress Report No. 2 On Studies in the Fields of Space Flight and Guidance Theory," NASA-MSFC Report MTP-AERO-62-52, June 26, 1962.

3. Hinz, H.K., Optimal Low-Thrust Near-Circular Orbital Transfer, "Progress Report No. 2 On Studies in the Fields of Space Flight and Guidance Theory" and AIAA Journal, 1367-1371, June 1963.

FIG. 1 TRANSFER TIMES FOR OPTIMUM EARTH-TO-MARS RENDEZVOUS TRAJECTORIES — THRUST CONSTANT

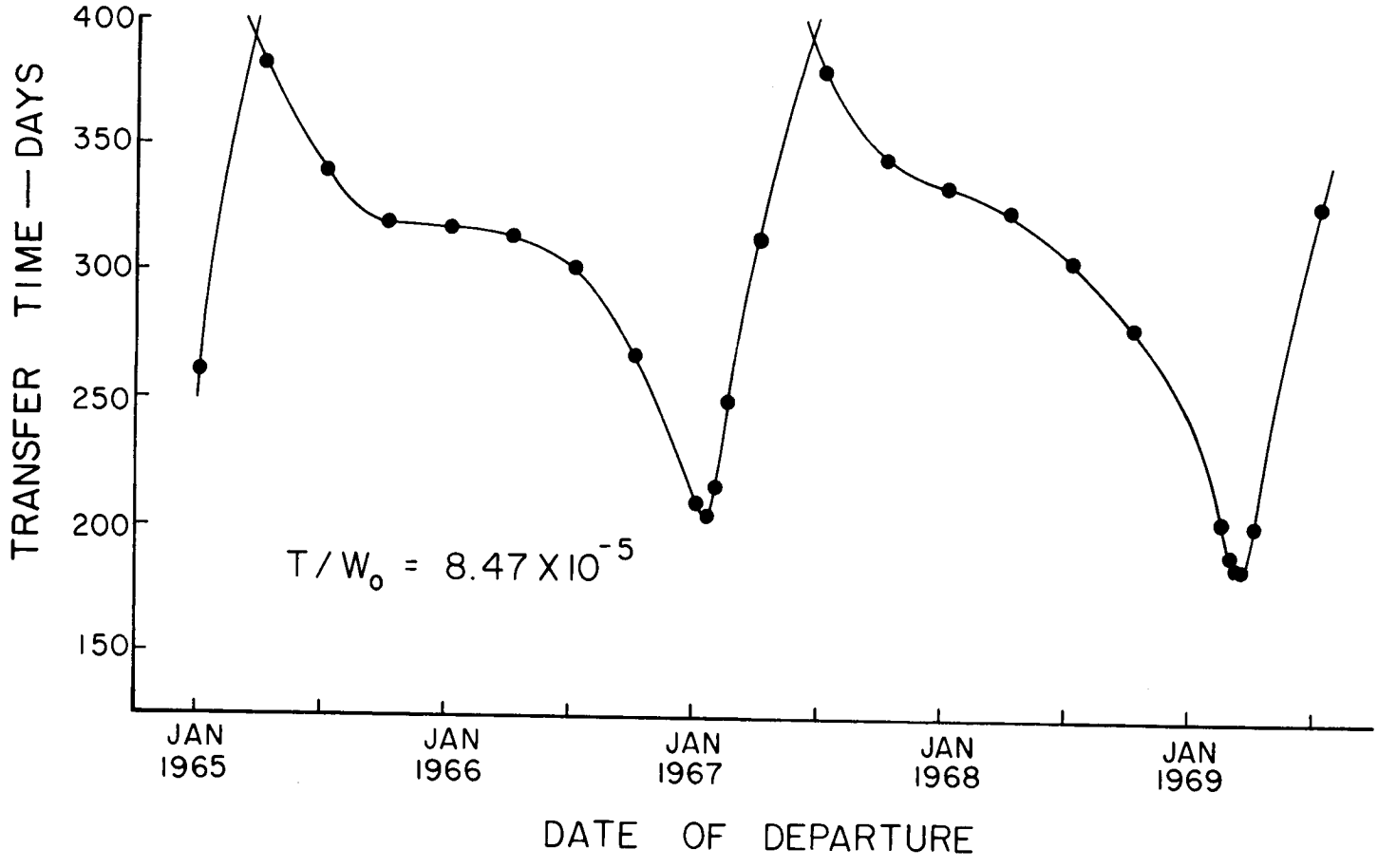

FIG. 2 THREE TYPES OF OPTIMUM EARTH-TO-MARS RENDEZVOUS TRAJECTORIES

$T/W_0 = 8.47 \times 10^{-5}$

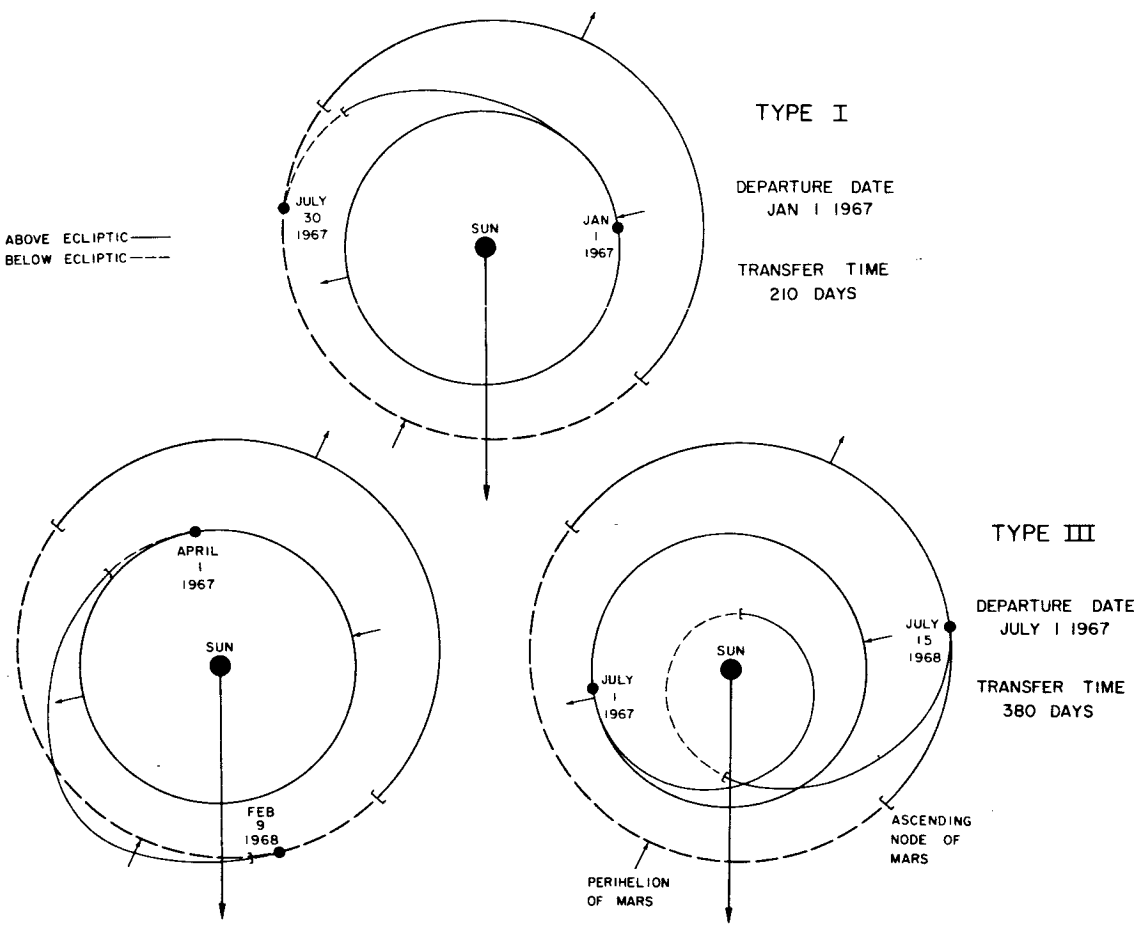

FIG. 3 TRANSFER TIMES FOR OPTIMUM CONTINUOUS LOW-THRUST EARTH-TO-MARS RENDEZVOUS TRAJECTORIES

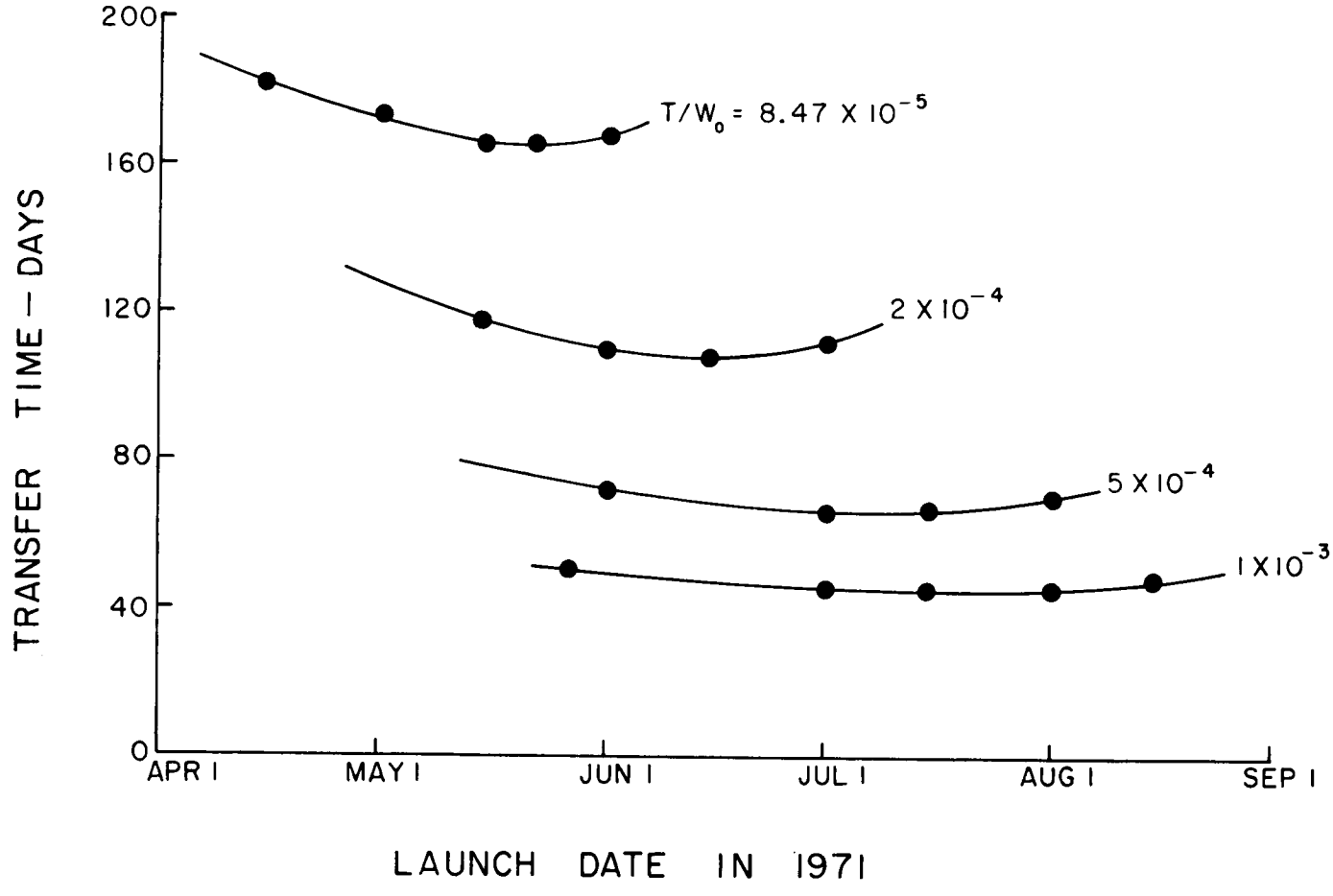

FIG. 4 MINIMUM TRANSFER TIMES FOR OPTIMUM CONTINUOUS LOW-THRUST EARTH-TO-MARS RENDEZVOUS TRAJECTORIES

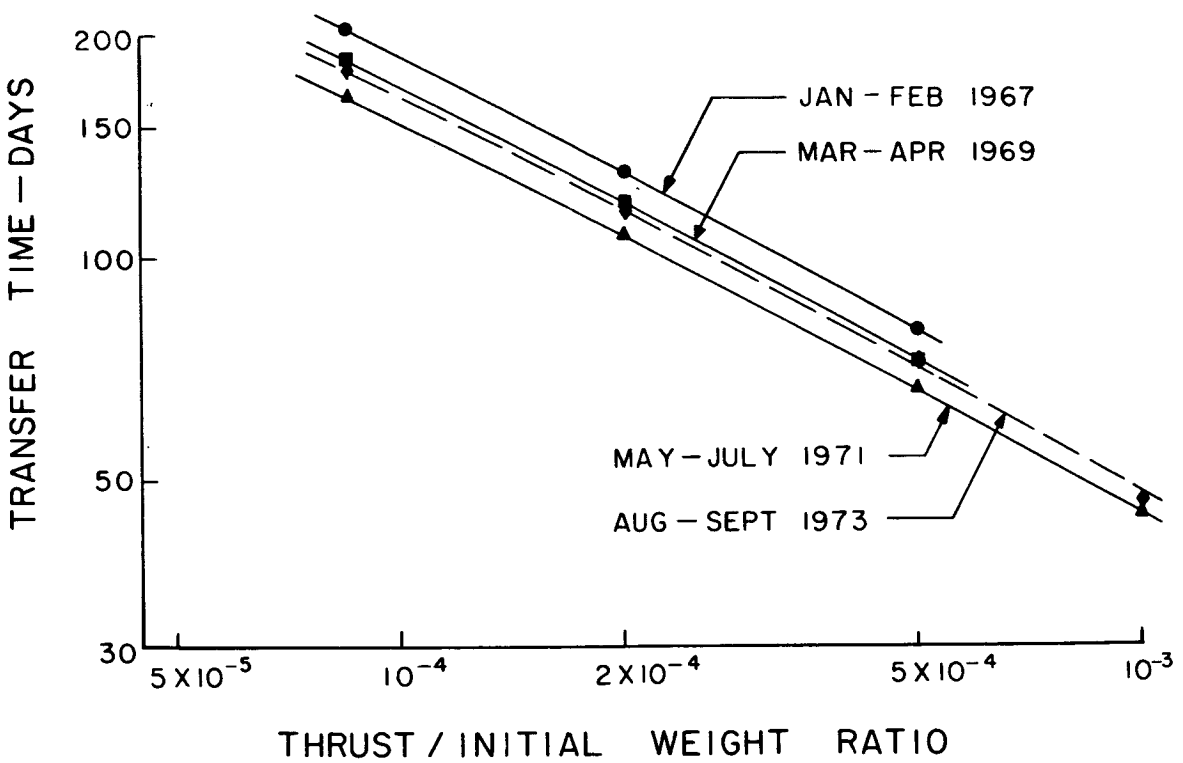

FIG. 5 MINIMUM-TIME OPTIMUM EARTH-TO-MARS RENDEZVOUS TRAJECTORIES

$T/W_0 = 8.47 \times 10^{-5}$

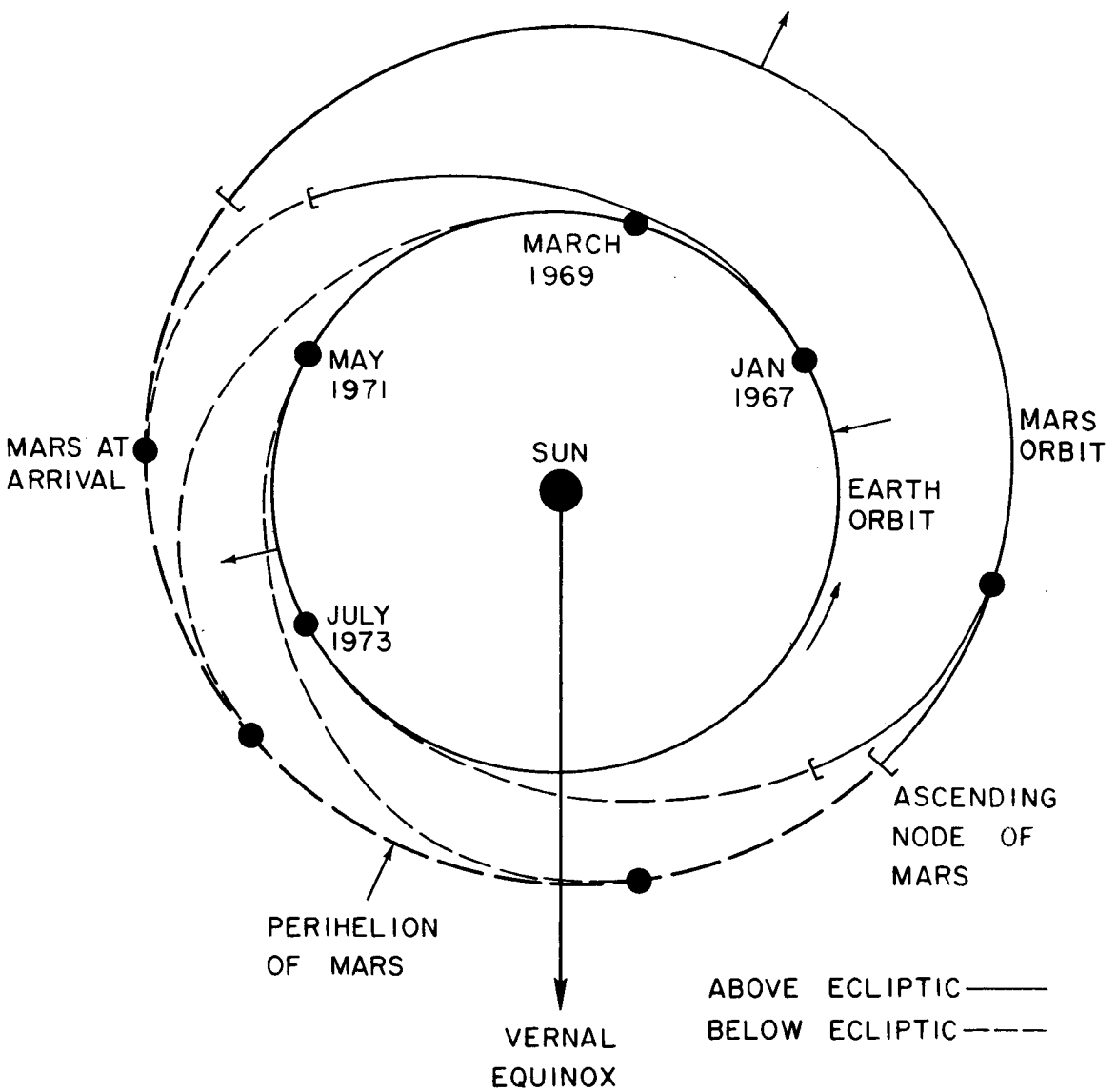

FIG. 6 MINIMUM-TIME OPTIMUM EARTH-TO-MARS RENDEZVOUS TRAJECTORIES

$T/W_0 = 2 \times 10^{-4}$

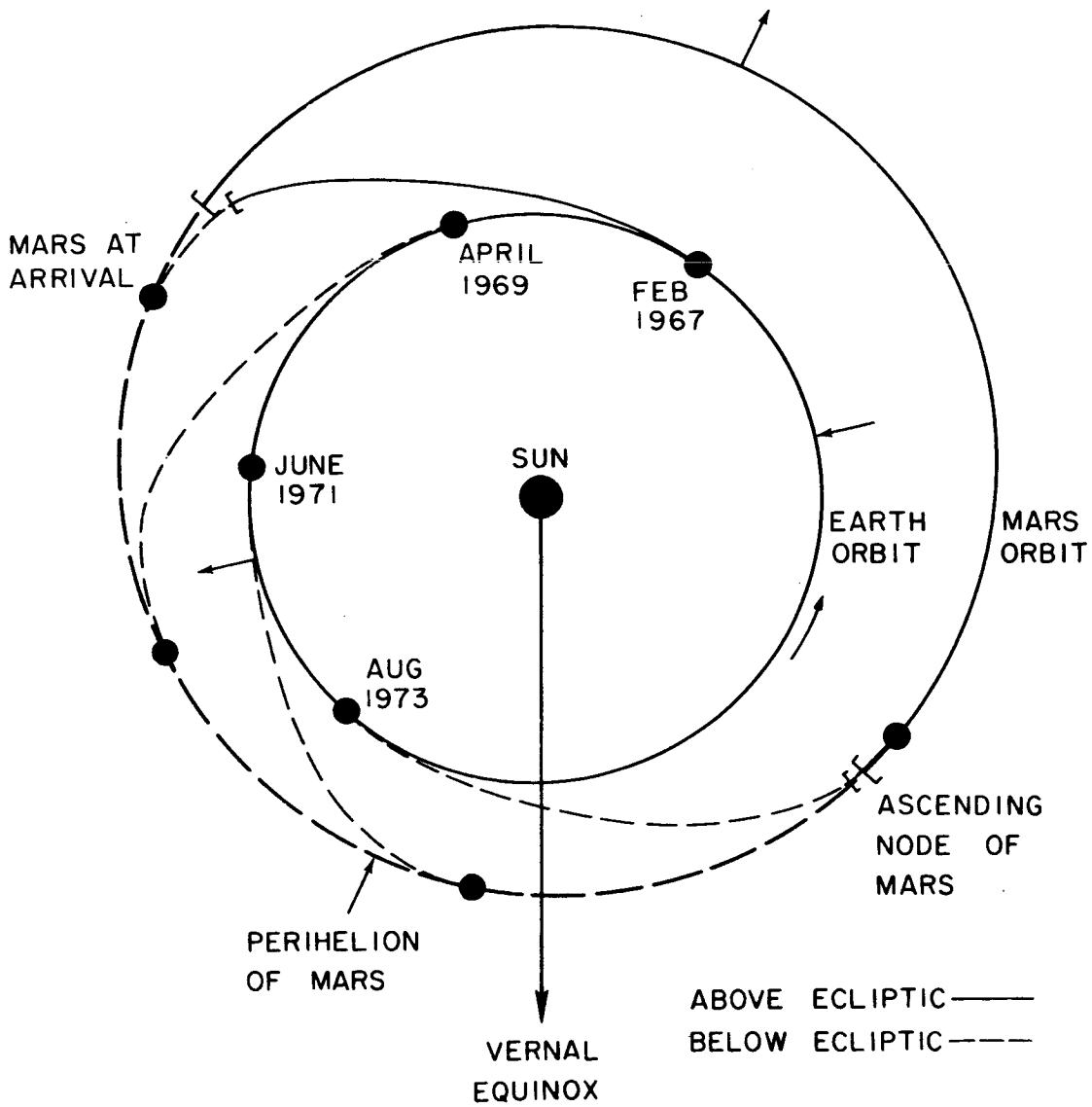

FIG. 7 MINIMUM-TIME OPTIMUM EARTH-TO-MARS RENDEZVOUS TRAJECTORIES

$T/W_0 = 5 \times 10^{-4}$

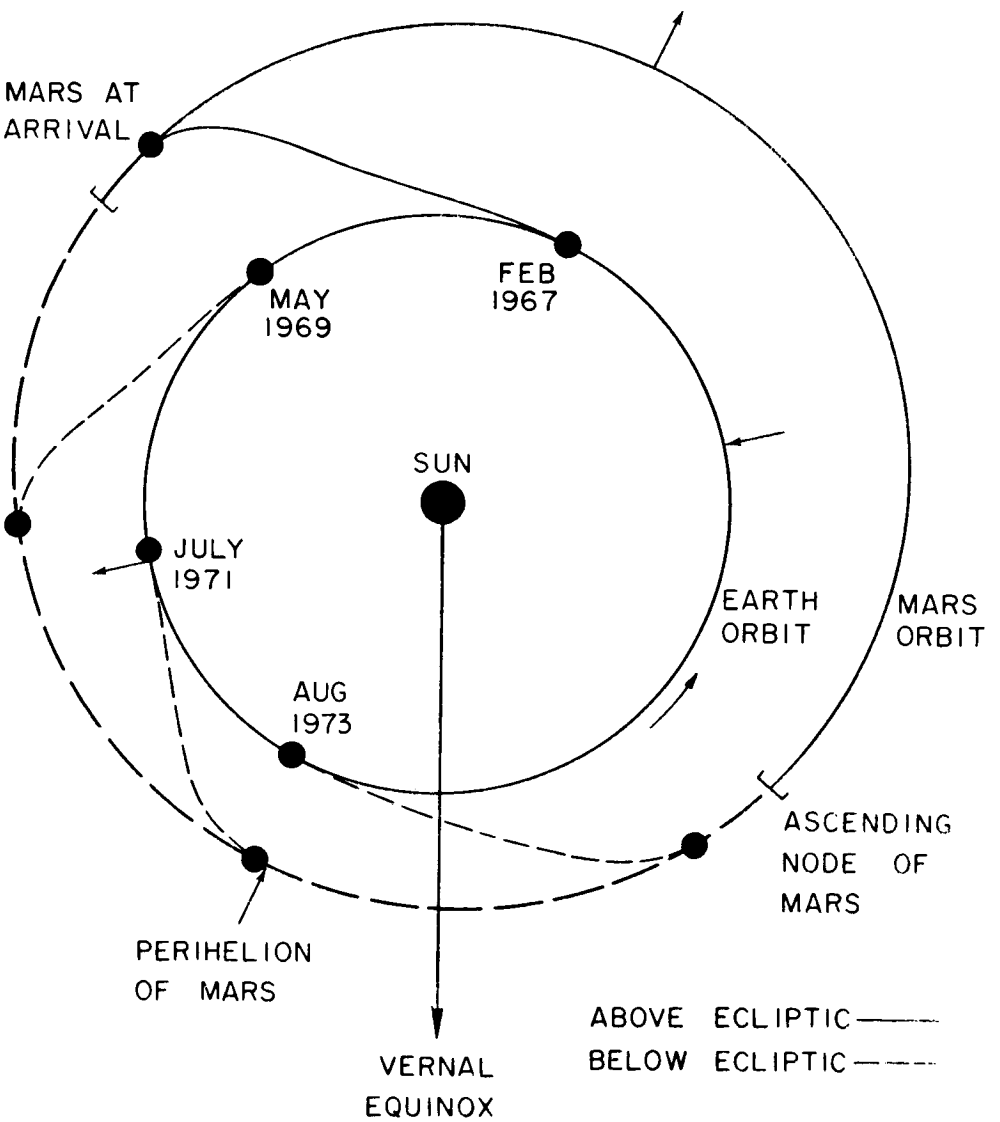

FIG. 8 MINIMUM-TIME OPTIMUM EARTH-TO-MARS RENDEZVOUS TRAJECTORIES

$T/W_0 = 10^{-3}$

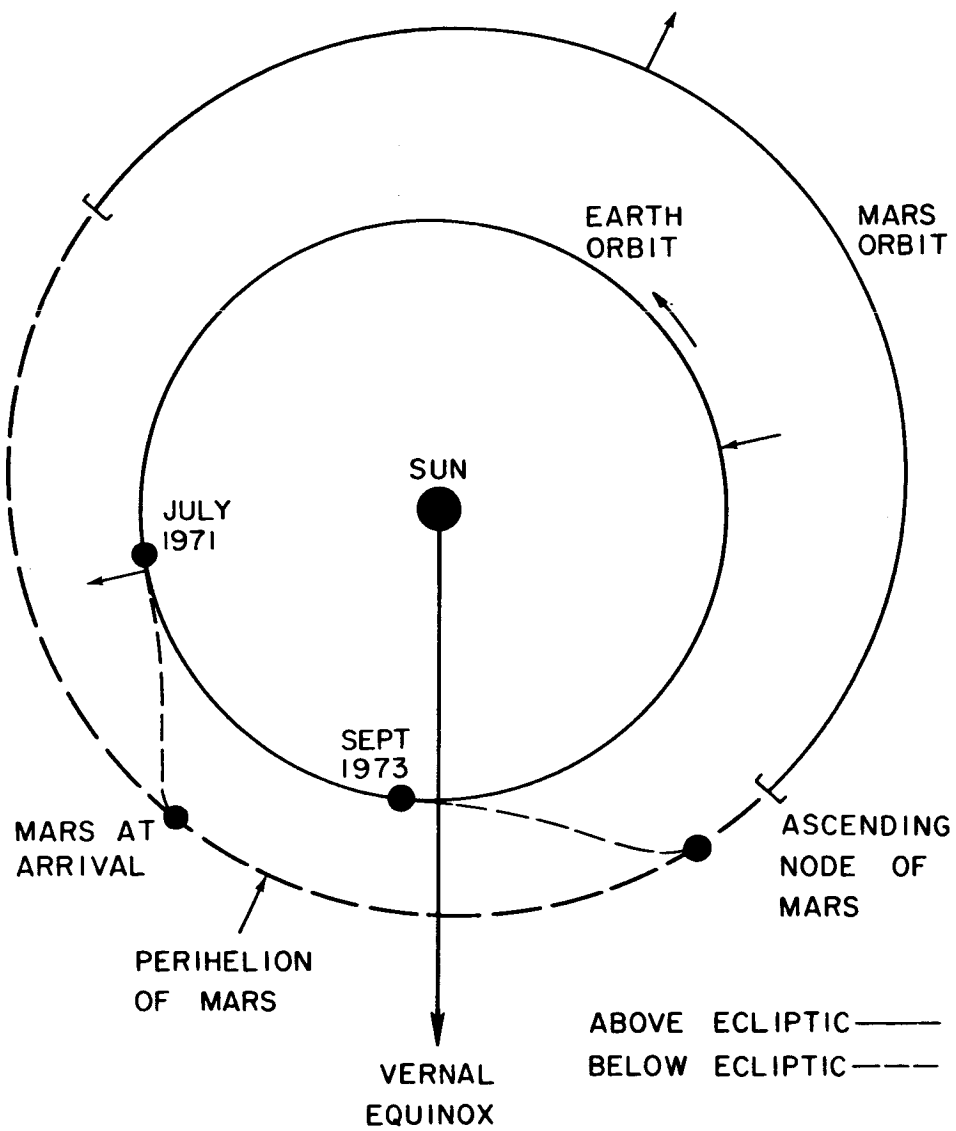

FIG. 9 THRUST STEERING ANGLE VARIATION ALONG A MINIMUM-TIME OPTIMUM EARTH-TO-MARS RENDEZVOUS TRAJECTORY

$T/W_0 = 8.47 \times 10^{-5}$

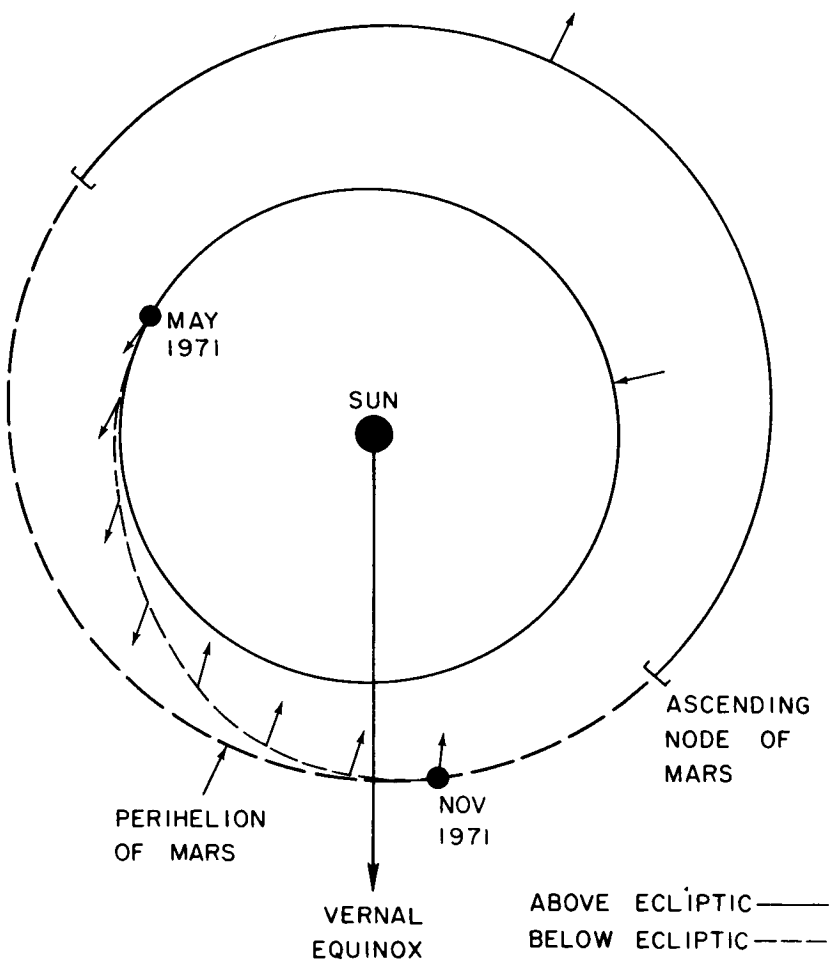

FIG. 10 THRUST STEERING ANGLE FOR MINIMUM-TIME OPTIMUM EARTH-TO-MARS RENDEZVOUS TRAJECTORIES

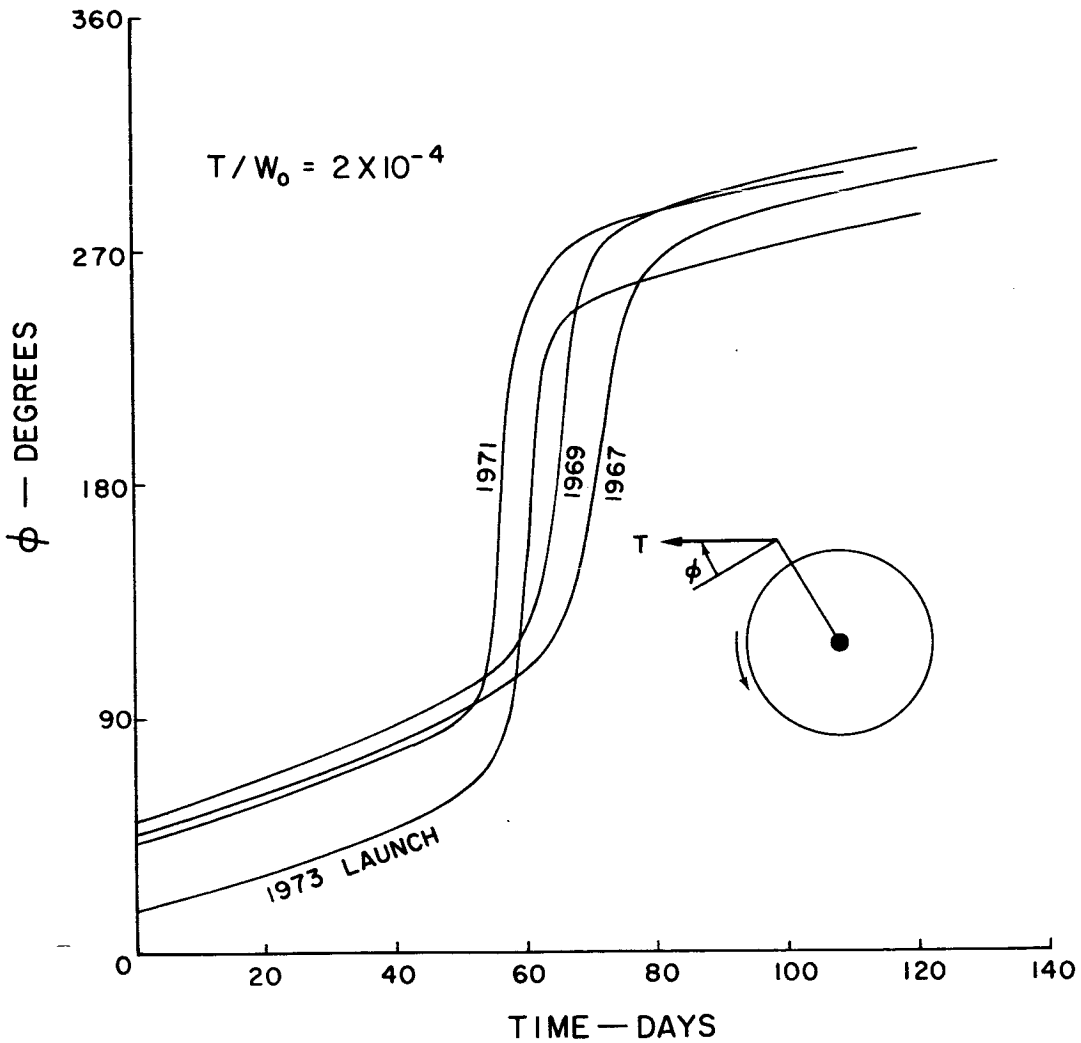

FIG. 11 COMPARISON OF OPTIMUM THRUST STEERING PROGRAM WITH CORRESPONDING SOLUTION OBTAINED FROM LINEAR COPLANAR STUDIES

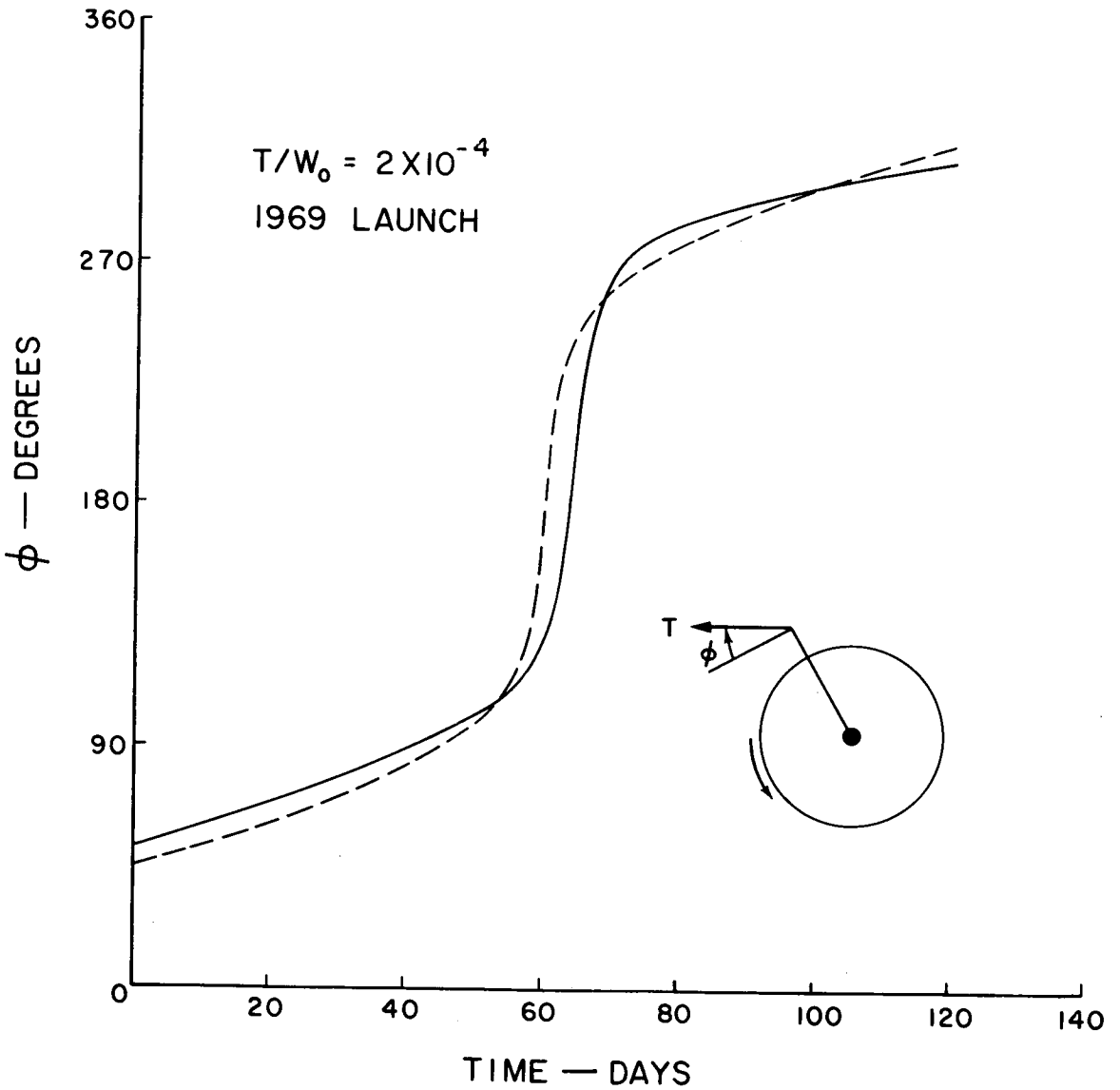

RESEARCH DEPARTMENT

GRUMMAN AIRCRAFT ENGINEERING CORPORATION

OPTIMAL MULTISTAGE ROCKET FLIGHT AND OTHER DISCONTINUOUS VARIATIONAL PROBLEMS

by

H. Gardner Moyer

Bethpage, New York

Research Department
GRUMMAN AIRCRAFT ENGINEERING CORPORATION
Bethpage, New York

OPTIMAL MULTISTAGE ROCKET FLIGHT AND OTHER DISCONTINUOUS VARIATIONAL PROBLEMS

by

H. Gardner Moyer

SUMMARY

Variational problems characterized by discontinuities artificially introduced by the problem formulation are examined. The discontinuities apply not only to the parameters in the differential equations of constraint but also to the state variables themselves. Two approaches to these problems are presented. The optimal flight of a throttleable, multistage rocket is discussed extensivelv.

INTRODUCTION

This report has as its subject two methods of treating discontinuous variational problems and their application to the optimal flight of throttleable, multistage rockets. The discontinuities considered are introduced artifically by the problem formulation and involve not only parameters in the differential system equations but also the state variables themselves.

One of the methods has been presented by Cicala in Ref. 1. It is both flexible and powerful. However, it has received little attention, perhaps because of the high degree of ingenuity by which it is established.

The alternative method utilizes the wavelet-wavefront approach to the calculus of variations. It provides an excellent introduction to discontinuous variational problems in that it is established by elementary and straightforward reasoning. By expressing all the control alternatives in terms of geometric figures there is no doubt as to the validity of the results. However, these properties prove more cumbersome than helpful as we pass from simpler to more complex problems.

The properties of wavelets and wavefronts will be summarized in the following section in order to establish nomenclature and notation.

WAVELETS AND WAVEFRONTS AS A THEORETICAL BASIS FOR THE CALCULUS OF VARIATIONS

Wavelets

We consider minimum and maximum time trajectories (extremals) obeying differential system equations of the type

$$\dot{x}_i = f_i(x_j, u_k, t) \qquad i = 1, \ldots, n \tag{1}$$

The n differentiated variables x_i are designated the state vector and the m undifferentiated variables u_k the control vector. Restrictions on the range of some or all of the u_k may be given in the problem formulation. The independent variable t is as usual designated time.

A wavelet is defined in x-space through the following equations

$$dx_i = \dot{x}_i\, dt = f_i(x_j, u_k, t)\, dt \qquad i = 1, \ldots, n \tag{2}$$

In the above equation the state vector is held fixed. The control vector takes on all admissible directions and magnitudes. We assume that f remains finite. The value of the differential dt is of course the same in each of the n equations. U does not change during the interval dt.

To illustrate some of the dimensional possibilities of a wavelet we assume for the moment that n equals three. Then if $m = 1$ the wavelet is a line which may or may not be closed. If $m = 2$ the wavelet is a surface. If $m = 3$ the wavelet is a solid.

The wavelet in control variables problems is thus a generalization of the indicatrix (Ref. 2) of the non-control-variable problems of the classical theory.

Wavefronts

When U is given as a function of time between t_o and t_1 a trajectory is defined by Eqs. 1. As $U(t)$ is varied (with t_o, t_1 and $x(t_o)$ fixed) the end-points of these trajectories cover a region in x-space. A wavefront, or transversal surface as it is usually called in the calculus of variations, is defined as the boundary between the reachable and the non-reachable points. It is thus an n-dimensional hypersurface regardless of the dimensionality of the wavelets.

Clearly the wavelets of the points on the transversal for time t_1 determine the transversal at time $t_1 + dt$ in the same way as wavefronts are determined in Huygens' theory of optics. This is true again regardless of the dimensionality and other properties of the wavelet.

Optimal Control

Given a point on a wavefront we desire to know the point on the associated wavelet that will lie on the new wavefront. Let us assume that the wavefront possesses a unique tangent hyperplane at the point in question. We designate the n-dimensional vector that is normal to the plane and points away from the wavefront (outward) as λ. The control vector that transfers the trajectory to the new wavefront is the one that imparts to f the largest component in the λ direction. That is, we must choose the admissible U that maximizes the scalar product $\lambda \cdot f$. The relation that distinguishes the optimal U from an aribtrary admissible U' is thus

$$\lambda \cdot f(X, U, t) \geqslant \lambda \cdot f(X, U', t) \qquad (3)$$

Eq. 3 denotes the maximum principle of Pontryagin. It can be derived using wavelets (Ref. 3) in the same way as the Weierstrass excess function is derived in the classical theory using indicatrixes.

As a general rule Eq. 3 determines a unique U for a given λ. If the direction of λ is not fixed by a wavefront we may regard U as function of this direction. Under these circumstances the λ direction replaces U as the independent variable. U is not, of course, a function of the magnitude of the λ vector. In addition, many directions will determine the same U when U is absent from some of the Eqs. 1, or when there are constraints on some of the components of U. If we replace U with λ as the independent variable in Eqs. 2 the points generated will be on the outer boundary of the wavelet.

The product $\lambda \cdot f$ is called the Hamiltonian and is denoted by H.

The Normal Vector

If we follow λ along a trajectory we find that it obeys the following differential equation

$$\dot{\lambda}_i = - \sum_{j=1}^{n} \frac{\partial f_j}{\partial x_i} \lambda_j \qquad i = 1, \ldots, n \qquad (4)$$

λ is thus identical with the Lagrange multiplier vector of Mayer problems (integrand identically zero) and when $H = +1$ with the $\partial t/\partial x_i$ vector of the Hamilton-Jacobi theory.

Minimum and Maximum Time Trajectories

Figure 1 shows the projection of wavefronts and extremals on a plane containing the initial point. We have assumed that motion is possible in all directions from the initial point. Thus by "chattering" it is possible to remain indefinitely in the vicinity of this point. For this reason solutions to a maximum time problem do not exist. We note that the wavefronts surround the initial point and that the f vector maintains a positive component in the λ direction ($H>0$).

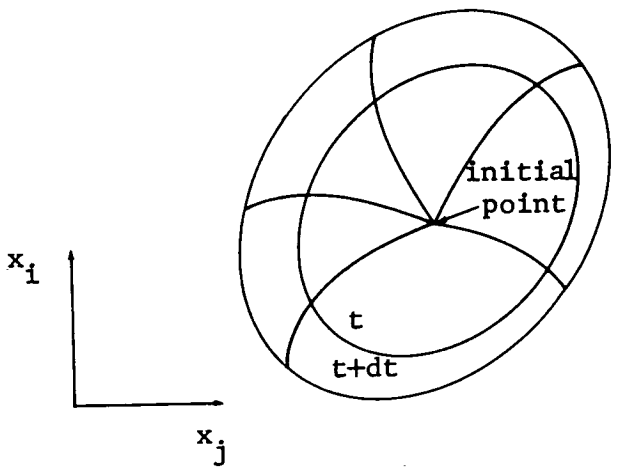

Fig. 1 Wavefronts with Minimum-Time Trajectories

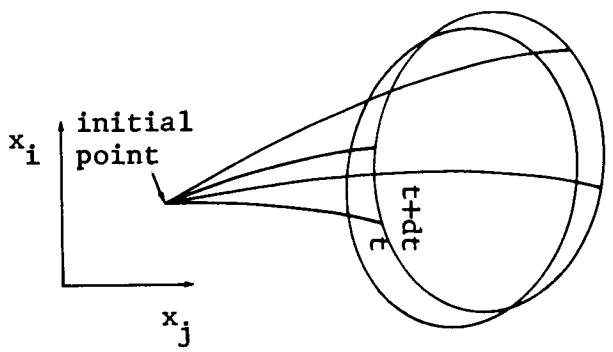

Fig. 2 Wavefronts with Minimum-and Maximum-Time Trajectories

In Fig. 2 motion is not possible in all directions. Some extremals of the family provide the minimum time and some the maximum time to their end points. The wavefronts do not surround the initial point. Minimum and maximum time trajectories are characterized by final values of H that are positive and negative respectively.

Wavefront Corners

We now discuss the effect of constraints on U on the shape of the wavefront. When there are constraints, a sub-family of extremals with varying λ time histories might have identical U (and therefore X) time histories. Thus what we actually have is a single extremal associated with a sub-family of λ vectors. As we move along a wavefront to this extremal the normal vectors defined along our path will approach an outer member of the λ sub-family. The particular member approached will be a function of the path taken. The tangent hyperplane that is approached will therefore also be a function of the path so that the wavefront must have a corner at this extremal.

A PROBLEM WITH DISCONTINUOUS STATE VARIABLES

We are now ready to apply the wavelet-wavefront basis of the calculus of variations to a problem with discontinuous state variables. To illustrate the basic principles of the method a simple problem will be discussed.

We seek the extremals having a common orgin, obeying system equations of the form

$$\dot{x}_1 = \dot{x}_1(x_1, x_2, u, t) \tag{5a}$$

$$\dot{x}_2 = \dot{x}_2(x_1, x_2, u, t) \tag{5b}$$

and subject to the condition that whenever the variable x_1 reaches the value $\bar{x}_1$ it is incremented by the constant Δx_1 whose magnitude is arbitrary. The control variable u is unbounded; $\dot{x}_1$ and $\dot{x}_2$ are finite at all points.

The problem is depicted in Fig. 3. Since the transversals surround P the figure indicates that only minimum-time extremals (H>0) originate from this point. The case with both minimizing and maximizing extremals will not be discussed.

The extremal to point A is incremented to point A' at time t_A. Recalling the discussion on optimal control, we regard u in Eqs. 5 as determined by the λ direction (i.e. λ_1/λ_2). We introduce the following notation:

$$f \equiv \dot{x}(\bar{x}_1,\ x_2,\ \lambda_1/\lambda_2,\ t_A)$$

$$g \equiv \dot{x}(\bar{x}_1 + \Delta x_1,\ x_2,\ \mu_1/\mu_2,\ t_A)$$

λ is the Lagrange multiplier at A

μ is a Lagrange multiplier at A'

At time $t_A + dt$ a wavelet has formed around the point A'. Also at this time an extremal has reached $x_1 = \bar{x}_1$ at B and been incremented to B'. The wavefront at $t_A + dt$ must pass through the point B', and be tangent to the wavelet. Also the line segments A B and A' B' must have equal lengths. Utilizing relations from plane geometry, we see from Fig. 3 that

$$\frac{\lambda_1}{\lambda_2}\ f_1\ dt + f_2\ dt = \frac{\mu_1}{\mu_2}\ g_1\ dt + g_2\ dt$$

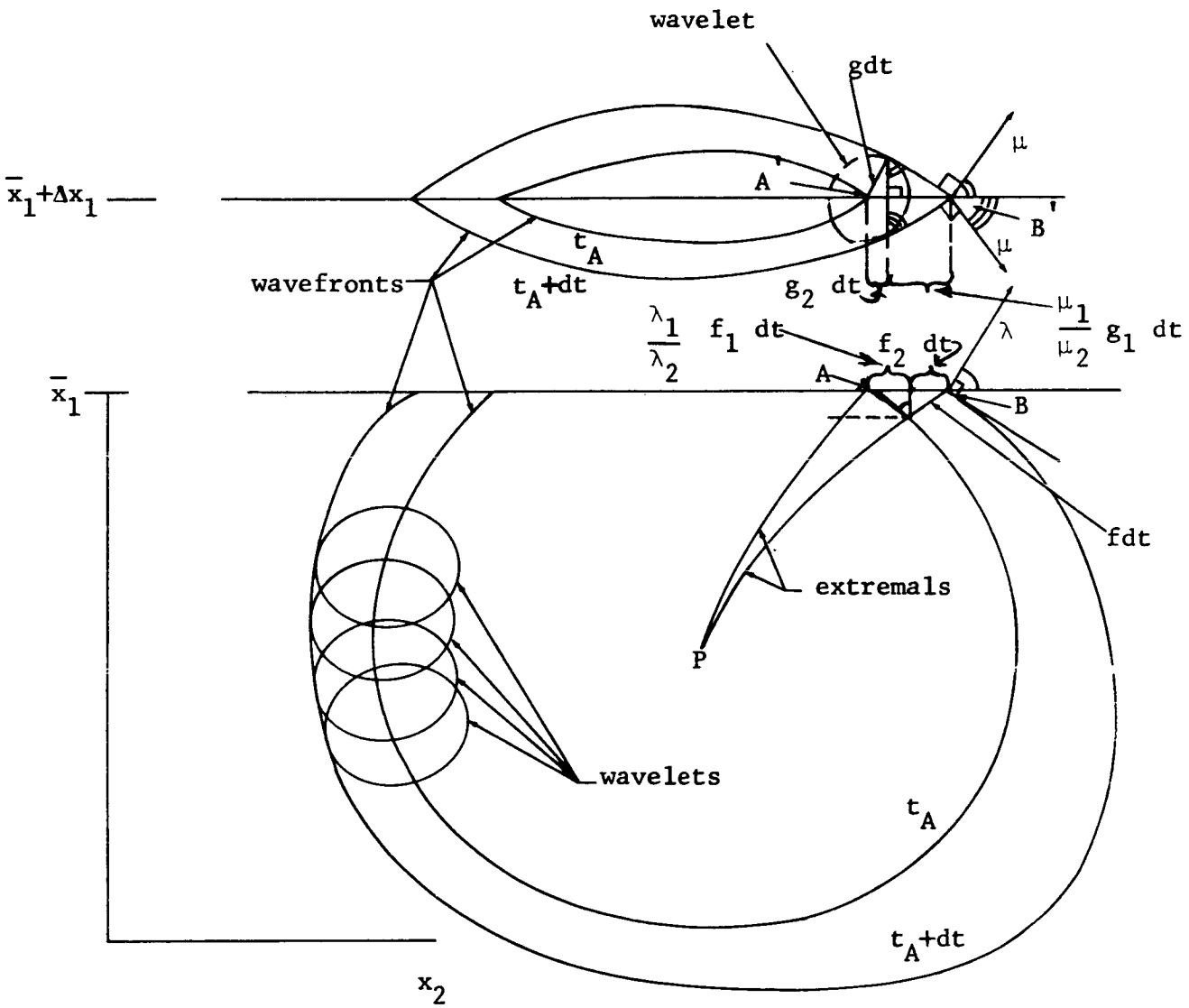

Fig. 3 Wavelets and Wavefronts for a Problem with Discontinuous State Variables

This equation determines the unknown μ_1/μ_2. But should the multipliers be $+\mu_1$ and $+\mu_2$ or $-\mu_1$ and $-\mu_2$? From Fig. 3 (as well as Fig. 4 below) we see that that μ_2 must be given the same sign as λ_2. Since the subsequent course of the extremal is independent of the magnitude of μ we will scale this vector so that our results will have a simple form. We therefore take $\mu_2 = \lambda_2$. We can now write

$$\lambda_1 f_1 + \lambda_2 f_2 = \mu_1 g_1 + \lambda_2 g_2 \equiv H \qquad (6)$$

In this form the solution requires λ_2 to be continuous and λ_1 to be incremented so that the Hamiltonian is also continuous.

If the wavelet has no regions of concave curvature (and B' is outside the wavelet) there will be two tangent lines from B'. If concave regions are present there will be more than two tangent lines. Clearly the wavefront will be defined by the two outer lines. Solutions corresponding to inner lines were eliminated from Eq. 6, when we employed Eq. 3 which incorporates the Pontryagin maximum principle. (That is, when we replaced U using Eq. 3, a portion of the complete outer boundary of the wavelet might have been eliminated.)

However, we must not always expect two solutions to Eq. 6. This is because in some regions of the wavelet, g may have a negative component in the μ direction making $H<0$ along part of the wavelet. (We have indicated that the left side of Eq. 6 is positive.) For the example of Fig. 3 we know that there are two solutions since the wavelet surrounds A'. In this example the extremal PAA' splits into two branches at A'.

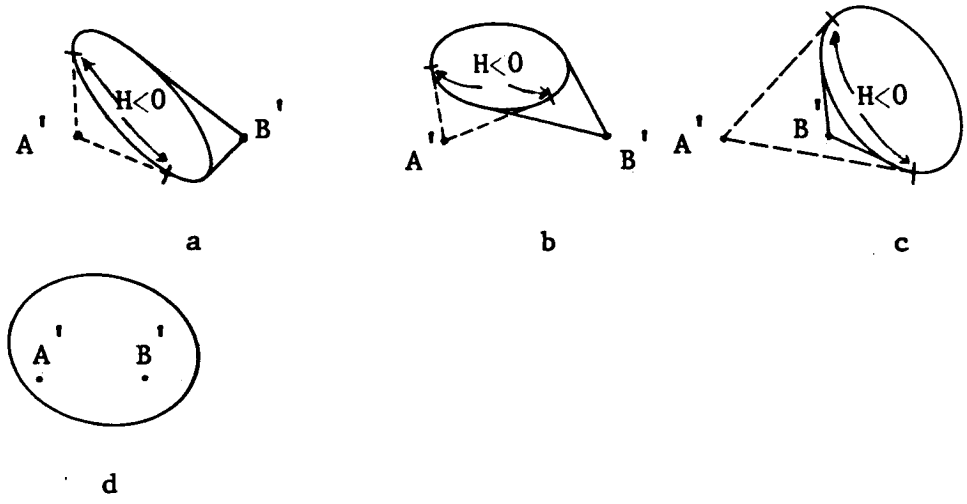

Fig. 4 Possible Relations between B' and the A' Wavelet

Equation 6 also has two solutions when the wavelet has the properties shown in Fig. 4a. Figure 4b shows how but one solution can be present. Figures 4c and 4d show that there can be no solution. In these cases the extremal $PAA'B$ takes less time than the extremal PBB'. The latter must therefore be terminated at point B.

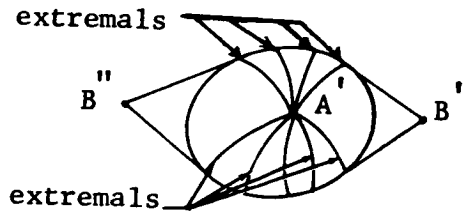

Fig. 5 Hypothetical Initial State of the Incremented Wavefront

Perhaps the initial state of the incremented wavefront is worthy of some discussion. Let us assume that PA is the first of all the extremals that originate at P to reach the Line $x_1 = \bar{x}_1$ and be

incremented to A'. The new wavefront will be determined by the A' wavelet and points B' and B'' on either side of A'. We ask whether the tangent lines from B' and B'' will be horizontal. If they are not a sub-family of extremals will emerge from the channel PAA' (Fig. 5). This would give the first extremal to be incremented a character quite different from those that are incremented afterwards.

At point A the line $x_1 = \bar{x}_1$ is tangent to the wavefront. Therefore, the normal vector is vertical ($\lambda_2 = 0$). Assuming $f_1 > 0$, the ratios of the distance $(\lambda_1/\lambda_2)f_1\,dt$ (cf. Fig. 3) to the distances $g_1\,dt$ and $g_2\,dt$ will both be infinite. We conclude that points B' and B'' in Fig. 5 should be moved out to infinity and that the tangent lines from B' and B'' will be horizontal, contacting the wavelet at its highest and lowest points. Thus the extremal PAA' splits into two branches at A' in common with those of Fig. 3.

Let us assume that parameters are present in Eqs. 5 and that they are changed when x_1 is discontinuous, that is, the parameters have different values in the equations for f and g. Reviewing the analysis of this section we see that it applies without change. The solution given by Eq. 6 also applies to problems with changing parameters.

The range of problems to which the wavelet-wavefront approach can be applied could now be gradually extended until the multistage rocket problem is included. This will not be done, however, since complex problems can be handled more readily by the analytic method presented in the next section.

METHOD OF ADJOINED DISCONTINUITY RELATIONS

In this section we present the analytic method devised by Cicla (Ref. 1, p.34). The specific example we will use to explain the method is a generalization of the previous example. As before the extremals are incremented when x_1, equals $\bar{x}_1$. Instead of two state variables we will have n and increments will will be allowed in all of them. The possibility of constraints on some of the control variables will be considered.

To be definite we will assume that there is a pay-off function $P(x_j(t_z), t_z)$. The functional is

$$J = P(x_j(t_z), t_z) + \int_{t_P}^{t_A} \left[\sum_{i=1}^{n} \lambda_i (\dot{x}_i - f_i(x_j, u_k, t, c_\ell)) \right] dt$$

$$+ \int_{t_A'}^{t_z} \left[\sum_{i=1}^{n} \mu_i (\dot{x}_i - g_i(x_j, u_k, t, c'_\ell)) \right] dt$$

$$+ \tilde{e} (x_1(t_A) - \bar{x}_1) + \sum_{i=1}^{n} e_i (x_i(t_A') - x_i(t_A) - \Delta x_i)$$

The constraint adjoined by the multiplier $\tilde{e}$ states that the extremal must intersect the hyperplane $x_1 = \bar{x}_1$ at an undetermined intermediate time t_A. The constraints adjoined by the multipliers e_i state that at the time $t_A' = t_A$ the state variable x_i must have been incremented by the constant Δx_i. Note that at the time t_A the parameters c_ℓ change to c'_ℓ.

Throughout the rest of this section we will employ the Einstein summation convention. The first variation is

$$\delta J = \int_{t_p}^{t_A} \left[\delta\lambda_i(\dot{x}_i - f_i) + \lambda_i\delta\dot{x}_i - \lambda_i\left(\frac{\partial f_i}{\partial x_j}\ \delta x_j + \frac{\partial f_i}{\partial u_k}\ \delta u_k\right)\right] dt$$

$$+ \int_{t_A'}^{t_z} \left[\delta\mu_i(\dot{x}_i - g_i) + \mu_i\delta\dot{x}_i - \mu_i\left(\frac{\partial g_i}{\partial x_j}\ \delta x_j + \frac{\partial g_i}{\partial u_k}\ \delta u_k\right)\right] dt$$

$$+ \tilde{e}\ (\delta x_1(t_A) + \dot{x}_1(t_A)\delta t_A) + e_i\ (\delta x_i(t_A') + \dot{x}_i(t_A')\delta t_A - \delta x_i(t_A)$$

$$-\dot{x}_i(t_A)\delta t_A) + \delta\ \tilde{e}(x_1(t_A) - \bar{x}_i) + \delta e_i(x_i(t_A') - x_i(t_A) - \Delta x_i)$$

$$+ \lambda_i(\dot{x}_i(t_A) - f_i(t_A))\ \delta t_A - \mu_i(\dot{x}_i(t_A') - g_i(t_A'))\delta t_A + \mu_i(\dot{x}_i(t_z)$$

$$- g(t_z))\ \delta t_z + \frac{\partial P}{\partial x_j}\ (\delta x_j(t_z) + \dot{x}_j(t_z)\delta t_z) + \frac{\partial P}{\partial t}\ \delta t_z$$

After the usual integration by parts we have

$$\delta J = \int_{t_p}^{t_A} \left[\delta\lambda_i(\dot{x}_i - f_i) - (\dot{\lambda}_i + \frac{\partial f_j}{\partial x_i}\ \lambda j)\ \delta x_i - \lambda_i \frac{\partial f_i}{\partial u_k}\ \delta u_k \right] dt$$

$$+ \int_{t_A'}^{t_z} \left[\delta\mu_i(\dot{x}_i - g_i) - (\dot{\mu}_i + \frac{\partial g_j}{\partial x_i}\ \mu_j)\ \delta x_i - \mu_i \frac{\partial g_i}{\partial u_k}\ \delta u_k \right] dt$$

$$+ \lambda_i \delta x_i(t_A) - \mu_i \delta x_i(t_A') + \mu_i \delta x_i(t_z) + \tilde{e} \, (\delta x_1(t_A) + \dot{x}_1(t_A) \, \delta t_A)$$

$$+ e_i \, (\delta x_i(t_A') + \dot{x}_i(t_A') \, \delta t_A - \delta x_i(t_A) - \dot{x}_i(t_A) \, \delta t_A)$$

$$+ \delta \tilde{e}(x_1(t_A) - \bar{x}_1) + \delta e_i \, (x_i(t_A') - x_i(t_A) - \Delta x_i) + \lambda_i(\dot{x}_i(t_A) - f(t_A))\delta t_A$$

$$- \mu_i(\dot{x}_i(t_A') - g(t_A')) \, \delta t_A + \mu_i(\dot{x}(t_z) - g(t_z)) \, \delta t_z + \frac{\partial P}{\partial x_j} \, (\delta x_j(t_z)$$

$$+ \dot{x}(t_z)\delta t_z) + \frac{\partial P}{\partial t} \, \delta t_z$$

If there are no constraints on u_k the equality sign applies in Eq. 3 and we set $\lambda_i \, \partial f_i / \partial u_k = 0$. If there are constraints the

inequality sign applies and we must have $\lambda_i \frac{\partial f_i}{\partial u_k} \delta u_k < 0$ (summation over i only). Since our conclusions will hold in either case we will assume the former possibility. The rest of the integrands vanish in virtue of Eqs. 1 and 4. Setting the coefficients of δe and δe_i to zero satisfies the discontinuity relations. After making the substitution $Dx_i(t) \equiv \delta x_i(t) + \dot{x}_i(t)\delta t$ we have

$$\delta J = \lambda_i Dx_i(t_A) - H(t_A)\,\delta t_A - \mu_i\, Dx_i(t_A') + H(t_A')\,\delta t_A + \mu_i Dx_i(t_z)$$

$$- H(t_z)\,\delta t_z + \tilde{e}\, Dx_1(t_A) + e_i\,(Dx_i(t_A') - Dx_i(t_A)) + \frac{\partial P}{\partial x_j}\, Dx_j(t_z)$$

$$+ \frac{\partial P}{\partial t}\,\delta t_z$$

Setting to zero the coefficients of $Dx_i(t_A)$, $Dx_i(t_A')$, δt_A, $Dx_i(t_z)$, and δt_z, we have

$$\lambda_1(t_A) - e_1 + \tilde{e} = 0 \qquad (7)$$

$$\lambda_i(t_A) - e_i = 0 \qquad i = 2, \ldots, n \tag{8}$$

$$-\mu_1(t_A') + e_1 = 0 \tag{9}$$

$$-\mu_i(t_A') + e_i = 0 \qquad i = 2, \ldots, n \tag{10}$$

$$-H(t_A) + H(t_A') = 0 \tag{11}$$

$$\mu_i(t_z) + \frac{\partial P}{\partial x_i} = 0$$

$$-H(t_z) + \frac{\partial P}{\partial t} = 0$$

The $2n + 1$ equations(7 through 11) determine the $2n + 1$ unknowns $\mu_i(t_A')$, e_i, and $\tilde{e}$. In $H(t_A')$ of Eq. 11, U is replaced using Eq. 3 so that the equations are non linear and possibly do not possess a solution: Eliminating e_i from Eqs. 8 and 10, we see that the $\lambda_i(i = 2, \ldots, n)$ are continuous. We then choose $\mu_1(t_A')$ so that the Hamiltonian is continuous as required by Eq. 11. This leaves available e_1 and $\tilde{e}$ to satisfy Eqs. 7 and 9. Note that these results are in agreement with those of the previous section.

The trajectory thus determined makes P a smooth minimum with respect to changes in unconstrained control variables and a sharp minimum with respect to admissible changes in constrained control variables.

In the previous section the magnitude of μ was free whereas here it is fixed. The discrepancy lies in the fact that here a pay-off is specified as $P(x_j(t_z), t_z)$ whereas before we merely sought extremals and left the pay-off open. Due to the linearity and homogeneity of λ in Eqs. 3 and 4 the extremal that minimizes $P(x_j(t_z), t_z)$ is identical to the extremal that minimizes $k\,P(x_j(t_z), t_z)$ except for the magnitude of λ. When k is fixed at a particular value (in this case one), the λ magnitude is fixed; when k is left open, the λ magnitude is open.

Of course the discontinuity relations could be generalized so that the discontinuity occurs at a surface $F(x_j(t_A), t_A) = 0$ with $x_i(t_A') - x_i(t_A) = G(x_j(t_A), t_A)$. This method is therefore more flexible and powerful than the wavelet-wavefront approach.

MULTISTAGE ROCKET FLIGHT

System, Multiplier, and Control Variable Equations

We turn now to the optimal flight of a throttleable multistage rocket. The mass curve is discontinuous at staging points.

The specific examples of planar motion above a flat earth and in a central gravitational field will be discussed. Three dimensional examples would present no new difficulties. The system equations for the former case are

$$\dot{x}_1 = \frac{T}{m} \sin\theta - g$$

$$\dot{x}_2 = \frac{T}{m} \cos\theta$$

$$\dot{x}_3 = x_1$$

$$\dot{x}_4 = x_2$$

$$\dot{m} = - T/c$$

x_1 and x_3 are vertical velocity and distance; x_2 and x_4 are horizontal velocity and distance; m is the mass. The control variables are the thrust direction angle θ and the thrust magnitude T. T has an upper limit T_u and a lower limit T_ℓ. g is the acceleration of gravity and c the effective exhaust velocity.

The multiplier equations are

$$\dot{\lambda}_1 = - \lambda_3$$

$$\dot{\lambda}_2 = - \lambda_4$$

$$\dot{\lambda}_3 = 0$$

$$\dot{\lambda}_4 = 0$$

$$\dot{\lambda}_m = \frac{T}{m^2} (\lambda_1 \sin \theta + \lambda_2 \cos \theta)$$

$$= \frac{T}{m^2} (\lambda_1^2 + \lambda_2^2)^{\frac{1}{2}} \qquad (12)$$

In Eq. 12 we have substituted for θ using the optimizing relations

$$\sin\theta \frac{\lambda_1}{(\lambda_1^2 + \lambda_2^2)^{\frac{1}{2}}} \qquad \cos\theta = \frac{\lambda_2}{(\lambda_1^2 + \lambda_2^2)^{\frac{1}{2}}}$$

Collecting the terms of the Hamiltonian that contain T, we can write

$$H = H_Q + QT \tag{13}$$

where

$$\begin{aligned} Q &= \frac{\lambda_1}{m}\sin\theta + \frac{\lambda_2}{m}\cos\theta - \frac{\lambda_m}{c} \\ &= \frac{1}{m}(\lambda_1^2 + \lambda_2^2)^{\frac{1}{2}} - \frac{\lambda_m}{c} \end{aligned} \tag{14}$$

To maximize H we must set $T = T_u$ when Q is positive and $T = T_\ell$ when Q is negative. Thus the optimal trajectories are composed of periods of coasting and full throttle burning as determined by the switching function Q.

For motion in a central gravitational field the system equations are

$$\dot{x}_1 = \frac{x_2^2}{x_3} - \frac{gR^2}{x_3^2} + \frac{T}{m}\sin\theta$$

$$\dot{x}_2 = -\frac{x_1 x_2}{x_3} + \frac{T}{m}\cos\theta$$

$$\dot{x}_3 = x_1$$

$$\dot{m} = -\frac{T}{c}$$

Here x_1 is the radial velocity, x_2 the circumferential velocity, and x_3 is the radius. R is the radius at which the gravitational acceleration is g. The other symbols are defined as before.

The multiplier equations now are

$$\dot{\lambda}_1 = \frac{x_2}{x_3}\ \lambda_2 - \lambda_3$$

$$\dot{\lambda}_2 = -\frac{2x_2}{x_3}\ \lambda_1 + \frac{x_1}{x_3}\ \lambda_2$$

$$\dot{\lambda}_3 = \left[\frac{x_2^2}{x_3^2} - 2\frac{gR^2}{x_3^3} \right] \lambda_1 - \frac{x_1 x_2}{x_3^2}\ \lambda_2$$

$$\dot{\lambda}_m = \frac{T}{m^2}\ (\lambda_1 \sin\theta + \lambda_2 \cos\theta) = \frac{T}{m^2}\ (\lambda_1^2 + \lambda_2^2)^{\frac{1}{2}}$$

It is interesting the expressions for $\dot{\lambda}_m$, $\sin\theta$, $\cos\theta$, and Q are the same in both problems.

Wavefronts

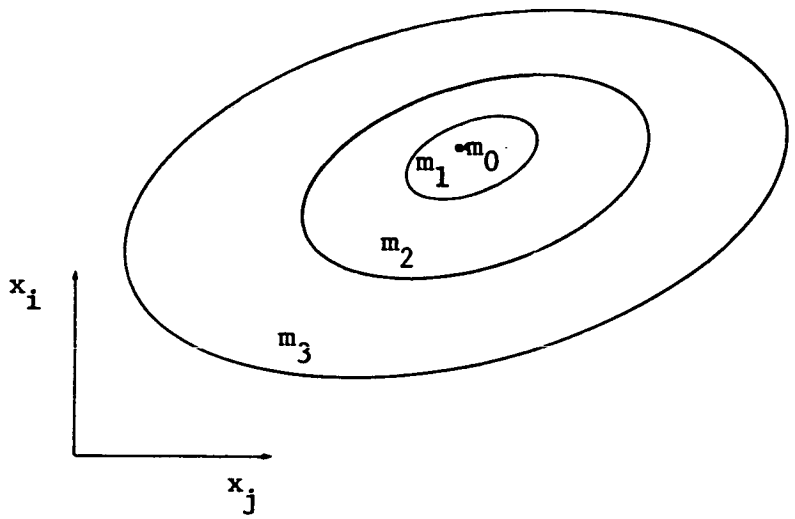

Fig. 6 Final Points of Optimal Trajectories - Fixed Final Time

To gain some conception of the form of the wavefronts we consider the following pair of problems. The final values of time, mass, and x_j are fixed in advance. The final values of the other state variables except x_j are free. The final value of x_i is to be maximized for one problem and minimized for the other. As the final x_j is varied, with different choices of the final mass parameter, we obtain a family of curves of the general form of Fig. 6. The final points of trajectories with continual full-throttle burning lie on the outer curve ($m = m_3$). The point designated m_0 results from continual coasting: Thus Fig. 6 as well as Figs. 7 and 10 to follow imply $T_\ell = 0$. It is reasonable to assume that a curve corresponding to a certain fuel expenditure will enclose a curve corresponding to less fuel. This conclusion will be made rigorous later on.

Fig. 7 is identical to Fig. 6 except that there is an axis for the final mass. The x_j axis is assumed to be perpendicular to the page. Instead of a family of curves we have a surface. This surface is the projection of the complete n-dimensional transversal surface for the given final time onto the three-space of the figure. This statement is justified by noting that the transversality relations for the state variables with free final values (those other than x_i, x_j, and m) require the corresponding components of the normal vector to be zero.

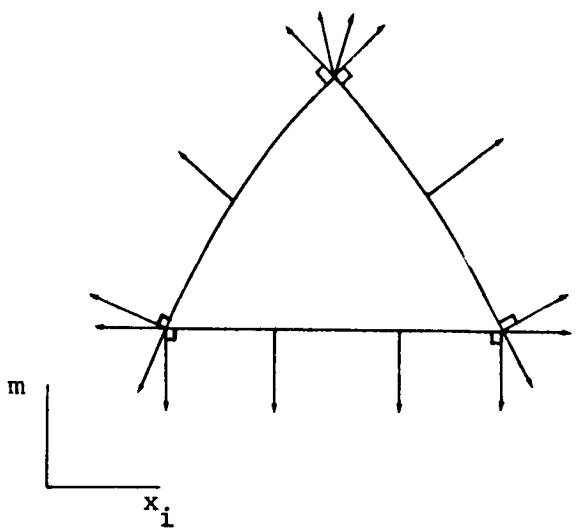

Fig. 7 Wavefront Projection with Multiplier Vectors for the Rocket Problem

Whether the wavefront of Fig. 7 is determined entirely by minimum time trajectories (as is the case in Fig. 1) or by both minimum and maximum time trajectories (as in Fig. 2) will not be relevant to our discussion.

We note that in Fig. 7 the λ_m component of the normal vectors along the lateral sides is always positive. This is required by Eq. 12 which states that $\lambda_m(t)$ increases monotonically and Eq. 14 which states that λ_m must be positive at switching points. This verifies the statement that curves of lower final mass enclose curves of higher final mass in Fig. 6.

We now consider a problem identical to one of the pair previously stated except that the roles of x_i and m are interchanged; that is, the final values of x_i as well as x_j and t are fixed and m is to be maximized. The maximum value of m is determined by the intersection (assuming one exists) of the surface of Fig. 7 with a vertical line having coorinates x_i, x_j.

We now ask if under the above circumstances there is also a minimum value of m. This question is of interest to the mathematician although the engineer never tries to maximize the fuel. Since there is an upper limit on the fuel-flow rate the minimum could not be below m_3 (as defined for Fig. 6). There are of course trajectories that reach the point x_i, x_j, and m_3 at the given final time although their θ time-histories are not unique. Therefore, for the sake of mathematical completeness, we close the surface with a portion of the plane $m = m_3$.

The upper point and lower edge of the surface of Fig. 7 are the result of the restrictions on the range of the control variable T. There is a sub-family of λ vectors associated with each corner point. Each vector in the sub-family associated with a point on the lower edge lies in the vertical plane that is normal to the edge.

Staging with Thrust On

We will assume that staging occurs as soon as a given amount of fuel has been consumed - that is, when the trajectory plotted in state variable space intersects the $m = \bar{m}$ hyperplane. The time (t_A) at which this occurs will vary with the $T(t)$ history. The only state variable to be incremented at staging is mass. The parameters T_u, T_ℓ, and c may also change. Writing the discontinuity relations explicitly we have

$$m(t_A) - \bar{m} = 0$$

$$x_i(t_A') - x_i(t_A) = 0 \qquad i = 1, \ldots, n-1$$

$$m(t_A') - m(t_A) + \Delta m = 0$$

This is precisely the form treated in the previous section. We therefore know that staging does not affect the multipliers $\lambda_i (i = 1, \ldots, n-1)$ and that λ_m must be incremented so that the Hamiltonian is continuous

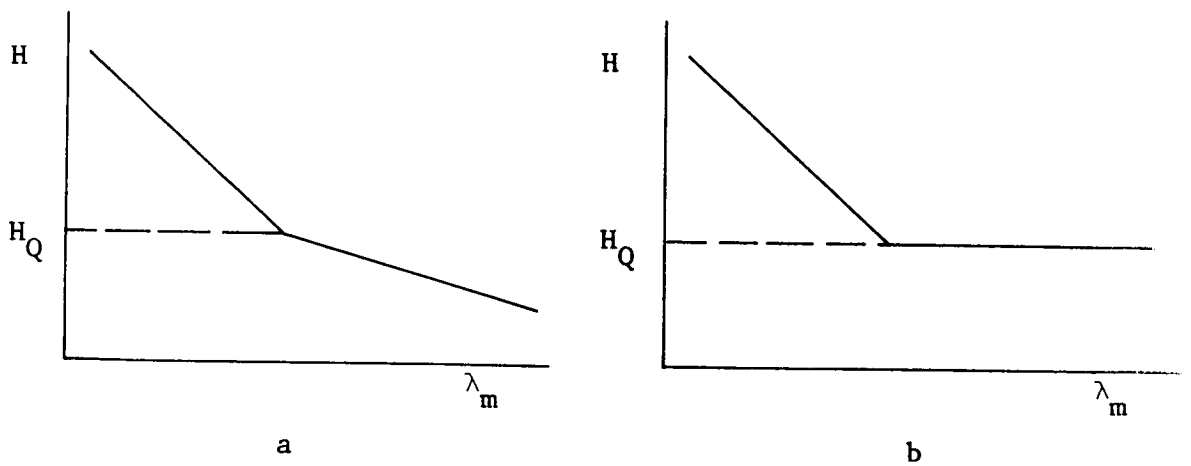

Fig. 8 The Hamiltonian vs. λ_m for the Rocket Problem

Fig. 8a shows H as a function of λ_m for the case $T_\ell > 0$. We see that a value of λ_m exists for every H and that the value λ_m must take on after staging to make H continuous is always uniquely determined.

It is interesting to note that staging can not induce a change in the thrust from its upper to its lower level (or vice versa). This conclusion follows from the fact that the discontinuous terms (m and λ_m) do not appear in H_Q (cf. Eq. 13). Therefore the quantities H, H_Q, $H - H_Q = QT$, and the sign of Q are all continuous.

If $T(t_A) > 0$ the expression for λ_m after staging is

$$\lambda_m(t_A') \equiv \mu_m(t_A') = \frac{c(t_A')}{T(t_A')} \left[\frac{T(t_A')}{m(t_A')} (\lambda_1^2 + \lambda_2^2) - Q(t_A)\, T(t_A) \right] \quad (15)$$

Staging with Thrust Off

In Fig. 8b T_ℓ equals zero. When staging occurs with $H > H_Q$ ($Q > 0$ and thrust on), everything is well behaved and there is no difficulty in drawing all conclusions of the $T_\ell > 0$ case. However, suppose $H = H_Q$ ($Q = 0$) at precisely the time that the trajectory reaches the $\overline{m}$ hyperplane. The trajectory will then move on this hyperplane during its thrust-off period. Each point during this period qualifies as the staging point. Two questions arise. (1) How is the succeeding motion affected by the choice of the staging point? (2) How should $\mu_m(t_A')$ be chosen since it is not determined by Fig. 8b?

Let us define trajectory A as the one for which staging does not occur until the end of the coasting period. During this period $\dot{m}$ and $\dot{\lambda}_m$ are zero and Q is negative. From Eq. 14 $(\lambda_1^2 + \lambda_2^2)^{\frac{1}{2}}$ must decrease to a minimum and then increase until Q is again zero. $(\lambda_1^2 + \lambda_2^2)^{\frac{1}{2}}$ will have identical values at the start and finish of the coasting period.

Let us move along points with $Q > 0$ of the $t = t_A$ transversal surface until trajectory A is reached. We have said that QT is continuous at staging. Therefore as trajectory A is approached and $Q(t_A)$ goes to zero $Q(t_A')$ will also go to zero. Question 2 is therefore answered for trajectory A by stating that $\mu_m(t_A')$ must be chosen so that $Q(t_A')$ is zero.

Let us define trajectory B as the one for which staging occurs as soon as the $m = \bar{m}$ hyperplane is reached. Using the above argument we see again that λ_m must be incremented so that $Q = 0$ after staging. It also follows from the above discussion about the terms that appear in Eq. 14 that the value λ_m takes on after staging on trajectory A equals the value λ_m had after staging on trajectory B (Fig. 9).

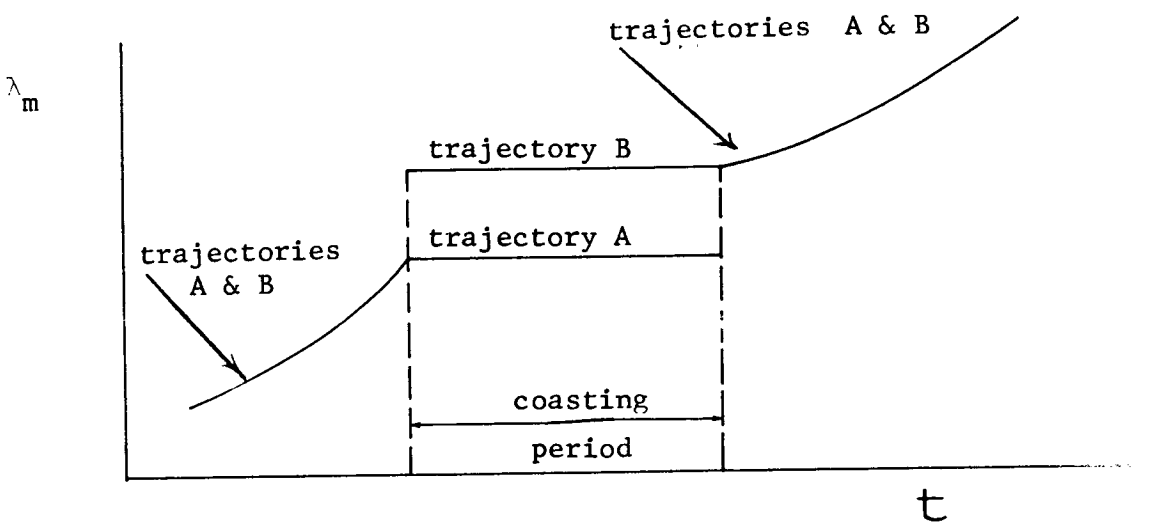

Fig. 9 . λ_m vs. Time for Staging at the Switching Points

After staging, trajectory B lies on the wavefront. We will assume that in order to remain on the wavefront it must coast on the $m = \bar{m} - \Delta m$ hyperplane. We will show that this assumption does not lead to a contradiction.

The position and velocity of the rocket during coasting are not affected by the value of the mass. Therefore, during coasting the differential equations for the Lagrange multipliers (except λ_m) are independent not only of λ_m but also of the mass. Therefore, the characteristics of Q for trajectory B will be identical to those of trajectory A. Q will become negative immediately after the staging and will return to zero at the same time as the Q for trajectory A. This behavior of Q is in agreement with the assumption that coasting will occur.

To summarize - during the coasting the state variables and mulitpliers (except for m and λ_m) are the same for trajectories A and B. After the staging for trajectory A the trajectories are completely identical.

Let us define trajectory C as representative of those for which staging occurs at an intermediate coasting point. After staging the mass as well as the other state variables will have values identical to those of trajectory B . This means that the wavefront defined on the hyperplane $m = \bar{m} - \Delta m$ by trajectory B without regard to trajectory C is valid even after trajectory C is taken into account. After the staging for trajectory C, λ_m must be incremented so that λ is normal to the existing wavefront. This means that λ_m must take on the value it has on trajectory B and that trajectories B and C will thereafter be identical.

We note that Eq. 15 cannot be used to calculate λ_m for trajectory C because $T(t_A) = T(t_A') = 0$. However, we have demonstrated that trajectories A, B, and C are identical after the staging for trajectory A. Since we know how to treat trajectories A and B, trajectory C can be ignored.

Continual Burning Before Staging

In this section we consider those trajectories that lie along the bottom edge of the transversal surface (Fig. 7). Q must be non-negative and must have been non-negative at all earlier times. As mentioned above there is a sub-family of λ vectors associated with each trajectory (Fig. 7). The subfamily is bounded by vectors normal to the bottom and lateral side of the transversal surface. After staging there will continue to be a sub-family of λ vectors that transfer each trajectory to the wavefront and therefore the latter will continue to possess an edge.

We will show that when any λ of the pre-staging sub-family has been incremented so that H is continuous (i.e., using Eq. 15), it will be included in the post-staging sub-family. To do this we scale the vectors of both sub-families so that their elements except for λ_m equal those of the vector under consideration. The values of λ_m in both sub-families now run from finite upper values (given by the vectors normal to the lateral sides) to minus infinity (for the vectors normal to the bottoms).

The two vectors normal to the lateral side are related by Eq. 15. If we replace $Q(t_A)$ using Eq. 14 we see that $\lambda_m(t_A')$ varies directly with $\lambda_m(t_A)$. Therefore, as $\lambda_m(t_A)$ is varied from its upper limit to minus infinity $\lambda_m(t_A')$ takes on the values of the post-staging sub-family - Q. E. D.

Next we show that if λ_m is incremented so that H is continuous, there will be a one-to-one correspondence between the vectors of the sub-families for points before and after staging. That is, if two vectors have distinct directions before staging they will continue to have distinct directions after staging regardless of how they are scaled. This property is of value when a search procedure is used to find the particular initial λ vector determining the trajectory that meets specified terminal conditions.

We consider the vectors λ and λ' of the sub-family corresponding to a point at t_A. They obey the following relations - $\lambda_i = k_1 \lambda_i'$ $(i = 1, \ldots, n - 1)$; $\lambda_m = k_2 \lambda'_m$. To make the Hamiltonians continuous we have

$$\sum_{i=1}^{n-1} \lambda_i f_i + \lambda_m f_m = \sum_{i=1}^{n-1} \lambda_i g_i + \mu_m g_m \qquad (16)$$

$$\sum_{i=1}^{n-1} k_1 \lambda_i f_i + k_2 \lambda_m f_m = \sum_{i=1}^{n-1} k_1 \lambda_i g_i + k_3 \mu_m g_m \qquad (17)$$

The vectors will have the same direction after staging if $k_3 = k_1$. Multiplying Eq. 16 by k_1 and subtracting from Eq. 17, we have

$$(k_2 - k_1) \lambda_m f_m = (k_3 - k_1) \mu_m g_m$$

k_3 will equal k_1 only when $k_2 = k_1$. But this contradicts our assumption that the vectors had different directions before staging.

Therefore the procedure derived by the method of adjoined discontinuity relations should be applied not only to trajectories on the lateral side on the transversal but also to trajectories on the bottom edge.

Low T/m after Staging

We have said that the mathematically complete extremal family should include trajectories that end on the horizontal bottom (excluding the edge) of the transversal surface. They are without value for the engineer since there other extremals that attain the same values the time and x_i ($i = 1, \ldots, n - 1$) but with less fuel.

In multistage rocket flight it is possible to find similar valueless trajectories that terminate not on the bottom but on the lateral side. This situation is illustrated by Fig. 10 which shows a wavefront projection similar to that of Fig. 7. The circumstances described above arise because a vertical line that intersects the lateral side with $m < \bar{m} - \Delta m$ will intersect again with $m > \bar{m}$.

The situation is characterized by $\lambda_m < 0$. From Eq. 15 we see that λ_m will take on a negative value when the T/m after staging is low. In engineering terms the first stage so far outperforms the second that the latter should never be used. Thus engineers should reject those trajectories that lie on the lateral side of the transversal (i.e., those that have undergone a switch in the thrust level) and have $\lambda_m < 0$.

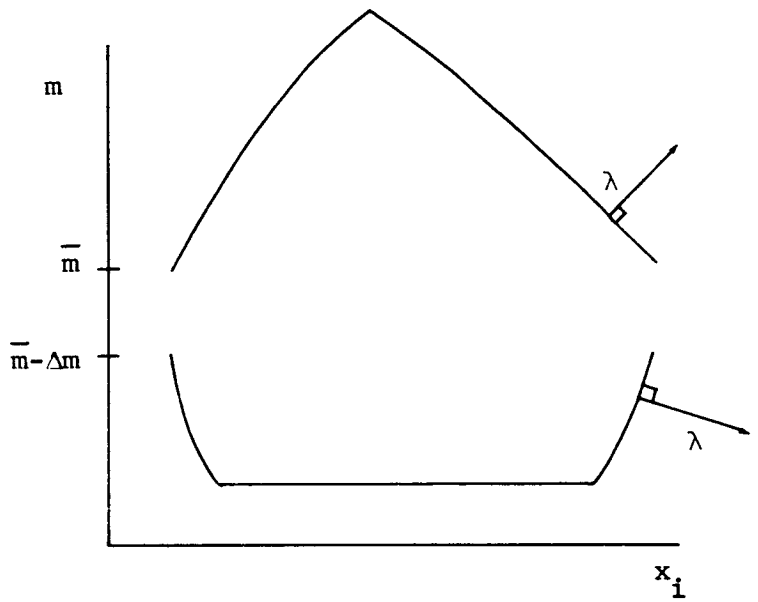

Fig. 10 Transversal Surface with Low T/m After Staging

Unfortunately this test cannot be applied directly to trajectories that lie on the bottom edge of the transversal. It is necessary to compute a neighboring trajectory that possesses a very short coasting period and then apply the test.

In this section we have seen the advantage of looking at a problem in the large. Our result could not have been obtained if we had restricted ourselves entirely to the method of adjoined discontinuity relations.

CONCLUSIONS

Two methods of treating discontinuous variational problems have been presented. The advantages of the wavelet-wavefront method are that the problem is viewed in the large and that it is easily comprehended by the student. The advantage of the method of adjoined discontinuity relations is in flexiability.

We have reached the following conclusions regarding optimal multistage rocket flight:

At staging the $\lambda_i (i = 1, \ldots, n - 1)$ are continuous but λ_m should be incremented to make the Hamiltonian continuous.

Staging never induces a simultaneous switching of the thrust level.

When the lower thrust level is at zero, staging at either a switching point or an intermediate coasting point will result in the same restart time and subsequent motion.

Trajectories that have undergone a switch in the thrust level and have the final $\lambda_m < 0$ are not fuel-optimal.

ACKNOWLEDGMENTS

This research was sponsored by USAF Office of Scientific Research under Contract AF 49(638)-1207 and under NASA Contract NAS 8-1549 with the Aeroballistics Division of the Marshall Space Flight Center, Huntsville Alabama.

REFERENCES

1. Cicala, P., An Engineering Approach to the Calculus of Variations, Levrotto-Bella, Torino, Italy, 1959.

2. Courant, R., and Hilbert, D., Methods of Mathematical Physics, Vol. I, Interscience Publishers, New York, 1953.

3. Flugge-Lotz, I, and Halkin, H., Pontryagin's Maximum Principle and Optimal Control, Stanford University Department of Engineering Mechanics, Technical Report No. 130, September 15, 1961.

REPUBLIC AVIATION CORPORATION

DIFFERENTIAL CORRECTION SCHEME FOR THE CALCULUS OF VARIATIONS

by

George N. Nomicos

Farmingdale, L. I., N. Y.

SUMMARY

A differential correction scheme is developed for the improvement of the approximate initial values of the adjoint variables so that an integral functional satisfying desired boundary conditions is optimized. The adjoint variables satisfy a system of equations that are developed by applying the classical methods of the calculus of variations, properly extended, or Pontryagin's maximum principle. Approximate initial values for the adjoint variables are assumed.

A general transition matrix is derived for the variations of the end conditions caused by the variations of the initial values of the adjoint variables, including the variations of the thrusting program and of the final time of the nominal optimum trajectory. An iteration scheme also is discussed for the convergence of the differential corrections to the desired end conditions.

LIST OF SYMBOLS

a	Semimajor axis of Kepler orbit
c	Gas exhaust velocity
E	Eccentric anomaly
$\underline{e}$	Unit vector along the thrust direction
$F(t)$	Partials of the vector functions $\underline{f}$ and $\underline{g}$ with respect to the vectors of state variables $\underline{x}$ and adjoint variables $\underline{y}$
$f_o(\underline{x},\underline{u})$	Integral functional to be optimized
$\underline{f}(\underline{x},\underline{u})$	Vector function of state variables (n-dimensional)
$\underline{f}(\underline{x},\underline{u},\underline{y})$	General form of vector state variables
$f, g, \dot{f}, \dot{g}$	Scalar functions relating position and velocity vectors a time t with initial position and velocity vectors for the Kepler problem
$\underline{g}(\underline{x},\underline{u},\underline{y})$	General form of vector adjoint variables
$\mathcal{H}(\underline{x},\underline{u},\underline{y})$	Hamiltonian
$\underline{H}$	Angular momentum vector $\underline{R} \times \dot{\underline{R}}$
h	Magnitude of angular momentum
$m(t)$	Mass of space vehicle
N	Number of switchings of thrusting program
n	Mean motion
$\underline{R}$	Position vector of the vehicle
$\dot{\underline{R}}$	Velocity vector of the vehicle
$P(t)$	Transformation of variations of conventional state variables to those of the orbit parameters

$\underline{r}$	General vector of state and adjoint variables
r	Magnitude of position vector
$S(t)$	Switching function for engine, "on" or "off"
T	Final time
t	Time
$\underline{u}(t)$	Control function of time
U	Control region (independent of time)
$\underline{V}$	Velocity vector of vehicle
v	Magnitude of velocity vector
$X_{x,y}(T, t_o)$	Transition matrix of the partials $\frac{\partial \underline{x}(T)}{\partial \underline{x}(t_o)}$ and $\frac{\partial \underline{x}(T)}{\partial \underline{y}(t_o)}$
$x_o(T)$	Integral to be optimized
$\underline{x}(t)$	State vector variables (n-dimensional)
$\underset{\sim}{x}(t)$	Augmented state vector $(x_o, \underline{x})$
$\underline{y}(t)$	Vector of adjoint variables (n-dimensional)
$\underset{\sim}{y}(t)$	Augmented vector of adjoint variables $(y_o, \underline{y})$
$Y_{x,y}(T, t_o)$	Transition matrix of the partials $\frac{\partial \underline{y}(T)}{\partial \underline{x}(t_o)}$ and $\frac{\partial \underline{y}(T)}{\partial \underline{y}(t_o)}$ respectivly

GREEK LETTERS

$\underline{\alpha}(t)$	Set of orbit parameters
$[\Gamma(T, t_o)]$	General transition matrix of $\frac{\partial \underline{x}(T)}{\partial \underline{y}(t_o)}$ including the optimum change of thrusting program
$[\hat{\Gamma}]$	The first six rows of the general transition matrix $[\Gamma]$
Γ_7	The last row of the general transition matrix $[\Gamma]$
$\delta \dot{\underline{x}}(t_j)$	$\lim_{\epsilon \to o} [\dot{\underline{x}}(t_j - \epsilon) - \dot{\underline{x}}(t_j + \epsilon)]$ at time t_j of change of thrusting program
$\delta \dot{\underline{y}}(t_j)$	$\lim_{\epsilon \to o} [\dot{\underline{y}}(t_j - \epsilon) - \dot{\underline{y}}(t_j + \epsilon)]$ at time t_j of change of thrusting program
δ_{ij}	Kroneker's delta
$\Delta \underline{\alpha}(t)$	Variation of the set of orbit parameters

$\Delta\underline{h}(t)$	Variation of the general vector of state and adjoint variables due to the control vector change $\Delta\underline{u}$
$\Delta\underline{f}(t)$	Variation of the vector function of the state variables due to control vector change $\Delta\underline{u}$
$\Delta\underline{g}(t)$	Variation of the vector function of the adjoint variables due to the control vector change $\Delta\underline{u}$
$\Delta\underline{r}(t)$	Variation of the general vector of state and adjoint variables
$\Delta S(t)$	Variation of the switching function S(t)
ΔT	Variation of the final time T
θ	Eccentric anomaly measured from initial position
$\underline{\lambda}$	Vector of adjoint variables (y_4, y_5, y_6)
μ	Gravitational constant times mass of the attracting body
$\underline{\nu}$	Vector of adjoint variables (y_1, y_2, y_3)
$\Phi(t, t_o)$	Transition matrix relating variations of the state variables $\underline{x}$ and the adjoint variables $\underline{y}$ at time t with those at t_o
$\Psi(t, t_o)$	Transition matrix of the set of orbit parameters
$[\Omega]$	General transition matrix of $\frac{\partial \underline{y}(T)}{\partial \underline{y}(t_o)}$ including the optimum change of the thrusting program
$[\hat{\Omega}]$	The first six rows of the general transition matrix $[\Omega]$
Ω_7	The last row of the general transition matrix $[\Omega]$

SUBSCRIPTS

i, j	Components
o	Initial value of time t_o

SUPERSCRIPTS

$\bullet$	Differentiation wrt time
T	Transpose of a matrix
$\hat{}$	Vector or matrix reduced to six rows
-1	Inverse of a matrix

INTRODUCTION

In the problems of the calculus of variations, a system of partial differential equations must be solved with specified boundary conditions. In addition to the state and control variables that appear in the equations of motion, the inequalities of constraints, and the functional that should be optimized, there is a number of adjoint variables that satisfy additional equations for the optimization of the given system. These equations are derived by the application of the classical methods of the calculus of variations, properly extended, or from Pontryagin's maximum principle [1], [2].

When some approximate values of the adjoint variables at the initial time t_o have been calculated, then, by numerical integration of the above systems of equations, an optimal solution is obtained that does not satisfy the desired end conditions. In this paper, a differential correction scheme is developed that will improve the approximate initial values of the adjoint variables so that the optimal solution will satisfy the desired end conditions. A general transition matrix is derived for the variations of the end conditions caused by the variations of the initial values of the adjoint variables, including the variations of the thrusting program of the nominal optimum trajectory and the variation of the final time. An iteration scheme also is presented for the convergence of the improved values of the adjoint variables to those of the optimum solution.

First, the general equations of the state variables, used mostly as constraints, are given, together with the equations of the adjoint variables. Second, the variational equations for the above systems of equations are derived, and an application to the problem of minimizing the fuel of a space vehicle flying between two given boundary points is given as an example. Third, a differential correction scheme is derived for the improvement of the approximate initial values of the adjoint variables, and an iteration scheme is presented for the convergence of the improved values of the adjoint variables, so that the optimum solution will satisfy the desired end conditions. Finally, conclusions and recommendations are presented for the application of this scheme to the actual flight of space vehicles.

FUNDAMENTAL SYSTEM OF EQUATIONS

State Variables

The motion of a vehicle is characterized by the vector variable $\underline{x}(t)$ belonging to the vector space W at any instant of time t. It is assumed that this motion is controlled by a control vector $\underline{u}(t)$.

The fundamental system of equations of state variables is given by

$$\dot{x}_i(t) = f_i(\underline{x}(t), \underline{u}(t)) \qquad (i = 1, 2, \ldots n) \tag{1}$$

where $\underline{x}(t)$ is an n-dimensional piecewise differentiable state vector, and $\underline{u}(t)$ is an r-dimensional piecewise continuous control vector belonging to an arbitrary control region U that is independent of time. The functions f_i are defined for $\underline{x} \in W$ and for $\underline{u} \in U$ and are assumed to be continuous in the variables $\underline{x}(t)$ and $\underline{u}(t)$ and continuously differentiable with respect to $\underline{x}(t)$. For a certain admissible control $\underline{u}(t)$, the motion of the vehicle $\underline{x}(t)$ is uniquely determined.

The integral functional to be optimized is

$$x_o(T) = \int_{t_o}^{T} f_o(\underline{x}(t), \underline{u}(t))dt \tag{2}$$

The necessary conditions for the optimum control vector $\underline{u}(t)$ of Eq.(2) are formulated for fixed boundary conditions of the state variables $\underline{x}(t_o)$ and $\underline{x}(T)$ and for free end time T.

Adjoint Variables

For the optimum solution of Eq. (2), another system of equations is considered. This system is linear and homogeneous in the adjoint variables $\underline{y}(t) = (y_o, y_1, \ldots y_n) = (y_o, \underline{y})$ which is an (n+1)-dimensional continuous vector, and is given by

$$\dot{y}_i(t) = -\sum_{j=0}^{n} \frac{\partial f_j(\underline{x}(t), \underline{u}(t))}{\partial x_i} y_j(t) \qquad (i = 0, 1, \ldots n) \tag{3}$$

The Hamiltonian $\mathcal{H}(\underset{\sim}{x}(t), \underline{u}(t), \underset{\sim}{y}(t))$ is defined by

$$\mathcal{H}(\underset{\sim}{x}, \underline{u}, \underset{\sim}{y}) = \sum_{i=0}^{n} y_i(t) f_i(\underline{x}(t), \underline{u}(t)) \tag{4}$$

and the systems of Eqs. (1), (2), and (3) correspond to the Hamiltonian system

$$\begin{aligned} \dot{x}_i(t) &= \frac{\partial \mathcal{H}}{\partial y_i} \\ \dot{y}_i(t) &= \frac{-\partial \mathcal{H}}{\partial x_i} \end{aligned} \tag{5}$$

Pontryagin's maximum principle and transversality condition give, for optimal $x_o(T)$, the function $\mathcal{H}(\underset{\sim}{x}(t), \underline{u}(t), \underset{\sim}{y}(t))$ of $\underline{u}(t)$ belonging to U attains its maximum at the point $\underline{u}(t)$, i.e.

$$\begin{aligned} &\mathcal{H}(\underset{\sim}{x}(t), \underline{u}(t), \underset{\sim}{y}(t)) = \sup_{\underline{u} \in U} \mathcal{H}(\underset{\sim}{x}(t), \underline{u}(t), \underset{\sim}{y}(t)) = 0 \\ &y_o(t_o) \leq 0 \quad \text{and} \quad y_k(T) = 0 \end{aligned} \tag{6}$$

where the subscript k corresponds to the subscript of the state variables for which the terminal value $x_k(T)$ is free. For most of the engineering applications, we have $y_o \neq 0$, which is normalized to $y_o = -1$.

The Lagrangian multipliers $\underset{\sim}{\overset{(L)}{\lambda}}(t)$ of the classical calculus of variations are related to the adjoint variables $\underset{\sim}{y}(t)$ by the relationship

$$\underset{i \neq 0}{\overset{(L)}{\lambda_i}}(t) = \frac{\partial f_o(\underline{x}(t), \dot{\underline{x}}(t), \underline{u}(t))}{\partial \dot{x}_i} y_o(t) + y_i(t) \tag{7}$$

If the time t appears explicitly in the system of functions f or f_o, then it always can be transformed to an autonomous system by introducing an auxiliary state variable that is defined by

$$\dot{x}_{n+1}(t_o) = 1 \qquad \text{with} \qquad x_{n+1}(t_o) = t_o \tag{8}$$

Example

For a space vehicle powered by a throttled engine and flying in the gravitational field of only one attracting body, the system of equations of the state variables, i.e., Eq. (1), reduces to

$$\begin{aligned} \dot{\underline{R}} &= \underline{V} && f_1, f_2, f_3 \\ \dot{\underline{V}} &= -\frac{\mu}{r^3}\underline{R} + \frac{u(t)}{m}\underline{e} && f_4, f_5, f_6 \\ \dot{m} &= -\frac{u(t)}{c} && f_7 \end{aligned} \tag{9}$$

where $\underline{e}$ is a unit vector in the direction of the thrust, and $u(t)$ is the control variable belonging to the range $0 \le u(t) \le K$.

For minimizing the fuel between $\underline{x}(t_o)$ and $\underline{x}(T)$ with free end time, the integral functional to be optimized, i.e., Eq. (2), becomes

$$x_o(T) = \int_{t_o}^{T} f_o(\underline{x}(t), u(t))\,dt \tag{10}$$

with $f_o = -\dot{m} = \frac{u(t)}{c}$.

The system of the adjoint variables, i.e., Eq. (3), reduces to

$$\begin{aligned} \dot{y}_o(t) &= 0 && \\ \dot{\underline{\nu}}(t) &= \frac{\mu}{r^3}\underline{\lambda} - 3\mu\frac{\underline{R}\cdot\underline{\lambda}}{r^5}\underline{R} && \underline{\nu} = \begin{bmatrix} y_1 \\ y_2 \\ y_3 \end{bmatrix} \\ \dot{\underline{\lambda}}(t) &= -\underline{\nu} && \\ \dot{y}_7(t) &= \frac{u(t)}{m^2}(\underline{\lambda}\cdot\underline{e}) && \underline{\lambda} = \begin{bmatrix} y_4 \\ y_5 \\ y_6 \end{bmatrix} \end{aligned} \tag{11}$$

The maximum principle and the transversality conditions of Eq. (6) become

$$\mathcal{H} = \sup_{u \in U} \mathcal{H} = y_o f_o + \underline{\nu} \cdot \underline{V} + \underline{\lambda} \cdot \left(\frac{\mu}{r^3}\underline{R} + \frac{u(t)}{m}\underline{e}\right) - y_7 \frac{u(t)}{c} = 0$$

$$y_o(t) = -1 \qquad \text{and} \qquad y_7(T) = 0 \tag{12}$$

where $f_o = \frac{u(t)}{c}$.

From Eq. (1), it is obvious that $\underline{\lambda} // \underline{e}$ and that the switching function for $u = 0$ or $u = K$ is defined by

$$S(t) = \frac{|\lambda|}{m} - \frac{y_7 - y_o}{c} \gtrless 0 \tag{13}$$

when $u(t) = \begin{cases} K \text{ (max)} \\ 0 \text{ (min)} \end{cases}$ respectively.

VARIATIONAL EQUATIONS

In this section, the variational equations of the optimum trajectory of a space vehicle are derived. The formulation of these equations is required for the application of the differential correction scheme that is developed in the next section.

The application of Pontryagin's maximum principle for the solution of optimal problems yields additional information for the synthesis of optimal controls. Making use of this principle, the system of Eqs. (1) and (3) may be rewritten in the following general form.

$$\dot{\underline{r}}(t) \equiv \begin{bmatrix} \dot{\underline{x}}(t) \\ \dot{\underline{y}}(t) \end{bmatrix} = \begin{bmatrix} \underline{f}(\underline{x}, \underline{y}, \underline{u}) \\ \underline{g}(\underline{x}, \underline{y}, \underline{u}) \end{bmatrix} \tag{14}$$

The variations of this system are obtained by

$$\Delta\dot{\underline{r}}(t) = F(t)\,\Delta\underline{r}(t) + \Delta\underline{h}(t) \tag{15}$$

where the matrix $F(t)$ and the vector $\Delta\underline{h}(t)$ are given by

$$F(t) = \begin{bmatrix} \dfrac{\partial \underline{f}}{\partial \underline{x}} & \dfrac{\partial \underline{f}}{\partial \underline{y}} \\ \dfrac{\partial \underline{g}}{\partial \underline{x}} & \dfrac{\partial \underline{g}}{\partial \underline{y}} \end{bmatrix}$$

$$\Delta\underline{h}(t) = \begin{bmatrix} \Delta\underline{f} \\ \Delta\underline{g} \end{bmatrix} = \begin{bmatrix} \underline{f}(\underline{u} + \Delta\underline{u}) - \underline{f}(\underline{u}) \\ \underline{g}(\underline{u} + \Delta\underline{u}) - \underline{g}(\underline{u}) \end{bmatrix} \tag{16}$$

Transition Matrix

The fundamental solution matrix for the homogeneous part of Eq. (15), i.e.,

$$\dot{\Phi}(t) = F(t)\,\Phi(t)$$

with initial conditions $\Phi(t_o, t_o) = I$ (unit matrix), is the transition matrix $\Phi(t, t_o)$ of the system. From the properties of the fundamental solution matrix and the transition matrix $\Phi(t, t_o)$, we obtain

$$\Delta\underline{r}(t) = \Phi(t, t_o)\,\Delta\underline{r}(t_o) + \int_{t_o}^{t} \Phi(t, \tau)\,\Delta\underline{h}(\tau)\,d\tau \tag{17}$$

which is the solution of the non-homogeneous Eq. (15).

In the example of the powered space vehicle flying in the gravitational field of one attracting body, Eq. (17) reduces to

$$\Delta\underline{r}(T) = \Phi(T, t_o)\,\Delta\underline{r}(t_o) + \sum_{j=1}^{N} \Phi(T, t_j)\,\Delta\underline{h}(t_j)\,\Delta t_j \tag{18}$$

where t_j is the time at which the thrusting program of the optimum nominal trajectory with the approximate values of initial conditions $\underline{r}(t_o)$ switches "on" or "off" during the time interval $t_o < t_j < T$, and $\Delta\underline{r}(T)$ gives the deviations of the nominal end conditions from the desired end conditions, i.e.

$$\Delta\underline{r}(T) = \begin{bmatrix} \Delta\underline{x}(T) \\ \Delta\underline{y}(T) \end{bmatrix}$$

$$\Phi(T, t_o) = \begin{bmatrix} \dfrac{\partial\underline{x}(T)}{\partial\underline{x}(t_o)} & \dfrac{\partial\underline{x}(T)}{\partial\underline{y}(t_o)} \\ \dfrac{\partial\underline{y}(T)}{\partial\underline{x}(t_o)} & \dfrac{\partial\underline{y}(T)}{\partial\underline{y}(t_o)} \end{bmatrix} = \begin{bmatrix} X_x(T, t_o) & X_y(T, t_o) \\ Y_x(T, t_o) & Y_y(T, t_o) \end{bmatrix} \tag{19}$$

$$\Delta\underline{h}(t_j) = \lim_{\epsilon \to 0} \begin{bmatrix} \dot{\underline{x}}(t_j - \epsilon) - \dot{\underline{x}}(t_j + \epsilon) \\ \dot{\underline{y}}(t_j - \epsilon) - \dot{\underline{y}}(t_j + \epsilon) \end{bmatrix} = - \begin{bmatrix} \delta\dot{\underline{x}}(t_j) \\ \delta\dot{\underline{y}}(t_j) \end{bmatrix}$$

Because the boundary conditions of the state variables at the initial time t_o are given, we have $\Delta\underline{x}(t_o) \equiv 0$, and Eq. (18) becomes (see Fig. 1)

$$\Delta\underline{r}(T) = \Phi(T, t_o)\, \Delta\underline{r}(t_o) - \sum_{j=1}^{N} \Phi(T, t_j)\, \delta\dot{\underline{r}}(t_j)\, \Delta t_j \tag{20}$$

or

$$\begin{bmatrix} \Delta\underline{x}(T) \\ \Delta\underline{y}(T) \end{bmatrix} = \begin{bmatrix} X_x & X_y \\ Y_x & Y_y \end{bmatrix} \begin{bmatrix} 0 \\ \Delta\underline{y}(t_o) \end{bmatrix} - \sum_{j=1}^{N} \begin{bmatrix} X_x^{(j)} & X_y^{(j)} \\ Y_x^{(j)} & Y_y^{(j)} \end{bmatrix} \begin{bmatrix} \delta\dot{\underline{x}}(t_j) \\ \delta\dot{\underline{y}}(t_j) \end{bmatrix} \Delta t_j \tag{21}$$

where $X = X(T, t_o)$, and $X^{(j)} = X(T, t_j)$.

From Eq. (21), we get

$$\Delta \underline{x}(T) = X_y \Delta \underline{y}(t_o) - \sum_{j=1}^{N} \left[X_x^{(j)} \delta \dot{\underline{x}}(t_j) + X_y^{(j)} \delta \dot{\underline{y}}(t_j) \right] \Delta t_j \tag{22}$$

and

$$\Delta \underline{y}(T) = Y_y \Delta \underline{y}(t_o) - \sum_{j=1}^{N} \left[Y_x^{(j)} \delta \dot{\underline{x}}(t_j) + Y_y^{(j)} \delta \dot{\underline{y}}(t_j) \right] \Delta t_j \tag{23}$$

Thrusting Program

In the formulation of the variational equations of the optimum nominal trajectory, the time variation Δt_j of the optimum thrusting program has been included where t_j is the time at which the thrust switches "on" or "off" and the switching function of the nominal trajectory is zero, i.e., $S(t_j) = 0$. The time variation Δt_j is calculated from the variation of the switching function $\Delta S(t_j + \Delta t_j)$ for which

$$S(t_j + \Delta t_j) + \Delta S(t_j + \Delta t_j) = 0 \tag{24}$$

From the linear expansion of Eq. (24) we get

$$\dot{S}(t_j) \Delta t_j \simeq - \frac{\partial S}{\partial \underline{r}} \Delta \underline{r}(t_j + \Delta t_j) \tag{25}$$

Because $\Delta \underline{r}(t_j + \Delta t_j) \simeq \Delta \underline{r}(t_j) + \Delta \dot{\underline{r}}(t_j) \Delta t_j$ and $\frac{\partial S}{\partial \underline{r}} \Delta \dot{\underline{r}}(t_j) = 0$, Eq. (25) becomes

$$\dot{S}(t_j) \Delta t_j \simeq - \frac{\partial S}{\partial \underline{r}} \Delta \underline{r}(t_j) \tag{26}$$

Expanding the variation $\Delta r(t_j)$ from Eq. (20), we get

$$\Delta \underline{r}(t_j) = \Phi(t_j, t_o) \Delta \underline{r}(t_o) - \sum_{i=1}^{i<j} \Phi(t_j, t_i) \delta \dot{\underline{r}}(t_i) \Delta t_i \tag{27}$$

$$\Delta t_j = \frac{-1}{\dot{S}(t_j)} \frac{\partial S(t_j)}{\partial \underline{r}(t_j)} \left[\Phi(t_j, t_o)\, \Delta \underline{r}(t_o) - \sum_{i=1}^{i<j} \Phi(t_j, t_i)\, \delta \dot{\underline{r}}(t_i)\, \Delta t_i \right] \tag{28}$$

and, in terms of the variations $\Delta \underline{y}(t_o)$, it becomes

$$\begin{aligned} \Delta t_j = & -\frac{1}{\dot{S}(t_j)} \left[\frac{\partial S(t_j)}{\partial \underline{x}(t_j)} X_y(t_j, t_o) + \frac{\partial \dot{S}(t_j)}{\partial \underline{y}(t_j)} Y_y(t_j, t_o) \right] \Delta \underline{y}(t_o) \\ & + \frac{1}{\dot{S}(t_j)} \frac{\partial S(t_j)}{\partial \underline{x}(t_j)} \sum_{i=1}^{i<j} \left[X_x(t_j, t_i)\, \delta \dot{\underline{x}}(t_i) + X_y(t_j, t_i)\, \delta \dot{\underline{y}}(t_i) \right] \Delta t_i \\ & + \frac{1}{\dot{S}(t_j)} \frac{\partial S(t_j)}{\partial \underline{y}(t_j)} \sum_{i=1}^{i<j} \left[Y_x(t_j, t_i)\, \delta \dot{\underline{x}}(t_i) + Y_y(t_j, t_i)\, \delta \dot{\underline{y}}(t_i) \right] \Delta t_i \end{aligned} \tag{29}$$

From Eq. (13) for the switching function S(t), we find that

$$\begin{aligned} S(t) &= \frac{|\lambda|}{m} - \frac{y_7 - y_o}{c} \qquad \dot{S}(t) = \frac{\underline{\lambda} \cdot \dot{\underline{\lambda}}}{m|\lambda|} \\ \frac{\partial S(t_j)}{\partial \underline{x}(t_j)} &= \left\{ 0,\ 0,\ 0,\ 0,\ 0,\ 0,\ -\frac{|\lambda|}{m^2} \right\} \\ \frac{\partial S(t_j)}{\partial \underline{y}(t_j)} &= \left\{ \frac{y_4}{m|\lambda|},\ \frac{y_5}{m|\lambda|},\ \frac{y_6}{m|\lambda|},\ 0,\ 0,\ 0,\ -\frac{1}{c} \right\} \end{aligned} \tag{30}$$

DIFFERENTIAL CORRECTION SCHEME

Correction Scheme

In this section, a differential correction scheme is developed for the improvement of the approximate initial values of the adjoint variables so that the optimum solution of the problem can be found. The variations of the nominal optimum trajectory of the space vehicle, calculated for the approximate initial values of the adjoint variables, have been derived previously.

Making use of Eqs. (17), we solve for $\Delta\underline{r}(t_o)$ if we know the variation $\Delta\underline{r}(T)$ at the terminal time T. In the example of the powered space vehicle we derived Eqs. (22) and (23) for the variations of $\Delta\underline{x}(T)$ and $\Delta\underline{y}(T)$ caused by the variations of the adjoint variables $\Delta\underline{y}(t_o)$ at the initial time t_o and the variations Δt_j at the time t_j of the thrusting program, which corresponds to the optimum nominal trajectory for the approximate adjoint variables.

Free End Time .

In the case of free end time T, a variation in the terminal time also is taken into consideration, and, making use of Eqs. (29), we find that

$$\Delta\underline{x}(T) = [\Gamma]\,\Delta\underline{y}(t_o) + \dot{\underline{x}}(T)\,\Delta T \tag{31}$$

$$\Delta\underline{y}(T) = [\Omega]\,\Delta\underline{y}(t_o) + \dot{\underline{y}}(T)\,\Delta T \tag{32}$$

Separating the seventh row of Eqs. (31) and (32), we get

$$\Delta\hat{\underline{x}}(T) = [\hat{\Gamma}]\,\Delta\underline{y}(t_o) + \dot{\hat{\underline{x}}}(T)\,\Delta T \tag{33}$$

$$\Delta y_7(T) = \Omega_7\,\Delta\underline{y}(t_o) + \dot{y}_7(T)\,\Delta T \tag{34}$$

where Eqs. (33) and (34) are of the form

$$[6\times1] = [6\times7]\,[7\times1] + [6\times1][1\times1]$$

$$[1\times1] = [1\times7]\,[7\times1] + [1\times1][1\times1]$$

respectively, $[\hat{\Gamma}]$ represents the first six rows of $[\Gamma]$, and Ω_7 represents the seventh row of $[\Omega]$.

For the solution of the system of Eqs. (33) and (34) for $\Delta\underline{y}(t_o)$ and ΔT from the deviations $\Delta\hat{\underline{x}}(T)$ and $\Delta y_7(T) = 0$, we need one more relationship, and this is obtained from Eq. (12), i.e.

$$\mathcal{H}(\underline{x}, \underline{u}, \underline{y}) = \sum_{j=1}^{7} y_j \cdot f_j(t) - f_o(t) = 0 \tag{35}$$

Taking the variation of $\mathcal{H}(t)$ at time t_o, we get

$$\sum_{j=1}^{7} f_j(t_o)\,\Delta y_j(t_o) + \sum_{j=1}^{7} y_j(t_o)\,\Delta f_j(t_o) - \Delta f_o(t_o) = 0 \tag{36}$$

Because $\Delta f_j(t_o) = 0$ and $\Delta f_o(t_o) = 0$ if the variation of the switching function $\Delta S(t_o)$ does not change the sign of $S(t_o)$, Eq. (36) becomes

$$\sum_{j=1}^{7} f_j(t_o)\,\Delta y_j(t_o) = 0 \tag{37}$$

or

$$\underline{V}(t_o) \cdot \Delta\underline{\nu}(t_o) + \ddot{\underline{R}}(t_o) \cdot \Delta\underline{\lambda}(t_o) - \frac{u(t_o)}{c}\,\Delta y_7(t_o) = 0 \tag{38}$$

Thus, combining Eqs. (33), (34), and (38), we get eight equations with eight unknown variations that are given by

$$\begin{bmatrix} \Delta\hat{\underline{x}}(T) \\ 0 \\ 0 \end{bmatrix} = \begin{bmatrix} [\hat{\Gamma}] & \dot{\hat{\underline{x}}}(T) \\ \Omega_7 & \dot{y}_7(T) \\ \dot{\underline{x}}(t_o)^T & 0 \end{bmatrix} \begin{bmatrix} \Delta\underline{y}(t_o) \\ \\ \Delta T \end{bmatrix} \tag{39}$$

Solving for $\Delta\underline{y}(t_o)$ and ΔT, we find that

$$\begin{bmatrix} \Delta\underline{y}(t_o) \\ \\ \Delta T \end{bmatrix} = \begin{bmatrix} [\hat{\Gamma}] & \dot{\hat{\underline{x}}}(T) \\ \Omega_7 & \dot{y}_7(T) \\ \dot{\underline{x}}(t_o)^T & 0 \end{bmatrix}^{-1} \begin{bmatrix} \Delta\hat{\underline{x}}(T) \\ 0 \\ 0 \end{bmatrix} \tag{40}$$

Iteration Scheme

For the calculation of the optimum trajectory of a space vehicle, the differential correction scheme described in this section is applied, and the variation of the adjoint vector $\Delta\underline{y}(t_o)$ at the initial time t_o, as well as the varia-

tion of the final time ΔT, are derived to match the desired conditions at the final time T in space. Making use of the corrected adjoint variables $\underline{y}_1(t_o) = \underline{y}(t_o) + \Delta\underline{y}(t_o)$, a new optimum nominal trajectory is computed by integrating the system of equations of the state and adjoint variables, i.e., Eqs. (9) and (11), by making use of Eq. (13) for the optimum thrusting program as described previously. Because the differential correction scheme has been derived for linear variations of highly nonlinear equations, it is expected that there still will be a discrepancy between the desired and the new computed values of the end conditions $\Delta\underline{x}_1(T_1)$, where $T_1 = T + \Delta T$.

In general, successive iterations generate corrections $\Delta\underline{y}_k(t_o)$ to the adjoint variables at time t_o from $\Delta\underline{x}_k(T_k)$ such that

$$\underline{y}_{k+1}(t_o) = \underline{y}_k(t_o) + \Delta\underline{y}_k(t_o) = \underline{y}(t_o) + \sum_{i=0}^{k} \Delta\underline{y}_i(t_o) \tag{41}$$

which, in turn, gives end conditions with deviations $\Delta\underline{x}_{k+1}(T_{k+1})$ from their desired values, and

$$T_{k+1} = T + \sum_{i=0}^{k} \Delta T_i \tag{42}$$

This iteration scheme converges to the desired end conditions of the state vector, provided that the deviations are within the linear range. Departure from the linear range will be indicated when the deviations of the computed nominal end conditions from the desired end conditions $\Delta\underline{x}_1(T_1)$ are comparable to or exceed the deviations $\Delta\underline{x}(T)$. In this case, each step of the iteration scheme described above contains a sub-iteration carried out on a parameter γ_k introduced as a factor multiplying the deviations $\Delta\underline{x}_k(T_k)$. Thus

$$\Delta\underline{x}_k^*(T_k) = \gamma_k \, \Delta\underline{x}_k(T_k) \tag{43}$$

From $\Delta\underline{x}_k^*(T_k)$, we obtain the correction $\Delta\underline{y}_k^*(t_o)$, which is added to $\underline{y}_k^*(t_o)$ for the k^{th} estimate of the adjoint variables at time t_o. The sub-iteration consists of the determination of a value of γ_k $(0 < \gamma_k \leq 1)$ such that the deviations $\Delta\underline{x}_{k+1}(T_{k+1})$ computed from the corrected adjoint variables, i.e.

$$\underline{y}_{k+1}(t_o) = \underline{y}_k(t_o) + \Delta\underline{y}_k^*(t_o) = \underline{y}(t_o) + \sum_{i=0}^{k} \Delta\underline{y}_i^*(t_o) \tag{44}$$

are comparable to or less than the deviations $\Delta\underline{x}_k(T_k)$. This procedure is continued until the linear range is reached for which $\gamma_k = 1$ and the iteration scheme converges to the desired end conditions.

It should be noted that the same procedure is followed when parameters other than the state variables are specified as end conditions. Of course, these parameters must be expressible as functions of the state variables.

CONCLUSIONS AND RECOMMENDATIONS

A differential correction has been developed for the improvement of the approximate values of the adjoint variables so that the optimal solution of the problems of the calculus of variations is obtained. The mathematical analysis for the differential correction scheme for the optimum trajectory of a space vehicle with minimum fuel consumption between fixed boundary conditions has been presented. The method developed relies on the variations of the nominal optimum trajectory of the space vehicle calculated for the approximate initial values of the adjoint variables, which are assumed to be given. Techniques for the calculation of these approximate values are not considered in this report.

A general transition matrix has been derived for the variations of the end conditions caused by the variations of the initial values of the adjoint variables, including the variations of the thrusting program of the nominal optimum trajectory and the variation of the final time. An iteration scheme also has been discussed for the convergence of the improved values of the adjoint variables to those of the optimum problem satisfying the desired end conditions. In addition, a method for the case of variations beyond the linear range has been outlined.

This program will be highly useful for the determination of optimum space missions and for optimum orbit transfer for intercept and rendezvous of space

vehicles as well as for optimum navigation and guidance of a space vehicle. Further work in this area is readily suggested. First, techniques should be developed for the approximate initial values of the adjoint variables that are used for the optimum nominal trajectory. Second, this correction scheme could be extended readily to optimum problems with more general types of end conditions than those considered in this report. Finally, a more general differential correction scheme is required for the optimum pursuit of a powered spacecraft, which would involve a statistical-control scheme for the probability law of a randomly moving point.

APPENDIX

VARIATIONAL PARAMETERS

For the calculation of variations of the optimum space trajectories, there is a general matrix introduced that relates the variations of the state and adjoint variables at time t to those at time t_o. This matrix, called the general transition matrix, requires the computation of the partial derivatives of the state and adjoint variables at two different times, i.e., t_o and T, and relates their linear variations at these times, including the optimum changes of the thrusting program.

When the thrust is "off," the system of equations for the adjoint variables is "adjoint" to the system of equations for the variations of the state variables, which, in this case, is homogeneous, and the transition matrix of the state variables is used for the calculations of the adjoint variables during the coasting intervals of time, i.e., $t_i<t<t_{i+1}$. In this case, the transition matrix of the state variables $\hat{X}(t_{i+1}, t_i)$ is found from the corresponding Kepler problem, and it is expressed in closed form from the solution of this problem.

The variations of the state variables and the values of the adjoint variables for the coasting interval are given by [3].

$$\Delta\underline{\hat{x}}(t_{i+1}) = \hat{X}(t_{i+1}, t_i)\, \Delta\underline{\hat{x}}(t_i)$$

$$\underline{\hat{y}}(t_{i+1}) = \left[\hat{X}^T(t_{i+1}, t_i)\right]^{-1} \underline{\hat{y}}(t_i) \tag{45}$$

where

$$\underline{\hat{x}}(t)^T = (x_1, x_2, x_3, x_4, x_5, x_6)$$

$$\underline{\hat{y}}(t)^T = (y_1, y_2, y_3, y_4, y_5, y_6) \tag{46}$$

and

$$\hat{X}(t_{i+1}, t_i) = \frac{\partial\underline{\hat{x}}(t_{i+1})}{\partial\underline{\hat{x}}(t_i)} \tag{47}$$

The use of the conventional state variables $\underline{\hat{x}}(t)$, which are position and velocity vectors $\underline{R}$ and $\dot{\underline{R}}$ in cartesian coordinates, has the disadvantage that all of their elements have secular terms that vary rapidly with time. If, instead of the conventional state variables, other parameters are used as state variables, the resultant matrix might be simplified considerably. For example, consider the following parameters and their variations:

$\Delta\alpha_1$	Rotation of $\underline{R}$ about $\dot{\underline{R}}$
$\Delta\alpha_2$	Rotation of $\dot{\underline{R}}$ about $\underline{R}$
$\Delta\alpha_3$	Rotation of both $\underline{R}$ and $\dot{\underline{R}}$ about $\underline{H}$
$\Delta\alpha_4$	Change in cos $(\underline{R}, \dot{\underline{R}})$, keeping v and $\underline{R}$ constant
$\Delta\alpha_5$	Relative change in the semimajor axis $\Delta a/a$, keeping $\underline{R}$ and $\dot{\underline{R}}/v$ constant
$\Delta\alpha_6$	Relative change in the magnitude of the position vector $(\Delta r/r)$, keeping $\underline{R}/r$ and $\dot{\underline{R}}/v$ constant.

The transition matrix corresponding to the above parameters, i.e.

$$\Delta\underline{\alpha}(t) = \Psi(t, t_o)\, \Delta\underline{\alpha}(t_o) \tag{48}$$

$$\Psi(t,t_o) = \begin{bmatrix} \frac{fv}{v_o} & \frac{-gv}{r_o} & 0 & 0 & 0 & 0 \\ \frac{-\dot{f}r}{v_o} & \frac{\dot{g}r}{r_o} & 0 & 0 & 0 & 0 \\ 0 & 0 & 1 & \frac{\partial\alpha_3}{\partial\alpha_{40}} & \frac{\partial\alpha_3}{\partial\alpha_{50}} & \frac{\partial\alpha_3}{\partial\alpha_{60}} \\ 0 & 0 & 0 & \frac{\partial\alpha_4}{\partial\alpha_{40}} & \frac{\partial\alpha_4}{\partial\alpha_{50}} & \frac{\partial\alpha_4}{\partial\alpha_{60}} \\ 0 & 0 & 0 & 0 & 1 & 0 \\ 0 & 0 & 0 & \frac{r_o v_o g}{r^2} & \frac{\partial\alpha_6}{\partial\alpha_{50}} & \frac{\partial\alpha_6}{\partial\alpha_{60}} \end{bmatrix} \tag{49}$$

where some of the non-zero elements are listed as partials of the orbital parameters and are given by Ref. [4] as

$$\frac{\partial\alpha_3}{\partial\alpha_{40}} = -\frac{r_o v_o}{r^2} g\left[\frac{r_o v_o}{h}\left(\frac{v_o g}{r_o} + f\alpha_{40}\right) + \frac{rh}{\mu g}\left(f-1\right)\left(\dot{g}-1\right)\right]$$

$$\frac{\partial\alpha_3}{\partial\alpha_{50}} = \frac{h}{r^2}\left[\frac{\mu}{v_o^2 r_o} g - \frac{3}{2}(t-t_o) - 3f\left(g-(t-t_o)\right) + (f-1)\frac{r_o}{v_o}\left(\alpha_{40} - \frac{rv}{r_o v_o}\alpha_4\right)\right] \tag{51}$$

$$\frac{\partial\alpha_3}{\partial\alpha_{60}} = \frac{h}{r^2}\left[fg\left(1 - \frac{\mu}{r_o v_o^2}\right) - 2g + (f-1)^2 \frac{r_o}{v_o}\alpha_{40}\right] \tag{52}$$

$$\frac{\partial\alpha_4}{\partial\alpha_{40}} = \frac{r_o v_o}{rv}\left[\dot{g} - \frac{\mu\alpha_4}{r^2 v}\left(1-\frac{r}{a}\right) g\right] \tag{53}$$

$$\frac{\partial\alpha_4}{\partial\alpha_{50}} = \frac{\mu}{rv^2}\left[\left(1-\frac{r}{a}\right)\left\{\alpha_4\left(f\frac{r_o}{v_o}\alpha_{40} + \dot{g}\right) - \frac{3v(t-t_o)}{2r}\left(1-\alpha_4^2\right)\right\} - \frac{v}{v_o}\left(1-\frac{r_o}{a}\right)\alpha_{40}\right.$$
$$\left. + \frac{v}{r}\left\{1-\left(1-\frac{r}{a}\right)\alpha_4^2\right\}\left\{\frac{\mu}{v_o^2 r_o} g - \frac{r_o}{v_o}\left(\alpha_{40} - \frac{rv}{r_o v_o}\alpha_4\right\}\right\}\right] \tag{54}$$

$$\frac{\partial \alpha_4}{\partial \alpha_{60}} = \frac{\mu}{rv^2}\left[\frac{v}{v_o}\left(1-\frac{r_o}{a}\right)\alpha_{40} - \frac{v}{r}\left\{1-\alpha_4{}^2\left(1-\frac{r}{a}\right)\right\}\left\{g+\frac{r_o}{v_o}(f-1)\alpha_{40}\right\}\right.$$

$$\left. - \frac{\mu}{v_o^2 r_o}\left(1-\frac{r}{a}\right)\left\{\dot{g}+\frac{r_o}{r}\left(1-\frac{r}{a}\right)\right\}\right] \qquad (55)$$

$$\frac{\partial \alpha_6}{\partial \alpha_{50}} = 1 - \frac{r_o}{v_o}\dot{f}\alpha_{40} - \dot{g} + \frac{v}{r}\alpha_4\left[\frac{\mu}{v_o^2 r_o}g - \frac{r_o}{v_o}\left(\alpha_{40} - \frac{rv}{r_o v_o}\alpha_4\right) - \frac{3}{2}(t-t_o)\right] \qquad (56)$$

$$\frac{\partial \alpha_6}{\partial \alpha_{60}} = \frac{\mu}{v_o^2 r_o}\left[\dot{g}+\frac{r_o}{r}\left(1-\frac{r}{a}\right)\right] - \frac{v\alpha_4}{r}\left[g+\frac{r_o}{v_o}(f-1)\alpha_{40}\right] \qquad (57)$$

The transformation relating the variation of the conventional state variable $\Delta\hat{\underline{x}}^T = (\Delta\underline{R}, \Delta\dot{\underline{R}})$ to the variations of the above set of parameters $\Delta\underline{\alpha}^T = (\Delta\alpha_1, \Delta\alpha_2, \ldots \Delta\alpha_6)$ is given by

$$\Delta\hat{\underline{x}}(t) = P(t)\,\Delta\underline{\alpha}(t) \qquad \text{and} \qquad \Delta\underline{\alpha}(t) = P(t)^{-1}\,\Delta\hat{\underline{x}}(t) \qquad (58)$$

where

$$P(t) = \begin{bmatrix} \frac{-\underline{H}}{v} & 0 & \frac{\underline{H}\times\underline{R}}{h} & 0 & 0 & \underline{R} \\ 0 & \frac{\underline{H}}{r} & \frac{\underline{H}\times\dot{\underline{R}}}{h} & \frac{-rv}{R^2}\underline{H}\times\dot{\underline{R}} & \frac{\mu}{2v^2 a}\dot{\underline{R}} & \frac{-\mu}{rv^2}\dot{\underline{R}} \end{bmatrix} \qquad (59)$$

and

$$P(t)^{-1^T} = \begin{bmatrix} \frac{-v\underline{H}}{h^2} & 0 & \frac{\underline{H}\times\underline{R}}{hr^2} & \frac{\underline{H}\times\underline{R}}{r^3 v} & \frac{2a}{r^3}\underline{R} & \frac{\underline{R}}{r^2} \\ 0 & \frac{r\underline{H}}{h^2} & 0 & \frac{-\underline{H}\times\dot{\underline{R}}}{rv^3} & \frac{2a}{\mu}\dot{\underline{R}} & 0 \end{bmatrix} \qquad (60)$$

The relationship between the transition matrix $\hat{X}(t,t_o)$ for the conventional state variables $\underline{\hat{x}}(t)$ and $\Psi(t,t_o)$ for the above set of parameters $\underline{\alpha}(t)$ is given by

$$\hat{X}(t,t_o) = P(t)\,\Psi(t,t_o)\,P(t_o)^{-1} \text{ and } \Psi(t,t_o) = P(t)^{-1}\hat{X}(t,t_o)\,P(t_o) \qquad (61)$$

The scalar functions $f, g, \dot{f}$, and $\dot{g}$ are given by

(Elliptic)	(Hyperbolic)
$f = \frac{a}{r_o}(\cos\theta - 1) + 1$	$f = \frac{a}{r_o}(\cosh\theta - 1) + 1$
$g = (t-t_o) - \frac{\theta - \sin\theta}{n}$	$g = (t-t_o) - \frac{\sinh\theta - \theta}{n}$
$\dot{f} = \frac{-a^2 n}{r r_o}\sin\theta$	$\dot{f} = -\frac{\sqrt{-\mu a}}{r r_o}\sinh\theta$
$\dot{g} = \frac{a}{r}(\cos\theta - 1) + 1$	$\dot{g} = \frac{a}{r}(\cosh\theta - 1) + 1$

(62)

REFERENCES

1) Pontryagin, L.S., Maximum Principles in the Theory of Optimum Systems Parts I, II, III, Vol. 20, "Soviet Journal on Automation and Remote Control"

2) Pontryagin, L.S., Boltyanskii, V.G., Gamkrelidze, R.V., and Mishchenko, E.F., "The Mathematical Theory of Optimal Processes (Interscience Publishers, Inc., New York, 1962)

3) Richman, J., Two-Point Boundary-Value Problem of the Calculus of Variations for Optimum Orbits, MTP-AERO-63-12, George C. Marshall Space Flight Center, Huntsville, Ala., 6 February 1963

4) Nomicos, G. and Fang, T.C., Transition Matrix for Two-Body Problems, RAC-1295 (RD-TR-63-33) Republic Aviation Corporation, Farmingdale, N.Y., 10 March 1963

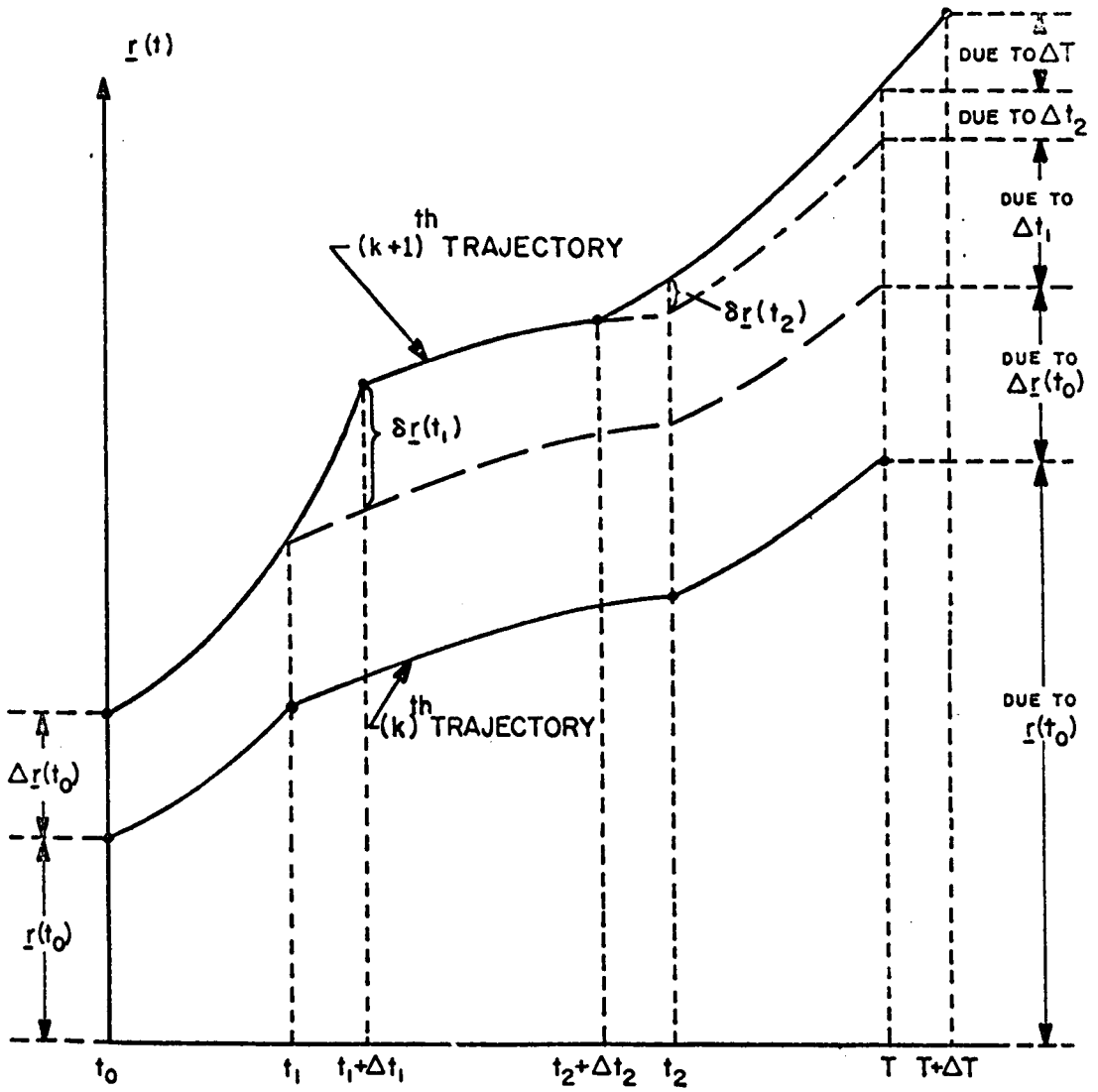
r(t)
(k+1)th TRAJECTORY
(k)th TRAJECTORY
δr(t1)
δr(t2)
DUE TO ΔT
DUE TO Δt2
DUE TO Δt1
DUE TO Δr(t0)
DUE TO r(t0)
Δr(t0)
r(t0)
t0
t1
t1+Δt1
t2+Δt2
t2
T
T+ΔT

FIGURE 1

AUBURN UNIVERSITY

PRELIMINARY INVESTIGATIONS ON SIX DIMENSIONAL OPTIMUM RE-ENTRY TRAJECTORIES

By

Douglas Raney
W. A. Shaw

AUBURN, ALABAMA

AUBURN UNIVERSITY
AUBURN, ALABAMA

PRELIMINARY INVESTIGATIONS ON SIX DIMENSIONAL OPTIMUM RE-ENTRY TRAJECTORIES

By

Douglas Raney
W. A. Shaw

SUMMARY

It is desired to find the point-to-point re-entry trajectory for a space vehicle with an off-set center of gravity which will minimize the integral of drag squared over time. The magnitude of the roll control force is used as a control variable. The problem takes the form of a Lagrange problem in the Calculus of Variations, with the first order equations of motion of the vehicle as constraint equations. The Euler characteristic equations are written and a computational procedure recommended so that trajectories can be generated on a digital computer.

Trajectories so generated satisfy the Euler necessary condition for stationary values of the given integral but do not necessarily satisfy the sufficiency conditions of Weierstrass.

SYMBOLS AND ABBREVIATIONS

G	Gravitational constant
M	Mass of the earth
m	Mass of the vehicle
g_i	Constraint equations
$\bar{r}$	Plumbline position vector
$\bar{r}_M$	Missile-fixed position vector
$\bar{r}_A$	Position vector in the aerodynamic coordinate system
$[\varphi]_1$	A rotation about the X axis
$[\varphi]_2$	A rotation about the Y axis
$[\varphi]_3$	A rotation about the Z axis
φ_p	Gimbal angle for pitch
φ_y	Gimbal angle for yaw
φ_r	Gimbal angle for roll
SP	Sine φ_p
CP	Cosine φ_p
SY	Sine φ_y
CY	Cosine φ_y
SR	Sine φ_r
CR	Cosine φ_r
$\bar{F}_A$	Aerodynamic force in the aerodynamic coordinate system
$\bar{F}_{AM}$	Aerodynamic force with components in the missile-fixed coordinate system

α	Absolute angle of attack
α_y	Angle of attack in yaw
A	Projected cross-sectional area of the vehicle
q	Dynamic pressure
$f(\alpha)$	A configuration dependent function of α
$\bar{\omega}_e$	Earth's angular velocity vector
$\bar{V}_r$	Relative wind vector
$\bar{V}_{rM}$	Relative wind vector with components in the missile-fixed system
$\bar{X}_{MCp}$	Position vector of the center of pressure in the missile-fixed coordinate system
$\bar{M}_{AM}$	Aerodynamic moment about the center of gravity
$\bar{F}_{r_1} = -\bar{F}_{r_2}$	Roll control forces
$\bar{M}_{Mr}$	Roll control moment
T	Kinetic energy
t	time
$\bar{\omega}$	Vehicle angular velocity vector with components in the missile system

$\bar{\omega}^T$ Transpose of $\bar{\omega}$

$\bar{X}_{Rc}$ Position vector of roll jets

λ_i Lagrangian multipliers

$$f' = \bar{F}_{AM} \cdot \bar{F}_{AM} + \lambda_i g_i$$

$$\bar{V} = \dot{\bar{r}} = \begin{bmatrix} u & v & w \end{bmatrix}^T$$

$$\bar{\Psi} = \dot{\bar{\varphi}} = \begin{bmatrix} \dot{\varphi}_p & \dot{\varphi}_y & \dot{\varphi}_r \end{bmatrix}^T$$

$$B_i = \dot{\bar{\varphi}}^T \frac{\partial [A_\omega]}{\partial \varphi_i} [\mu] [A_\omega] \dot{\bar{\varphi}}$$

$$\bar{B} = \begin{bmatrix} B_p & B_y & B_r \end{bmatrix}^T$$

$$[C] = \left\{ [A_\omega]^T [\mu] [A_\omega] \right\}^{-1}$$

$$[S] = \frac{d}{dt} [A_\omega]^T [\mu] [A_\omega]$$

$$[T] = [A_\omega]^T [\mu] \frac{d}{dt} [A_\omega]$$

$$[M] = \frac{\partial}{\partial \varphi_y} [A_\omega]^T [\mu] [A_\omega]$$

$$[N] = \frac{\partial}{\partial \varphi_r} [A_\omega]^T [\mu] [A_\omega]$$

$$[\mu] = \begin{bmatrix} I_{xx} & -I_{xy} & -I_{xZ} \\ -I_{xy} & I_{yy} & -I_{yZ} \\ -I_{xZ} & -I_{yZ} & I_{ZZ} \end{bmatrix}$$

$$[A_\omega] = \begin{bmatrix} SRCY & CR & 0 \\ SY & 0 & -1 \\ CRCY & -SR & 0 \end{bmatrix}$$

I. INTRODUCTION

In this paper an attempt is made to treat the optimum re-entry problem in a dynamically realistic manner. The condition for optimality used herein is that the integral $\int(\text{Drag})^2 dt$ be a minimum for fixed end-point trajectories. The six degrees of freedom, rigid body constraints are used in the form of first order differential equations of motion. It is assumed that the attractive force due to Earth and atmospheric drag are the only forces influencing the vehicle's motion. A re-entry vehicle with an off-set center of gravity is used so that maneuvering can be accomplished by properly placed roll jets. The performance optimization analysis which results from the statement of the problem is a Lagrange problem in the classical Calculus of Variations with fixed end points.

II. STATEMENT OF THE PROBLEM

From an initial point above the earth's surface, a space vehicle is assumed to re-enter the atmosphere under the influence of gravitational attraction due to the earth and atmospheric drag. The performance optimization study herein presented is predicated on the assumption that an automatic control system is desired to satisfy the following criteria:

1. Maneuvering capability for a point landing.
2. Minimization of the accumulated physiological strain on a human crew.

The exact mathematical statement of the latter criterion as used in this paper will be the minimization over the trajectory of the integral $\int(\text{Drag})^2 dt$. The term "drag" is here used to denote the total aerodynamic force acting on the vehicle. The basic performance problem so formulated is the fixed end point variational problem of Lagrange, where the integral $\int(\text{Drag})^2 dt$ is to be minimized subject to n differential side conditions $g_i = 0$ $(i = 1, \ldots, n)$ and boundary conditions $f_k = 0$ $(k = 1, \ldots, 2m + 2)$, where m is the number of state variables. The constraint equations $g_i = 0$ $(i = 1, \ldots, 12)$ will be the first order equations of motion of the vehicle written in three degrees of translational freedom and three degrees of angular freedom in the gimbal angles for pitch, yaw, and roll. The boundary conditions $f_k = 0$ $(k = 1, 2, \ldots, 24)$ will be the initial and terminal values of position, velocity, gimbal angles, and angular rates. These boundary conditions seem realistic for the performance problem if adaptive control is to be used. The magnitude of the roll jet force

will appear as a control variable and is left unspecified at the end-points. The problem is formulated subject to the following additional assumptions:

1. The mass of the vehicle is an invariant with respect to time.
2. The vehicle center of gravity is an invariant.
3. The only forces acting on the vehicle are the gravitational force and drag.
4. The vehicle has an off-set center of gravity so that maneuvering can be accomplished solely by roll jets, properly placed so as to create a pure couple.
5. The earth is spherical and the inverse gravity law is valid. $\bar{F} = \dfrac{-GMm\,\bar{r}}{|\bar{r}|^3}$

III. COORDINATE SYSTEMS

Two coordinate systems will be used, one earth-centered, space-fixed Cartesian set and one Cartesian set fixed in the vehicle.

PLUMBLINE SYSTEM

The plumbline system is a space-fixed Cartesian system and is defined at the initial time of re-entry by taking the origin at the center of the earth with the Y axis parallel to the gravity gradient at some fixed reference site on the earth's surface. The X axis is parallel to some earth-fixed azimuth at the reference point. The Z axis is taken so as to form a right hand set.

MISSILE SYSTEM

The missile system is defined by having its origin at the center of gravity of the vehicle and its Y_M axis parallel to the longitudinal axis of the vehicle. The X_M and Z_M axes are taken so as to form a right hand Cartesian set. The coordinate systems are illustrated in Figure 1.

GIMBAL SYSTEM

As the vehicle moves in flight, the two coordinate systems are related through Eulerian angles, which are measured by the gimbal system. Starting with the space-fixed system, three successive

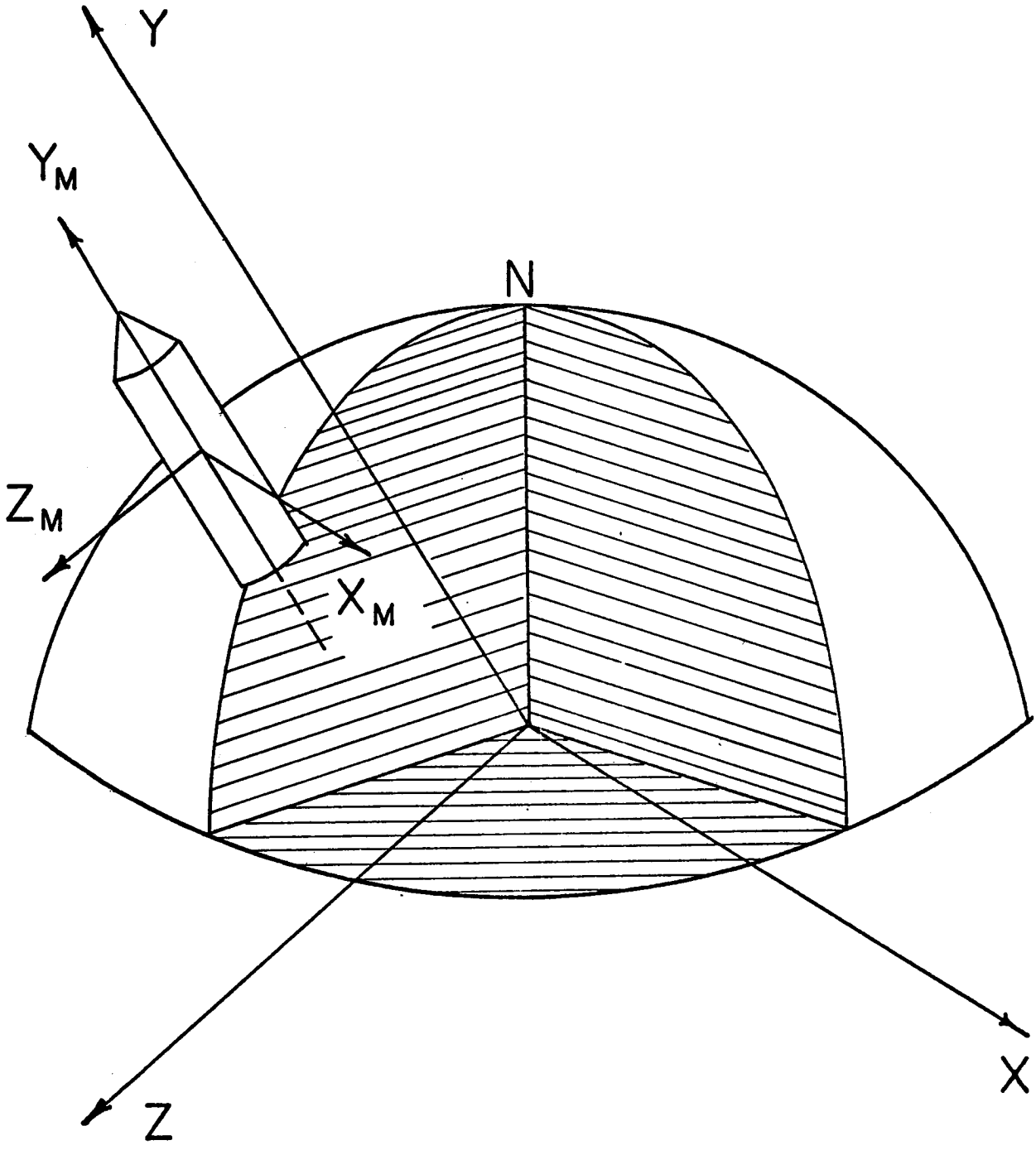

FIGURE 1. COORDINATE SYSTEMS

rotations of coordinate axes are defined in terms of the Eulerian angles so that a transformation relating the two Cartesian sets can be written. Specifically, the attitude of the missile in flight is defined by first rotating about the Z axis by φ_p then around the new intermediate X axis by φ_y, and finally around the Y_M axis by $-\varphi_r$. So that

$$(1) \qquad \bar{r}_M = [-\varphi_r]_2 \; [\varphi_y]_1 \; [\varphi_p]_3 \, \bar{r} = [A_D] \, \bar{r}$$

or

$$\bar{r}_M = \begin{bmatrix} CR & 0 & SR \\ 0 & 1 & 0 \\ -SR & 0 & CR \end{bmatrix} \begin{bmatrix} 1 & 0 & 0 \\ 0 & CY & SY \\ 0 & -SY & CY \end{bmatrix} \begin{bmatrix} CP & SP & 0 \\ -SP & CP & 0 \\ 0 & 0 & 1 \end{bmatrix} \bar{r}$$

$$(2) \qquad \bar{r}_M = \begin{bmatrix} CRCP + SPSYSR & CRSP-SRSYCP & SRCY \\ -CYSP & CYCP & SY \\ -SRCP + CRSYSP & -SRSP-CRSYCP & CRCY \end{bmatrix} \bar{r} = [A_D] \, \bar{r}$$

Where, for example, CR is used to denote Cosine φ_r. At the time the gimbal system is actuated, the transformation between the two systems is taken as the identity transformation. The gimbal angles are illustrated in Figure 2.

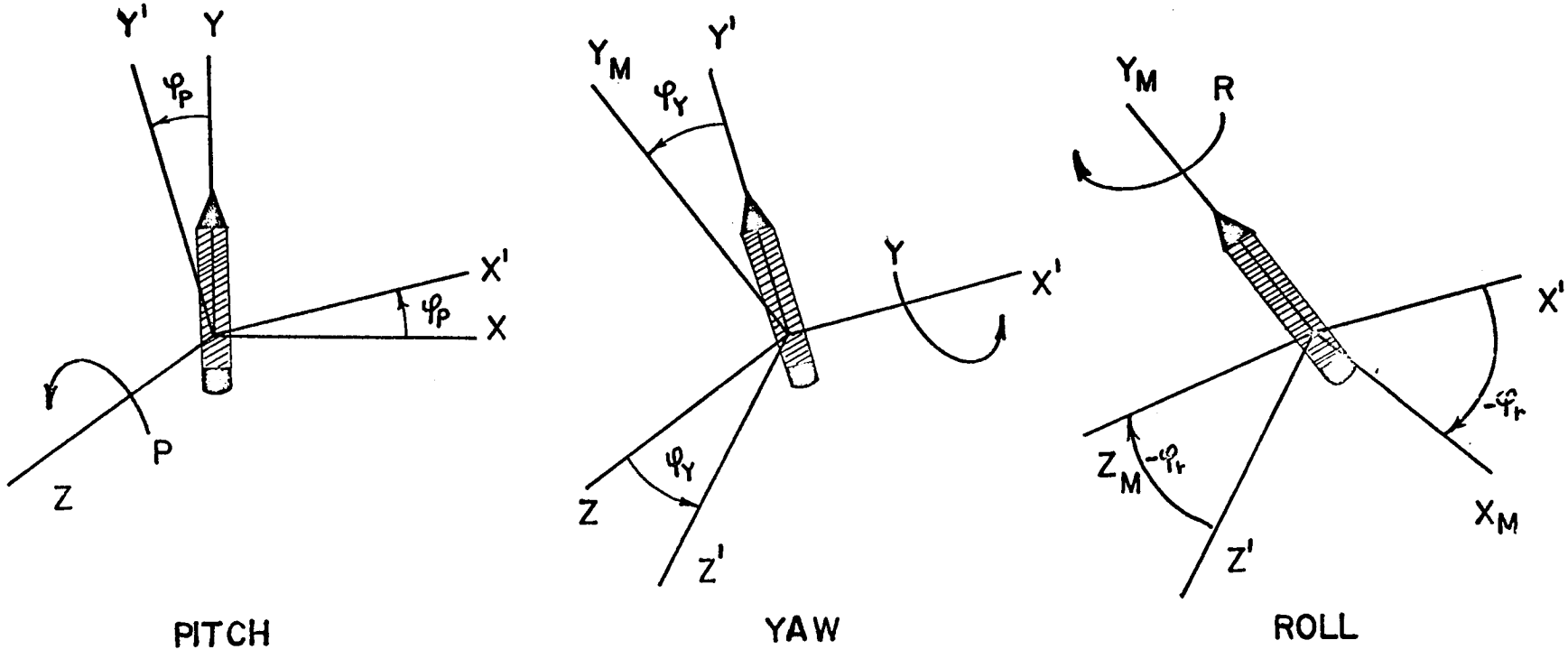

FIGURE 2. EULERIAN ANGLES

IV. BASIC MECHANICS

Before the variational problem can be formulated, a mathematical model for the basic mechanics must be deduced from the previously stated physical assumptions.

FORCES

Aerodynamic Force

The aerodynamics used is essentially that given by Miner (6) except winds have been ignored. An aerodynamic force, $\bar{F}_A$, is assumed to act at the vehicle's center of pressure. The direction of the aerodynamic force is found in terms of two consecutive rotations of coordinate axes starting with the missile system and forming a new Cartesian system denoted by $\bar{r}_A$. The rotations are made so that the aerodynamic force is parallel to the new Y_A axis. The rotations are defined as follows, turning from the missile system:

1. Rotate about the Y_M axis such that the X_M axis is brought to lie in the plane which contains the Y_M axis and the relative velocity vector; denote the angle turned through as α_y.
2. Rotate about the new Z_A axis to bring the Y_M axis to lie along the relative velocity vector; denote this angle as α, the absolute angle of attack.

So that

$$(3)\quad \bar{r}_A = \left[-\alpha\right]_3 \left[\alpha_y\right]_2 \bar{r}_M$$

Now consider the magnitude of the aerodynamic force to be given by $|\bar{F}_A| = Aqf(\alpha)$; where $f(\alpha)$ is determined by the vehicle configuration. The aerodynamic force in the missile system is then given by:

$$(4)\quad \bar{F}_{AM} = [-\alpha_y]\ 2\ [\alpha]_3\ \bar{F}_A = \begin{bmatrix} \cos\alpha_y & 0 & \sin\alpha_y \\ 0 & 1 & 0 \\ -\sin\alpha_y & 0 & \cos\alpha_y \end{bmatrix} \begin{bmatrix} \cos\alpha & \sin\alpha & 0 \\ -\sin\alpha & \cos\alpha & 0 \\ 0 & 0 & 1 \end{bmatrix} \bar{F}_A$$

$$(5)\quad \bar{F}_{AM} = \begin{bmatrix} -Aq\ \sin\alpha\cos\alpha_y\ f(\alpha) \\ -Aq\ \cos\alpha\ f(\alpha) \\ Aq\ \sin\alpha\ \sin\alpha_y\ f(\alpha) \end{bmatrix}$$

The equations of motion for the vehicle will be written in the plumbline system, since this system is space-fixed and assumed to be a primary inertial system. It will be assumed that the atmosphere moves with the earth so that there is an air mass movement relative to the plumbline system defined by $(\bar{r} \times \bar{\omega}_e)$, where $\bar{\omega}_e$ is the earth's angular velocity vector written in the plumbline system. The relative velocity vector is then given by

$$(6)\quad \bar{V}_r = \dot{\bar{r}} + (\bar{r} \times \bar{\omega}_e)$$

and in the missile system

$$(7)\quad \bar{V}_{rM} = [A_D]\ \bar{V}_r = \begin{bmatrix} V_{rMx} \\ V_{rMy} \\ V_{rMZ} \end{bmatrix}$$

From the definitions of α and α_y the following relations are now deduced:

$$(8)\quad \cos\alpha_y = \frac{V_{rMx}^2}{|V_{rMx}|\sqrt{V_{rMx}^2 + V_{rMZ}^2}} \quad \text{if} \quad \begin{matrix} V_{rMX} < 0 & \cos\alpha_y < 0 \\ V_{rMX} > 0 & \cos\alpha_y > 0 \end{matrix}$$

$$(9) \qquad \text{Sin } \alpha_y = \pm \sqrt{1 - \text{Cos}^2 \alpha_y} \quad \text{if} \quad \begin{matrix} V_{rMZ} < 0 & \text{Sin } \alpha_y > 0 \\ V_{rMZ} > 0 & \text{Sin } \alpha_y < 0 \end{matrix}$$

$$(10) \qquad \text{Cos } \alpha = \frac{V_{rMy}^2}{\sqrt{V_{rMx}^2 + V_{rMy}^2 + V_{rMZ}^2}} \quad \text{if} \quad \begin{matrix} V_{rMy} < 0 & \text{Cos } \alpha < 0 \\ V_{rMy} > 0 & \text{Cos } \alpha > 0 \end{matrix}$$

$$(11) \qquad \text{Sin } \alpha = + \sqrt{1 - \text{Cos}^2 \alpha} \qquad \text{where} \qquad 0 \leq \alpha \leq 180^\circ$$

Reference to Figure 3 may be convenient at this point.

Gravitational Force

Since the earth is assumed to be spherical, from Newton's Law of Universal Gravitation, there is an attractive force acting at the center of gravity of the vehicle given by:

$$(12) \qquad \bar{F} = \frac{-GMm\bar{r}}{|\bar{r}|^3}$$

MOMENTS

Aerodynamic Moment

The aerodynamic force acting at the center of pressure causes a moment about the center of gravity of $(\bar{X}_{MCp} \times \bar{F}_{AM})$ where $\bar{X}_{MCp}$ is the position vector of the center of pressure in the missile system.

$$(13) \qquad \bar{M}_{AM} = \begin{bmatrix} X_{MCp} \\ Y_{MCp} \\ Z_{MCp} \end{bmatrix} \times \begin{bmatrix} -Aq\, f(\alpha) & \text{Sin } \alpha \text{ Cos } & \alpha_y \\ -Aq\, f(\alpha) & \text{Cos } \alpha & \\ Aq\, f(\alpha) & \text{Sin } \alpha \text{ Sin } & \alpha_y \end{bmatrix}$$

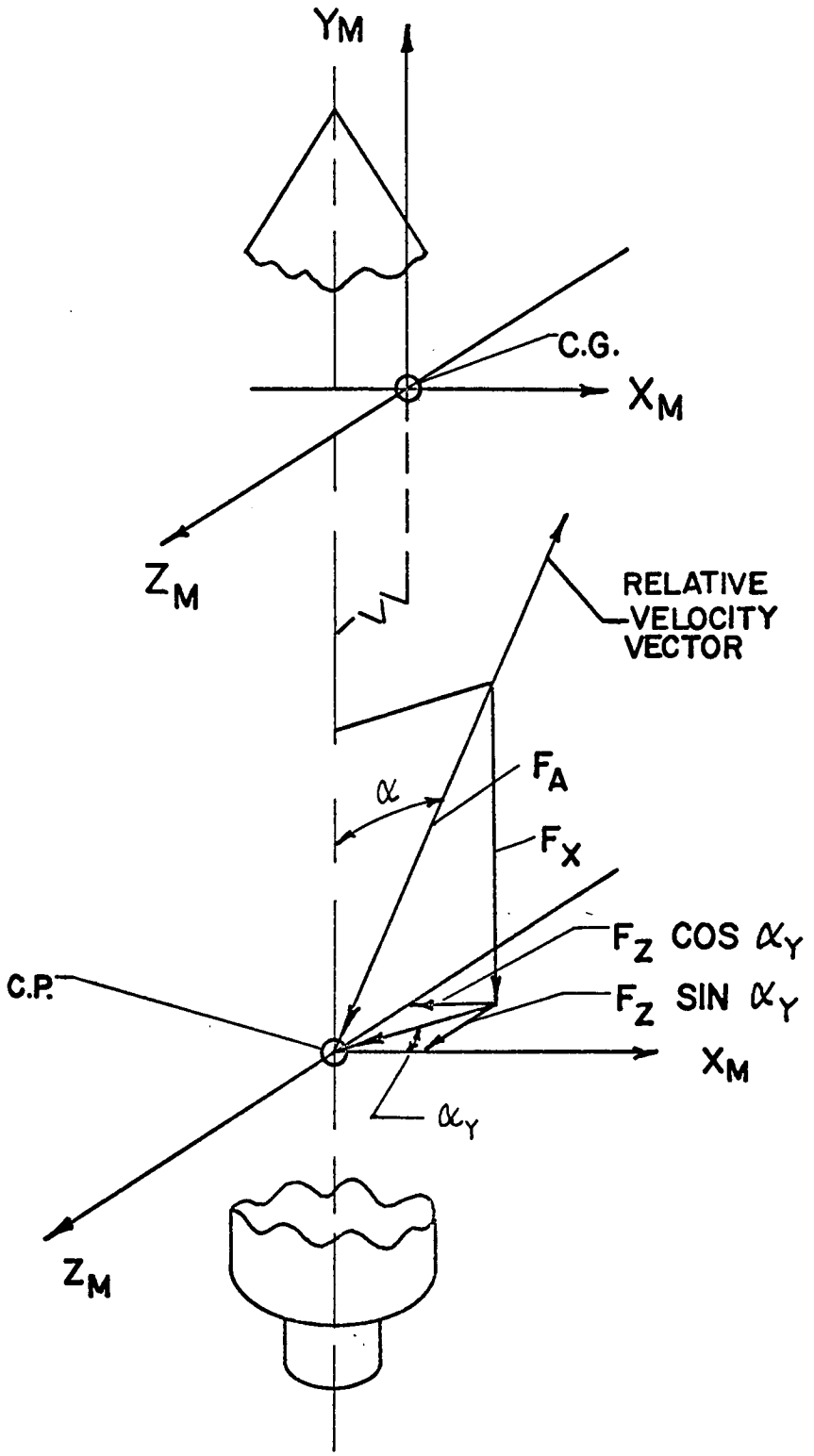

FIGURE 3. AERODYNAMIC FORCE SYSTEM

Roll Control Moment

The roll jets are placed in the positions shown in Figure 4, so that in the missile system

$$\bar{F}_{r_1} = \begin{bmatrix} F_r \\ 0 \\ 0 \end{bmatrix}, \quad \text{located at} \quad \begin{bmatrix} 0 \\ 0 \\ Z_{RC} \end{bmatrix}$$

and

$$\bar{F}_{r_2} = \begin{bmatrix} -F_r \\ 0 \\ 0 \end{bmatrix}, \quad \text{located at} \quad \begin{bmatrix} 0 \\ 0 \\ -Z_{RC} \end{bmatrix}$$

so that the moment about the center of gravity due to the roll jets is given by

$$\bar{M}_{MR} = \begin{bmatrix} 0 \\ 2F_r Z_{RC} \\ 0 \end{bmatrix} \tag{14}$$

The total moment about the center of gravity in the missile system is then the sum of the aerodynamic and roll control moments.

$$\bar{M}_{MT} = \bar{M}_{AM} + \bar{M}_{MR}$$

TRANSLATIONAL MOTION

Since it has been assumed that the only forces acting on the vehicle are the attractive force due to Earth and the atmospheric drag, the equation of motion for the translation of the vehicle center of gravity takes the following form:

$$\ddot{\bar{r}} = \frac{-GM\bar{r}}{|\bar{r}|^3} + \frac{[A_D]}{m}^T \bar{F}_{AM} \tag{15}$$

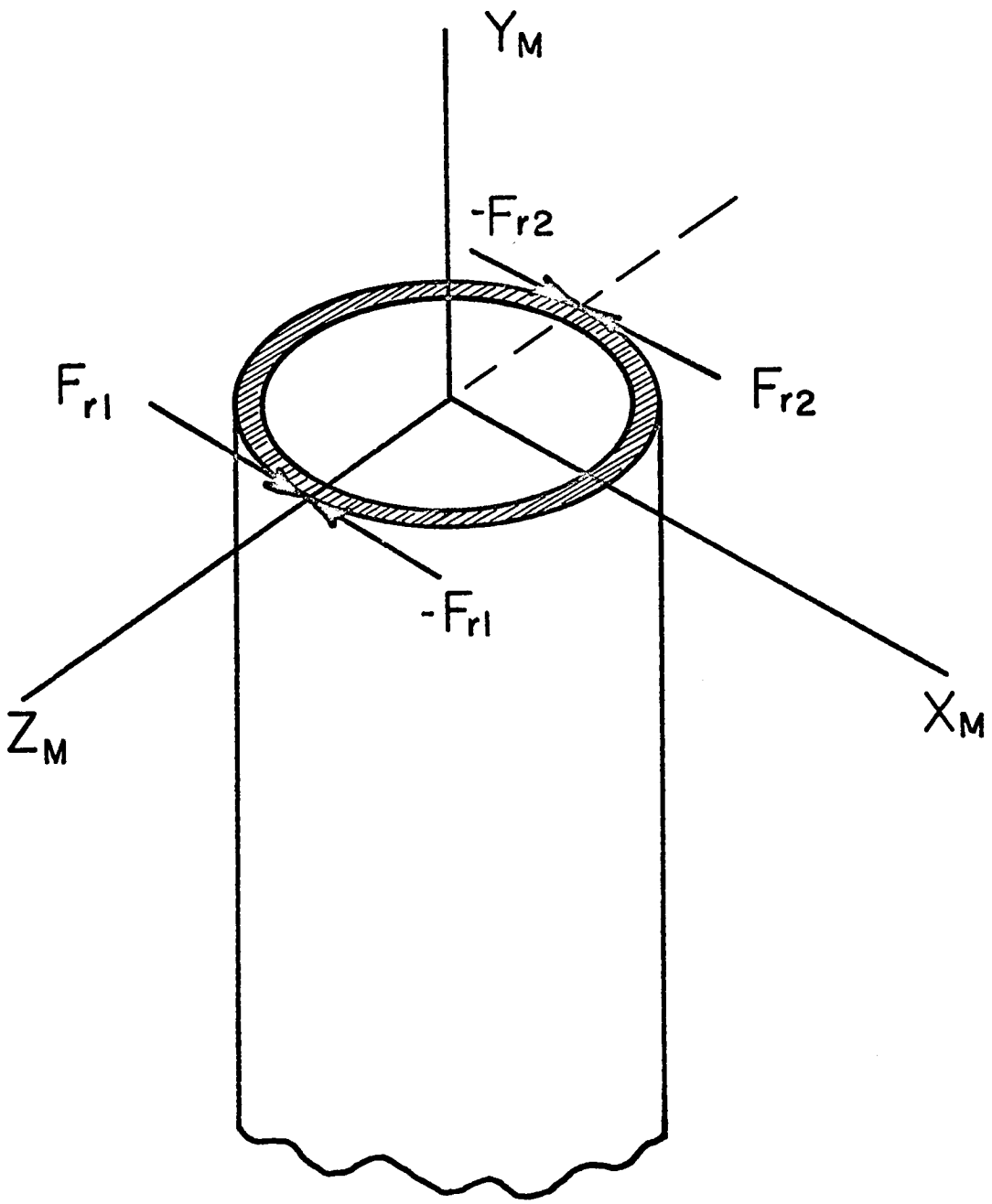

FIGURE 4. ROLL CONTROL FORCE SYSTEM

ROTATIONAL DYNAMICS

In general, a rigid body in three-dimensional space has six degrees of freedom since six coordinates are required to fix its position relative to a given space-fixed set of axes. In this analysis, the six degrees of freedom are the plumbline coordinates of the vehicle center of gravity and the three gimbal angles which fix the missile system axes with respect to the plumbline axes. Clasle's theorem states that it is possible to split the problem of rigid body motion into two separate phases, one concerned solely with the translational motion of the body, the other, with its rotational motion. Since an expression has previously been written for the translational motion of the vehicle center of gravity, expressions are now needed to describe the rotational motion of the vehicle about its center of gravity. These equations are determined from energy considerations.

A transformation can be carried out from a given Cartesian coordinate system to another by means of three successive rotations of coordinate axes. In this analysis, starting with the plumbline system and transforming to the missile system, these angles of rotation have been defined to be the gimbal angles for pitch, yaw, and roll. These gimbal angles are ideal generalized coordinates for setting up the rotational motion of rigid bodies using the Lagrangian formulation of mechanics. For generalized coordinates of angular character, such as the gimbal angles, the Lagrangian form becomes

$$(16)\qquad \frac{d}{dt}\left(\frac{\partial T}{\partial \dot{\varphi}_i}\right) - \frac{\partial T}{\partial \varphi_i} = M_{\varphi_i}$$

where T is the kinetic energy and M_{φ_i} is the moment causing the φ_i rotation. The subscript i takes the values pitch, yaw, and roll. Since an off-set center of gravity has been assumed, all six components of the inertia tensor are taken as non-zero. The expression for kinetic energy takes the following form:

$$T = \frac{1}{2} I_{xx}\omega_x^2 + \frac{1}{2} I_{yy}\omega_y^2 + \frac{1}{2} I_{ZZ}\omega_Z^2$$

$$-2I_{xy}\omega_x\omega_y - 2I_{xZ}\omega_x\omega_Z - 2I_{yZ}\omega_y\omega_Z$$

or using matrix notation

$$(17)\qquad T = \frac{1}{2}\begin{bmatrix}\omega_x & \omega_y & \omega_Z\end{bmatrix}\begin{bmatrix} I_{xx} & -I_{xy} & -I_{xZ} \\ -I_{xy} & I_{yy} & -I_{yZ} \\ -I_{xZ} & -I_{yz} & I_{ZZ}\end{bmatrix}\begin{bmatrix}\omega_x \\ \omega_y \\ \omega_Z\end{bmatrix} = \frac{1}{2}\bar{\omega}^T[\mu]\bar{\omega}$$

where $[\mu]$ is the inertia tensor for motion about the missile axes, $\bar{\omega}$ is the missile-fixed angular velocity vector and $\bar{\omega}^T$ is the transpose of $\bar{\omega}$. By carrying out the indicated differentiation on the above expressions for kinetic energy, the Lagrangian equations take the following form:

$$(18)\qquad \frac{d}{dt}\left(\frac{\partial \bar{\omega}^T}{\partial \dot{\varphi}_i}\right)[\mu]\bar{\omega} + \frac{\partial \bar{\omega}^T}{\partial \varphi_i}[\mu]\frac{d\bar{\omega}}{dt} - \frac{\partial \bar{\omega}^T}{\partial \varphi_i}[\mu]\bar{\omega} = M_{\varphi_i}$$

The $\bar{\omega}$ vector in the missile system is obtained by establishing the angular velocity components in the missile system due to the trans-

formation of each of the vectors $\dot{\bar{\varphi}}_p$, $\dot{\bar{\varphi}}_y$, and $\dot{\bar{\varphi}}_r$. These vectors are in the directions of the axes of rotation. The gimbal system used in this analysis measures pitch, yaw, and roll in order turning from the space-fixed system. Therefore, $\dot{\bar{\varphi}}_r$ is already in the missile system, whereas, $\dot{\bar{\varphi}}_y$ must be rotated through the roll angle and $\dot{\bar{\varphi}}_p$ must be rotated first through the yaw angle and then through the roll angle. The $\bar{\omega}$ vector in the missile system is then written

$$\bar{\omega} = \begin{bmatrix} 0 \\ -\dot{\varphi}_r \\ 0 \end{bmatrix} + \begin{bmatrix} CR & 0 & SR \\ 0 & 1 & 0 \\ -SR & 0 & CR \end{bmatrix} \begin{bmatrix} \dot{\varphi}_y \\ 0 \\ 0 \end{bmatrix} + \begin{bmatrix} CR & 0 & SR \\ 0 & 1 & 0 \\ -SR & 0 & CR \end{bmatrix} \begin{bmatrix} 1 & 0 & 0 \\ 0 & CY & SY \\ 0 & -SY & CY \end{bmatrix} \begin{bmatrix} 0 \\ 0 \\ \dot{\varphi}_p \end{bmatrix}$$

or

$$\bar{\omega} = \begin{bmatrix} SRCY & CR & 0 \\ SY & 0 & -1 \\ CRCY & -SR & 0 \end{bmatrix} \begin{bmatrix} \dot{\varphi}_p \\ \dot{\varphi}_y \\ \dot{\varphi}_r \end{bmatrix} = [A_\omega] \dot{\bar{\varphi}} \tag{19}$$

and

$$\bar{\omega}^T = \dot{\bar{\varphi}}^T [A_\omega]^T \tag{20}$$

Using these expressions in equation (18) the Lagrangian equations in pitch, yaw, and roll can be written as follows in vector form:

$$\ddot{\bar{\varphi}} = [C] \left\{ [A_\omega]^T \bar{M}_{M_T} - [S] \dot{\bar{\varphi}} - [T] \dot{\bar{\varphi}} + \bar{B} \right\} \tag{21}$$

where $$B_i = \dot{\bar{\varphi}}^T \frac{\partial [A_\omega]^T}{\partial \varphi_i} [\mu] [A_\omega] \dot{\bar{\varphi}}$$

and $$\bar{B} = \begin{bmatrix} B_p \\ B_y \\ B_r \end{bmatrix}$$

$$\dot{\bar{\varphi}} = \begin{bmatrix} \dot{\varphi}_p \\ \dot{\varphi}_y \\ \dot{\varphi}_r \end{bmatrix}$$

$$\ddot{\bar{\varphi}} = \begin{bmatrix} \ddot{\varphi}_p \\ \ddot{\varphi}_y \\ \ddot{\varphi}_r \end{bmatrix}$$

$$[C] = \left\{ [A_\omega]^T [\mu] [A_\omega] \right\}^{-1}$$

$$[S] = \frac{d}{dt} [A_\omega]^T [\mu] [A_\omega]$$

$$[T] = [A_\omega]^T [\mu] \frac{d}{dt} [A_\omega]$$

In developing $\bar{B}$, it will be noted that

$$\frac{\partial}{\partial \varphi_p} [A_\omega]^T = 0$$

$$\frac{\partial}{\partial \varphi_y} [A_\omega]^T = \begin{bmatrix} -SRSY & CY & -SYCR \\ 0 & 0 & 0 \\ 0 & 0 & 0 \end{bmatrix}$$

$$\frac{\partial}{\partial \varphi_r} [A_\omega]^T = \begin{bmatrix} CRCY & 0 & -SRCY \\ -SR & 0 & -CR \\ 0 & 0 & 0 \end{bmatrix}$$

Also, in the development the following additional notation is used:

$$[M] = \frac{\partial}{\partial \varphi_y} [A_\omega]^T [\mu] [A_\omega]$$

$$[N] = \frac{\partial}{\partial \varphi_r} [A_\omega]^T [\mu] [A_\omega]$$

V. FIRST ORDER EQUATIONS OF MOTION

In light of the preceding discussion the first order equations of motion for the vehicle can readily be written in vector form by defining the velocity, $\bar{V} = \dot{\bar{X}} = [u \quad v \quad w]^T$, and the angular velocity vector, $\bar{\Psi} = \dot{\bar{\varphi}} = [\dot{\varphi}_p \quad \dot{\varphi}_y \quad \dot{\varphi}_r]^T$. The equations are written assuming the validity of Newton's second postulate in the plumbline system.

$$(22) \qquad \dot{\bar{r}} - \bar{V} = 0$$

$$(23) \qquad \dot{\bar{V}} + \frac{GM\,\bar{r}}{|\bar{r}|^3} - \frac{[A_D]^T}{m}\,\bar{F}_{AM} = 0$$

$$(24) \qquad \dot{\bar{\varphi}} - \bar{\Psi} = 0$$

$$(25) \qquad \dot{\bar{\Psi}} - [C]\left\{[A_\omega]^T \bar{M}_{MT} - [S]\,\bar{\Psi} - [T]\,\bar{\Psi} + \bar{B}\right\} = 0$$

These vector equations can be written as twelve scalar equations as follows:

$$(26) \qquad g_1 = \dot{x} - u = 0$$

$$(27) \qquad g_2 = \dot{y} - v = 0$$

$$(28) \qquad g_3 = \dot{z} - w = 0$$

$$(29) \qquad g_4 = \dot{u} + GM\,x\,(x^2 + y^2 + z^2)^{-\frac{3}{2}}$$

$$-\frac{Aqf(\alpha)}{m}\left\{(CRCp + SRSYSp)(-\text{Sin}\,\alpha\,\text{Cos}\,\alpha_y) + CYSp\text{Cos}\,\alpha + (-SRCp + CRSYSp)(\text{Sin}\,\alpha\ \text{Sin}\,\alpha_y)\right\} = 0$$

$$(30) \qquad g_5 = \dot{v} + GMY(x^2 + Y^2 + Z^2)^{-\frac{3}{2}}$$

$$+\frac{Aqf(\alpha)}{m}\left\{(CRSp - SRSYCp)(\text{Sin}\,\alpha\,\text{Cos}\,\alpha_y) + CYCp\text{Cos}\,\alpha + (SRSP + CRSYCp)(\text{Sin}\,\alpha\ \text{Sin}\,\alpha_y)\right\} = 0$$

(31) $$g_6 = \dot{w} + GMZ\,(X^2 + Y^2 + Z^2)^{-\frac{3}{2}} + \frac{Aqf(\alpha)}{m}\left\{ SRCY\ SIN\alpha \cos \alpha_y + SY \cos\alpha - CRCY \sin\alpha \sin \alpha_y \right\} = 0$$

(32) $$g_7 = \dot{\varphi}_p - \psi_p = 0$$

(33) $$g_8 = \dot{\varphi}_y - \psi_y = 0$$

(34) $$g_9 = \dot{\varphi}_r - \psi_r = 0$$

(35) $$g_{10} = \dot{\psi}_p - Aqf(\alpha)\left\{ (C_{11}SRCY+C_{12}CR)(Y_{MCP}\sin\alpha \sin \alpha_y + Z_{MCP} \cos\alpha) - (C_{11}SY-C_{13})(Z_{MCP}\sin\alpha \cos \alpha_y + X_{MCP} \sin\alpha \sin \alpha_y) + (C_{11}CRCY-C_{12}SR)(-X_{MCP} \cos\alpha + Y_{MCP} \sin\alpha \cos \alpha_y) \right\} - (C_{11}SY-C_{13})(2FrZ_{RC}) + (C_{11}S_{11}+C_{12}S_{21}+C_{13}S_{31})\psi_p + (C_{11}S_{12}+C_{12}S_{22}+C_{13}S_{32})\psi_y + (C_{11}S_{13}+C_{12}S_{23} + C_{13}S_{33})\psi_r + (C_{11}T_{11}+C_{12}T_{21}+C_{13}T_{31})\psi_p + (C_{11}T_{12}+C_{12}T_{22}+C_{13}T_{32})\psi_y + (C_{11}T_{13}+C_{12}T_{23}+C_{13}T_{33})\psi_r - C_{12}\left\{ \psi_p(M_{11}\psi_p + M_{12}\psi_y + M_{13}\psi_r) + \psi_y(M_{21}\psi_y + M_{22}\psi_y + M_{23}\psi_r) + \psi_r(M_{31}\psi_p + M_{32}\psi_y + M_{33}\psi_r) \right\} - C_{13}\left\{ \psi_p(N_{11}\psi_p + N_{12}\psi_y + N_{13}\psi_r) + \psi_y(N_{21}\psi_p + N_{22}\psi_y + N_{23}\psi_r) + \psi_r(N_{31}\psi_p + N_{32}\psi_y + N_{33}\psi_r) \right\} = 0$$

(36) $$g_{11} = \dot{\psi}_y - Aqf(\alpha)\left\{ (C_{21}SRCY+C_{22}CR)(Y_{MCP}\sin\alpha \sin \alpha_y + Z_{MCP} \cos\alpha) - (C_{21}SY-C_{23})(Z_{MCP}\sin\alpha \cos \alpha_y + X_{MCP}\sin\alpha \sin \alpha_y) + (C_{21}CRCY-C_{22}SR)(-X_{MCP}\cos\alpha + Y_{MCP}\sin\alpha\cos \alpha_y) \right\} - (C_{21}SY-C_{23})(2F_rZ_{RC}) + (C_{21}S_{11}+C_{22}S_{21}+C_{23}S_{31})\psi_p + (C_{21}S_{12}+C_{22}S_{22}+C_{23}S_{32})\psi_y + (C_{21}S_{13}+C_{22}S_{23} + C_{23}S_{33})\psi_r + (C_{21}T_{11}+C_{22}T_{21}+C_{23}T_{31})\psi_p + (C_{21}T_{12}+C_{22}T_{22}+C_{23}T_{32})\psi_y + (C_{21}T_{13}+C_{22}T_{23}+C_{23}T_{33})\psi_r - C_{23}\left\{ \psi_p(M_{11}\psi_p + M_{12}\psi_y + N_{13}\psi_r) + \psi_y(M_{21}\psi_p + M_{22}\psi_y + M_{23}\psi_r) + \psi_r(M_{31}\psi_p + M_{32}\psi_y + M_{33}\psi_r) \right\} - C_{23}\left\{ \psi_p(N_{11}\psi_p + N_{12}\psi_y + N_{13}\psi_r) + \psi_y(N_{21}\psi_p + N_{22}\psi_y + N_{23}\psi_r) + \psi_r(N_{31}\psi_p + N_{32}\psi_y + N_{33}\psi_r) \right\} = 0$$

$$(37)\quad g_{12} = \dot{\psi}_r - Aqf(\alpha)\Big\{(C_{31}SRCY+C_{32}CR)(Y_{MCP}Sin\alpha\ Sin\ \alpha_y + Z_{MCP}Cos\ \alpha) - (C_{31}SY-C_{33})(Z_{MCP}Sin\alpha\ Cos\ \alpha_y + X_{MCP}Sin\alpha\ Sin\ \alpha_y) + (C_{31}CRCY-C_{32}SR)(-X_{MCP}Cos\ \alpha + Y_{MCP}Sin\alpha\ Cos\ \alpha_y)\Big\} - (C_{31}SY-C_{33})(2F_rZ_{RC}) + (C_{31}S_{11}+C_{32}S_{21}+C_{33}S_{31})\psi_p + (C_{31}S_{12}+C_{32}S_{22}+C_{33}S_{32})\psi_y + (C_{31}S_{13}+C_{32}S_{23} + C_{33}S_{33})\psi_r + (C_{31}T_{11}+C_{32}T_{21}+C_{33}T_{31})\psi_p + (C_{31}T_{12}+C_{32}T_{22}+C_{33}T_{32})\psi_y + (C_{31}T_{13}+C_{32}T_{23}+C_{33}T_{33})\psi_r - C_{32}\Big\{\psi_p(M_{11}\psi_p+M_{12}\psi_y+M_{13}\psi_r) + \psi_y(M_{21}\psi_p + M_{22}\psi_y+M_{23}\psi_r) + \psi_r(M_{31}\psi_p+M_{32}\psi_y+M_{33}\psi_r)\Big\} - C_{33}\Big\{\psi_p(N_{11}\psi_p+N_{12}\psi_y + N_{13}\psi_r) + \psi_y(N_{21}\psi_p+N_{22}\psi_y+N_{23}\psi_r) + \psi_r(N_{31}\psi_p+N_{32}\psi_y+N_{33}\psi_r)\Big\} = 0$$

VI. FORMULATION OF THE VARIATIONAL PROBLEM

As previously stated, it is desired to find stationary values of the integral $\int(\text{Drag})^2\,dt$ between fixed end points subject to the first order equations of motion as constraints. Using the aerodynamic force previously derived, the integral becomes

$$(38)\quad \int(\bar{F}_{AM}\cdot\bar{F}_{AM})dt = \int q^2 f^2(\alpha)\quad(\text{Sin}^2\alpha\,\text{Cos}^2\alpha_y+\text{Cos}^2\alpha+\text{Sin}^2\alpha\,\text{Sin}^2\alpha_y)\,dt$$

The concept of the Lagrangian multiplier is used to handle the constraint equations in the usual way; thus f' is defined as follows:

$$f' = f + \lambda_i g_i = \bar{F}_{AM}\cdot\bar{F}_{AM} + \lambda_i g_i \quad (i = 1, \ldots 12)$$

or in vector form

$$(39)\quad f' = (\bar{F}_{AM}\cdot\bar{F}_{AM}) + \bar{\lambda}_1\cdot(\dot{\bar{r}} - \bar{V}) + \bar{\lambda}_4\cdot\left(\dot{\bar{V}} + \frac{GM\bar{r}}{|\bar{r}|^3} - \frac{[A_D]}{m}^T\bar{F}_{AM}\right)$$

$$+ \bar{\lambda}_7\cdot(\dot{\bar{\Psi}} - \bar{\Psi}) + \bar{\lambda}_{10}\cdot\left\{\dot{\bar{\Psi}} - [C]\left([A_\omega]^T\bar{M}_{M_T} - [S]\bar{\Psi}\right.\right.$$

$$\left.\left. - [T]\bar{\Psi} + \bar{B}\right)\right\}$$

where

$$\bar{\lambda}_1 = \begin{bmatrix}\lambda_1\\ \lambda_2\\ \lambda_3\end{bmatrix} \qquad \bar{\lambda}_4 = \begin{bmatrix}\lambda_4\\ \lambda_5\\ \lambda_6\end{bmatrix} \qquad \bar{\lambda}_7 = \begin{bmatrix}\lambda_7\\ \lambda_8\\ \lambda_9\end{bmatrix} \quad \text{and} \quad \bar{\lambda}_{10} = \begin{bmatrix}\lambda_{10}\\ \lambda_{11}\\ \lambda_{12}\end{bmatrix}$$

The Euler characteristic equations are given by

$$(40)\quad \frac{\partial f'}{\partial q} = \frac{d}{dt}\left(\frac{\partial f'}{\partial \dot{q}}\right) \qquad q = (X,Y,Z,U,V,W,\varphi_p,\varphi_y,\varphi_r,\psi_p,\psi_y,\psi_r,F_r)$$

The characteristic equations for the respective variables are given as equations (41) through (53) below:

$$(41)\quad 2\bar{F}_{AM}\cdot\frac{\partial \bar{F}_{AM}}{\partial x} + \bar{\lambda}_4\cdot\left(\frac{GM}{|\bar{r}|^3}\frac{\partial \bar{r}}{\partial x} + 3GM\,|\bar{r}|^2\frac{\partial|\bar{r}|}{\partial x}\,\bar{r}\right.$$

$$\left. - \frac{[A_D]}{m}^T\frac{\partial \bar{F}_{AM}}{\partial x}\right) + \bar{\lambda}_{10}\cdot\left(-[C][A_\omega]^T\frac{\partial \bar{M}_{MT}}{\partial x}\right) = \frac{d}{dt}\left(\bar{\lambda}_1\cdot\frac{\partial \dot{\bar{r}}}{\partial \dot{x}}\right)$$

$$(42)\quad 2\bar{F}_{AM}\cdot\frac{\partial \bar{F}_{AM}}{\partial y} + \bar{\lambda}_4\cdot\left(\frac{GM}{|\bar{r}|^3}\frac{\partial \bar{r}}{\partial y} + 3GM\,|\bar{r}|^2\frac{\partial|\bar{r}|}{\partial y}\,\bar{r}\right.$$

$$\left. - \frac{[A_D]}{m}^T\frac{\partial \bar{F}_{AM}}{\partial y}\right) + \bar{\lambda}_{10}\cdot\left(-[C][A_\omega]^T\frac{\partial \bar{M}_{MT}}{\partial y}\right) = \frac{d}{dt}\left(\bar{\lambda}_1\cdot\frac{\partial \dot{\bar{r}}}{\partial \dot{y}}\right)$$

$$(43)\quad 2\bar{F}_{AM}\cdot\frac{\partial \bar{F}_{AM}}{\partial Z} + \bar{\lambda}_4\cdot\left(\frac{GM}{|\bar{r}|^3}\frac{\partial \bar{r}}{\partial Z} + 3GM\,|\bar{r}|\frac{\partial|\bar{r}|}{\partial Z}\,\bar{r}\right.$$

$$\left. - \frac{[A_D]}{m}^T\frac{\partial \bar{F}_{AM}}{\partial Z}\right) + \bar{\lambda}_{10}\cdot\left(-[C][A_\omega]^T\frac{\partial \bar{M}_{MT}}{\partial Z}\right) = \frac{d}{dt}\left(\bar{\lambda}_1\cdot\frac{\partial \dot{\bar{r}}}{\partial \dot{Z}}\right)$$

$$(44)\quad 2\bar{F}_{AM}\cdot\frac{\partial \bar{F}_{AM}}{\partial u} - \bar{\lambda}_1\cdot\frac{\partial \bar{V}}{\partial u} + \bar{\lambda}_4\cdot\left(\frac{[A_D]}{m}^T\frac{\partial \bar{F}_{AM}}{\partial u}\right)$$

$$+ \bar{\lambda}_{10}\cdot\left(-[C][A_\omega]^T\frac{\partial \bar{M}_{MT}}{\partial u}\right) = \frac{d}{dt}\left(\bar{\lambda}_4\cdot\frac{\partial \dot{\bar{V}}}{\partial \dot{u}}\right)$$

$$(45)\quad 2\bar{F}_{AM}\cdot\frac{\partial \bar{F}_{AM}}{\partial v} - \bar{\lambda}_1\cdot\frac{\partial \bar{V}}{\partial v} + \bar{\lambda}_4\cdot\left(-\frac{[A_D]}{m}^T\frac{\partial \bar{F}_{AM}}{\partial v}\right)$$

$$+ \bar{\lambda}_{10}\cdot\left(-[C][A_\omega]^T\frac{\partial \bar{M}_{MT}}{\partial v}\right) = \frac{d}{dt}\left(\bar{\lambda}_4\cdot\frac{\partial \dot{\bar{V}}}{\partial \dot{v}}\right)$$

$$(46)\ 2\bar{F}_{AM} \cdot \frac{\partial \bar{F}_{AM}}{\partial w} - \bar{\lambda}_1 \cdot \frac{\partial \bar{V}}{\partial w} + \bar{\lambda}_4 \cdot \left(- \frac{[A_D]}{m}^T \frac{\partial \bar{F}_{AM}}{\partial w}\right)$$

$$+ \bar{\lambda}_{10} \cdot \left(- [C]\,[A_\omega]^T \frac{\partial \bar{M}_{MT}}{\partial w}\right) = \frac{d}{dt}\left(\bar{\lambda}_4 \cdot \frac{\partial \dot{\bar{V}}}{\partial \dot{w}}\right)$$

$$(47)\ 2\bar{F}_{AM} \cdot \frac{\partial \bar{F}_{AM}}{\partial \varphi_p} + \bar{\lambda}_4 \cdot \left(- \frac{1}{m} \frac{\partial [A_D]}{\partial \varphi_p}^T \bar{F}_{AM} - \frac{1}{m} [A_D]^T \frac{\partial \bar{F}_{AM}}{\partial \varphi_p}\right)$$

$$+ \bar{\lambda}_{10} \cdot \left(- [C]\,[A_\omega]^T \frac{\partial \bar{M}_{MT}}{\partial \varphi_p}\right) = \frac{d}{dt}\left(\bar{\lambda}_7 \cdot \frac{\partial \dot{\bar{\varphi}}}{\partial \dot{\varphi}_p}\right)$$

$$(48)\ 2\bar{F}_{AM} \cdot \frac{\partial \bar{F}_{AM}}{\partial \varphi_y} + \bar{\lambda}_4 \cdot \left(-\frac{1}{m} \frac{\partial [A_D]}{\partial \varphi_y} \bar{F}_{AM} - \frac{1}{m} [A_D]^T \frac{\partial \bar{F}_{AM}}{\partial \varphi_y}\right)$$

$$+ \bar{\lambda}_{10} \cdot \left(- [C]\,[A_\omega]^T \left(\frac{\partial \bar{M}_{MT}}{\partial \varphi_y}\right) - \frac{\partial [C]}{\partial \varphi_y} [A_\omega]^T \bar{M}_{MT} - [C] \frac{\partial [A_\omega]}{\partial \varphi_y}^T\right.$$

$$\left.\bar{M}_{MT} - \frac{\partial [S]}{\partial \varphi_y} - \frac{\partial [T]}{\partial \varphi_y} \bar{\psi} + \frac{\partial \bar{B}}{\partial \varphi_y}\right) = \frac{d}{dt}\left(\bar{\lambda}_7 \cdot \frac{\partial \dot{\bar{\varphi}}}{\partial \dot{\varphi}_y}\right)$$

$$(49)\ 2\bar{F}_{AM} \cdot \frac{\partial \bar{F}_{AM}}{\partial \varphi_r} + \bar{\lambda}_4 \cdot \left(-\frac{1}{m} \frac{\partial [A_D]}{\partial \varphi_r}^T \bar{F}_{AM} - \frac{1}{m} [A_D]^T \frac{\partial \bar{F}_{AM}}{\partial \varphi_r}\right)$$

$$+ \bar{\lambda}_{10} \cdot \left(- [C]\,[A_\omega]^T \frac{\partial \bar{M}_{MT}}{\partial \varphi_r} - \frac{\partial [C]}{\partial \varphi_r} [A_\omega]^T \bar{M}_{M_T} - [C] \frac{\partial [A_\omega]}{\partial \varphi_r}^T\right.$$

$$\left.\bar{M}_{M_T} - \frac{\partial [S]}{\partial \varphi_r} \bar{\psi} - \frac{\partial [T]}{\partial \varphi_r} \bar{\psi} + \frac{\partial \bar{B}}{\partial \varphi_r}\right) = \frac{d}{dt}\left(\bar{\lambda}_7 \cdot \frac{\partial \dot{\bar{\varphi}}}{\partial \dot{\varphi}_r}\right)$$

$$(50)\ - \bar{\lambda}_7 \cdot \frac{\partial \bar{\Psi}}{\partial \psi_p} + \bar{\lambda}_{10} \cdot \left(- [S] \frac{\partial \Psi}{\partial \psi_p} - [T] \frac{\partial \Psi}{\partial \psi_p} + \frac{\partial \bar{B}}{\partial \psi_p}\right) = \frac{d}{dt}\left(\bar{\lambda}_{10} \cdot \frac{\partial \dot{\bar{\Psi}}}{\partial \dot{\psi}_p}\right)$$

$$(51) - \bar{\lambda}_7 \cdot \frac{\partial \bar{\Psi}}{\partial \Psi_y} + \bar{\lambda}_{10} \cdot \left(-\frac{\partial [S]}{\partial \Psi_y} \bar{\Psi} - [S] \frac{\partial \bar{\Psi}}{\partial \Psi_y} - \frac{\partial [T]}{\partial \Psi_y} \bar{\Psi} - [T] \frac{\partial \bar{\Psi}}{\partial \Psi_y} + \frac{\partial \bar{B}}{\partial \Psi_y}\right) = \frac{d}{dt}\left(\bar{\lambda}_{10} \cdot \frac{\partial \dot{\bar{\Psi}}}{\partial \dot{\Psi}_y}\right)$$

$$(52) - \bar{\lambda}_7 \cdot \frac{\partial \bar{\Psi}}{\partial \Psi_r} + \bar{\lambda}_{10} \cdot \left(-\frac{\partial [S]}{\partial \Psi_r} \bar{\Psi} - [S] \frac{\partial \bar{\Psi}}{\partial \Psi_r} - \frac{\partial [T]}{\partial \Psi_r} \bar{\Psi} - [T] \frac{\partial \bar{\Psi}}{\partial \Psi_r} + \frac{\partial \bar{B}}{\partial \Psi_r}\right) = \frac{d}{dt}\left(\bar{\lambda}_{10} \cdot \frac{\partial \dot{\bar{\Psi}}}{\partial \dot{\Psi}_r}\right)$$

$$(53) \quad \bar{\lambda}_{10} \cdot \left(-[C][A_\omega]^T \frac{\partial \bar{M}_{MT}}{\partial F_r}\right) = 0$$

VII. COMPUTATIONAL PROCEDURE

The desired trajectory then is one which satisfies the original twelve first order equations of motion and the thirteen Euler characteristic equations. The equations are such that a solution in closed form seems improbable to obtain. However, if the Runge-Kutta method is used as a basic numerical integration scheme, the system can be programmed for the digital computer. Starting with initial values for the state variables and the Lagrangian multipliers, trajectories can be generated that satisfy the system of governing equations to a high degree of accuracy. Since the equations involved are long and hard to work with, it is convenient to outline a computational scheme from the system of equations written in functional form. The system can be written as follows, where the longer equations are not written out but represented in functional notation:

$$\dot{x} - u = 0 \tag{54}$$

$$\dot{y} - v = 0 \tag{55}$$

$$\dot{z} - w = 0 \tag{56}$$

$$\dot{u} = \dot{u}(x,y,z,u,v,w, \varphi_r, \varphi_p, \varphi_y) \tag{57}$$

$$\dot{v} = \dot{v}(x,y,z,u,v,w, \varphi_r, \varphi_p, \varphi_y) \tag{58}$$

$$\dot{w} = \dot{w}(x,y,z,u,v,w, \varphi_r, \varphi_p, \varphi_y) \tag{59}$$

$$\dot{\varphi}_p - \psi_p = 0 \tag{60}$$

$$\dot{\varphi}_y - \psi_y = 0 \tag{61}$$

$$\dot{\varphi}_r - \psi_r = 0 \tag{62}$$

$$\dot{\psi}_p = \dot{\psi}_p (x,y,z,u,v,w, \varphi_p, \varphi_r, \varphi_y, \psi_p, \psi_r, \psi_y, F_r) \tag{63}$$

(64) $\dot{\psi}_y = \dot{\psi}_y (x, y, z, u, v, w, \varphi_p, \varphi_r, \varphi_y, \psi_p, \psi_r, \psi_y, F_r)$

(65) $\dot{\psi}_r = \dot{\psi}_r (x, y, z, u, v, w, \varphi_p, \varphi_r, \varphi_y, \psi_p, \psi_r, \psi_y, F_r)$

(66) $\dot{\lambda}_1 = \dot{\lambda}_1 (x, y, z, u, v, w, \varphi_p, \varphi_r, \varphi_y, \lambda_4, \lambda_5, \lambda_6, \lambda_{10}, \lambda_{11}, \lambda_{12})$

(67) $\dot{\lambda}_2 = \dot{\lambda}_2 (x, y, z, u, v, w, \varphi_p, \varphi_r, \varphi_y, \lambda_4, \lambda_5, \lambda_6, \lambda_{10}, \lambda_{11}, \lambda_{12})$

(68) $\dot{\lambda}_3 = \dot{\lambda}_3 (x, y, z, u, v, w, \varphi_p, \varphi_r, \varphi_y, \lambda_4, \lambda_5, \lambda_6, \lambda_{10}, \lambda_{11}, \lambda_{12})$

(69) $\dot{\lambda}_4 = \dot{\lambda}_4 (x, y, z, u, v, w, \varphi_p, \varphi_r, \varphi_y, \lambda_1, \lambda_4, \lambda_5, \lambda_6, \lambda_{10}, \lambda_{11}, \lambda_{12})$

(70) $\dot{\lambda}_5 = \dot{\lambda}_5 (x, y, z, u, v, w, \varphi_p, \varphi_r, \varphi_y, \lambda_2, \lambda_4, \lambda_5, \lambda_6, \lambda_{10}, \lambda_{11}, \lambda_{12})$

(71) $\dot{\lambda}_6 = \dot{\lambda}_6 (x, y, z, u, v, w, \varphi_p, \varphi_r, \varphi_y, \lambda_3, \lambda_4, \lambda_5, \lambda_6, \lambda_{10}, \lambda_{11}, \lambda_{12})$

(72) $\dot{\lambda}_7 = \dot{\lambda}_7 (x, y, z, u, v, w, \varphi_r, \varphi_p, \varphi_y, \lambda_4, \lambda_5, \lambda_6, \lambda_{10}, \lambda_{11}, \lambda_{12})$

(73) $\dot{\lambda}_8 = \dot{\lambda}_8 (x, y, z, u, v, w, \varphi_r, \varphi_p, \varphi_y, \lambda_4, \lambda_5, \lambda_6, \lambda_{10}, \lambda_{11}, \lambda_{12}, \psi_p, \psi_y, \psi_r, F_r)$

(74) $\dot{\lambda}_9 = \dot{\lambda}_9 (x, y, z, u, v, w, \varphi_r, \varphi_p, \varphi_y, \lambda_4, \lambda_5, \lambda_6, \lambda_{10}, \lambda_{11}, \lambda_{12}, \psi_p, \psi_y, \psi_r, F_r)$

(75) $\dot{\lambda}_{10} = \dot{\lambda}_{10} (\lambda_7, \lambda_{10}, \lambda_{11}, \lambda_{12}, \varphi_r, \varphi_y, \psi_p, \psi_y, \psi_r)$

(76) $\dot{\lambda}_{11} = \dot{\lambda}_{11} (\lambda_8, \lambda_{10}, \lambda_{11}, \lambda_{12}, \varphi_r, \varphi_y, \psi_p, \psi_y, \psi_r)$

(77) $\dot{\lambda}_{12} = \dot{\lambda}_{12}(\lambda_9, \lambda_{10}, \lambda_{11}, \lambda_{12}, \varphi_r, \varphi_y, \psi_p, \psi_y, \psi_r)$

(78) $f(\lambda_{10}, \lambda_{11}, \lambda_{12}, \varphi_y, \varphi_r) = 0$

Before integration of the system forward through time can be accomplished, an expression must be found for F_r in terms of the state variables. Therefore, the following analytical steps must be taken to get the system of equations in proper form to integrate:

1. Solve (78) for λ_{10}, obtaining $\lambda_{10} = \lambda_{10}(\lambda_{11}, \lambda_{12}, \varphi_y, \varphi_r)$

2. Differentiate the expression for λ_{10} with respect to time, obtaining $\dot{\lambda}_{10} = \dot{\lambda}_{10}(\lambda_{11}, \lambda_{12}, \varphi_y, \varphi_r, \dot{\lambda}_{11}, \dot{\lambda}_{12}, \psi_y, \psi_r)$

3. Substitute in the above expression the values of $\dot{\lambda}_{11}$ and $\dot{\lambda}_{12}$ from equations (76) and (77), obtaining
$\dot{\lambda}_{10} = \dot{\lambda}_{10}(\lambda_8, \lambda_9, \lambda_{10}, \lambda_{11}, \lambda_{12}, \varphi_y, \varphi_r, \psi_p, \psi_y, \psi_r)$

4. Differentiate this expression for $\dot{\lambda}_{10}$, finding an expression for $\ddot{\lambda}_{10}$.
$\ddot{\lambda}_{10} = \ddot{\lambda}_{10}(\lambda_8, \lambda_9, \lambda_{10}, \lambda_{11}, \lambda_{12}, \varphi_y, \varphi_r, \psi_p, \psi_y, \psi_r, \dot{\lambda}_8, \dot{\lambda}_9, \dot{\lambda}_{10}, \dot{\lambda}_{11}, \dot{\lambda}_{12}, \dot{\psi}_p, \dot{\psi}_y, \dot{\psi}_r)$

5. Substitute into the above expression the respective values for $\dot{\lambda}_8, \dot{\lambda}_9, \dot{\lambda}_{10}, \dot{\lambda}_{11}, \dot{\lambda}_{12}, \dot{\psi}_p, \dot{\psi}_y$ and $\dot{\psi}_r$ from equations (73), (74), (75), (76), (77), (63), (64), and (65), obtaining the following:

(79) $\ddot{\lambda}_{10} = \ddot{\lambda}_{10}(\lambda_4, \lambda_5, \lambda_6, \lambda_7, \lambda_8, \lambda_9, \lambda_{10}, \lambda_{11}, \lambda_{12}, x, y, z, u, v, w, \varphi_p, \varphi_y, \varphi_r, \psi_p, \psi_y, \psi_r, F_r)$

6. Differentiate equation (75) with time, obtaining

$$\ddot{\lambda}_{10} = \ddot{\lambda}_{10}(\lambda_7, \lambda_{10}, \lambda_{11}, \lambda_{12}, \varphi_r, \varphi_y, \psi_p, \psi_y, \psi_r, \dot{\lambda}_7, \dot{\lambda}_{10}, \dot{\lambda}_{11}, \dot{\lambda}_{12}, \dot{\psi}_p, \dot{\psi}_y, \dot{\psi}_r)$$

7. Substitute in the above expression the respective values of $\dot{\lambda}_7$, $\dot{\lambda}_{10}$, $\dot{\lambda}_{11}$, $\dot{\lambda}_{12}$, $\dot{\psi}_p$, $\dot{\psi}_y$ and $\dot{\psi}_r$ from equations (72), (75), (76), (77), (63), (64), and (65), obtaining the following:

(80) $\ddot{\lambda}_{10} = \ddot{\lambda}_{10}(\lambda_4, \lambda_5, \lambda_6, \lambda_7, \lambda_8, \lambda_9, \lambda_{10}, \lambda_{11}, \lambda_{12}, \varphi_r, \varphi_y, \varphi_p, \psi_r, \psi_y, \psi_p, x, y, z, u, v, w, F_r)$

8. Equate the two expressions for $\ddot{\lambda}_{10}$ given as equations (79) and (80) and solve for F_r.

(81) $F_r = F_r(\lambda_4, \lambda_5, \lambda_6, \lambda_7, \lambda_8, \lambda_9, \lambda_{10}, \lambda_{11}, \lambda_{12}, \varphi_r, \varphi_y, \varphi_p, \psi_r, \psi_y, \psi_p, x, y, z, u, v, w)$

9. Now that an expression for F_r has been obtained in terms of the state variables, the original system of equations can be simplified by elimination of one of the Lagrangian multipliers.

10. Use the expressions for λ_{10} and $\dot{\lambda}_{10}$ from (78) to eliminate λ_{10} from equations (54) through (77) and (81).

11. Equation (75) now becomes a relation between $\dot{\lambda}_{11}$ and $\dot{\lambda}_{12}$. Using this equation and the expressions for $\dot{\lambda}_{11}$ and $\dot{\lambda}_{12}$ given by equations (76) and (77), new expressions are obtained for $\dot{\lambda}_{11}$ and $\dot{\lambda}_{12}$ as follows:

(82) $\dot{\lambda}_{11} = \dot{\lambda}_{11}(\lambda_7, \lambda_8, \lambda_9, \lambda_{12}, \varphi_y, \varphi_r, \psi_y, \psi_r, \psi_p)$.

(83) $\dot{\lambda}_{12} = \dot{\lambda}_{12}(\lambda_7, \lambda_8, \lambda_9, \lambda_{12}, \varphi_y, \varphi_r, \psi_y, \psi_r, \psi_p)$.

A computational procedure can now be given as follows:

(a) Assume initial values for $\lambda_1, \lambda_2, \lambda_3, \lambda_4, \lambda_5, \lambda_6, \lambda_7, \lambda_8, \lambda_9, \lambda_{10}, \lambda_{11}, \lambda_{12}, x, y, z, u, w, \varphi_p, \varphi_y, \varphi_r, \psi_p, \psi_y$, and ψ_r.

(b) Calculate an initial value for F_r from (81).

(c) Calculate:

$\dot{u}$ from (57)
$\dot{v}$ from (58)
$\dot{w}$ from (59)
$\dot{\psi}_p$ from (63)
$\dot{\psi}_y$ from (64)
$\dot{\psi}_r$ from (65)
$\dot{\lambda}_1$ from (66)
$\dot{\lambda}_2$ from (67)
$\dot{\lambda}_3$ from (68)
$\dot{\lambda}_4$ from (69)
$\dot{\lambda}_5$ from (70)
$\dot{\lambda}_6$ from (71)
$\dot{\lambda}_7$ from (72)

$\dot{\lambda}_8$ from (73)

$\dot{\lambda}_9$ from (74)

$\dot{\lambda}_{11}$ from (82)

$\dot{\lambda}_{12}$ from (83).

(d) Integrate the following expressions twice for values at the n + 1 time step:

Equation (57) for u and x

Equation (58) for v and y

Equation (59) for w and z

Equation (63) for ψ_p and φ_p

Equation (64) for ψ_y and φ_y

Equation (65) for ψ_r and φ_r

(e) Integrate the following equations once for values at the n + 1 time step:

Equation (66) for λ_1

Equation (67) for λ_2

Equation (68) for λ_3

Equation (69) for λ_4

Equation (70) for λ_5

Equation (71) for λ_6

Equation (72) for λ_7

Equation (73) for λ_8

Equation (74) for λ_9

Equation (82) for λ_{11}

Equation (83) for λ_{12}

(f) Repeat the process starting with n + 1 values.

VIII. CONCLUSIONS

The problem presented in this paper is similar to other vehicle performance optimization studies that have been published recently with the following exceptions:

1. The full six-degrees of freedom, rigid body constraint equations are used. In most of the available literature either the rotational equations of motion have been ignored entirely or else the assumption is made that the dynamical motion of the attitude loop can be replaced by its instantaneous steady state solution.
2. The vehicle used is assumed to have an off-set center of gravity so that maneuvering is possible using roll control only.
3. The magnitude of the roll control force is used as a control variable. In most of the previous work one or more of the gimbal angles have been used as control variables.

It is not known by this investigator whether hardware can be designed to give the F_r specified by this analysis in an actualy flight. However, the problem formulation does show that F_r appears to be the "natural" control variable when the vehicle is treated as a rigid body with the full six-degrees of freedom. F_r always appears linearly and computational problems are not nearly as bad as might have been expected if the control had appeared in the constraint equations in a more complicated manner.

The trajectories generated from the system of equations derived herein satisfy the original constraint equations as well as the Euler characteristic equations. However, satisfaction of the Euler equations is a necessary but not sufficient condition for a minimum. In order to insure that a trajectory gives a minimum value to the given integral, the Legendre and Jacobi conditions must be satisfied.

BIBLIOGRAPHY

Bliss, G. A. Lectures On The Calculus of Variations. Chicago: The University of Chicago Press, 1946.

Fox, Charles. An Introduction to The Calculus of Variations. London: Oxford University Press, 1954.

Goldstein, Herbert. Classical Mechanics. Reading, Massachusetts: Addison-Wesley Publishing Company, Inc., 1959.

Lanczos, Cornelius. The Variational Principles of Mechanics. Toronto: University of Toronto Press, 1949.

McCuskey, S. W. An Introduction to Advanced Dynamics. Reading, Massachusetts: Addison-Wesley Publishing Company, Inc., 1959.

Miner, W. E. Methods for Trajectory Computation, NASA - Marshall Space Flight Center, Internal Note, May 10, 1961.

AERONUTRONIC

TRAJECTORIES WITH CONSTANT NORMAL FORCE STARTING FROM A CIRCULAR ORBIT

by

Richard R. Auelmann

Newport Beach, California

TRAJECTORIES WITH CONSTANT NORMAL FORCE STARTING FROM A CIRCULAR ORBIT

Richard R. Auelmann

Aeronutronic, Newport Beach, California

The totality of motions for a particle initially in a circular Kepler orbit and acted upon by a constant, in-plane normal force is determined. The orbits lie in a ring bounded by two circles, the first with radius equal to the radius of the initial Kepler orbit and the second with radius dependent on the normal force. The second circle lies outside the first circle when the normal force is outward and lies inside when the normal force is inward. The radius of the second circle cannot exceed twice the radius of the first circle and is reached only when the normal force is 0.230 times the gravity force at the initial radius. The point of central attraction is reached only when the normal force is 2.809 times the gravity force at the initial radius. The orbit path oscillates periodically between the two circles. However, the orbits are not in general periodic since they do not close. When the magnitude of the normal force is small, the orbits are direct, while when the force is large, the orbits are direct near the first circle and retrograde near the second circle.

Introduction

A particle is moving in a circular Kepler orbit when a constant force is applied perpendicular to the instantaneous velocity vector and in the plane of motion. What is the resulting motion of the particle?

This problem with the applied force in the normal direction and three other closely related problems with the applied force in the radial, circumferential and tangential directions have received considerable attention during the past ten years. Of the four problems only the radial case has been solved in terms of tabulated integrals (elliptic integrals of the first, second and third kinds). Next to the radial case, the normal case appears to be the easiest to analyze. In spite of this fact, the motion with normal force has not been solved in the sense that Copeland[1] (with corrections by Karrenberg[2] and Au[3]) has solved the radial case.

The possibility of reducing the normal case to quadratures was revealed by Rodriques.[4] The complete solution is developed in this paper for the entire range of normal force. Since the applied force is perpendicular to the velocity, the energy is conserved. Consequently, the semi-major axis of the instantaneous Kepler ellipse (the path which would be traced by the particle if the normal force were removed) is equal to the radius of the initial circular orbit. The particle can never move farther than twice the radius of the initial orbit from the point of central attraction.

The energy integral may be used to reduce the fourth order system of equations, which describe the motion, by two orders. A complete reduction to quadratures is possible when the problem is formulated in plane

polar coordinates but, unlike in the radial case, the quadratures are not tabulated integrals. However, even without evaluating the quadratures, the totality of motions can be determined. The first step in this direction is to determine the angular momentum as an explicit function of the distance from the point of central attraction.

Reduction to Quadratures

Let O be the point of central attraction and P be the particle. The constant normal force f (divided by the mass of P) is positive in the direction shown in Fig. 1. The angle between the radial direction and the instantaneous velocity vector v is ϕ. The unit of mass is selected so that the universal constant of gravitation is unity. The energy and angular momentum are given by

$$E = \frac{1}{2} v^2 - \frac{1}{r}, \qquad h = r^2\dot{\theta}$$

respectively. E is a constant but h is not. Its time derivative is given by

$$\dot{h} = - fr \cos \phi = - fr\dot{r}/v$$

Using the energy integral to eliminate v, the differential form

$$dh = - fr\left[2(E + \frac{1}{r})\right]^{-\frac{1}{2}} dr$$

is obtained. Integration in the case when E is negative (corresponding to a Kepler ellipse) provides

$$h = \frac{- f}{2(2)^{\frac{1}{2}}E}\left\{r^2(E + \frac{1}{r})^{\frac{1}{2}}(1 - \frac{3}{2Er}) - \frac{3}{2E}(-E)^{-\frac{1}{2}} \tan^{-1}\left[(E + \frac{1}{r})/-E\right]^{\frac{1}{2}}\right\} + c$$

where c is the constant of integration.

The following analysis is based on the condition that the initial Kepler orbit is circular with radius r_0. E and the initial value for h are given by

$$E = -\frac{1}{2r_0}, \qquad h_0 = r_0^{\frac{1}{2}}$$

With the nondimensional parameters

$$x = r/r_0, \qquad \alpha = fr_0^2$$

the constant of integration becomes

$$c = r_0^{\frac{1}{2}}\left[1 - \alpha(2 + \frac{3\pi}{4})\right]$$

and

$$h = r_0^{\frac{1}{2}}(1 - \alpha U) \tag{1}$$

where

$$U(x) = 2 + \frac{3\pi}{4} - \frac{1}{2}(x + 3)(2x - x^2)^{\frac{1}{2}} - 3\tan^{-1}\left(\frac{2}{x} - 1\right)^{\frac{1}{2}}$$

U is imaginary when $x > 2$. The reason is that the semi-major axis of the instantaneous Kepler ellipse would exceed r_0 which is impossible since energy is conserved. The critical values for U are

$$U(0) = 2 - \frac{3\pi}{4} \approx -0.356$$

$$U(1) = 0$$

$$U(2) = 2 + \frac{3\pi}{4} \approx 4.356$$

U is positive for $x > 1$ and negative for $x < 1$.

Having determined h as an explicit function of x it is possible to obtain the time in quadrature. The energy equation may be written as

$$\left(\frac{dr}{dt}\right)^2 = 2\left(E + \frac{1}{r}\right) - \frac{h^2}{r^2}$$

$$= \left(\frac{2}{r} - \frac{1}{r_0}\right) - \frac{r_0}{r^2}(1 - \alpha U)^2$$

The nondimensional form

$$\left(\frac{dx}{d\tau}\right)^2 = \frac{1}{x^2}\left[2x - x^2 - (1 - \alpha U)^2\right] \tag{2}$$

is obtained after multiplying by r_0 and replacing t by $\tau = n_0 t$ where $n_0 = r_0^{-3/2}$ is the mean motion along the instantaneous Kepler ellipse. The time quadrature

$$\tau = \int x\left[2x - x^2 - (1 - \alpha U)^2\right]^{-\frac{1}{2}} dx + \text{constant} \tag{3}$$

is analogous to the Kepler equation for the Kepler problem.

The differential equation for the orbit

$$\left(\frac{dx}{d\theta}\right)^2 = \left(\frac{x}{1 - \alpha U}\right)^2\left[2x - x^2 - (1 - \alpha U)^2\right] \tag{4}$$

is obtained from (2) by the operation

$$\frac{dx}{d\theta} = \frac{dx}{d\tau}\frac{d\tau}{d\theta}$$

where

$$\frac{d\theta}{d\tau} = \frac{1}{x^2}(1 - \alpha U) \tag{5}$$

which follows from the definition $h = r^2\dot{\theta}$. The orbit equation is also reducible to quadrature:

$$\theta = \int \frac{1 - \alpha U}{x}\left[2x - x^2 - (1 - \alpha U)^2\right]^{-\frac{1}{2}} dx + \text{constant} \tag{6}$$

The quadratures (3) and (6) appear to be intractable. Nevertheless a complete qualitative description of the motion can be obtained without carrying out the integration.

The Regions of Motion

From Eq. (2) the motion is imaginary if

$$f(\rho) = -(x-1)^2 + 2\alpha U - \alpha^2 U^2$$

is negative. A necessary (though not sufficient) condition for the motion to be real is that αU be positive. An examination of the sign of U shows that, if the normal force is directed initially outward (inward), the trajectory will never move interior (exterior) to the initial circular orbit.

The question arises whether or not f(x) vanishes at any other value x = a besides 1. Certainly a would depend on α. The two roots for α which satisfy the equation f(x) = 0 are

$$\alpha(x) = \frac{1}{U}\left[1 \pm (2x - x^2)^{\frac{1}{2}}\right] \tag{7}$$

from which

$$\alpha(0) = \left(2 - \frac{3\pi}{4}\right)^{-1} \approx -2.809$$

$$\alpha(1) = \pm\infty$$

$$\alpha(2) = \left(2 + \frac{3\pi}{4}\right)^{-1} \approx 0.230$$

The values for α which satisfy Eq. (7) are shown as functions of x in Fig. 2. The solid curve in Fig. 2 occurs when the minus sign is taken in Eq. (7), while the two dashed curves occur when the plus sign is used. The value for x along these curves is denoted by a. For any given value of α the function f(x) is

positive and the motion is real in the region between x = 1 and x = a. The exterior regions are inaccessible and are so labeled in Fig. 2.

It is significant that a unique value $\alpha(0)$ is required to reach the origin x = 0 and that a second unique value $\alpha(2)$ is required to reach the outer limit x = 2. Indeed it is logical to expect the motion to be qualitatively different in the regions: $\alpha < \alpha(0)$, $\alpha(0) < \alpha < 0$, $0 < \alpha < \alpha(2)$ and $\alpha > \alpha(2)$.

Qualitative Description of the Motion

Considerable information can be obtained by examining Eq. (2):

$$\left(\frac{dx}{d\tau}\right)^2 = R(x) , \qquad R(x) = \frac{1}{x^2}\left[2x - x^2 - (1 - \alpha U)^2\right]$$

R(x) has the following properties:

1) It is continuous.
2) It is zero at x = 1 and x = a. The only exception occurs when a = 0.
3) It is positive in the region between x = 1 and x = a.
4) dR/dx does not vanish at x = 1 and x = a.

Consequently the trajectory $x = x(\tau)$ has the following characteristics:

1) $x(\tau)$ lies between x = 1 and x = a for all values of τ.
2) $dx/d\tau$ only vanishes at x = 1 and x = a. However, at a = 0 the derivative does not exist.
3) $x(\tau) = x(-\tau)$ when the origin $\tau = 0$ is taken at x = 1 or x = a.
4) $x(\tau)$ is periodic with period 2K, that is, $x(\tau) = x(\tau + 2K)$.

The trajectories have the forms shown in Fig. 3. It remains to establish the forms for the orbits, $x = x(\theta)$.

The direction of motion along the boundary $x = 1$ is direct. In fact $d\theta/d\tau = 1$. The direction of motion along the boundary $x = a$ can be established from Eq. (5) which provides:

$d\theta/d\tau > 0$ for $\alpha(0) < \alpha < \alpha(2)$

$d\theta/d\tau < 0$ for $\alpha < \alpha(0)$ and $\alpha > \alpha(2)$

$d\theta/d\tau = 0$ at $\alpha = \alpha(2)$

$d\theta/d\tau = +\infty$ as $\alpha \to \alpha(0)$ from the positive side

$d\theta/d\tau = -\infty$ as $\alpha \to \alpha(0)$ from the negative side

An examination of Eq. (4) shows that $dx/d\theta$ vanishes at $x = 0$ and $x = a$ except at $a = 2$ where $dx/d\theta$ does not exist.

A complete picture (Fig. 4) of the orbits can now be formed. x is periodic in τ and θ, however, the orbits themselves are not in general periodic since they do not close. Indeed the only periodic orbits which do exist are isolated. The sign of $d\theta/d\tau$ determines whether the motion is direct or retrograde. For $\alpha = \alpha(2)$ the orbits have cusps at the outer boundary and for $\alpha = \alpha(0)$ the orbits pass through 0.

REFERENCES

1. Copeland, J., "Interplanetary Trajectories Under Low Thrust Radial Acceleration," ARS J. 29, 267-271 (1959).

2. Karrenberg, H. K., "Note on 'Interplanetary Trajectories Under Low Thrust Radial Acceleration'," ARS J. 30, 130-131 (1960).

3. Au, G., "Corrections for 'Interplanetary Trajectories Under Low Thrust Radial Acceleration'," ARS J. 30, 708 (1960).

4. Rodriquez, E., "A Method for Determining Steering Programs for Low-Thrust Interplanetary Vehicles," ARS J. 29, 783-788 (1959).

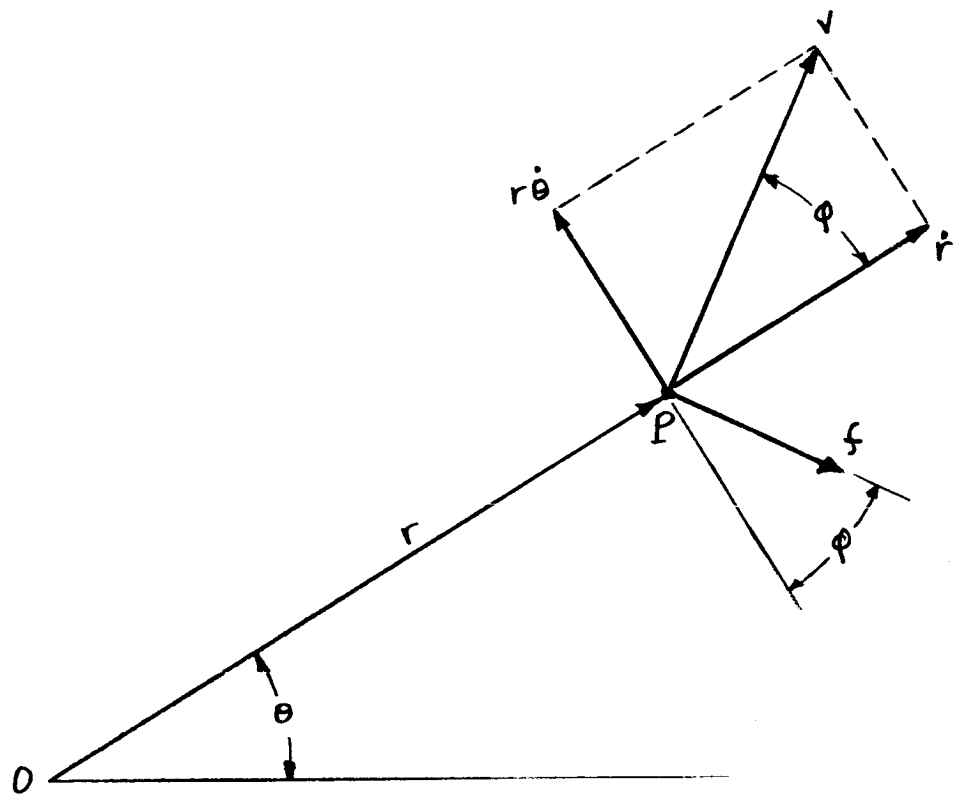

Fig. 1. Geometry for the normal force, f

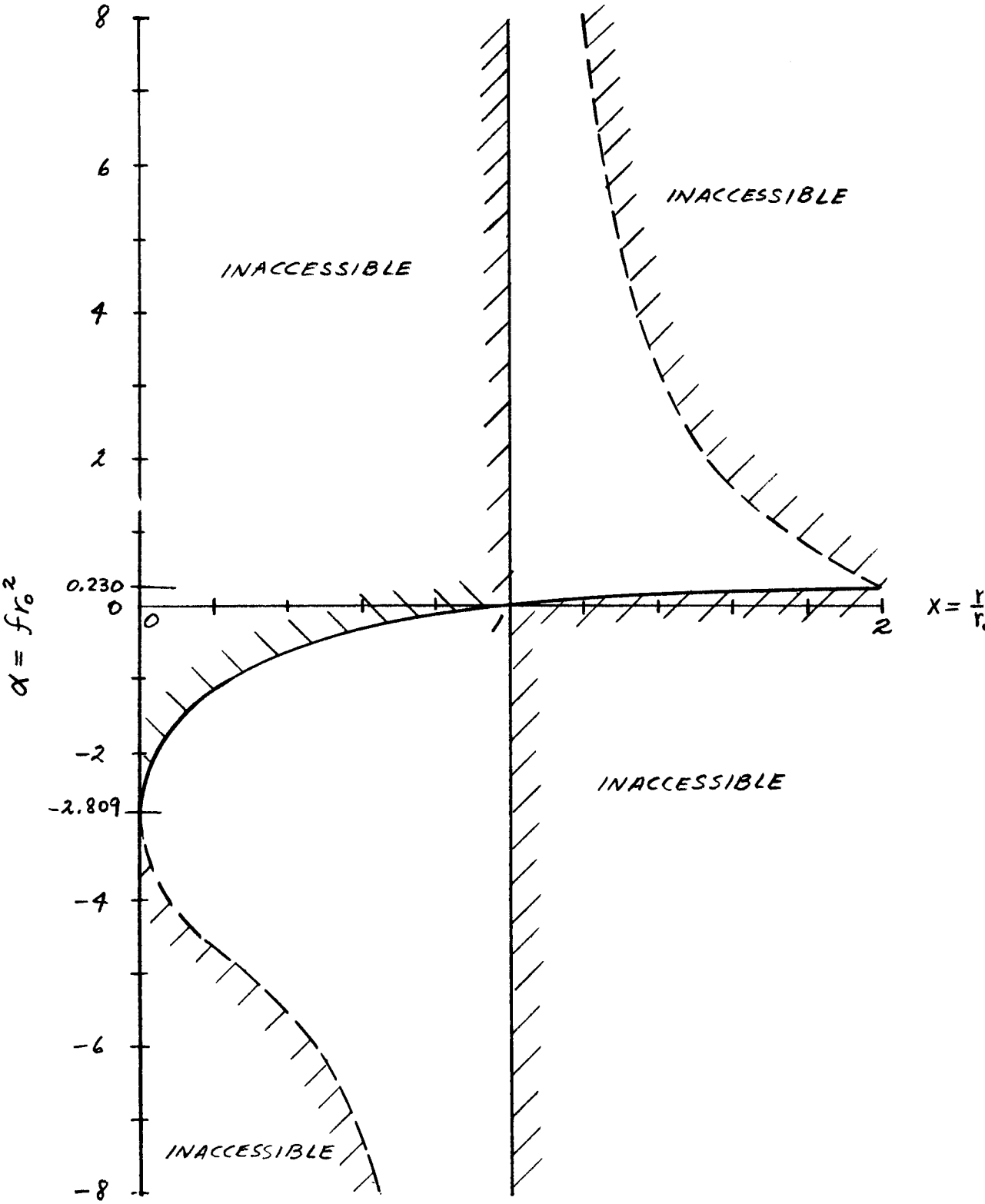

Fig. 2 Regions of motion

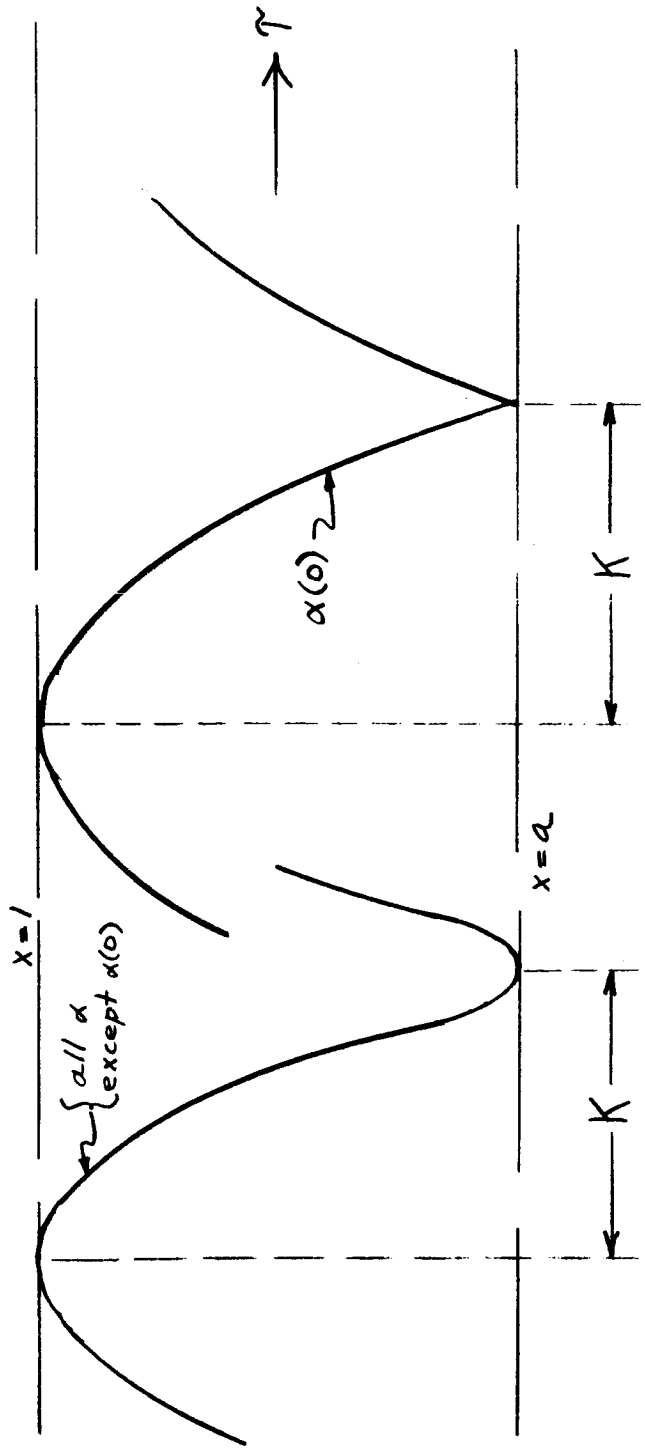

Fig. 3 The trajectories $x = x(\tau)$

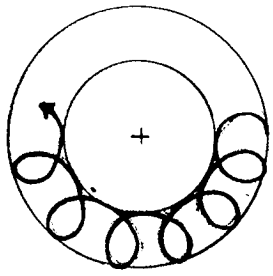

a) $\alpha < \alpha(0)$

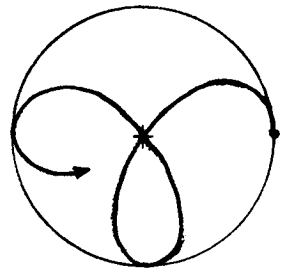

b) $\alpha = \alpha(0)$

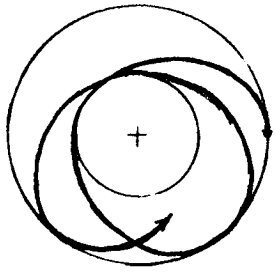

c) $\alpha(0) < \alpha < 0$

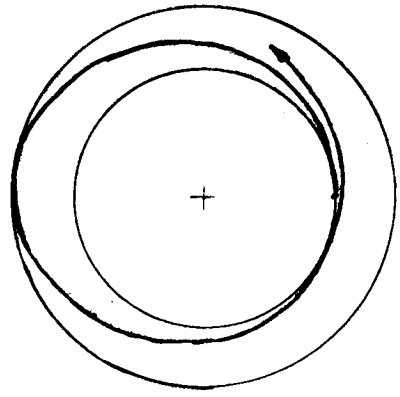

d) $0 < \alpha < \alpha(2)$

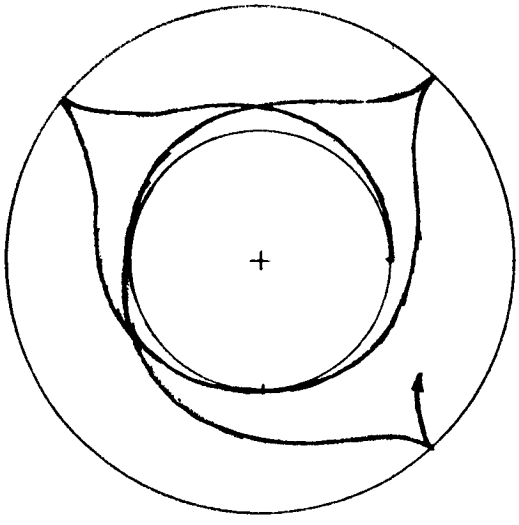

e) $\alpha = \alpha(2)$

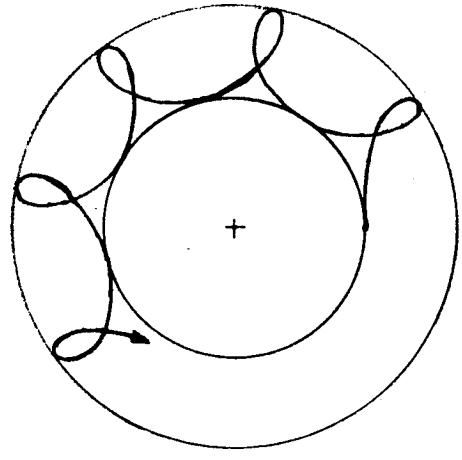

f) $\alpha > \alpha(2)$

Fig 4 Totality of Motions

OPTIMUM TWO-IMPULSE ORBITAL TRANSFER AND RENDEZVOUS BETWEEN INCLINED ELLIPTICAL ORBITS

by

Gary A. McCue

Space Sciences Laboratory
Space & Information Systems Division
North American Aviation, Inc.
Downey, California

Special Report No. 2

July 18, 1963

Contracts NAS8-1582 and NAS8-5211

Prepared For

George C. Marshall Space Flight Center
National Aeronautics and Space Administration
Huntsville, Alabama

FOREWARD

The study presented here constitutes an extension of work performed for Marshall Space Flight Center under Contract NAS8-1582 and is being used extensively in work under Contract NAS8-5211. Much of this work was done in the interim between contracts NAS8-1582 and NAS8-5211. It is presented here with the aim of providing in these progress reports on Space Flight and Guidance Theory a series of papers giving the results of rendezvous studies made at the Space Sciences Laboratory of the Space & Information Systems Division of North American Aviation.

The author wishes to acknowledge the assistance and technical suggestions of H. W. Bell, Assistant Director of Space Sciences Laboratory. The contributions of P. R. Des Jardins, who participated in studies which led to many of the results presented here, are also acknowledged.

ABSTRACT

Mathematical formulations of the general--inclined orbits and free end points--optimum two-impulse orbital transfer problem lead to expressions which, except for special cases, are analytically intractable. Numerical techniques were developed and used to study optimum transfer modes--many orbit pairs yield four useful relative optima. A parameter space was adopted to represent the impulse function; that is, impulse is a function of take-off point, arrival point, and transfer orbit semi-latus rectum. This abstraction allowed visualization and detailed examination of surfaces of constant impulse--thus revealing the structure of the impulse function. As a result of this study, one may predict the gross properties of "impulse function spaces" and consequently determine the optimum two-impulse orbital transfer circumstances for any pair of elliptical orbits. The entire procedure of impulse optimization, requiring less than one minute of IBM 7090 time, is accomplished for free end points; i.e., impulse is minimized with respect to take-off and arrival points, as well as transfer orbit geometry. The method is easily extended to computation of time constraints for two-impulse rendezvous. An approximation to optimum two-impulse rendezvous when time constraints are specified is also explored.

TABLE OF CONTENTS

LIST OF FIGURES

I. INTRODUCTION

Success of a variety of space missions depends ultimately upon an ability to maneuver in orbit. The high fuel requirements usually associated with orbit-changing maneuvers make it essential that optimum orbital transfer modes be investigated--optimum in the sense of minimum fuel requirements. While these modes might not be employed in the actual mission, they do represent lower bounds against which vehicle design compromises may be measured.

This paper concerns optimum two-impulse orbital transfer and rendezvous between any pair of unperturbed elliptical orbits. The objective of the orbital transfer maneuver is to transform the five orbital elements, p, e, ω, i, Ω of an initial orbit to match corresponding elements of a final orbit. This is accomplished by instantaneous velocity changes (impulses) which may be applied at arbitrary points on the initial and final orbits. Impulse optimization is accomplished for free end points; i.e., impulse is minimized with respect to take-off and arrival points, as well as transfer orbit geometry. The term rendezvous is used to imply an additional constraint to the two-impulse orbital transfer process--that of physically meeting a vehicle in the final orbit.

Little analytic information is known about the optimum orbital transfer when end points are unspecified. Like many problems of celestial mechanics, the formulation is straightforward and, except for special cases, the equations are analytically intractable. Thus, for the general problems, one accepts simplifications in the mathematical model or utilizes numerical techniques.

Numerical methods were employed to allow visualization of an "impulse function space"--a geometrical abstraction of the impulse function. This technique allowed concise graphical presentation of all optimum impulse information concerning any pair of elliptical orbits. As a result, it was possible to understand the nature and structure of the entire impulse function.

II. TWO-IMPULSE ORBITAL TRANSFER FORMULATION

This study involves a two-impulse transfer process between an initial orbit with elements p_1, e_1, ω_1, i_1, and a final orbit with elements p_2, e_2, ω_2 (Fig. 1). The formulation assumes Keplerian orbits and results from

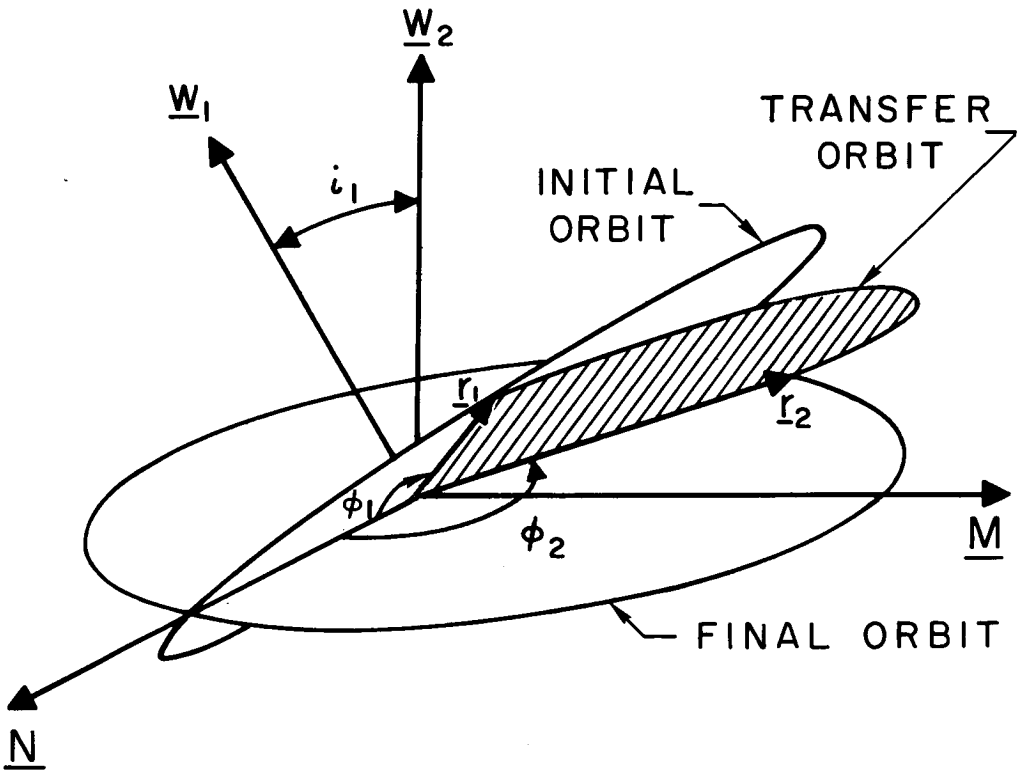

FIGURE I. TRANSFER GEOMETRY

choosing the final orbit as the reference plane ($i_2 = 0$). i_1 is the relative inclination of the two orbit planes ($\cos i_1 = \underline{W}_1 \cdot \underline{W}_2$, where $\underline{W}_1$ and $\underline{W}_2$ are unit vectors directed along the angular momentum vectors of the initial and final orbits). For coplanar orbits the reference direction ($\underline{N}$) is arbitrary, but for inclined orbits $\underline{N}$ is defined as the line of intersection of the two orbit planes ($\underline{N} = \underline{W}_2 \times \underline{W}_1 / |\underline{W}_2 \times \underline{W}_1|$).

For the general case, there is a three parameter family of transfer orbits joining any two specific orbits. The objective of this study was to select transfer orbits which minimized the sum of the two velocity increments required to perform the transfer. Optimization was accomplished by numerical means---a fact that has an important bearing on the choice of independent variables. The angles from the reference line to departure point (ϕ_1) and to arrival point (ϕ_2) are a natural choice for two of the three optimizing variables since they, along with the given orbital elements, specify position and velocity in the known orbits (Fig. 1). Further, except for the special case when the arrival and departure points are colinear with the center of mass, ϕ_1 and ϕ_2 establish the plane of the transfer orbit.

The third independent variable must be one of the elements of the transfer orbit: p, e, or ω. p, the semi-latus rectum of the transfer orbit, was the third parameter used for this study. It was chosen since it simplified the structure of the impulse function $I(\underline{\phi}) = I(\phi_1, \phi_2, p)$. It also avoided several undesirable discontinuities which are present in other formulations. (A discussion of the use of alternate variables may be found in References 1 and 2.)

TRANSFER GEOMETRY

Unit vectors ($\underline{U}_1$, $\underline{U}_2$) and radius vectors ($\underline{r}_1$, $\underline{r}_2$) toward the departure and arrival points may be computed from ϕ_1, ϕ_2 and the elements of the initial and final orbits.*

$$\underline{U}_1 = (\cos \phi_1, \sin \phi_1 \cos i_1, \sin \phi_1 \sin i_1) \tag{1}$$

$$\underline{U}_2 = (\cos \phi_2, \sin \phi_2, 0) \tag{2}$$

$$\underline{r}_j = \left[\frac{p_j}{1 + e_j \cos(\phi_j - \omega_j)}\right] \underline{U}_j \qquad j = 1, 2 \tag{3}$$

*The subscripts 1, 2, and t indicate initial, final, and transfer orbits. Lack of a subscript is also employed to denote a transfer orbit parameter.

Unit vectors normal to the initial, final, and transfer orbit planes are defined as follows:

$$\underline{W}_1 = (0 , - \sin i_1 , \cos i_1) \tag{4}$$

$$\underline{W}_2 = (0 , 0 , 1) \tag{5}$$

$$\underline{W}_t = \frac{\underline{U}_1 \times \underline{U}_2}{|\underline{U}_1 \times \underline{U}_2|} \qquad \underline{U}_1 \times \underline{U}_2 \neq 0 \tag{6}$$

Two vectors which define the shape and orientation of the initial and final orbits complete the transfer geometry description, (This formulation has been suggested by Herget[4]).

$$\underline{e}_j = e_j [\cos \omega_j , \sin \omega_j \cos i_j , \sin \omega_j \sin i_j] \qquad j = 1, 2 \tag{7}$$

The true anomaly interval traversed in the transfer orbit ($\Delta\theta$) may be determined directly.

$$\cos \Delta\theta = (\underline{U}_1 \cdot \underline{U}_2) \qquad 0° < \Delta\theta < 180° \tag{8}$$

Note that $\Delta\theta$ is arbitrarily limited to the first two quadrants ("short" transfers). A reversal of the algebraic signs of the transfer orbit velocity vectors is employed to compute "long" transfer circumstances. For elliptical transfer orbits, optimum impulse is defined as the least of the optimum long and short transfer impulses. Note that this particular formulation is singular if $\Delta\theta = 180°$ or $\Delta\theta = 0°$. For these cases the impulse required is not unique since any transfer orbit inclination will satisfy the geometry. In many special cases the optima occur when $\Delta\theta = 180°$ and an alternate set of computations is necessary to avoid this singularity.

IMPULSE COMPUTATION

The function to be minimized is the total impulse for the two-impulse maneuver:

$$I = |\underline{I}_1| + |\underline{I}_2| \tag{9}$$

where

$$\underline{I}_1 = \pm \underline{V}_{t_1} - \underline{V}_1 \tag{10}$$

$$\underline{I}_2 = \underline{V}_2 \mp \underline{V}_{t_2} \tag{11}$$

(When a double sign is used, the upper sign refers to the short transfer case.) Velocity vectors in the initial and final orbits at the departure and arrival points ($\underline{V}_1$ and $\underline{V}_2$) and the corresponding velocity vectors in the transfer orbit ($\underline{V}_{t_1}$ and $\underline{V}_{t_2}$) are computed as follows:

$$\left.\begin{aligned} \underline{V}_j &= \left(\frac{\mu}{p_j}\right)^{1/2} \underline{W}_j \times (\underline{e}_j + \underline{U}_j) \qquad (12) \\ \underline{V}_{t_j} &= \left(\frac{\mu}{p}\right)^{1/2} \underline{W}_t \times (\underline{e} + \underline{U}_j) \qquad (13) \end{aligned}\right\} \quad j = 1, 2$$

Equations 12 and 13 may be derived from Equation 3.26 of Herget.[4] An expression for $\underline{e}$ is not included since this transfer orbit parameter is not required in the final equations for impulse computation. The final impulse equations are obtained from Equations 10 - 13 by substituting Equation 6 and performing several algebraic manipulations.

$$\underline{I}_1 = \pm [\underline{v} + z\,\underline{U}_1] - \underline{V}_1 \tag{14}$$

$$\underline{I}_2 = \underline{V}_2 \mp [\underline{v} - z\,\underline{U}_2] \tag{15}$$

where

$$\underline{v} = \frac{(\mu p)^{1/2} (\underline{r}_2 - \underline{r}_1)}{|\underline{r}_1 \times \underline{r}_2|} \tag{16}$$

$$z = \left(\frac{\mu}{p}\right)^{1/2} \tan \frac{\Delta\theta}{2} \tag{17}$$

Impulses corresponding to long and short transfers are compared and the combination producing the lesser impulse is utilized for the remaining optimization procedures.

III. IMPULSE FUNCTION INVESTIGATION

While the formulation of the expressions for impulse computation is relatively straightforward, the exact mathematical expressions are not susceptible to analytical solution. One must therefore resort to numerical techniques for optimizing the solution vector, $I(\underline{\phi}) = I(\phi_1, \phi_2, p)$.

At best, conventional numerical search techniques only provide information concerning a function's local properties. Yet a detailed understanding of the impulse function's structure is essential for interpretation of numerical results. The number, shape, and relative importance of minima are requisites to a complete analysis of transfer problems since numerical optimization methods (e.g., steepest descent) find only that minimum impulse which is closest to the point of search initiation.[2, 3]

A geometric ("ϕ-space") representation of the impulse function was adopted for this investigation. In Figure 2, p, ϕ_1, and ϕ_2 are measured along the principal axes of an orthogonal coordinate system. All possible transfers between a pair of orbits (excluding the $\Delta\theta = 0°$ and $\Delta\theta = 180°$ function singularities) lie within the volume defined by $0° \leq \phi_1 < 360°$, $0° \leq \phi_2 < 360°$, $0 < p < +\infty$. Of course, ϕ_1 and ϕ_2 undergo cyclical repetition outside this volume.

Studying the impulse function in ϕ-space requires visualization of surfaces which are the loci of points having the same impulse. These "impulse surfaces" are generally closed and surround optima in much the same manner that the successive layers of an onion enclose its center. Impulse surfaces may be visualized and studied by considering their traces upon a cutting plane (Fig. 2). The resulting contours of equivalent impulse that appear in most of the figures presented here will be shown to provide a wealth of data in a concise easily understood form.

These contour maps are produced from an array of impulse values which are parametrically generated from Equation 9 with ϕ_1, ϕ_2, or p being held constant. Constant impulse contour lines, consisting of short straight-line segments, are then fitted between the survey points. It is important to note that the fidelity of the contouring technique depends directly upon the number of survey points. This fact should be remembered when examining certain structural details of the figures presented here.

Several seconds of IBM 7090 time are required to contour a typical array of survey data (500-1,000 points). A Stromberg Carlson 4020 CRT is then employed to plot the contour maps. A description of the contouring technique appears in Reference 5.

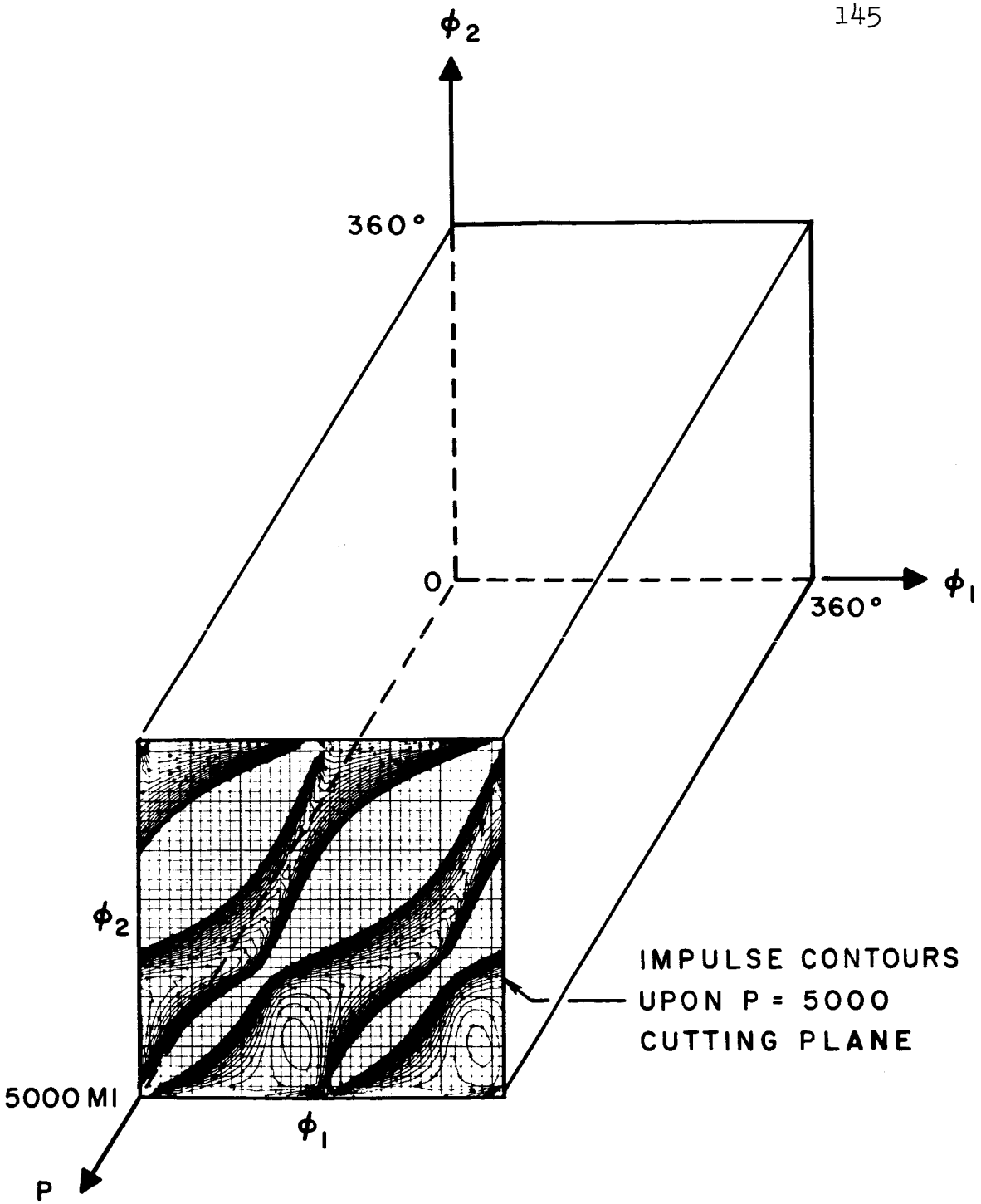

FIGURE 2. SCHEMATIC VIEW OF IMPULSE FUNCTION SPACE AND IMPULSE CONTOURS

TABLE 1. IDENTIFICATION OF OPTIMA

OPTIMUM	ϕ_1	ϕ_2	p (miles)	IMPULSE (ft/sec)
1	75°	190°	6650	4900
2	40°	300°	6600	5300
3	175°	75°	4600	5400
4	310°	40°	4600	5800

IV. p-OPTIMIZATION

The technique of passing a number of cutting planes through a given ϕ-space suffices to isolate optima and other pertinent features. However, as a ϕ-space becomes more complex, this technique requires that numerous contour maps be generated--each of them providing additional information concerning the optimum transfer modes.

A "p-optimization" technique was developed to overcome the above difficulties and thus present one contour map containing only optimum impulse information.

Given ϕ_1 and ϕ_2, (i.e., $\underline{r}_1$ and $\underline{r}_2$), it is desired to find that p which minimizes the impulse defined by Equation 9. Differentiating Equation 9 yields

$$dI = \frac{\underline{I}_1 \cdot d\underline{I}_1}{|\underline{I}_1|} + \frac{\underline{I}_2 \cdot d\underline{I}_2}{|\underline{I}_2|} \tag{18}$$

Since $\underline{V}_1$ and $\underline{V}_2$ are independent of p,

$$\frac{\partial \underline{I}_1}{\partial p} = \pm \frac{\partial \underline{V}_{t_1}}{\partial p} \tag{19}$$

$$\frac{\partial \underline{I}_2}{\partial p} = \mp \frac{\partial \underline{V}_{t_2}}{\partial p} \tag{20}$$

This leads to an expression for the derivative of impulse with respect to p, which may be set equal to zero.

HOHMANN TRANSFER ϕ-SPACE

Figure 3 was produced by cutting the ϕ-space associated with coplanar circular orbits having $p_1 = 5,000$ and $p_2 = 6,000$ miles. Cutting planes corresponded to $\phi_2 = 0°$ and $p = 5,454.54$ miles. In this case the symmetry is so complete that an adequate description of the ϕ-space is possible with the two contour maps presented. Symmetry about the $\phi_1 - \phi_2 = 180°$ plane is apparent. The Hohmann transfer corresponds to the straight line $\underline{\phi} = (\phi_1, \phi_1 + 180°, p)$ with ϕ_1 arbitrary and $p = 5,454.54$ miles. All other impulse surfaces are cylinders having elements parallel to the Hohmann line minimum. In Figure 3 the minimum impulse contour corresponds to 2500 ft/sec.

INCLINED ASYMMETRIC ORBIT PAIR

Figure 4 concerns an orbit pair having the following elements:

$p_1 = 5,000$ mi $\qquad p_2 = 6,000$ mi

$e_1 = 0.2 \qquad e_2 = 0.2$

$\omega_1 = -90° \qquad \omega_2 = +30°$

$i_1 = 5°$

The five p = constant contour maps presented here adequately illustrate the ϕ-space associated with a typical unsimplified problem. The perfect symmetry and simplicity of the circle-to-circle case is in sharp contrast with the seemingly amorphous impulse contours of asymmetrical cases. The shapes and relative orientations of the two orbits are apparent from the illustration which projects the initial orbit upon the final orbit plane.

The existence of four distinct relative optimum transfers between these two orbits is apparent. The approximate coordinates and impulse associated with each of the optima are summarized in Table 1. Uncontoured portions of each survey plane correspond to hyperbolic and elliptical transfer orbits which require excessive impulses.

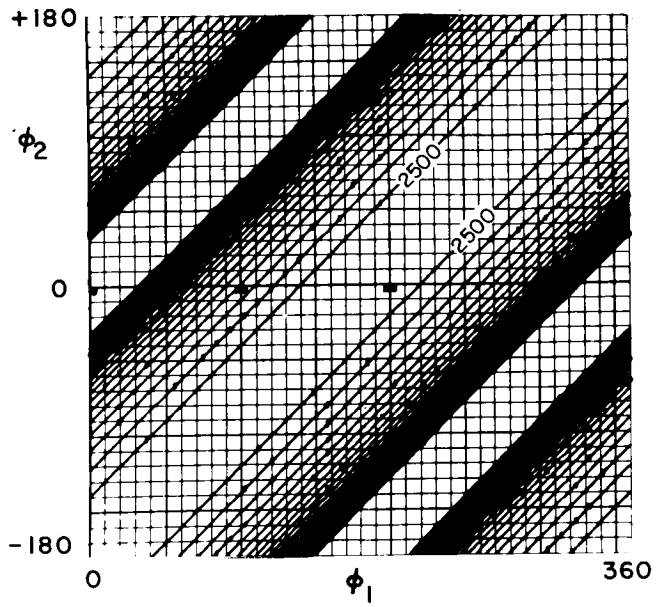

a.) p = CONSTANT = 5454 MI.

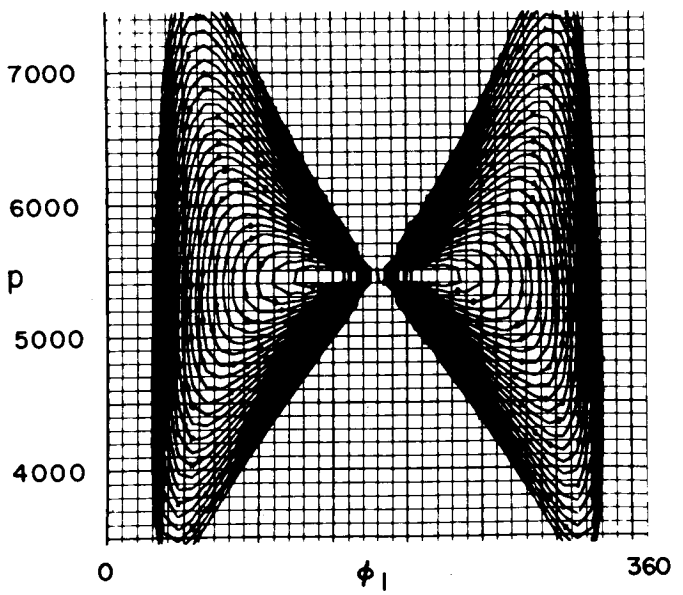

b.) ϕ_2 = CONSTANT = 0.0

FIGURE 3. IMPULSE CONTOURS FOR COPLANAR CIRCULAR ORBITS (CONTOUR INTERVAL = 500 FT/SEC)

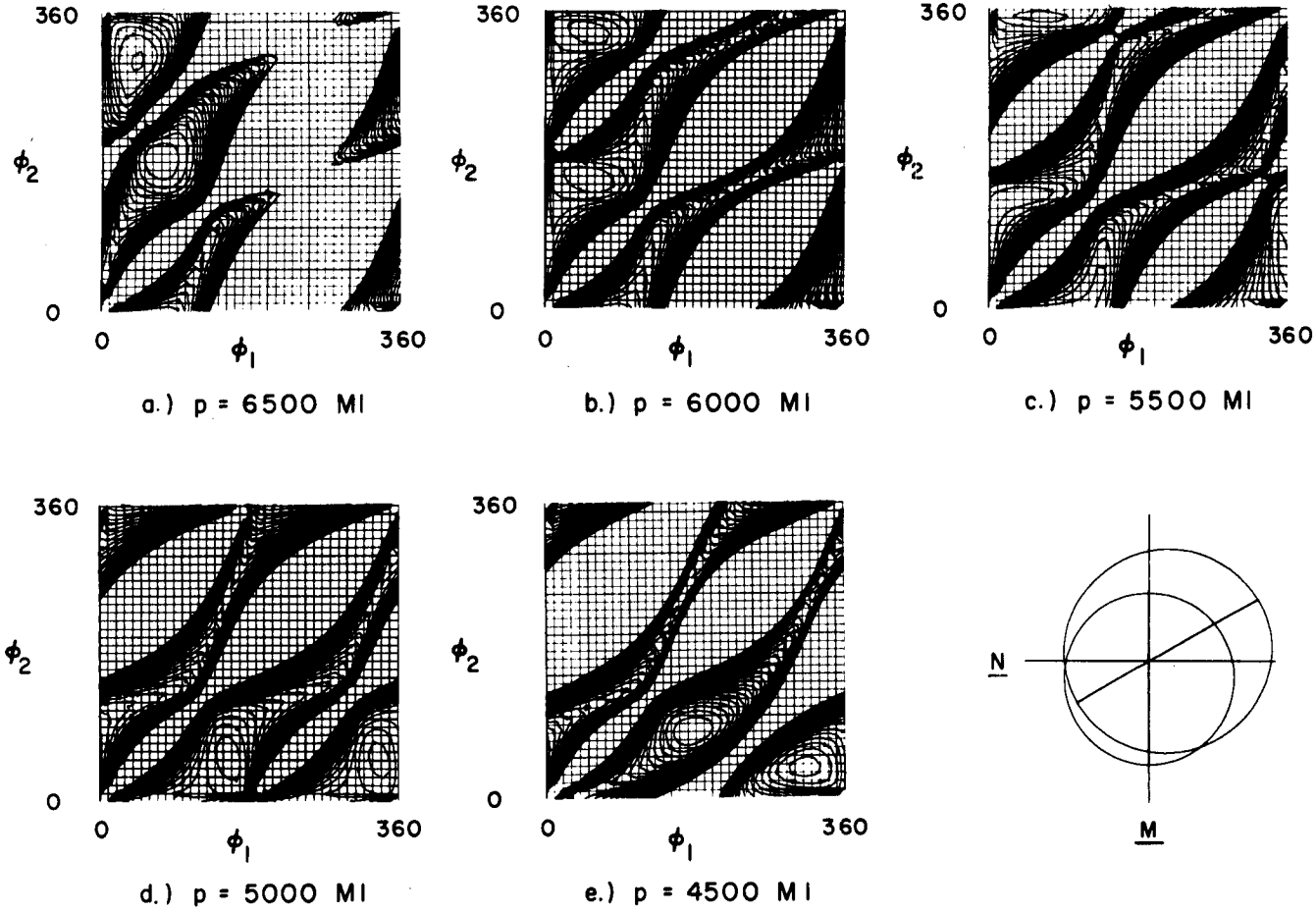

FIGURE 4. INCLINED ASYMMETRIC ORBIT PAIR -- IMPULSE CONTOURS FOR p = CONSTANT PLANES (CONTOUR INTERVAL = 500 FT/SEC)

Note that Figure 5 readily illustrates the circumstances of the four optimum transfers. At the same time it is possible to note their relative importance and to infer certain other properties such as error sensitivity, i.e., $\partial I/\partial \phi_1$ and $\partial I/\partial \phi_2$ may be approximated from the contour maps. Other features of ϕ-space structure such as regions of extreme impulse are apparent. The nature and properties of these features were the subject of considerable investigation.

The entire computational procedure necessary to produce Figures 5a and 5b required less than 1 minute of IBM 7090 time.

V. FORMATION OF LOCAL OPTIMA

This study resulted in the identification of mechanisms which guide the formation of optima and determine their multiplicity. It was found that the number, shape, and distribution of minima of the impulse function are controlled by the type of asymmetries present in the given orbit pair. Eccentricity, inclination, and the relative position of the lines of apsides all have distinct effects upon the structure of function space.

EFFECT OF ECCENTRICITY PERTURBATIONS

The first orbit pair of Figure 6 represents a transfer from an elliptical orbit ($e_1 = 0.2$, $p_1 = 5,000$ mi) to a circular orbit ($p_2 = 6,400$ mi). The Hohmann optimum region of the circle-to-circle case has been twisted into nearly horizontal and vertical optimum regions. The optimum transfer occurs at $\underline{\phi} = (0°, 180°, p_{opt})$, [7] but near optimum transfers are available throughout the entire range of ϕ_1. The strong warping of the impulse contours is associated with the varying radial distances separating the two orbits.

Addition of sufficient eccentricity ($e_1 = e_2 = 0.4$; $p_1 = 5000$ mi, $p_2 = 6000$ mi) to allow the orbits to intersect under the proper rotations disturbs the Hohmann line optimum and forms two distinct optima[5] at $\underline{\phi} = (0°, 180°, p_{opt})$ and $\underline{\phi} = (180°, 0°, p_{opt})$. As additional eccentricity ($e_1 = e_2 = 0.8$; $p_1 = 5000$ mi, $p_2 = 6000$ mi) is added, the optima become more pronounced and are separated by a larger impulse differential. If the orbits are coapsidal, the optima always correspond to perigee-to-apogee and apogee-to-perigee transfers.

COPLANAR ROTATION OF LINES OF APSIDES

When coplanar elliptical orbits ($e_1 = e_2 = 0.2$; $p_1 = 5,000$ mi and $p_2 = 6,000$ mi) are rotated, a new type of optimum modifying asymmetry is introduced (Fig. 7). As the orbits approach tangency, the optimum

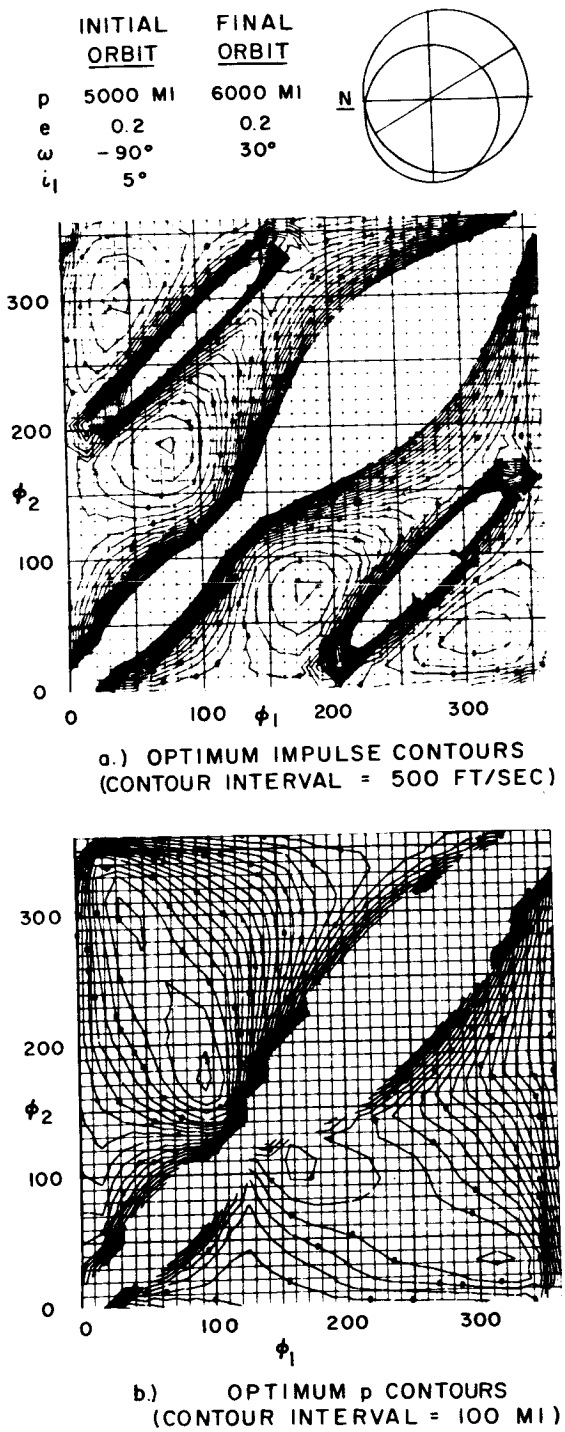

FIGURE 5. INCLINED ASYMMETRIC ORBIT PAIR

$$\frac{\partial I}{\partial p} = \pm \frac{1}{2p} \left[\frac{\underline{I}_1 \cdot (\underline{v} - z\,\underline{U}_1)}{|\underline{I}_1|} - \frac{\underline{I}_2 \cdot (\underline{v} + z\,\underline{U}_2)}{|\underline{I}_2|} \right] = 0 \qquad (21)$$

Equation 21 is used to direct a numerical search that seeks the value of p that minimizes impulse for the given ϕ_1 and ϕ_2. Though Equation 21 has several roots, usually only those roots which correspond to elliptical transfer orbits are useful for impulse minimization. For certain elliptical orbit pairs, it can be shown that optimum two-impulse transfers between particular groups of end points result in hyperbolic transfer orbits.(6) The range of p which produces an elliptical transfer orbit is bounded. These boundaries (parabolic orbit limits) are defined as follows:

$$p_{min} = \frac{r_1 r_2 - \underline{r}_1 \cdot \underline{r}_2}{r_1 + r_2 + \left[2(r_1 r_2 + \underline{r}_1 \cdot \underline{r}_2)\right]^{1/2}} \qquad (22)$$

$$p_{max} = \frac{r_1 r_2 - \underline{r}_1 \cdot \underline{r}_2}{r_1 + r_2 - \left[2(r_1 r_2 + \underline{r}_1 \cdot \underline{r}_2)\right]^{1/2}} \qquad (23)$$

Except for certain special cases, only one minimum impulse will occur between these limits.(6) An effective numerical technique has been devised to seek the required optimum impulse solutions where $p_{min} < p < p_{max}$. Each determination of an optimum p requires less than 0.1 second of IBM 7090 time.

The contour maps presented throughout the remainder of this paper were generated using this technique. Approximately 500 p-optimizations were required for the generation of each contour map.

Figure 5a is a p-optimized survey of the ϕ-space associated with the orbit pair which was examined in Figure 4. Note that the optimum impulse (feet per second) for any ϕ_1, ϕ_2 may be read directly from the contour map. The advantages of the p-optimization technique should be apparent from a comparison of Figures 4 and 5a. Complete description of a ϕ-space requires the generation of numerous cuts at various values of one of the variables. Once these cuts are available, it is difficult to extract the optimum impulse information. The p-optimization technique allows complete description of the optimum impulse regions of a ϕ-space in one contour map.

Another contour map (Figure 5b) presents the p contours associated with the optimum impulse contours. The optimum p associated with any ϕ_1, ϕ_2 is therefore available. One may easily proceed from these contour maps to numerical searching programs which permit exact detailed examination of regions of particular interest.(2)

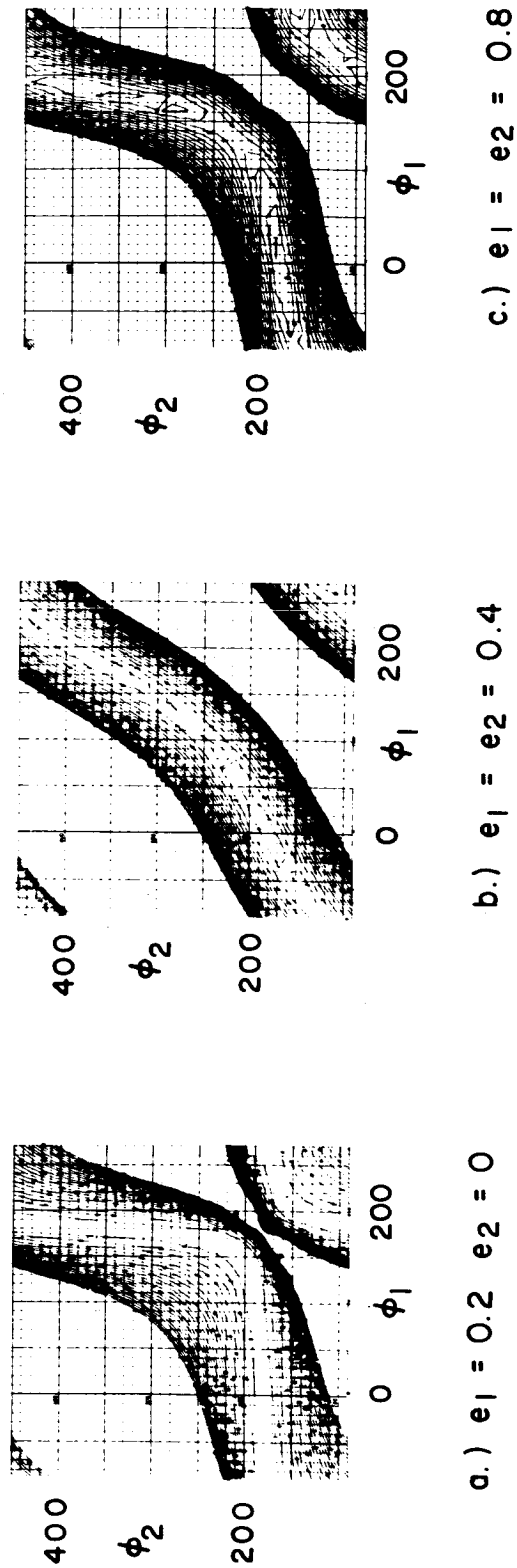

FIGURE 6. EFFECT OF ECCENTRICITY ADDITION--
COPLANAR COAPSIDAL ORBITS
(CONTOUR INTERVAL = 200 FT/SEC)

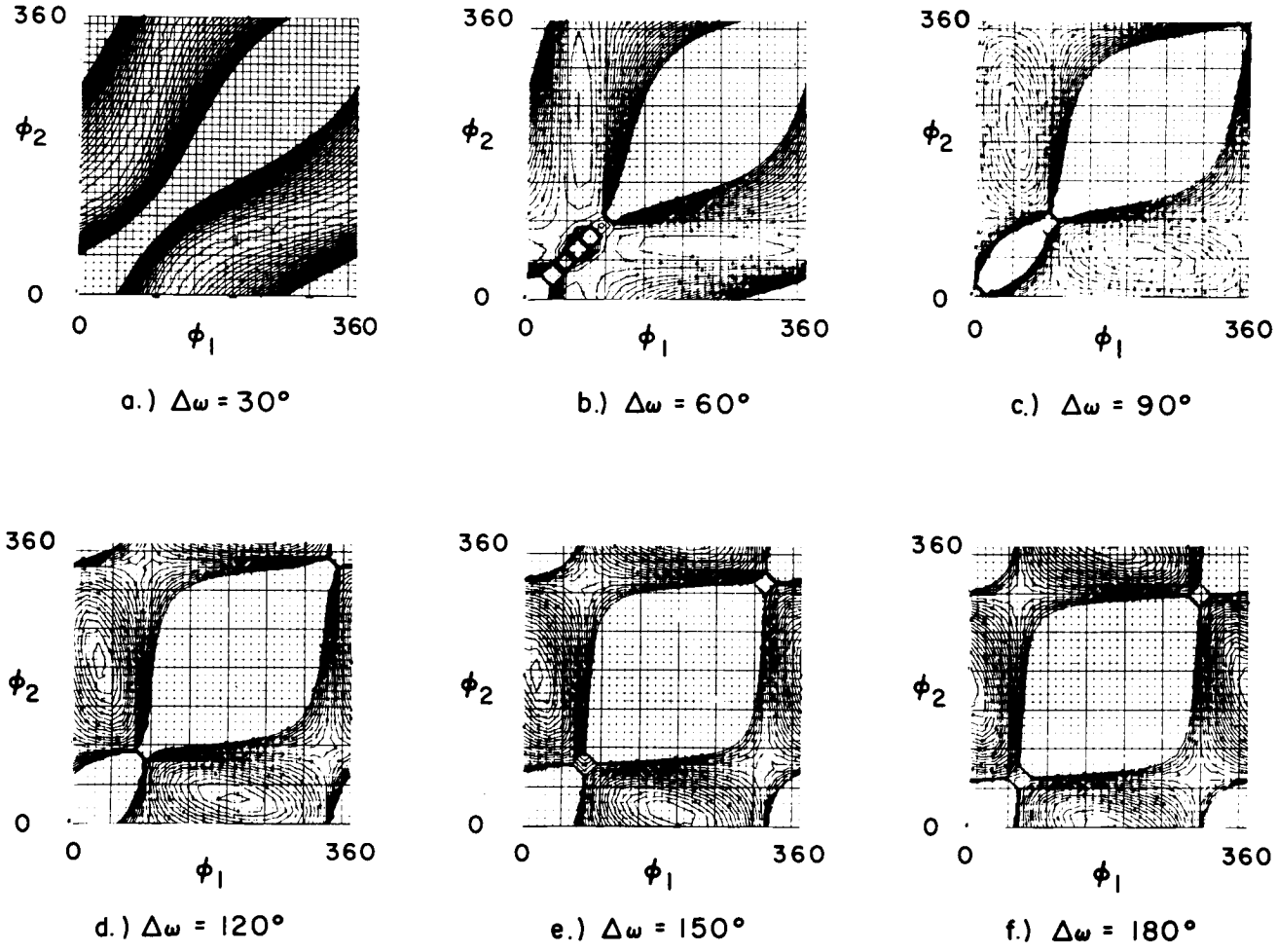

FIGURE 7. EFFECT OF COPLANAR ROTATION OF ELLIPTICAL ORBITS (CONTOUR INTERVAL = 200 FT/SEC)

impulse contours are bent into one section which is nearly horizontal and another which is nearly vertical ($\Delta\omega = 30°$). The optima migrate to locations adjacent to the coordinates of the point at which the orbits would become tangent under further rotation. Further rotation ($\Delta\omega = 60°$) causes the orbits to intersect and the optima to shift from near the tangency point to the horizontal and vertical regions mentioned earlier. These regions correspond to transfers which utilize most of the total impulse at either the departure or the arrival point---a single impulse transfer is possible if the orbits are tangent or intersecting.

Further rotation causes the two optima to become less elongated, to correspond to greater minimum impulse levels, and to migrate toward $\underline{\phi} = (0°, 180°, p_{opt})$ and $\underline{\phi} = (180°, 0°, p_{opt})$. The uncontoured regions indicate the excessive impulse which is required to transfer via high eccentricity orbits which pass near the center of mass.

TANGENT ORBITS

When coplanar orbits are tangent and also coapsidal, it can be shown that a one-impulse transfer at the point of tangency is optimum. However, if the orbits have undergone coplanar rotation this is no longer true.(7)

Figures 8a and 8b present the impulse and p contours which result from a pair of tangent orbits. The impulse for the one-impulse transfer $I(\underline{\phi}) = I(73.^{\circ}74, 73.^{\circ}74, 6000)$ is about 1971.3 feet per second. Two seemingly symmetrical regions corresponding to impulse levels of about 1963 feet per second are centered near $\underline{\phi} = (74°, 68°, p_{opt})$ and $\underline{\phi} = (68°, 74°, p_{opt})$. A quick glance at the p contours associated with these optima (Fig. 8b) indicates that a transfer orbit semi-latus rectum of about 5400 miles is optimum (note that $p_1 = 5000$ mi and $p_2 = 6000$ mi). This result indicates that approximately equal initial and final impulses will produce the optimum transfer.

INCLINATION

Inclination produces a division of a given ϕ-space about the $\phi_1 - \phi_2 = 180°$ plane (Fig. 9). In this case two circular orbits are inclined 10°. Contours appear to radiate from the $\underline{\phi} = (0°, 180°, p_{opt})$ and $\underline{\phi} = (180°, 0°, p_{opt})$ points which are singularities in the impulse computation formulation. These points are optima if the orbits are inclined about their semi-major axes, but for other orientations the optima may lie elsewhere. Increasing the inclination causes the ϕ-space division to become more pronounced.

All ϕ-spaces resulting from inclined orbits exhibit an inclination "wall" which, in general, tends to <u>double</u> the number of optima which

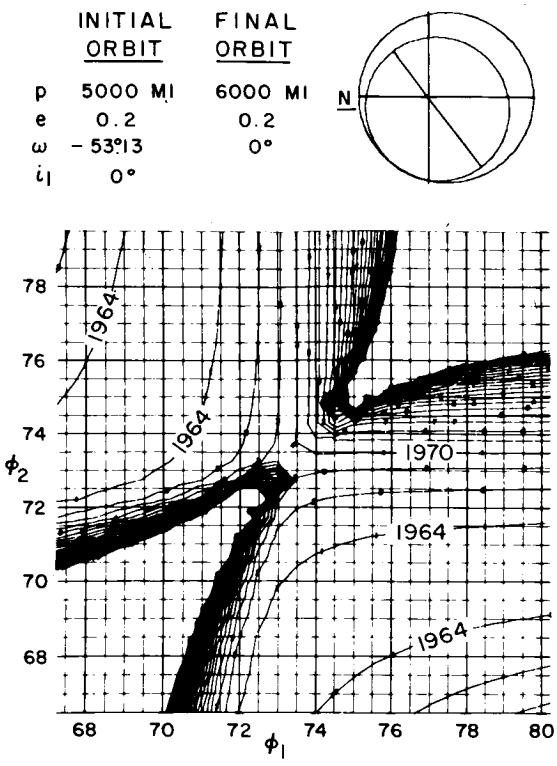

a.) OPTIMUM IMPULSE CONTOURS
(CONTOUR INTERVAL = 1 FT/SEC)

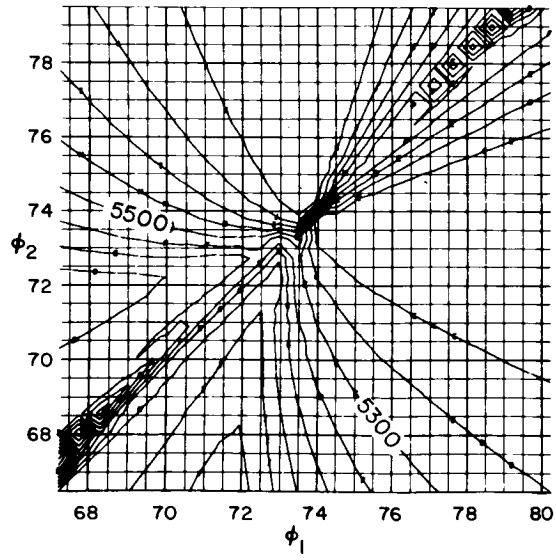

b.) OPTIMUM p CONTOURS
(CONTOUR INTERVAL = 100 MI)

FIGURE 8. TANGENT ELLIPTICAL ORBITS

	INITIAL ORBIT	FINAL ORBIT
p	5000 MI	6000 MI
e	0	0
ω	0	0
i_1	10°	

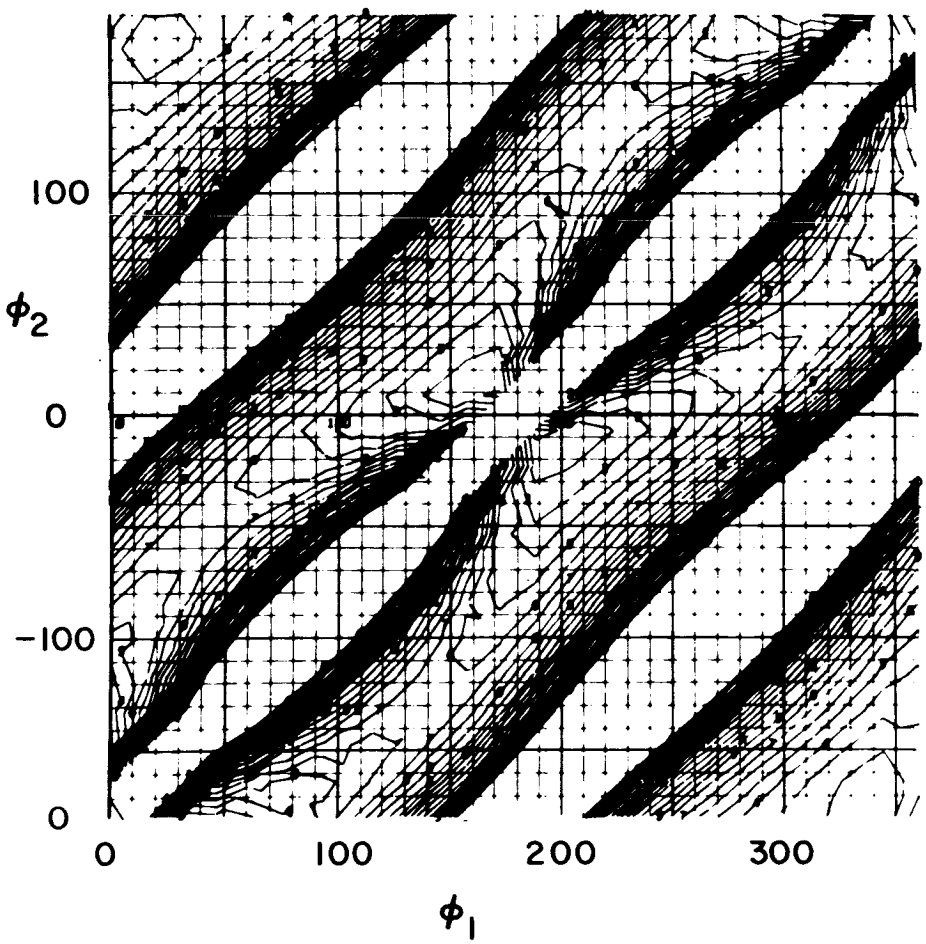

FIGURE 9. INCLINED CIRCULAR ORBITS (CONTOUR INTERVAL = 500 FT/SEC)

would have existed if the orbits had been coplanar. For instance Figure 5 results from adding inclination to a pair of elliptical orbits whose lines of apsides are separated by 120°.

VI. ADDITIONAL ϕ-SPACE STUDIES

Space does not permit the comprehensive examination of enough ϕ-spaces to develop a complete picture of the optimum orbital transfer circumstances which arise from all possible orbit combinations. Figures 10 and 11 are presented to answer several additional questions--and no doubt raise several more.

The asymmetrical orbit pair which produced Figure 5 was altered to produce Figures 10 and 11 (10: p_1 = 4800 mi, p_2 = 9000 mi, e_2 = 0.8; 11: p_1 = 4800 mi, p_2 = 7920 mi). The first pair of orbits can intersect under appropriate rotations. Even though the final orbit is considerably enlarged relative to the initial, the ϕ-space structure remains similar to that of Figure 5. The dominant role of orbit orientation is apparent from this illustration.

The non-intersecting orbit pair (Fig. 11) exhibits only two optima although the orbit orientations are identical. This example illustrates how the number of optima is multiplied when orbits are capable of intersection.

VII. TWO-IMPULSE RENDEZVOUS

An optimum two-impulse orbital transfer is also an optimum rendezvous for two vehicles with an appropriate phase relationship. The foregoing orbital transfer techniques may easily be extended to allow calculation of rendezvous time constraints for arbitrary ϕ_1, ϕ_2 and p.

In order to define a time constraint let zero time correspond to the arrival of a vehicle in the final orbit at the reference line ($\underline{N}$) and let τ be the time at which the vehicle in the initial orbit will cross the same reference. If t_1, t_2, and t_t are the traverse times associated with the true anomaly intervals ϕ_1, ϕ_2, and $\Delta\theta$, then a sufficient condition for rendezvous is that $t_1 + t_t = t_2 - \tau$. Expressing τ in units of the final orbit's period (T_2) yields

$$\tau = (t_2 - t_1 - t_t) / T_2 \tag{24}$$

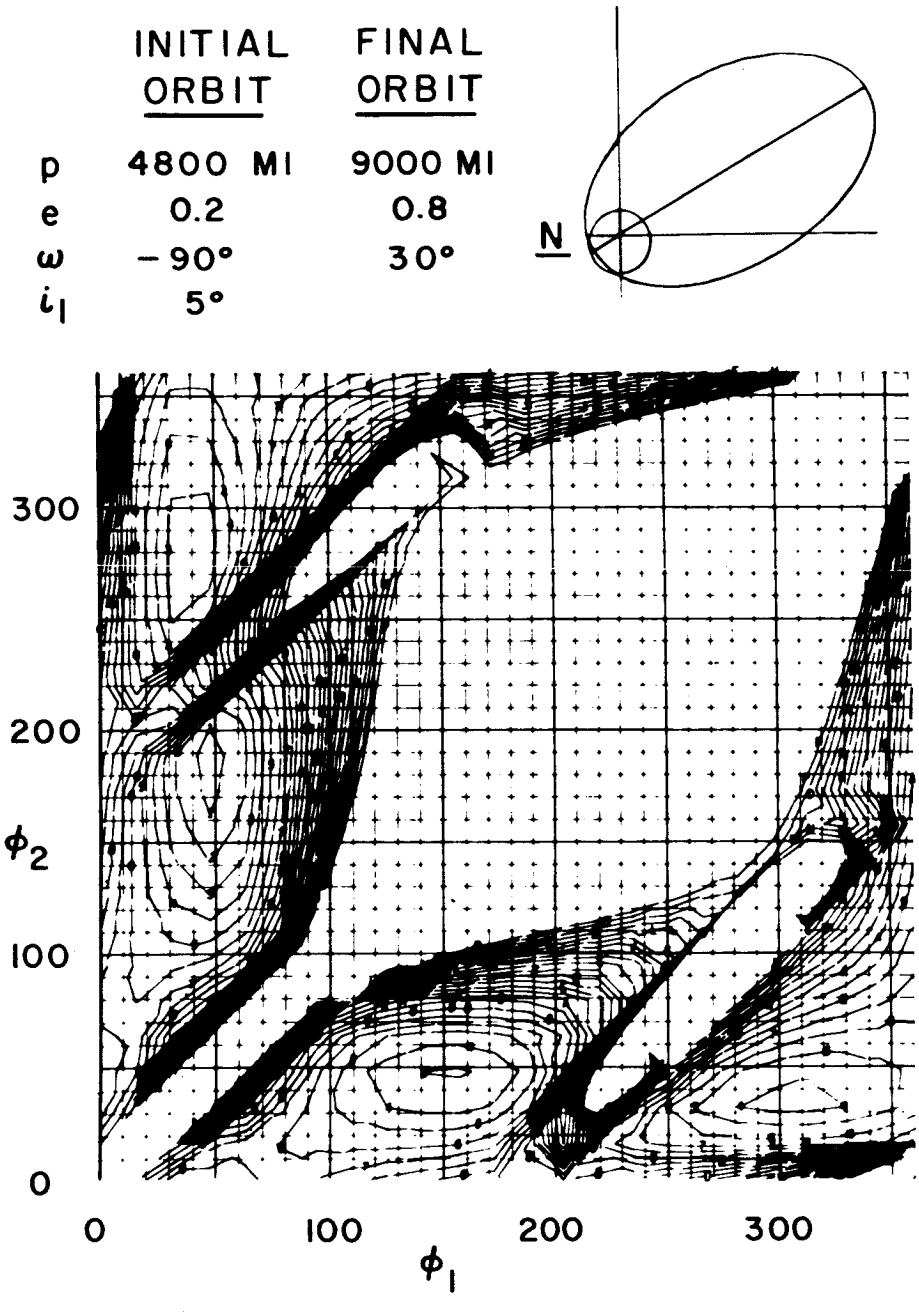

FIGURE 10. INCLINED ELLIPTICAL ORBITS (CONTOUR INTERVAL = 500 FT/SEC)

	INITIAL ORBIT	FINAL ORBIT
p	4800 MI	7920 MI
e	0.2	0.2
ω	-90°	30°
i_1	5°	

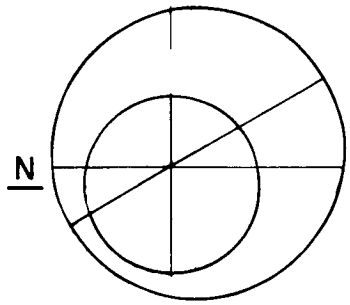

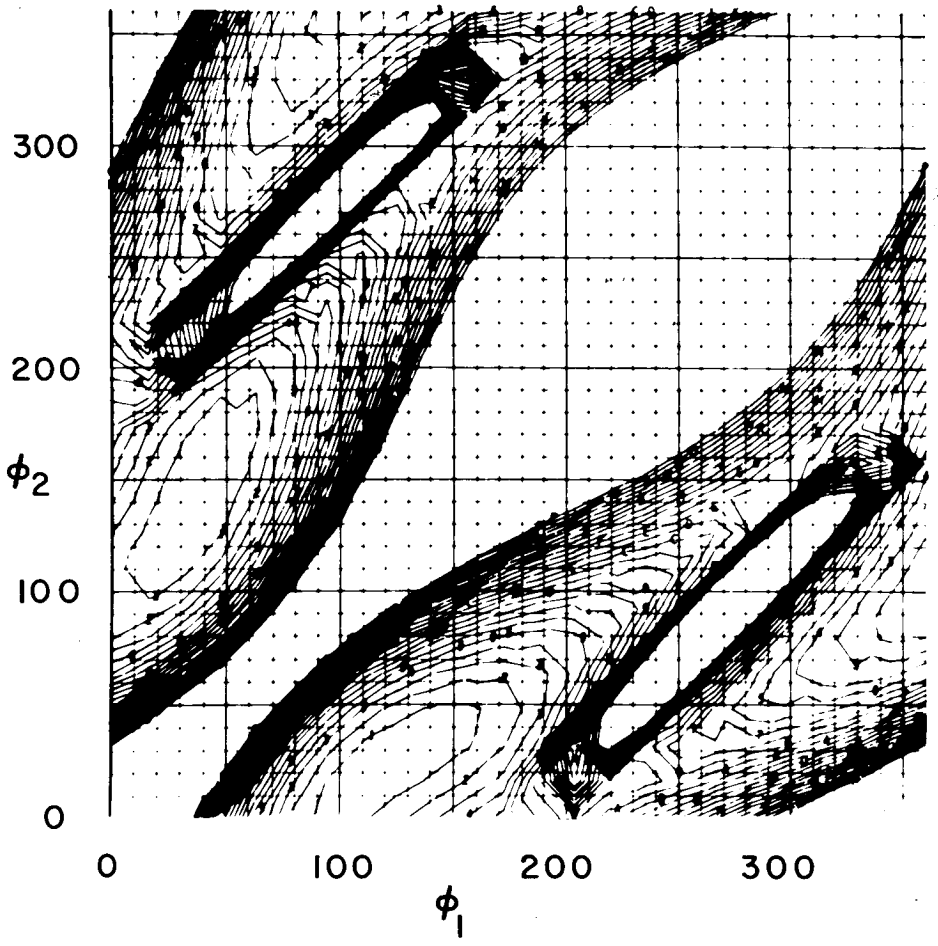

FIGURE II. NON-INTERSECTING ELLIPTICAL ORBI
(CONTOUR INTERVAL = 500 FT/SEC)

Utilizing Kepler's Equation, it is a simple matter to compute $\tau(\underline{\phi}) = \tau(\phi_1, \phi_2, p_{opt})$. Therefore, the values of τ associated with the p-optimized impulse may also be contoured. Figure 12 superimposes the p-optimized impulse and corresponding τ countours associated with the principal optimum of Figure 5. Clearly, τ must equal .913 for the optimum impulse rendezvous.

Of course, it will be a rare instance when τ is such that the optimum impulse rendezvous may be accomplished during a given revolution. Fortunately, for non-synchronous orbits τ changes each revolution, and a near optimum value will eventually result. An impulse splitting technique which is detailed in References 1 and 9 may be used to achieve a three-impulse rendezvous which requires no more impulse than the optimum two-impulse orbital transfer.* One may therefore avoid waiting a prolonged period in order to achieve the optimum impulse rendezvous.

When τ is specified, impulse optimization requires finding ϕ_1, ϕ_2 and p such that the impulse and τ surfaces are tangent. Numerical search techniques such as steepest descent have been employed to seek the required solutions.[1,8,9] Experience has demonstrated that economical and effective use of these numerical search methods requires adequate knowledge of a function's properties. With this knowledge it is possible to determine initial conditions which will assure rapid convergence to the required relative optimum.

Figure 12 allows one to approximate the conditions required for an optimum time constrained rendezvous. Given τ, one may locate the position where the corresponding τ line approaches nearest to the impulse optimum (the locus of these positions is shown as a dashed line). The ϕ_1, ϕ_2 and p located by this process will not usually yield an optimum time constrained rendezvous. Note, however, that the optimum impulse must be less than or equal to this approximate value. Therefore, the method provides a convenient means for determining whether the impulse required for rendezvous is within vehicle system capabilities. The method also provides information concerning the behavior of the impulse and τ functions. This information allows a good choice of initial conditions for subsequent investigation of exact solutions by other numerical procedures.

VIII. CONCLUSION

Methods for systematically studying optimum two-impulse orbital transfer between any pair of elliptical orbits have been developed and used to investigate the properties of an "impulse function space." The

*Reference 1 utilizes a τ which is the negative of the τ employed here.

	INITIAL ORBIT	FINAL ORBIT
p	5000 MI	6000 MI
e	0.2	0.2
ω	-90°	30°
i_1	5°	

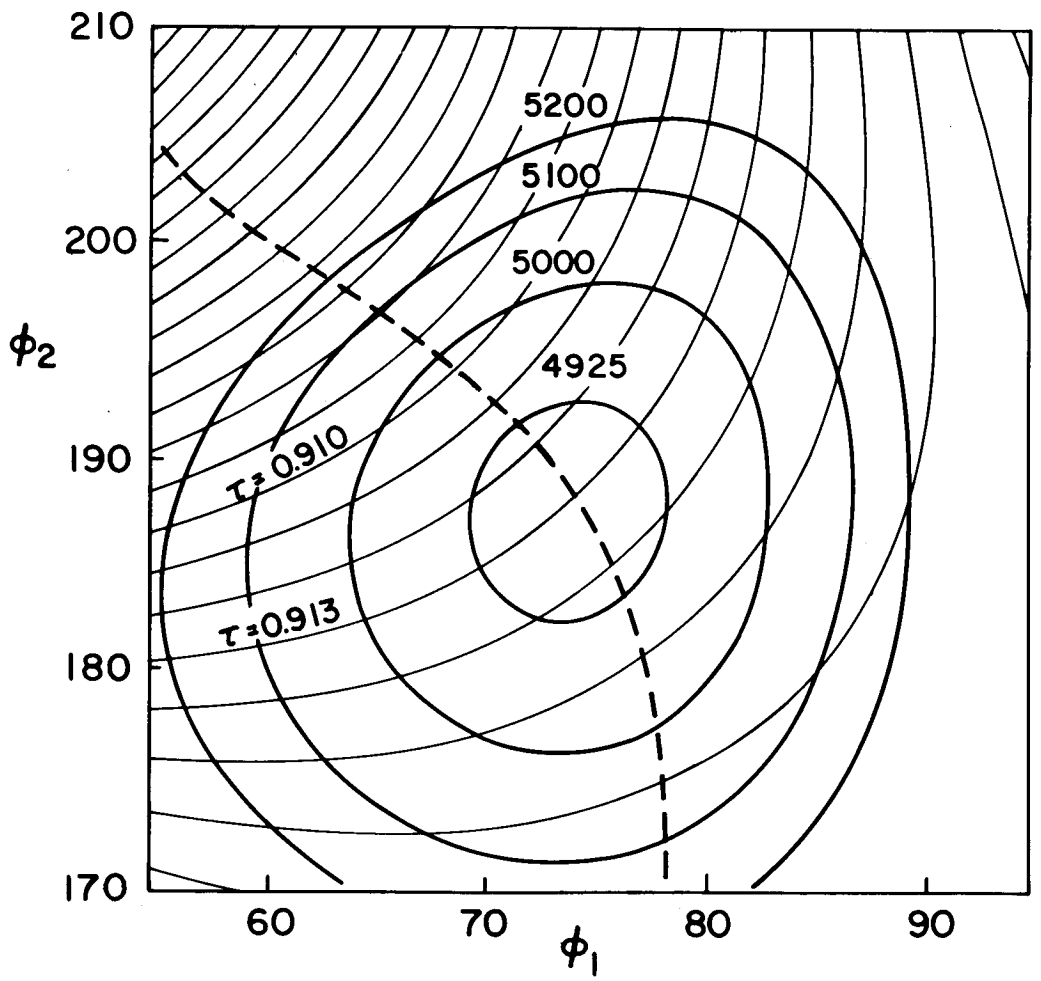

FIGURE 12. OPTIMUM IMPULSE AND CORRESPONDIN
τ CONTOURS NEAR PRINCIPAL OPTIMUM

mechanisms which govern the structure of this function space have been determined and may now be employed to predict the optimum transfers resulting from any pair of elliptical orbits.

A contouring technique was utilized to present large amounts of optimum impulse information in a concise easily understood form. The results obtained from function contouring have been verified through the use of steepest descent optimization procedures.(2, 8) Initial conditions taken from the contour maps always allowed the numerical search program to converge to the proper local optimum within a few seconds of IBM 7090 time. Optimum impulses obtained from this exact numerical optimization were only slightly better than those obtained from contouring. In all instances where exact numerical solutions were required, the insight gained through contouring methods proved to be an invaluable aid to subsequent optimization by conventional techniques.

While the methods presented here are oriented principally toward the area of space mission design, they also provide numerous clues which point the way to analytical solution of numerous sub-problems.

NOMENCLATURE

Scalars

a	Semi-major axis
e	Eccentricity (magnitude of $\underline{e}$)
i	Inclination
p	Semi-latus rectum
r	Radius to satellite
t	Time
$\Delta\theta$	Transfer angle (true anomaly difference in transfer orbit plane)
τ	Relative phase between vehicles--- rendezvous time constraint
μ	Gravitation constant

Scalars

ϕ_1	Angle from reference axis to departure position in initial orbit
ϕ_2	Angle from reference axis to arrival position in terminal orbit
ω	Argument of perigee, angle from reference axis to perigee point
Ω	Right ascension of ascending node

Vectors

$\underline{e}$	Orbit shape and orientation vector
$\underline{I}$	Impulse vector
$\underline{N}$	Unit vector denoting reference direction (line of intersection of initial and final orbit planes)
$\underline{r}$	Geocentric satellite position vector
$\underline{U}_1$	Unit vector directed toward point of departure from initial orbit
$\underline{U}_2$	Unit vector directed toward point of arrival in final orbit
$\underline{V}$	Velocity vector
$\underline{W}$	Unit vector directed along orbit's angular momentum vector
$\underline{\phi}$	Independent variable vector (ϕ_1, ϕ_2, p)
$\underline{N}\ \underline{M}\ \underline{W}_2$	Orthogonal unit vector set which establishes reference coordinate system

REFERENCES

1. Des Jardins, P. R., Bender, D. F., and McCue, G. A., "Orbital Transfer and Satellite Rendezvous," SID 62-870, North American Aviation, Inc., 31 August 1962.

2. Kerfoot, H. P., Bender, D. F., and Des Jardins, P. R., "Analytical Study of Satellite Rendezvous (Final Report)," MD 59-272, North American Aviation, Inc., 20 October 1960.

3. Des Jardins, P. R. and Bender, D. F., "Extended Satellite Rendezvous Study, (Quarterly Report, 31 May through 31 August 1961)," SID 61-304, North American Aviation, Inc., 14 September 1961.

4. Herget, Paul, "The Computation of Orbits," Published privately by the author, Ann Arbor, Michigan, 1948.

5. McCue, G. A., "Optimization by Function Contouring Techniques," SID 63-171, North American Aviation, Inc., 10 February 1963.

6. Bell, H. W. and Lee, B. G., "Analysis of Two-Impulse Orbital Transfer," Unpublished private communication, 1963.

7. Ting, L., "Optimum Orbital Transfer by Impulses," ARS Journal, Vol. 30, No. 11, pp. 1013-1018, November 1960.

8. Des Jardins, P. R. and Bender, D. F., "Extended Satellite Rendezvous Study, (Quarterly Report, 31 August through 30 November 1961)," SID 61-459, North American Aviation, Inc., 15 December 1961.

9. Bender, D. F., "Rendezvous Possibilities with the Impulse of Optimum Two-Impulse Transfer," Progress Report No. 3 on Studies in the Fields of Space Flight and Guidance Theory, MSFC, Feb. 6, 1963, page 138; and Preprint for A. A. S. Symposium on Space Rendezvous, Rescue, and Recovery, September 10-12, 1963.

AN ANALYSIS OF TWO-IMPULSE ORBITAL TRANSFER

Prepared by

Gentry Lee

Space Sciences Laboratory
Space and Information Systems Division
North American Aviation, Inc.

Special Report No. 3

July 18, 1963

Contract NAS8-5211
Prepared for

George C. Marshall Space Flight Center
National Aeronautics and Space Administration
Huntsville, Alabama

NOMENCLATURE

Scalars

a	Semi-major axis
e	Eccentricity
i	Inclination
Ω	Right ascension of ascending node
ω	Argument of perigee, angle from reference axis to perigee point
p	Semi-latus rectum
$\Delta\theta$	True anomaly angle traversed in transfer orbit plane
μ	Gravitation constant
ϕ_1	Angle from reference axis to departure position in initial orbit.
ϕ_2	Angle from reference axis to arrival position in terminal orbit
α	Angle between $\underline{r}_2$ and $\underline{r}_2 - \underline{r}_1$
β	Angle between $\underline{r}_1$ and $\underline{r}_1 - \underline{r}_2$
z	Term defined in equation (14)
Ψ_1	Functional form of 1st velocity increment
Ψ_2	Functional form of 2nd velocity increment
I	Functional representation of impulse
I^*	Function defined by equation (41), whose extrema are also located in equation (37)
f	One of test functions used in analyzing short transfer

Scalars

g	The other test function used in analyzing short transfer
h	One of test functions used in analyzing long transfer
k	Other test function used in analyzing long transfer
A-H	Coefficients that determine interval-finding polynomials
ϕ_1-ϕ_9	Coefficients that determine minimizing polynomial
σ	Function defined by equation (51)
τ	Function defined by equation (52)

Vectors

$\underline{e}$	Orbit shape and orientation vector
$\underline{r}_1$	Vector from reference position to point of departure on initial orbit
$\underline{r}_2$	Vector from reference position to point of arrival on final orbit
$\underline{W}$	Unit vector directed along orbit's angular momentum vector
$\underline{v}$	Vector defined by equation (13)
$\underline{V}_{tj}$	Velocity vectors in transfer orbit
$\underline{V}_j$	Velocity vectors in initial and final orbit
$\underline{V}_{par}$	Velocity vector in parabolic orbit
$\underline{V}_r$	Velocity vector in circular orbit
$\underline{U}_j$	Unit vectors in direction of radius vectors
$\underline{N}, \underline{M}, \underline{W}_2$	Unit vectors in Cartesian coordinates defining the reference plane

ABSTRACT

Analytical investigations of two-impulse transfers between elliptical orbits, using vector analysis and other mathematical techniques, have yielded pertinent, heretofore unknown facts about an orbital transfer function. One particular mode of analysis, the Bell-Arenstorf technique, helped show not only that the minimum velocity increment solution between two points on elliptical orbits could be along a hyperbola, but also that there could be two relative minima in this impulse function. Particular examples of both these phenomena are given.

Although prior published analysis has been restricted mostly to coplanar elliptical orbits, this analysis includes inclined elliptical orbits. An eighth-order polynomial expression, the real roots of which may refer to extrema in the impulse function, is determined. Since it can be shown that some of these roots are extraneous--not corresponding to impulse minima--two test functions are next determined that define regions in which all extrema must lie. These regions identify those roots that do correspond to extrema in the impulse function and those that are extraneous. These new analytical findings have been incorporated into an earlier computer contour mapping program that locates the optimum transfer between elliptical orbits.

I. INTRODUCTION

One of the major problems of the nascent space age is concerned with changing orbits in space. To transfer from orbit to orbit can require immense quantities of fuel, far beyond the limitations of today's engineering. It is, therefore, of extreme practical interest to be able to locate particular modes of transfer between these orbits that use the least possible fuel.

The most general problem of optimum two-impulse orbital transfer, in which the chief assumption is that the elliptical orbits are unperturbed, permits both the departure point and the arrival point to be arbitrary and finds the single best mode of transfer between the two given orbits. The most general constraint is to fix the end points; then the optimization procedure is carried out solely along a parameter defining all the transfer orbits that go through these given terminals.

The impulsive case of orbital transfer is, of course, an ideal situation. There is one instantaneous thrust from the initial orbit into

the transfer orbit; there is a second instantaneous thrust to get into the final orbit. The information gained from the solution of this problem should provide a basis for the study of orbital transfer with finite thrust.

The majority of the published two-impulse orbital transfer work deals with fixed terminals and co-planar orbits [2-4]. The recent work by G. A. McCue [5] represents an extension, by means of a numerical contour mapping approach, to include both free terminals and inclined orbits. The analysis in the paper presented here is valid for inclined orbits and is directed towards solving the fixed terminal problem. However, since it is necessary to solve this problem many times before the free terminal problem can be investigated by means of contour maps, the findings of this analysis have been incorporated into Mr. McCue's numerical program.

II. EXPLANATION OF PROBLEM FORMULATION

Two Keplerian elliptical orbits in space can be defined by their orbital elements, a, e, i, Ω, and ω. In the general two-impulse orbital transfer problem, it is desirable to locate the minimum velocity increment solution between any two such Keplerian orbits. If the plane of the second orbit of the transfer is the reference plane, then i_2, the inclination of the second orbit, is zero. The terms ordinarily referred to as the "nodal" parameters, Ω_1, and Ω_2, are made zero by selecting the line of intersection of the two orbit planes as the reference direction. (See Figure 1)

$$\left(\underline{N} = \frac{\underline{W}_2 \times \underline{W}_1}{\left| \underline{W}_2 \times \underline{W}_1 \right|} \right) \tag{1}$$

This leaves seven orbital elements (a_1, e_1, i_1, ω_1 and a_2, e_2, ω_2--subscripts one and two refer to elements in the first and second orbits respectively) that define the two orbits between which the transfer is to be accomplished.

Three variables which define all possible means of transferring from the first orbit to the second orbit are ϕ_1, the angle from reference line ($\underline{N}$) to a departure point on the first orbit; ϕ_2, the angle from reference line to arrival point on second orbit; and p, the semi-latus rectum of the transfer orbit between the two points. The parameter p is chosen as the third variable because it simplifies the nature of the impulse function. Other formulations for the third variable can produce serious discontinuities [5].

The "total impulse" used in transferring between the orbits is defined as the sum of the magnitudes of the velocity changes necessary to get from the first orbit into the transfer orbit and then from the transfer orbit into

the second orbit. In this paper, an optimum impulse solution refers to a particular configuration of the three variables that leads to the least possible impulse between two orbits. A minimum impulse solution refers to the transfer orbit which gives the least total impulse for a given arrival-point, departure-point configuration.

III. TRANSFER GEOMETRY

In rendering the orbital transfer problem subject to analysis, it is most convenient to express the important quantities in their vector representation. The vectors $\underline{r}_1$ and $\underline{r}_2$ represent the vectors from the attracting body to the departure and arrival points. Define unit vectors $\underline{U}_1$ and $\underline{U}_2$ in the direction of $\underline{r}_1$ and $\underline{r}_2$. The components of these vectors are then given by

$$\underline{U}_1 = \cos \phi_1 \, \underline{i} + \sin \phi_1 \cos i_1 \, \underline{j} + \sin \phi_1 \sin i_1 \, \underline{k} \tag{2}$$

$$\underline{U}_2 = \cos \phi_2 \, \underline{i} + \sin \phi_2 \, \underline{j} \tag{3}$$

$$\underline{r}_m = \left[\frac{p_m}{1 + e_m \cos (\phi_m - \omega_m)} \right] \underline{U}_m, \quad m = 1, 2 \tag{4}$$

where $\underline{i}$, $\underline{j}$, and $\underline{k}$ are unit vectors in a right-handed Cartesian system with $\underline{i}$ in the direction of N.

Three more useful vectors in the analysis are $\underline{W}_1$, $\underline{W}_2$, and $\underline{W}_t$--these are normal to the initial, final, and transfer orbit planes and are defined as follows:

$$\underline{W}_1 = -\sin i_1 \, \underline{j} + \cos i_1 \, \underline{k} \tag{5}$$

$$\underline{W}_2 = \underline{k} \tag{6}$$

$$\underline{W}_t = \frac{\underline{U}_1 \times \underline{U}_2}{|\underline{U}_1 \times \underline{U}_2|} \quad \text{where } |\underline{U}_1 \times \underline{U}_2| \neq 0 \tag{7}$$

To complete the vector description, define two vectors $\underline{e}_1$ and $\underline{e}_2$--these define the shape and orientation of the two orbits (6).

$$\underline{e}_m = e_m (\cos \omega_m \underline{i} + \sin \omega_m \cos i_m \underline{j} + \sin \omega_m \sin i_m \underline{k}) \quad (8)$$

where $m = 1, 2$

The part of the transfer orbit traversed in the transfer is a certain true anomaly interval $\Delta\theta$. This interval may be quickly determined from

$$\cos \Delta\theta = (\underline{U}_1 \cdot \underline{U}_2) \quad 0° < \Delta\theta < 180° \quad (9)$$

No generality is lost if the true anomaly interval is limited to the first two quadrants. Although this does restrict the problem to "short transfers," if the signs of the velocity vectors in the transfer orbit are changed, the long transfers may be considered. The singularities in the impulse function at $\Delta\theta = 180°$ and $\Delta\theta = 0°$ indicate that the problem is simplified by considering the long and short transfers separately. Thus, in order to determine the absolute optimum transfer between two elliptical orbits, it is necessary to compare the optima found from all the short transfers and all the long transfers.

For every elliptical transfer orbit between a given departure point and arrival point, there exists both a short transfer and a long transfer. However, when considering particular hyperbolic transfer orbits, it is important to realize that either the short transfer or the long transfer is meaningless--it would require going out to infinity and back.

IV. THE BELL-ARENSTORF TECHNIQUE

The "Bell-Arenstorf technique" refers to a geometrical method of analyzing the two impulse orbital transfer problem. This method is based upon some cogent variable relationships recognized separately by Mr. H. W. Bell of North American Aviation, Inc., [7] and Dr. Richard Arenstorf of Marshall Space Flight Center [8]. The fundamental idea of the method - that all possible transfers between fixed terminals on any elliptical orbits can be represented by two hyperbolae - provided the stimulus for much of this analysis.

For any two elliptical orbits, let $\underline{r}_1$ and $\underline{r}_2$ be the vectors from the reference position on the line of intersection to the departure and arrival points, respectively. The angle between them is $\Delta\theta$ and the size of this angle can be selected to be always in the first two quadrants without any loss of generality. By forming the vector $\underline{r}_2 - \underline{r}_1$, a triangle is made of the three vectors in the transfer orbit plane.

Define the two angles α and β (Figure 2) as follows:

$$\beta = \arcsin \frac{|\underline{r}_2| \sin \Delta\theta}{|\underline{r}_2 - \underline{r}_1|} \tag{10}$$

$$\alpha = \pi - (\beta + \Delta\theta) \tag{11}$$

Consider the locus of all possible velocity vectors that can act upon the point defined by $\underline{r}_1$ and trace a conical orbit path that goes through the point defined by $\underline{r}_2$. This locus defines all possible conic transfer orbits between the two points, since a particular orbit is uniquely defined by its velocity vector at a given position.

The velocity vector of any transfer orbit at the particular point $\underline{r}_1$ is given by (See Appendix 1)

$$\underline{V}_{t1} = \underline{v} + z\ \underline{U}_1 \tag{12}$$

where

$$\underline{v} = \frac{(\mu p)^{1/2} (\underline{r}_2 - \underline{r}_1)}{|\underline{r}_1 \times \underline{r}_2|} \tag{13}$$

$$z = \left(\frac{\mu}{p}\right)^{1/2} \tan \frac{\Delta\theta}{2} \tag{14}$$

where p is the semi-latus rectum of the transfer orbit. Then V_{t1} may be witten as a function of this variable p.

$$V_{t1}(p) = \left(\frac{\mu}{p}\right)^{1/2} \left[\frac{p\ |\underline{r}_2 - \underline{r}_1|}{|\underline{r}_1 \times \underline{r}_2|}\ \underline{m} + \tan \frac{\Delta\theta}{2}\ \underline{U}_1\right] \tag{15}$$

where $\underline{m}$ is unit vector in the direction of $\underline{r}_2 - \underline{r}_1$. Every positive value of p greater than zero defines a certain transfer orbit whose velocity vector at $\underline{r}_1$ has components in the direction of $\underline{m}$ and $\underline{U}_1$.

For any coordinate axes, the locus of all points such that the product of the coordinates is a constant forms a hyperbola with the axes as asymptotes. Since the product of the magnitudes of the components in the $\underline{m}$-direction and the $\underline{U}_1$ direction is independent of p,

$$\left[\frac{(\mu p)^{1/2} \; |\underline{r}_2 - \underline{r}_1|}{|\underline{r}_1 \times \underline{r}_2|}\right]\left[\left(\frac{\mu}{p}\right)^{1/2} \tan\frac{\Delta\theta}{2}\right] = \frac{\mu \tan\frac{\Delta\theta}{2} \; |\underline{r}_2 - \underline{r}_1|}{|\underline{r}_1 \times \underline{r}_2|} \qquad (16)$$

the formulation of V_{t1} defines a hyperbola with the oblique coordinates established by $\underline{m}$ and $\underline{U}_1$ as asymptotes. Thus the locus of all possible velocity vectors leaving $\underline{r}_1$ and arriving at $\underline{r}_2$ on a conic path forms a hyperbola.

Similarly, at $\underline{r}_2$ the velocity vector for any transfer orbit (dependent upon its semi-latus rectum) is given by

$$\underline{V}_{t2} = \underline{v} - z \; \underline{U}_2 \qquad (17)$$

This defines another hyperbola that represents the locus of all possible transfer orbits leaving from $\underline{r}_1$ and arriving at $\underline{r}_2$. These are shown in Figure 2. It is important to note that for every p, there is one point on each of these hyperbolae that represents the transfer orbit.

These two hyperbolae refer to the so-called short transfer, in which the true anomaly interval traversed in the transfer orbit is less than 180°. If the true anomaly interval is greater than 180° ("long transfer"), the other branches of these same two hyperbolae represent the locus of all transfer orbits. These are obtained by simply changing the sign of $\underline{V}_{t1}$ and $\underline{V}_{t2}$.

In Figure 2, the vectors $\underline{V}_1$ and $\underline{V}_2$, defining the initial and final orbits, are in the transfer orbit plane to simplify the analysis. Then this particular Bell-Arenstorf diagram represents a coplanar transfer and $\underline{V}_1$ and $\underline{V}_2$, defined by

$$\underline{V}_1 = \left(\frac{\mu}{p_1}\right)^{1/2} \underline{W}_1 \times (\underline{e}_1 + \underline{U}_1) \qquad (18)$$

$$\underline{V}_2 = \left(\frac{\mu}{p_2}\right)^{1/2} \underline{W}_2 \times (\underline{e}_2 + \underline{U}_2) \qquad (19)$$

must have magnitudes less than parabolic speed ($\underline{V}_{par}$).

$$\underline{V}^2_{par} = \frac{2\mu}{r} \qquad (20)$$

In the Bell-Arenstorf diagram, the vectors $\underline{V}_1$ and $\underline{V}_2$ (which uniquely define the initial and final orbits) emanate from $\underline{r}_1$ and $\underline{r}_2$ and must lie within a certain radius containing all elliptical orbits.

In finding the minimum velocity change solution for this two-impulse case, the function to be minimized is

$$I(p) = \Psi_1(p) + \Psi_2(p) \tag{21}$$

where

$$\Psi_1(p) = |\pm \underline{V}_{t1}(p) - \underline{V}_1| \tag{22a}$$

$$\Psi_2(p) = |\underline{V}_{2-} \mp \underline{V}_{t2}(p)| \tag{22b}$$

The double sign on the transfer velocity vector refers to short and long transfers (upper sign is short). In the diagram, this optimization procedure requires that the sum of the distances from $\underline{V}_1$ and $\underline{V}_2$ to their respective transfer loci be minimized. For every p, there is one and only one point on each hyperbola corresponding to that transfer orbit. The distances marked I_{1p} and I_{2p} (In Figure 2) represent simply a particular transfer orbit chosen for illustrative purposes. The sums of their magnitudes would represent the impulse necessary to transfer between these two points along that particular conic.

V. APPLICATION OF BELL-ARENSTORF TECHNIQUE

The Bell-Arenstorf technique provides an excellent geometrical image of what is occurring in the two-impulse orbital transfer. By comparing the magnitudes of the impulse vectors for different transfer orbits, one can gain an intuitive feeling for the size of the impulse for a particular transfer orbit. More important, though, was the fact that the Bell-Arenstorf technique offered clues to two of the more important questions in the field.

In Mr. McCue's paper [5] he conducts a numerical search for the minimum impulse for each arrival-point, departure-point configuration and then, by a method of contour mapping, locates the optimum transfer between any two elliptical orbits. One of his early assumptions was that there could only be one minimum in the impulse function (variable p, semi-latus rectum of transfer orbit) for a fixed pair of terminals. The Bell-Arenstorf technique clearly showed the existence of a double minimum for a certain case and thus implied the existence of certain configurations under which a double minimum may be present.

It has been implied in nearly all of the definitive analytical works in this area, such as that by Altman[3], that the minimum velocity increment solution between points on elliptical orbits was always an ellipse. The Bell-Arenstorf technique suggested the existence of hyperbolic minima for certain configurations--this fact was subsequently proved.

The use of the Bell-Arenstorf technique stimulated further analytic investigations whose findings have been incorporated into Mr. McCue's optimization program.

VI. LOCATION OF DOUBLE MINIMUM

In order to assert that there can be a double minimum in the impulse function for fixed terminals, it is necessary only to find an example. By considering a particular case with unique symmetry properties, this example can be readily illustrated.

Consider the case where $|r_1| = |r_2|$ (Figure 3). This makes the angle α (Figure 2) equal to the angle β. Then the hyperbolae formed between the oblique axes at both the departure point and the arrival point are equivalent. If the entire coordinate system at $\underline{r}_2$ were flipped over and translated to $\underline{r}_1$, then these two hyperbolae would become coincident--they would match up point for point, transfer orbit for transfer orbit. Then the impulse function for particular elliptical orbits (defined by $\underline{V}_1$ and $\underline{V}_2$, both of which now act at the same point) is only the sum of the distances from $\underline{V}_1$ and $\underline{V}_2$ to all points on the hyperbola. Then, for this case, the minimum impulse solution corresponds to the point on the hyperbola from which the sum of the distances to $\underline{V}_1$ and $\underline{V}_2$ is a minimum.

For points with equal radii, one possible transfer orbit corresponds to a circular transfer. This transfer has a velocity vector ($\underline{V}_r$) perpendicular to the radius vector and its magnitude is given by

$$\underline{V}_r^2 = \frac{\mu}{r} \tag{23}$$

All velocity vectors emanating from $\underline{r}_1$ that have magnitudes less than $\left(\frac{2\mu}{r}\right)^{1/2}$ define elliptical initial and final orbits. In the diagram this range for $\underline{V}_1$ and $\underline{V}_2$ is described by a circle marked parabolic orbit limit.

Suppose $\underline{V}_1$ and $\underline{V}_2$ are located in such positions (See Figure 3), relative to each other, that the line connecting them intersects the hyperbola (either short transfer branch or long transfer branch) twice. As p varies from zero to its unbounded upper value, all possible transfer orbits

have a corresponding point on the hyperbola. As p increases along the hyperbola, the value of the impulse is obviously decreasing until p reaches the value corresponding to a, where the line between $\underline{V}_1$ and $\underline{V}_2$ intersects the hyperbola. For values of p slightly larger than a (such as the p corresponding to point b), according to the triangle inequality the impulse must be higher. Thus the value of p at a must constitute a relative minimum in the impulse function.

As p nears the value corresponding to point c on the hyperbola, the triangle inequality states that the necessary transfer impulse is going down again. For points past c, the impulse is rising again, and thus c must also be a relative minimum. The fact that there can be two minima is thus demonstrated.

Numbers were placed into the diagram and indeed a double minimum (See Figure 4) occurred. The orbital elements for that particular fixed terminal case are given on the graph. For this case, the long transfer provides a greater impulse requirement for all transfers--thus only the short transfer is plotted.

In Appendix 2 a short mathematical investigation of the criteria for the existence of the double minimum in the case of equal radii is carried out. This investigation, which did lend some intuitive understanding to the problem, was not easily extendable to the case of non-equal radii.

VII. LOCATION OF HYPERBOLIC MINIMUM

The assumption has been made, in prior two-impulse orbital transfer studies, that the minimum transfer between two points on elliptical orbits always lies along an ellipse. Although this has never been proved, it has been generally accepted. Use of the Bell-Arenstorf technique showed this assumption to be false.

For the case of $|\underline{r}_1| = |\underline{r}_2|$, it is clear from Figure 5 that a hyperbolic minimum may exist. Once again, the coordinate system at $\underline{r}_2$ is rotated and flipped such that all possible transfer orbits are given by one hyperbola. If the vectors $\underline{V}_1$ and $\underline{V}_2$ lie in the shaded region (see insert), the shortest distance from each to the transfer orbit hyperbola arrives at a point on that hyperbola outside the parabolic orbit limit. Since the least velocity increment - both to arrive in the transfer orbit and depart from it - lies along hyperbolic transfers, the sum of the two, the impulse, must have its minimum along a hyperbolic orbit between these two.

In investigating the more general case of non-equal radii, the geometry yielded not only configurations for which the minimum velocity

increment solution could lie along a hyperbola, but also some other interesting properties about this orbital transfer function.

The general Bell-Arenstorf technique diagram can be modified (See Figure 6) in such a way as to orient both hyperbolae about the same coordinate axis with a common asymptote. Since for every p, the semi-latus rectum of the transfer orbit, there is one and only one point on each hyperbola, some manner of relating corresponding transfer orbits must be found. In Appendix 3 it is shown that there exist two families of circles, with centers on the $\underline{r}_2 - \underline{r}_1$ axis and radii dependent on the parameter p, that intersect the hyperbolae in such a way as to identify the points referring to the same transfer orbit. One family refers to the short transfers; the other, to the long. The short transfer family begins at the origin, with a member of infinite radius, and moves left through all possible values of p; the long transfer family goes in the opposite direction, also with increasing radius magnitude.

For every fixed arrival-point, departure-point configuration, there are two bounds on the values of the semi-latus rectum of the transfer orbit that define all elliptical transfer orbits. These "parabolic orbit limits" are defined by [5]

$$P_{max} = \frac{r_1 r_2 - \underline{r}_1 \cdot \underline{r}_2}{r_1 + r_2 + (2r_1 r_2 + 2\underline{r}_1 \cdot \underline{r}_2)^{1/2}} \tag{24}$$

$$P_{min} = \frac{r_1 r_2 - \underline{r}_1 \cdot \underline{r}_2}{r_1 + r_2 + (2r_1 r_2 + 2\underline{r}_1 \cdot \underline{r}_2)^{1/2}} \tag{25}$$

In the Bell-Arenstorf diagram, as p increases from zero to infinity, the radii of the family of circles diminish for both the long and short transfers. It is important to note that for $p > p_{max}$, the long transfer's being along a hyperbola is meaningless; similarly, for $p < p_{min}$, the short transfer implies going out to infinity to complete the orbit.

Regardless of what $\underline{r}_1$ and $\underline{r}_2$ are, there exists some value of p that defines the lower limit of elliptical transfer orbits. The circle marked "parabolic orbit limit" has its center at a point that is a value of p at which the long transfers change from hyperbolic into elliptical. Even though it is true that for every $\underline{r}_1$ and $\underline{r}_2$ this circle is located at a different place, it is important that it does exist somewhere and thus can be located arbitrarily. Then all initial orbits whose velocity vector at $\underline{r}_1$ lies inside the circle of radius A are elliptical; similarly for all final orbits whose velocity vector at $\underline{r}_2$ lies inside the circle of radius B. Suppose the initial and final orbits define velocity vectors $\underline{V}_1$ and $\underline{V}_2$ such that they are located as in Figure 5.

It is clear that the least first increment change (to get into the transfer orbit) and the least final increment change are to transfer orbits that are hyperbolic. It is an easy extension to see that the sum of these two is a minimum along a hyperbola somewhere between these.

In Figure 7, impulse is plotted against the semi-latus rectum of the transfer orbit for a particular configuration. The parabolic orbit limits are marked and the orbital parameters are given--clearly the minimum transfer is along a hyperbola.

VIII. ANALYSIS OF IMPULSE FUNCTION

The location of these peculiarities in the impulse function prompted an analytic search into the equations that describe the impulse problem. New analytic boundaries, different from the parabolic orbit limits, were sought for the minima. For fixed terminals (once again it should be pointed out that this is a restricted case of the more general problem of optimizing between any points on elliptical orbits), the impulse function is only dependent on p, the semi-latus rectum of the transfer orbit. This impulse function, defined by equation (21), has an extremum at all points p where

$$\frac{\partial I}{\partial p} = \frac{\partial \Psi_1}{\partial p} + \frac{\partial \Psi_2}{\partial p} = 0 \tag{26}$$

In the analysis of the impulse function carried out here, only the short transfers are considered. It is shown in a subsequent section that the extension to include the long transfers is very simple.

Now

$$\begin{aligned} \Psi_1(p) &= [\,(\underline{V}_{t1}(p) - \underline{V}_1) \cdot (\underline{V}_{t1}(p) - \underline{V}_1)\,]^{1/2} \\ &= [\,(\underline{v}(p) + z(p)\,\underline{U}_1 - \underline{V}_1) \cdot (\underline{v}(p) + z(p)\,\underline{U}_1 - \underline{V}_1)\,]^{1/2} \\ &= [\,f(p)\,]^{1/2} \end{aligned} \tag{27}$$

where

$$f(p) = \underline{v}(p) \cdot \underline{v}(p) + z^2(p) + \underline{V}_1 \cdot \underline{V}_1 - 2z(p)\, \underline{V}_1 \cdot \underline{U}_1$$

$$- 2\underline{V}_1 \cdot \underline{v}(p) + 2z(p)\, \underline{v}(p) \cdot \underline{U}_1$$

$$= Ap + 2Bp^{1/2} + G - 2Cp^{-1/2} - Dp^{-1} \tag{28}$$

where the coefficients are given in Table 1.

Similarly,

$$\Psi_2(p) = [\, g(p)]^{1/2} \tag{29}$$

where

$$g(p) = Ap + 2Ep^{1/2} + H - 2Fp^{-1/2} - Dp^{-1} \tag{30}$$

where the new coefficients are also given in Table 1.

Then, in order for impulse to be an extremum,

$$\frac{\partial \Psi_1}{\partial p} + \frac{\partial \Psi_2}{\partial p} = \frac{1}{2\Psi_1} \frac{\partial f}{\partial p} + \frac{1}{2\Psi_2} \frac{\partial g}{\partial p} = 0 \tag{31}$$

$$\Longrightarrow \quad \frac{\Psi_1(p)}{\Psi_2(p)} = -\frac{\frac{\partial f}{\partial p}}{\frac{\partial g}{\partial p}} \tag{32}$$

Since $\Psi_1(p)$ and $\Psi_2(p)$ are always positive, it is easy to see from equation (32) that $\partial f/\partial p$ and $\partial g/\partial p$ must be of different sign before an extremum can occur in the impulse function. This important fact permits the identification of the extraneous roots in the eighth-order polynomial that will be derived.

Then

$$\frac{\partial f}{\partial p} = A + Bp^{-1/2} + Cp^{-3/2} + Dp^{-2} \tag{33}$$

and

$$\frac{\partial g}{\partial p} = A + Ep^{-1/2} + Fp^{-3/2} + Dp^{-2} \tag{34}$$

Before a meaningful expression can be worked out for the extrema in the impulse, equation (32) must be squared. Then the necessary expression becomes

$$\frac{f(p)}{g(p)} = \frac{\left(\frac{\partial f}{\partial p}\right)^2}{\left(\frac{\partial g}{\partial p}\right)^2}$$

or

$$f(p)\left(\frac{\partial g}{\partial p}\right)^2 - g(p)\left(\frac{\partial f}{\partial p}\right)^2 = 0 \tag{35}$$

When this equation is multiplied out using equations (27), (28), (33), and (34), together with the substitution

$$s = p^{1/2} \tag{36}$$

the necessary condition for an extremum becomes

$$\phi_1 s^8 + \phi_2 s^7 + \phi_3 s^6 + \phi_4 s^5 + \phi_5 s^4 + \phi_6 s^3 + \phi_7 s^2 + \phi_8 s + \phi_9 = 0 \tag{37}$$

where the coefficients ϕ_i, i = 1-8 are given in Table 2. The real roots of this eighth-order polynomial must include all the values of p for which the impulse is an extremum.

The squaring process introduced in equation (35) added some extraneous roots to the octic--roots which do not correspond to extrema in I(p). These can be identified by factoring equation (35) as the difference of two squares.

$$f(p)\left(\frac{\partial g}{\partial p}\right)^2 - g(p)\left(\frac{\partial f}{\partial p}\right)^2 = 0$$

$$\Longrightarrow \left(\Psi_1(p)\frac{\partial g}{\partial p} + \Psi_2(p)\frac{\partial f}{\partial p}\right)\left(\Psi_1(p)\frac{\partial g}{\partial p} - \Psi_2(p)\frac{\partial f}{\partial p}\right) = 0 \tag{38}$$

Since $\frac{\partial f}{\partial p}$ and $\frac{\partial g}{\partial p}$ must be of different sign, only those real values of p which are roots of

$$\Psi_1(p) \frac{\partial g}{\partial p} + \Psi_2(p) \frac{\partial f}{\partial p} = 0 \tag{39}$$

are true extrema of I(p). It is easily shown (See Appendix 4) that the equation

$$\Psi_1(p) \frac{\partial g}{\partial p} - \Psi_2(p) \frac{\partial f}{\partial p} = 0 \tag{40}$$

contains the extraneous roots of the octic and refers to extrema in another function, I*(p). Then

$$I^*(p) = \Psi_1(p) - \Psi_2(p) \tag{41}$$

Inquiries into the nature of this octic suggest that four of these roots refer to extrema in I*(p). Although no general proof has been made, if this fact were true for all configurations, then there could be no more than two minima on either transfer branch. This would greatly simplify the application of the contour mapping approach.

In Mr. Altman's paper, he identifies an eighth-order polynomial, the roots of which refer to minima in the case of two-impulse orbital transfer between coplanar orbits. Equation (37) extends the analysis, using different techniques, both to include inclined orbits and to identify those roots of the equation that are extraneous and do not refer to minima in the impulse function.

IX. THE BOUNDARIES ON MINIMA

Since a necessary condition for the existence of an extremum in the impulse function is that $\partial f/\partial p$ and $\partial g/\partial p$ be of different sign, analyses were next directed to determine the values for p for which they could be of different sign.

From equations (33) and (34),

$$\lim_{p \to \infty} \frac{\partial f}{\partial p} = \lim_{p \to \infty} \frac{\partial g}{\partial p} = A \tag{42}$$

where

$$A = \frac{\mu \left| \underline{r}_2 - \underline{r}_1 \right|^2}{\left| \underline{r}_1 \times \underline{r}_2 \right|^2} > 0 \tag{43}$$

and

$$\lim_{p \to 0^+} \frac{\partial f}{\partial p} = \lim_{p \to 0^+} \frac{\partial g}{\partial p} = -\infty \tag{44}$$

because

$$D = -\mu \tan^2 \frac{\Delta\theta}{2} \tag{45}$$

Since for p both very small and very large, $\partial f/\partial p$ and $\partial g/\partial p$ have the same sign, we know that the region in which $\partial f/\partial p$ and $\partial g/\partial p$ are of different sign may definitely be bounded. The boundaries in which all minima in the impulse function (on short transfer side) must lie are given by the least positive value of p and the greatest positive value of p at which either

$$\frac{\partial f}{\partial p} = 0 \quad \text{or} \quad \frac{\partial g}{\partial p} = 0 \tag{46}$$

For $s = p^{1/2}$, $\partial f/\partial p = 0$ where

$$As^4 + Bs^3 + Cs + D = 0 \tag{47}$$

Similarly, $\partial g/\partial p = 0$ where

$$As^4 + Es^3 + Fs + D = 0 \tag{48}$$

These values for p that bound the minima can be readily obtained. It is shown in a subsequent section that these equations also give the intervals for the long transfer. Thus, definite, analytic boundaries on the possible range of the impulse minima have been ascertained.

X. THE INTERVALS

Since both $\partial f/\partial p$ and $\partial g/\partial p$ have negative values for p very small and positive values for p very large, both expressions (47 and 48) must have an odd number of positive real roots. Each of these quartic equations may

have either one or three real positive roots. Regardless how many of these roots each of these quartics has, all possible combinations of the roots can be studied by investigating two types of intervals in which $\partial f/\partial p$ and $\partial g/\partial p$ may be of different sign.

Type A: 1) $\frac{\partial f}{\partial p}$ and $\frac{\partial g}{\partial p}$ of different sign in [a, b]

2) $\left(\frac{\partial f}{\partial p}\right)_{p = a} = 0; \quad \left(\frac{\partial g}{\partial p}\right)_{p = b} = 0$ (49)

Type B: 1) $\frac{\partial f}{\partial p}$ and $\frac{\partial g}{\partial p}$ of different sign in [a, b]

2) $\left(\frac{\partial f}{\partial p}\right)_{p = a} = 0; \quad \left(\frac{\partial f}{\partial p}\right)_{p = a} = 0$ (50)

It is important to note that if, in equation (49), $\partial f/\partial p$ and $\partial g/\partial p$ are zero at opposite ends of the interval from those given, the problem is not really changed. Similarly, if in equation (50) it is $\partial g/\partial p$ which is zero at both ends, the analysis of the types of intervals still holds. In type A each of the functions is zero at one end of the interval; in type B, one function is zero at both ends of the interval. The two types of intervals are illustrated in Figure 8.

These intervals are divided into two types because the number of minima possible in a given interval is determined by its type. Define two functions $\sigma(p)$ and $\tau(p)$ as

$$\sigma(p) = -\frac{\frac{\partial f}{\partial p}}{\frac{\partial g}{\partial p}} \tag{51}$$

$$\tau(p) = \frac{\Psi_1(p)}{\Psi_2(p)} \tag{52}$$

Obviously, an extremum in the impulse function occurs for all p at which $\sigma(p) = \tau(p)$.

Consider an interval of Type A. τ is monotonic increasing and positive for all p in [a, b]. Also, note that

$$\sigma(a) = 0 \tag{53}$$

and

$$\lim_{p \to b} \sigma(p) = \infty \tag{54}$$

From Figure 8, it is clear σ and τ must intersect at least one time (producing one extremum) in that interval. If they are equal more than once, they must intersect an odd number of times.

Consider next an interval of Type B. Once again τ is monotonic increasing and positive for all p in [a, b]. Here, though

$$\sigma(a) = 0 \tag{55}$$

and

$$\sigma(b) = 0 \tag{56}$$

while for all p in [a, b], $\sigma(p) > 0$. It is evident from Figure 8 that σ and τ must intersect an even number of times in intervals of this type.

All possible permutations of the roots of these quartics can be manipulated to reduce the problem to an analysis of these intervals. Most frequently, both $\partial f/\partial p$ and $\partial g/\partial p$ have one real, positive root and produce an interval of type A in which σ and τ intersect one time. It is also true that, for the majority of the cases, the first and last real positive roots of the two quartics will limit the search for the minimum impulse to elliptical transfer orbits. These analyses do, however, explain the existence of the two peculiarities located earlier.

XI. LONG AND SHORT TRANSFER

For nearly all the equations derived in the preceding sections, it was assumed that the two-impulse orbital transfer was accomplished with a true anomaly interval in the transfer orbit of less than 180°--short transfer. The symmetry of the problem makes extension to include the long transfers very simple. To obtain the absolute minimum impulse, the two are then compared.

Because of the symmetry (See Appendix 5 for detailed derivation of long transfer equations) it can be shown that the real, negative roots of equations (33) and (34) determine intervals on the long transfer side that may produce minima. Similarly, it is the real, negative roots of the general octic (Equation 37) that appear within those specified intervals that determine values of p for which the long transfer may be an extremum.

This implies that all the analysis can be conducted by examining three equations--two quartic and one octic. The real roots of these equations--positive for short transfer and negative for long transfer--define all the intervals in which the extrema may exist and then locate the values of p at which extrema actually occur.

XII. MODIFICATION OF COMPUTER PROGRAM

In Mr. McCue's work, he optimizes the transfer between two elliptical orbits (not fixed terminals) by means of a contour mapping routine in the ϕ_1-ϕ_2 space that connects transfers of equal impulse requirement. In locating the minimum impulse for a particular ϕ_1-ϕ_2 configuration, he conducts a numerical search minimization along p that is confined within the parabolic orbit limits. The results of the analytic investigations presented here have been incorporated into the program to remove the limitations.

The solution of the two quartics (Equations 33 and 34) gives the intervals to which the numerical search for minima may be restricted. In nearly all cases a search within these limits will require fewer iterations than one conducted with the old arbitrary limits. If the steepest descent program should--in rare instances--converge on two different values within the same interval, the octic equation may be solved and its real roots compared to the intervals of possible minima. For nearly all ϕ_1-ϕ_2 configurations, this process will require no more computer time than it did before the limitations were removed.

XIII. SUMMARY

New analytical approaches to the two-impulse orbital transfer problem are developed in this paper. This development precipitated the discovery of both the hyperbolic minimum and the double minimum in the minimum velocity increment solution between points on elliptical orbits. Further analyses produced an eighth-order polynomial--applicable even for inclined orbits--whose roots contain all possible extrema in the impulse function. Next test functions were located that placed bounds on the regions in which these extrema could exist and identified those roots of the octic that were extraneous. The explanation of these extraneous roots--not corresponding to minima in the impulse function--was given.

All these results have been used to modify an earlier computer program. It is now possible to locate not only the absolute minimum two-impulse transfer between fixed terminals for any elliptical orbit pair, but also the absolute optimum transfer between any end points on those orbits.

TABLE 1

COEFFICIENTS OF TEST FUNCTIONS

$$A = \mu \frac{|\underline{r}_2 - \underline{r}_1|^2}{|\underline{r}_1 \times \underline{r}_2|^2}$$

$$B = - \frac{\mu}{(p_1)^{1/2} |\underline{r}_1 \times \underline{r}_2|} \left[(\underline{r}_2 - \underline{r}_1) \cdot (\underline{W}_1 \times (\underline{e}_1 + \underline{U}_1)) \right]$$

$$C = \frac{\mu \tan \frac{\Delta\theta}{2}}{(p_1)^{1/2}} \left[U_1 \cdot (\underline{W}_1 \times \underline{e}_1) \right]$$

$$D = - \mu \tan^2 \frac{\Delta\theta}{2}$$

$$E = - \frac{\mu}{(p_2)^{1/2} |\underline{r}_1 \times \underline{r}_2|} \left[(\underline{r}_2 - \underline{r}_1) \cdot (\underline{W}_2 \times (\underline{e}_2 + \underline{U}_2)) \right]$$

$$F = \frac{- \mu \tan \frac{\Delta\theta}{2}}{(p_2)^{1/2}} \left[\underline{U}_2 \cdot (\underline{W}_2 \times \underline{e}_2) \right]$$

$$G = \frac{\mu}{p_1} \left[\underline{W}_1 \times (\underline{e}_1 + \underline{U}_1) \right]^2 + \frac{2\mu \tan \frac{\Delta\theta}{2}}{|\underline{r}_1 \times \underline{r}_2|} \left[\underline{U}_1 \cdot (\underline{r}_2 - \underline{r}_1) \right]$$

$$H = \frac{\mu}{p_2} \left[\underline{W}_2 \times (\underline{e}_2 + \underline{U}_2) \right]^2 - \frac{2\mu \tan \frac{\Delta\theta}{2}}{|\underline{r}_1 \times \underline{r}_2|} \left[\underline{U}_2 \cdot (\underline{r}_2 - \underline{r}_1) \right]$$

TABLE 2

COEFFICIENTS OF EIGHTH-ORDER POLYNOMIAL

$$\phi_1 = A^2(G - H) + A(E^2 - B^2)$$

$$\phi_2 = A^2(4F - 4C) + A(2EG - 2BH) + 2E^2B - 2EB^2$$

$$\phi_3 = A(8BF - 8EC + 2EF - 2BC) + E^2G - HB^2$$

$$\phi_4 = A(4BD - 4ED + 2FG - 2CH) + 4BEF - 2CE^2 - 4BCE + 2FB^2$$

$$\phi_5 = D(2AG - 2HA - E^2 + B^2) + A(F^2 - C^2) - 2BCH + 2GEF$$

$$\phi_6 = D(4FA - 4AC + 2EG - 2BH) + 4FBC - 4CEF + 2BF^2 - 2EC^2$$

$$\phi_7 = D(8BF - 8EC + 2BC - 2EF) + F^2G - C^2H$$

$$\phi_8 = D^2(4B - 4E) + D(2FB - 2HC) + 2FC^2 - 2CF^2$$

$$\phi_9 = D^2(G - H) + D(C^2 - F^2)$$

ACKNOWLEDGMENTS

To Mr. H. W. Bell, the assistant director of the Space Sciences Laboratory, the author extends his gratitude--both for his patient advice during the research and the vital technical contributions that provided the stimuli for much of this work. I also am indebted to Dr. D. F. Bender, Mr. G. A. McCue, and the entire Space Mechanics section of the laboratory; their prior research in this area laid the foundation for this work.

REFERENCES

1. Smart, W. M., Celestial Mechanics, Longmans, Green and Company, London, 1953.

2. Bender, D. F., "Optimum Coplanar Two-Impulse Transfer Between Elliptic Orbits", Journal of Aerospace Engineering, Vol. 21, October 1962, p. 44-52.

3. Altman, S. P. and Pistiner, J. S., "Minimum Velocity Increment Solution for Two-Impulse Coplanar Orbital Transfer", AIAA Journal, Vol. 1, number 2, February 1963, pp. 435-442.

4. Vargo, L. G., "Optimal Transfer Between Coplanar Terminals in a Gravitational Field," Advances in Astronautical Sciences, Plenum Press, New York, 1958, Vol. 3, pp. 20-1 to 20-9.

5. McCue, G. A., "Optimum Two-Impulse Orbital Transfer and Rendezvous Between Inclined Elliptical Orbits", SID 62-1400, North American Aviation, Inc., November 20, 1962, (To be published in AIAA Journal).

6. Herget, Paul, "The Computation of Orbits", Published privately by author, Ann Arbor, Michigan, 1948, p. 30

7. Bell, H. W., Unpublished private communication, 1963.

8. Arenstorf, Richard A., "Solution of Two-Body Problem in Complex Form", Unpublished written analysis, 1960.

APPENDIX 1

Derivation of Transfer Velocity Expressions:

These equations appear in reference (5) and were originally derived by Mr. H. W. Bell.

Begin with the vector expressions for the transfer orbit velocities,

$$\underline{V}_{t1}(p) = \left(\frac{\mu}{p}\right)^{1/2} \underline{W}_t \times (\underline{e}_t + \underline{U}_1) \tag{A1-1}$$

$$\underline{V}_{t2}(p) = \left(\frac{\mu}{p}\right)^{1/2} W_t \times (\underline{e}_t + \underline{U}_2) \tag{A1-2}$$

where $\underline{e}_t$ is a vector, not necessarily explicitly defined, that has the magnitude of the eccentricity of the transfer orbit and is in the direction of its perigee.

Then for all transfer orbits that include $\underline{r}_1$ and $\underline{r}_2$,

$$|\underline{r}_1| = \frac{p}{1 + \underline{e}_t \cdot \underline{U}_1} \tag{A1-3}$$

$$|\underline{r}_2| = \frac{p}{1 + \underline{e}_t \cdot \underline{U}_2} \tag{A1-4}$$

and by algebraic manipulation

$$\underline{e}_t \cdot \underline{U}_1 = \frac{p}{|\underline{r}_1|} - 1 \tag{A1-5}$$

$$\underline{e}_t \cdot \underline{U}_2 = \frac{p}{|\underline{r}_2|} - 1 \tag{A1-6}$$

Then multiplying these equations by $\underline{U}_2$ and $\underline{U}_1$ gives

$$(\underline{e}_t \cdot \underline{U}_1)\,\underline{U}_2 = \underline{U}_2 \left(\frac{p}{|\underline{r}_1|} - 1\right) \tag{A1-7}$$

and

$$(\underline{e}_t \cdot \underline{U}_2)\,\underline{U}_1 = \underline{U}_1 \left(\frac{p}{|\underline{r}_2|} - 1\right) \tag{A1-8}$$

Then according to vector identities

$$(\underline{U}_1 \times \underline{U}_2) \times \underline{e}_t = -\underline{e}_t \times (\underline{U}_1 \times \underline{U}_2)$$

$$= -\underline{U}_1 (U_2 \cdot \underline{e}_t) + U_2 (\underline{U}_1 \cdot \underline{e}_t)$$

$$= \underline{U}_2 \left(\frac{p}{|\underline{r}_1|} - 1\right) - \underline{U}_1 \left(\frac{p}{|\underline{r}_2|} - 1\right) \tag{A1-9}$$

Notice that

$$\underline{W}_t \times (\underline{e}_t + \underline{U}_1) = \frac{(\underline{U}_1 \times \underline{U}_2)}{|\underline{U}_1 \times \underline{U}_2|} \times (\underline{e}_t + \underline{U}_1)$$

$$= \frac{(\underline{U}_1 \times \underline{U}_2) \times \underline{e}_t}{\underline{U}_1 \times \underline{U}_2} + \frac{(\underline{U}_1 \times \underline{U}_2) \times \underline{U}_1}{U_1 \times \underline{U}_2} \tag{A1-10}$$

$$= \frac{\underline{U}_2 \left(\frac{p}{|\underline{r}_1|} - 1\right) - \underline{U}_1 \left(\frac{p}{|\underline{r}_2|} - 1\right) + \underline{U}_2 (\underline{U}_1 \cdot \underline{U}_1) - \underline{U}_1 (\underline{U}_1 \cdot \underline{U}_2)}{|\underline{U}_1 \times \underline{U}_2|}$$

Similarly,

$$\underline{W}_t \times (\underline{e}_t + \underline{U}_2) = \frac{\underline{U}_2 \left(\frac{p}{|\underline{r}_1|} - 1\right) - \underline{U}_1 \left(\frac{p}{|\underline{r}_2|} - 1\right) - \underline{U}_1 (\underline{U}_2 \cdot \underline{U}_2) + \underline{U}_2 (\underline{U}_1 \cdot \underline{U}_2)}{\underline{U}_1 \times \underline{U}_2} \tag{A1-11}$$

Then from Equations (A1-1), (A1-2), (A1-10), and (A1-11),

$$V_{t1(p)} = \left(\frac{\mu}{p}\right)^{1/2} \frac{1}{|\underline{U}_1 \times \underline{U}_2|} \left[p \left(\frac{\underline{U}_2}{|\underline{r}_1|} - \frac{\underline{U}_1}{|\underline{r}_2|}\right) + (1 - \underline{U}_1 \cdot \underline{U}_2)\,\underline{U}_1\right] \tag{A1-12}$$

and

$$V_{t2}(p) = \left(\frac{\mu}{p}\right)^{1/2} \frac{1}{|\underline{U}_1 \times \underline{U}_2|} \left[p \left(\frac{\underline{U}_2}{|\underline{r}_1|} - \frac{\underline{U}_1}{|\underline{r}_2|} \right) - (1 - \underline{U}_1 \cdot \underline{U}_2)\, \underline{U}_2 \right] \tag{A1-13}$$

note that

$$U_1 \cdot U_2 = \cos \Delta\theta \tag{A1-14}$$

and

$$|\underline{U}_1 \times \underline{U}_2| = |U_1|\, |U_2| \sin \Delta\theta = \sin \Delta\theta \tag{A1-15}$$

Furthermore,

$$\frac{p}{|\underline{U}_1 \times \underline{U}_2|} \left[\frac{\underline{U}_2}{|\underline{r}_1|} - \frac{\underline{U}_1}{|\underline{r}_2|} \right] = \frac{p}{|\underline{U}_1 \times \underline{U}_2|} \left[\frac{\underline{U}_2\, \underline{r}_2 - \underline{U}_1\, \underline{r}_1}{|\underline{r}_1|\, |\underline{r}_2|} \right]$$

$$= \frac{p\,(\underline{r}_2 - \underline{r}_1)}{|\underline{r}_1 \times \underline{r}_2|} \tag{A1-16}$$

therefore,

$$\underline{V}_{t1}(p) = \left(\frac{\mu}{p}\right)^{1/2} \left[\frac{p\,(\underline{r}_2 - \underline{r}_1)}{\underline{r}_1 \times \underline{r}_2} + \frac{1 - \cos \Delta\theta}{\sin \Delta\theta}\, \underline{U}_1 \right] \tag{A1-17}$$

But

$$\frac{1 - \cos \Delta\theta}{\sin \Delta\theta} = \tan \frac{\Delta\theta}{2} \tag{A1-18}$$

*

which implies that

$$\underline{V}_{t1}(p) = \frac{\mu}{p}^{1/2} \left[\frac{p\,(\underline{r}_2 - \underline{r}_1)}{\underline{r}_1 \times \underline{r}_2} + \tan \frac{\Delta\theta}{2}\, \underline{U}_1 \right] = \underline{v} + z\underline{U}_1 \tag{A1-19}$$

---

* $\sin \Delta\theta = \underline{W}_t \cdot (\underline{U}_1 \times \underline{U}_2)$--this implies that angle from $\underline{U}_1$ to $\underline{U}_2$ is less than 180°.

Similarly, from (A1-13),

$$\underline{V}_{t2}(p) = \underline{v} - z\underline{U}_2 \tag{A1-20}$$

where

$$\underline{v} = \frac{(\mu p)^{1/2} (\underline{r}_2 - \underline{r}_1)}{|\underline{r}_1 \times \underline{r}_2|} \tag{A1-21}$$

and

$$z = \left(\frac{\mu}{p}\right)^{1/2} \left(\tan\frac{\Delta\theta}{2}\right) \tag{A1-22}$$

APPENDIX 2

On the Criteria for Existence of Double Minimum in Case of Equal Radii:

After the existence of the double minimum was first established the next research was directed toward finding the necessary and sufficient conditions for this existence. In the equal radii case, the answer was more or less obtainable.

If, for any $\underline{r}_1 - \underline{r}_2$ configuration where $|\underline{r}_1| = |\underline{r}_2|$, the transfer velocity (See Figure 2) hyperbola is considered to be symmetrical about an x-axis of a rectangular Cartesian coordinate system, the analytic equation of this hyperbola can be derived. From the general expression,

$$\frac{x^2}{a^2} - \frac{y^2}{b^2} = 1 \tag{A2-1}$$

and the knowledge that

$$\tan\left(45 - \frac{\Delta\theta}{4}\right) = \frac{a}{b} \tag{A2-2}$$

and the fact that there exists one point p_o on the hyperbola where

$$p_o = \left(\frac{\mu}{r}\right)^{1/2} \sin\Psi\,\underline{i} + \left(\frac{\mu}{r}\right)\cos\Psi\,\underline{j} \tag{A2-3}$$

$$\Psi = 45° + \frac{\Delta\theta}{4} \tag{A2-4}$$

the equation for this hyperbola is given as

$$r(y^2 \cos^2 \Psi - x^2 \sin^2 \Psi) = \mu \cos 2\Psi \tag{A2-5}$$

where

$$|\underline{r}_2| = |\underline{r}_1| = r \tag{A2-6}$$

$$a^2 = -\frac{\mu \cos 2\Psi}{r \sin^2 \Psi} \tag{A2-7}$$

$$b^2 = -\frac{\mu \cos 2\Psi}{r \cos^2 \Psi} \tag{A2-8}$$

The two elliptical orbits, initial and final, are defined by their velocity vectors at $\underline{r}_1$ and $\underline{r}_2$. The coordinates of these vectors in the same coordinate system as the hyperbola are readily found from the geometry and elementary celestial mechanics[1].

Suppose*

$$\underline{V}_1 = x_1 \underline{i} + y_1 \underline{j} \tag{A2-9}$$

$$\underline{V}_2 = x_2 \underline{i} + y_2 \underline{j} \tag{A2-10}$$

Then for every pair of elliptical orbits, two points in this system are determined. There is also a corresponding magnitude d_v, where

$$d_v = \left[(x_2 - x_1)^2 + (y_2 - y_1)^2\right]^{1/2} \tag{A2-11}$$

In the Bell-Arenstorf diagram, it is important to remember that for the case where $\underline{r}_1 = \underline{r}_2$, impulse for a particular transfer is nothing more than the sum of the distances from $\underline{V}_1$ and $\underline{V}_2$ to the point on the hyperbola representing that transfer.

---

* The actual analytic expressions for these coordinates have been omitted because of their detail.

For any initial and final elliptical orbits, let the points defined by $\underline{V}_1$ and $\underline{V}_2$ in this coordinate system be considered as the foci for a family of confocal ellipses. Each scalar value k,

$$\text{where } k \geq d_v \tag{A2-12}$$

defines a member of this family. Let

$$k = s_1 + s_2 \tag{A2-13}$$

Then s_1 and s_2 are, for any particular ellipse, the distances from $\underline{V}_1$ and $\underline{V}_2$ to that ellipse--their sum must be a constant for any member of the family.

In terms of the Bell-Arenstorf diagram, each member of the family corresponds to a certain impulse value--as k grows larger, eventually a member of the family (See Figure A2-1) intersects the hyperbola at a point of tangency. That point on the hyperbola, representing a particular transfer orbit, must be a relative minimum in impulse. This is easily seen if the next member of the family is considered--it intersects the hyperbola at two points, one on either side of the earlier point of tangency--it represents higher impulse. It is an easy intuitive extension to realize that every point at which a member of the family of ellipses is tangent to either branch of the hyperbola produces a relative extremum in either the long or short transfer.

In Figure A2-1, on the right, an example is given of a typical $\underline{V}_1$ - $\underline{V}_2$ configuration that produces one point of tangency--one relative minimum--on each of the two branches. The other example is a $\underline{V}_1$ - $\underline{V}_2$ configuration that produces a double minimum (see members 2 and 3 of the family) by having three points of tangency on one branch of the hyperbola. Note that if the family of ellipses has three members tangent to one branch of the hyperbola, there must exist some member of the family that intersects one branch of the hyperbola four times.

Since the analytic equation for this family of ellipses, using $s_1 + s_2 = k$ as the variable parameter, can be readily derived, the criteria for the existence of a double minimum can be simplified--for some member of the family, the fourth-order polynomial representing the intersection of that ellipse and the velocity hyperbola has four real roots of the same sign (on the same branch) if and only if a double minimum exists on that branch.

APPENDIX 3

Method of Determining Corresponding Transfers on Velocity Hyperbolae:

In Figure 6, the hyperbola representing all possible transfer orbits that arrive at $\underline{r}_2$ and pass through $\underline{r}_1$ is transformed so that both of the hyperbolae have the same reference point and one common asymptote. It is next necessary to determine the corresponding points on the hyperbolae: that is, to find some way of relating--transfer orbit for transfer orbit--the point on one hyperbola with the point defining the same transfer orbit on the other hyperbola. Because of the high symmetry and so that Figure 6 may be used, only the long transfer has been considered here.

Then if,

$$k = \frac{(\mu)^{1/2} \ |\underline{r}_2 - \underline{r}_1|}{|\underline{r}_1 \times \underline{r}_2|} \tag{A3-1}$$

and

$$h = \sqrt{\mu} \tan \frac{\Delta\theta}{2} \tag{A3-2}$$

and $\underline{m}$ is defined as a unit vector in the direction of $\underline{r}_2 - \underline{r}_1$.

$$V_{t1}(p) = - kp^{1/2} \underline{m} - hp^{-1/2} \underline{U}_1 \tag{A3-3}$$

$$V_{t2}(p) = - kp^{1/2} \underline{m} + hp^{-1/2} \underline{U}_2 \tag{A3-4}$$

It is obvious then that these two velocity hyperbolae have equal components in the m-direction. Furthermore, for each vector, the magnitude of the other component is the same. Thus the only significant difference in these functions is given by the different directions of $\underline{U}_1$ and $\underline{U}_2$.

For any real, positive value of p, the component of each of these transfer velocity vectors in the $\underline{r}_2 - \underline{r}_1$ direction is given by

$$\underline{V}_{t1} (\text{comp } \underline{r}_2 - \underline{r}_1) = \underline{V}_{t2} (\text{comp } \underline{r}_2 - \underline{r}_1) = - kp^{1/2} \tag{A3-5}$$

Therefore for any p, there exists some point on the $r_2 - r_1$ axis that corresponds to this component. Suppose a circle of radius r^*, where

$$r^* = hp^{-1/2} \tag{A3-6}$$

is circumscribed about that point as center. Then both the transfer velocity vectors for that particular transfer must end on that circle. Therefore, for any p, there exists a circle with center at a point on the $\underline{r}_2 - \underline{r}_1$ axis that will intersect the hyperbolae at the corresponding points.

It is an easy extension, therefore, to realize that the corresponding points on the hyperbolae are located by a family of circles with variable radii and centered on the $\underline{r}_2 - \underline{r}_1$ axis--the center and the radius being functions of the variable parameter p defining the transfer orbit.

APPENDIX 4

Identification of Extraneous Roots to Octic:

The eighth-order polynomial expression (Equation 37), whose roots contain the values of p at which the impulse function has a minimum, also has some roots that do not refer to impulse extrema.

This octic can be factored as the difference of two squares to produce equation (38),

$$\left(\Psi_1(p)\frac{\partial g}{\partial p} + \Psi_2(p)\frac{\partial f}{\partial p}\right)\left(\Psi_1(p)\frac{\partial g}{\partial p} - \Psi_2(p)\frac{\partial f}{\partial p}\right) = 0 \tag{A4-1}$$

It has already been shown that the equation

$$\left(\Psi_1(p)\frac{\partial g}{\partial p} + \Psi_2(p)\frac{\partial f}{\partial p}\right) = 0 \tag{A4-2}$$

gives roots to the octic whose p values do correspond to extrema in the impulse function.

The other factor

$$\left(\Psi_1(p)\frac{\partial g}{\partial p} - \Psi_2(p)\frac{\partial f}{\partial p}\right) = 0 \tag{A4-3}$$

produces roots to the octic that have no correspondence with impulse extrema.

Consider the function $I^*(p)$, where

$$I^*(p) = \Psi_1(p) - \Psi_2(p) \tag{A4-4}$$

Then $I^*(p)$ has extrema at every value p where

$$\frac{\partial \Psi_1}{\partial p} - \frac{\partial \Psi_2}{\partial p} = \frac{1}{2\Psi_1}\frac{\partial f}{\partial p} - \frac{1}{2\Psi_2}\frac{\partial g}{\partial p} = 0 \tag{A4-5}$$

This occurs whenever

$$\frac{\Psi_1(p)}{\Psi_2(p)} = \frac{\frac{\partial f}{\partial p}}{\frac{\partial g}{\partial p}}$$

or

$$\Psi_1(p)\frac{\partial g}{\partial p} - \Psi_2(p)\frac{\partial f}{\partial p} = 0 \tag{A4-6}$$

This identifies the extraneous roots.

This function $I^*(p)$ corresponds to the <u>difference</u> between the magnitudes of the two velocity increments. Cases where this function has extrema for real values of p are not hard to locate. However, every real extremum for this function must lie in an interval in which $\partial f/\partial p$ and $\partial g/\partial p$ are the same sign. By using the interval technique described in section XI, these roots can be identified.

APPENDIX 5

Derivation of Long Transfer Equations:

For the "long transfer", the lower sign on the double-sign expressions for $\Psi_1(p)$ and $\Psi_2(p)$ (see equations (22) and (23)) is used.

Thus

$$\Psi_1(p) = \left| -\underline{V}_{t1}(p) - \underline{V}_1 \right| = \left| \underline{V}_{t1}(p) + \underline{V}_1 \right|$$

$$= \left[(\underline{V}_{t1}(p) + \underline{V}_1) \cdot (\underline{V}_{t1}(p) + \underline{V}_1) \right]^{1/2}$$

$$= \left[(\underline{v}(p) + z(p)\,\underline{U}_1 + \underline{V}_1) \cdot (\underline{v}(p) + z(p)\,\underline{U}_1 + \underline{V}_1) \right]^{1/2}$$

$$= [h(p)]^{1/2} \qquad \text{(A5-1)}$$

where

$$h(p) = \underline{v}(p) \cdot \underline{v}(p) + z^2(p) + \underline{V}_1 \cdot \underline{V}_1 + 2z(p)\,\underline{v}(p) \cdot \underline{U}_1$$

$$+ 2\underline{V}_1 \cdot \underline{v}(p) + 2z(p)\,\underline{V}_1 \cdot \underline{U}_1$$

$$= Ap - 2Bp^{1/2} + G + 2Cp^{-1/2} - Dp^{-1} \qquad \text{(A5-2)}$$

where the coefficients are given in Table 1.

Similarly,

$$\Psi_2(p) = [k(p)]^{1/2} \qquad \text{(A5-3)}$$

where

$$k(p) = Ap - 2Ep^{1/2} + H + 2Fp^{-1/2} - Dp^{-1} \qquad \text{(A5-4)}$$

and these coefficients are also found in Table 1.

Equation (32) is now replaced by the following criterion for the value of p at which the long transfer impulse has a minimum

$$\frac{\Psi_1(p)}{\Psi_2(p)} = \frac{-\dfrac{\partial h}{\partial p}}{\dfrac{\partial k}{\partial p}} \qquad \text{(A5-5)}$$

Now $\partial h/\partial p$ and $\partial k/\partial p$ must be of different sign in order for the long transfer impulse to have a minimum. Then

$$\frac{\partial h}{\partial p} = A - Bp^{-1/2} - Cp^{-3/2} + Dp^{-2} \tag{A5-6}$$

and

$$\frac{\partial k}{\partial p} = A - Ep^{-1/2} - Fp^{-3/2} + Dp^{-2} \tag{A5-7}$$

Then

$$\lim_{p\to\infty} \frac{\partial h}{\partial p} = \lim_{p\to\infty} \frac{\partial k}{\partial p} = A \tag{A5-8}$$

and

$$\lim_{p\to 0^+} \frac{\partial k}{\partial p} = \lim_{p\to 0^+} \frac{\partial k}{\partial p} = -\infty \tag{A5-9}$$

Thus by an analogy similar to the short transfer case, the minima must be in bounded intervals. These intervals can be found by analyzing the roots of two fourth-order polynomials.

$$\frac{\partial h}{\partial p} = 0 \implies As^4 - Bs^3 - Cs + D = 0 \tag{A5-10}$$

where $s = p^{1/2}$

and

$$\frac{\partial k}{\partial p} = 0 \implies As^4 - Es^3 - Fs + D = 0 \tag{A5-11}$$

These fourth-order equations that produce bounds on the long transfer minima are very similar to those (see equations (47) and (48)) that provided the regions for the short transfer minima. In fact, if $s = a$ is a real root of equation (A5-10), then $s = -a$ must be a root of equation (47). The same correspondence holds for the roots $\partial k/\partial p = 0$ and $\partial g/\partial p = 0$.

Since the only values of p that are of practical interest in either case are for p real and positive, by simply analyzing the real roots of equations (47) and (48), both the long and short transfer intervals can be ascertained.

An eighth-order polynomial whose roots contain the impulse minima also exists for the long transfer. By squaring equation (A5-5), the necessary expression becomes

$$h(p)\left(\frac{\partial k}{\partial p}\right)^2 - k(p)\left(\frac{\partial h}{\partial p}\right)^2 = 0 \qquad \text{(A5-12)}$$

If this expression is multiplied out in terms of equations (A5-3), (A5-4), (A5-6), and (A5-7), the necessary condition for the existence of an extremum in the long transfer impulse becomes

$$\phi_1 s^8 - \phi_2 s^7 + \phi_3 s^6 - \phi_4 s^5 + \phi_5 s^4 - \phi_6 s^3 + \phi_7 s^2 - \phi_8 s + \phi_9 = 0 \qquad \text{(A5-13)}$$

where for i = 1-8, the ϕ_i coefficients are defined in Table 2.

Once again, if s = a is a real root of equation (A5-13), then s - -a is a real root of equation (37). Since the only values of p that are of practical interest are real and positive, both the long and short transfer extrema can be located in the analysis of the single octic. This symmetry would have been suggested by the Bell-Arenstorf technique.

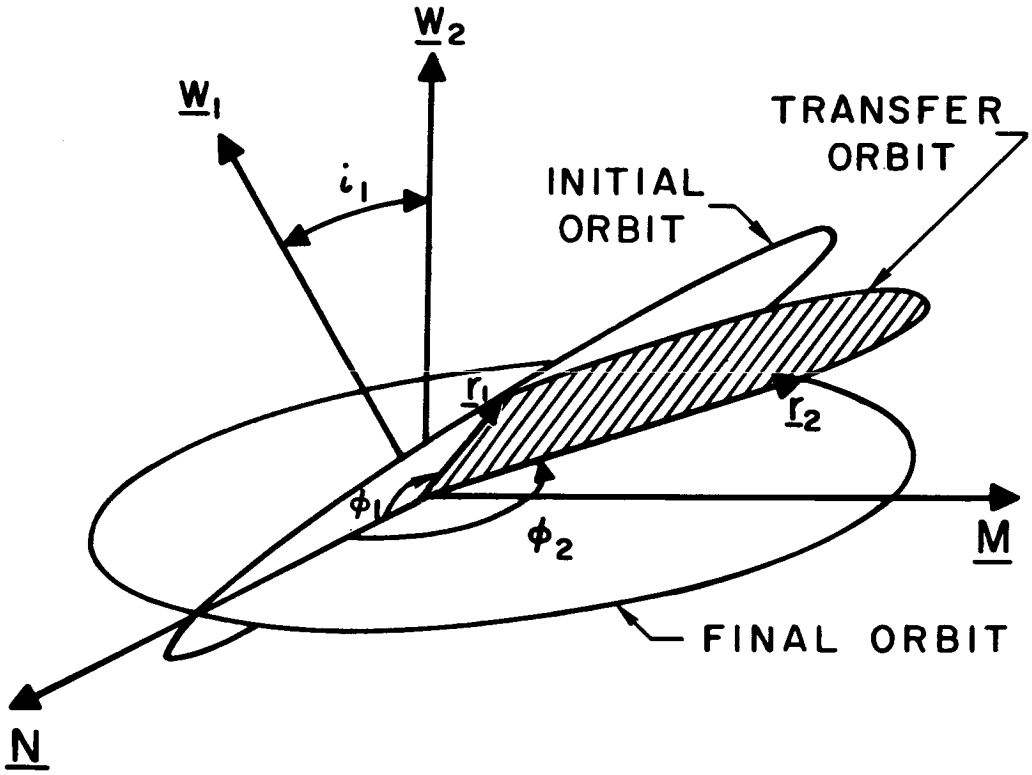

FIGURE I. TRANSFER GEOMETRY

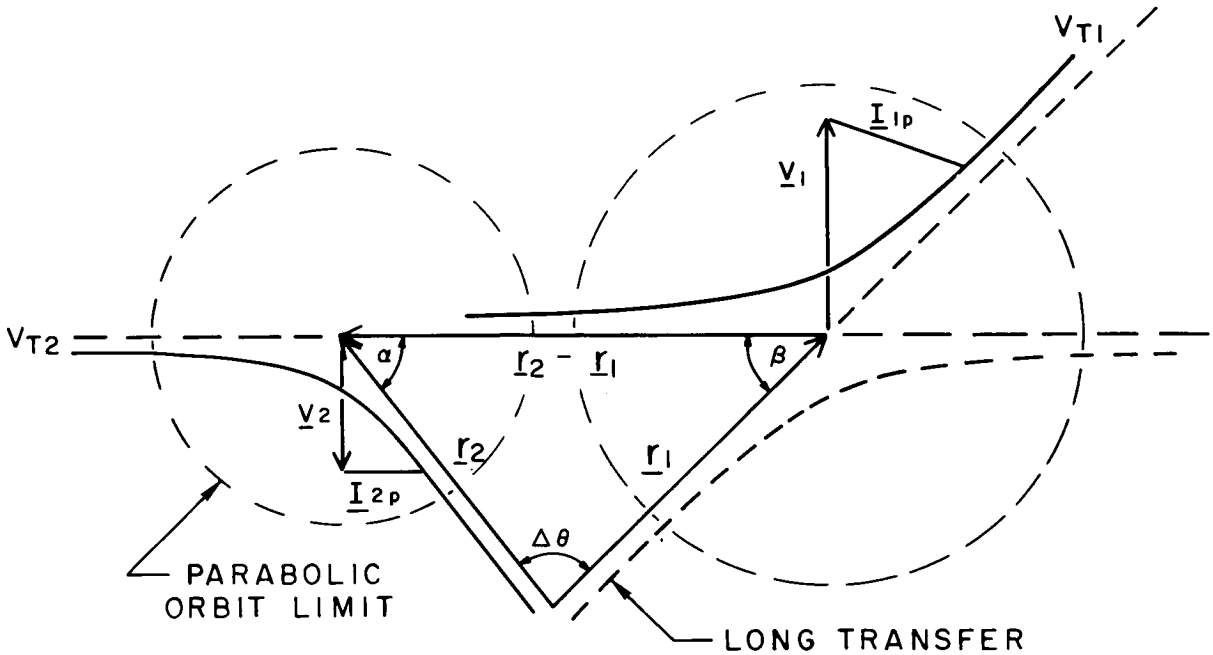

$$V_{T1} = \left(\frac{\mu}{p}\right)^{1/2} \left[\frac{p(\underline{r}_2 - \underline{r}_1)}{|\underline{r}_1 \times \underline{r}_2|} + \text{TAN}\ \frac{\Delta\theta}{2}\ \underline{U}_1\right]$$

$$V_{T2} = \left(\frac{\mu}{p}\right)^{1/2} \left[\frac{p(\underline{r}_2 - \underline{r}_1)}{|\underline{r}_1 \times \underline{r}_2|} - \text{TAN}\ \frac{\Delta\theta}{2}\ \underline{U}_2\right]$$

FIGURE 2. BELL-ARENSTORF TECHNIQUE

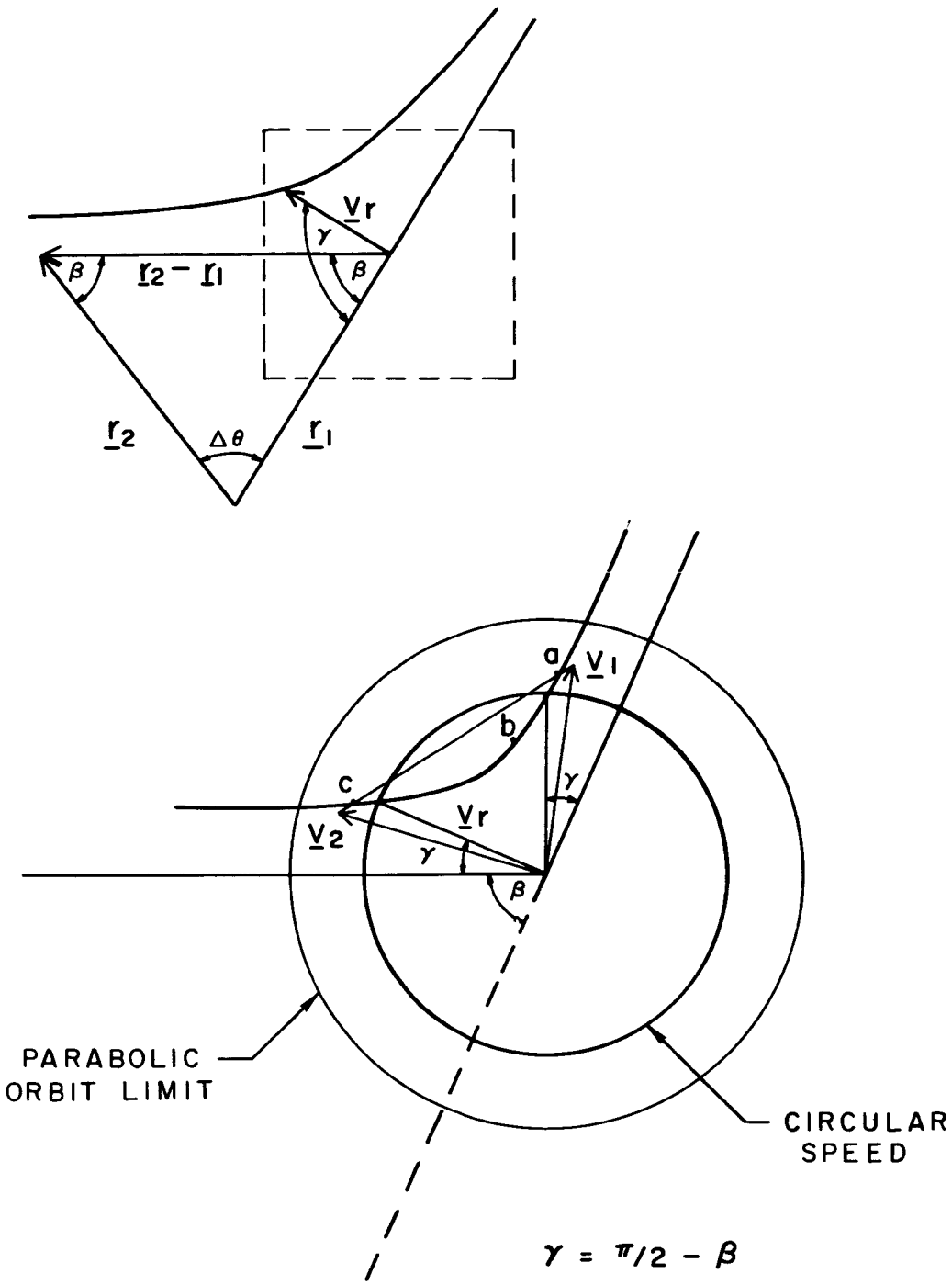

FIGURE 3. DOUBLE MINIMUM CASE OF EQUAL RADII

INITIAL ORBIT		FINAL ORBIT
6582	a (miles)	6582
0.93725	e	0.28355
0.0	i (degrees)	0.0
0.0	ω (degrees)	171.47

$\phi_1 = 153.7°$ $\phi_2 = 213.7°$

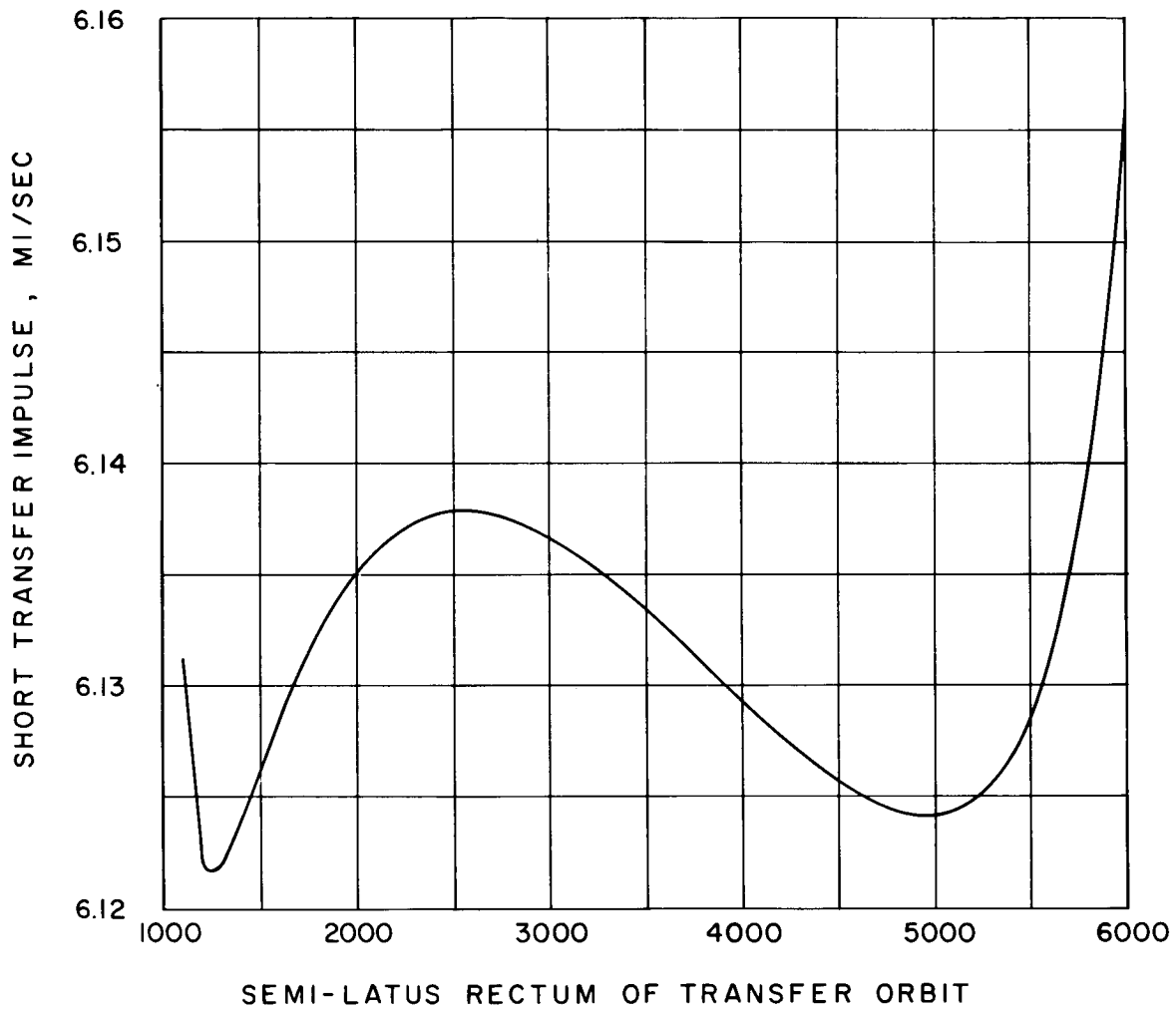

FIGURE 4. EXAMPLE OF DOUBLE MINIMUM

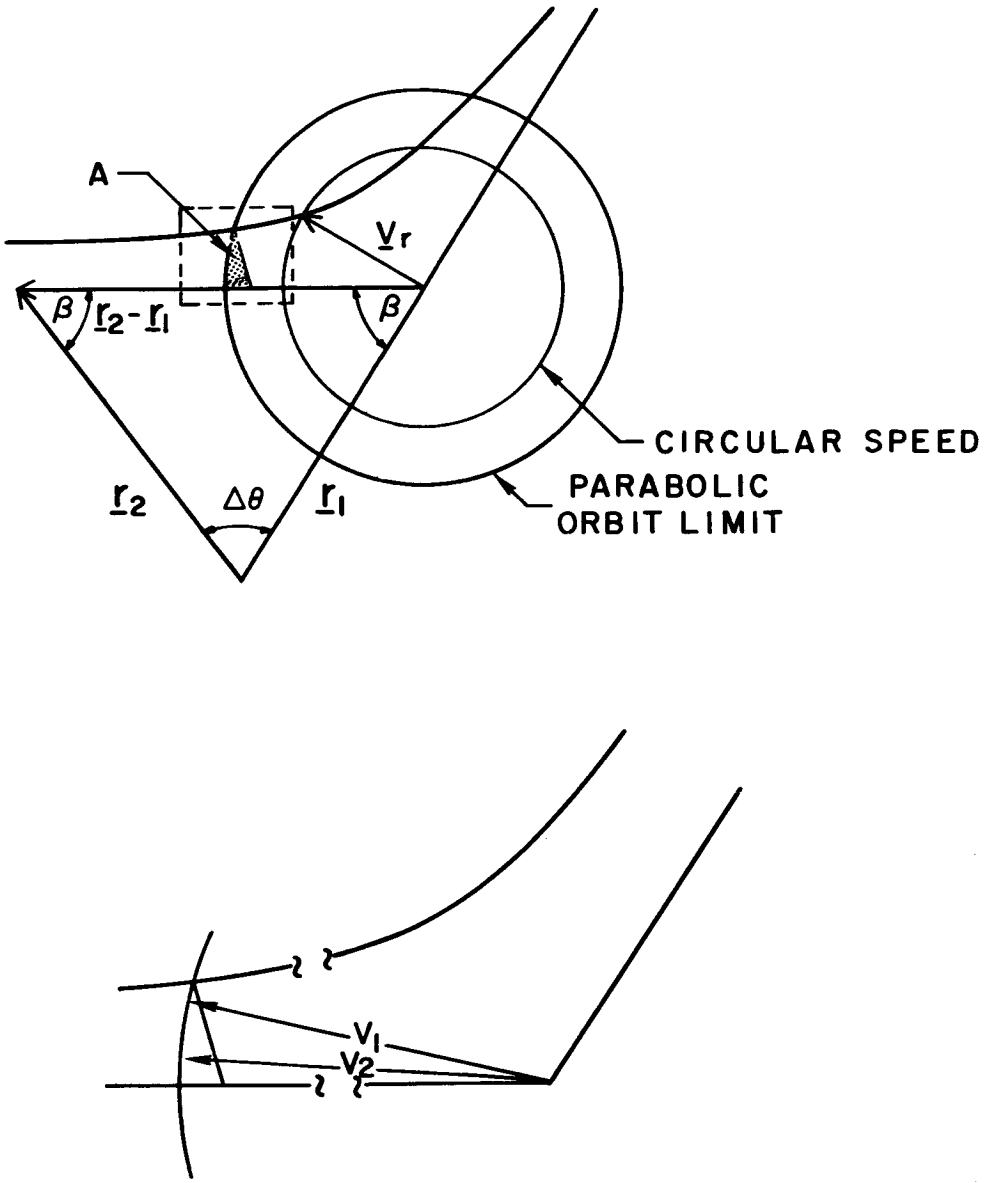

FIGURE 5. EXAMPLE OF HYPERBOLIC MINIMUM CASE OF EQUAL RADII

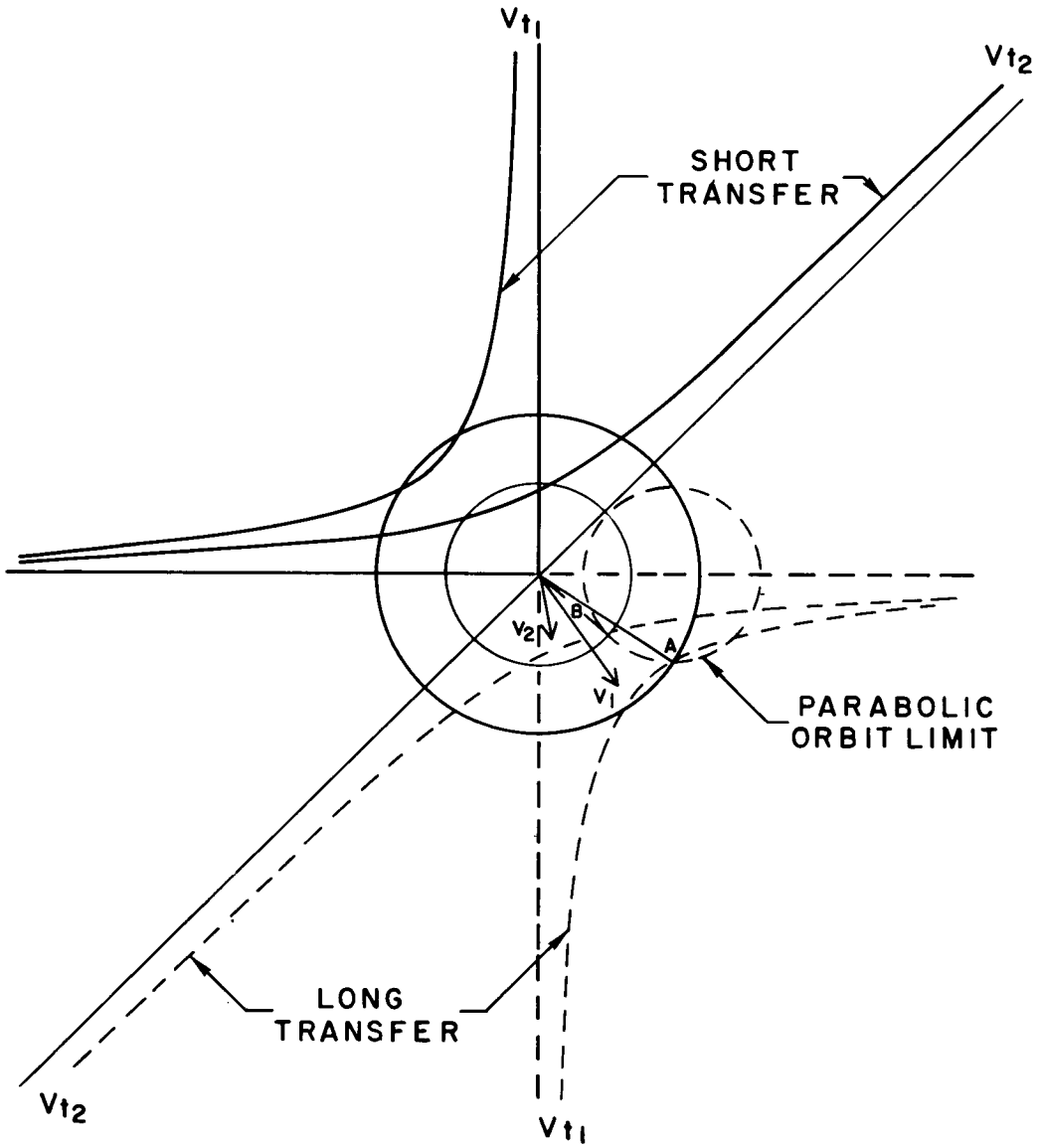

FIGURE 6. HYPERBOLIC MINIMUM TRANSFER — CASE OF NON-EQUAL RADII

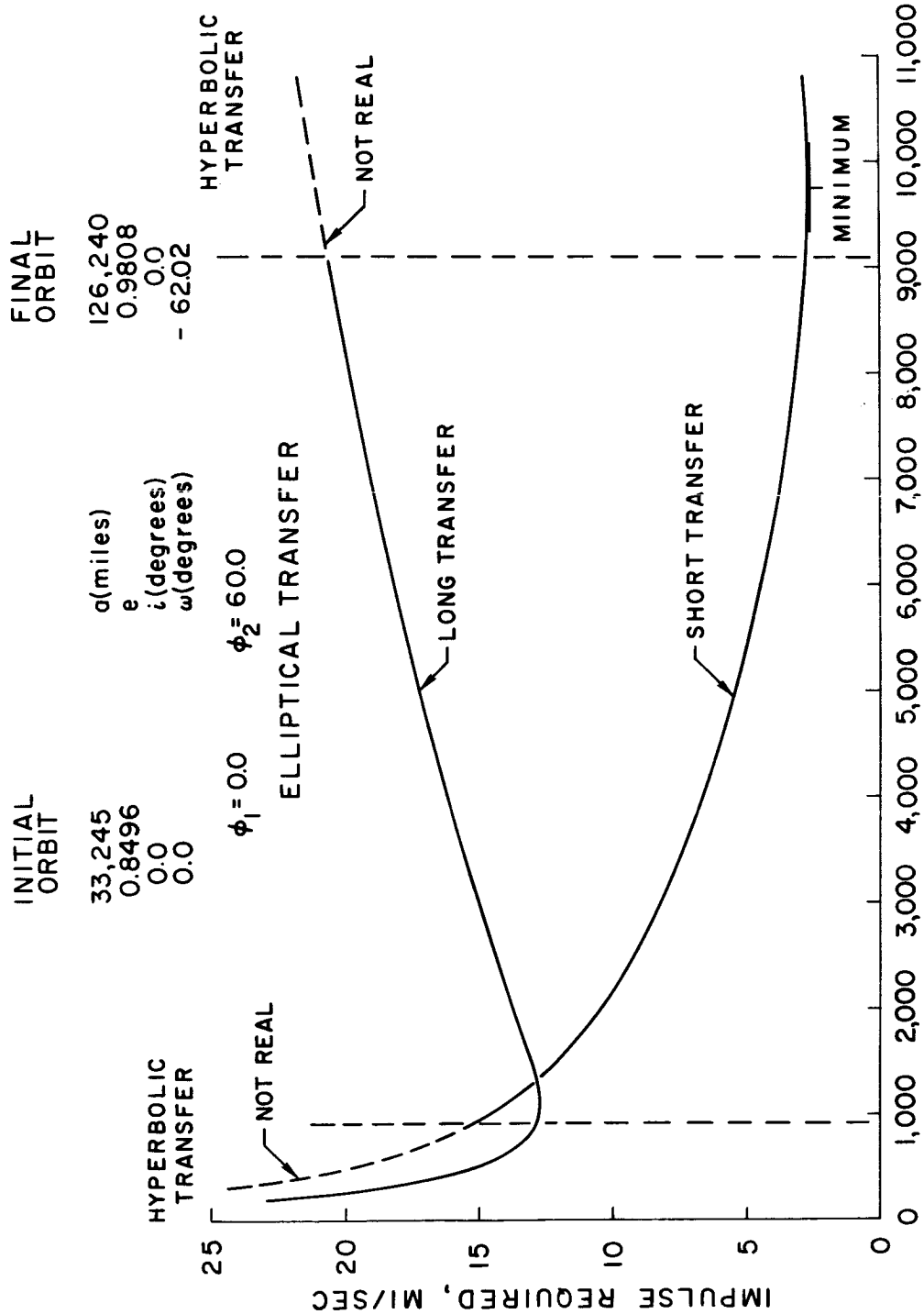

FIGURE 7. EXAMPLE OF HYPERBOLIC MINIMUM

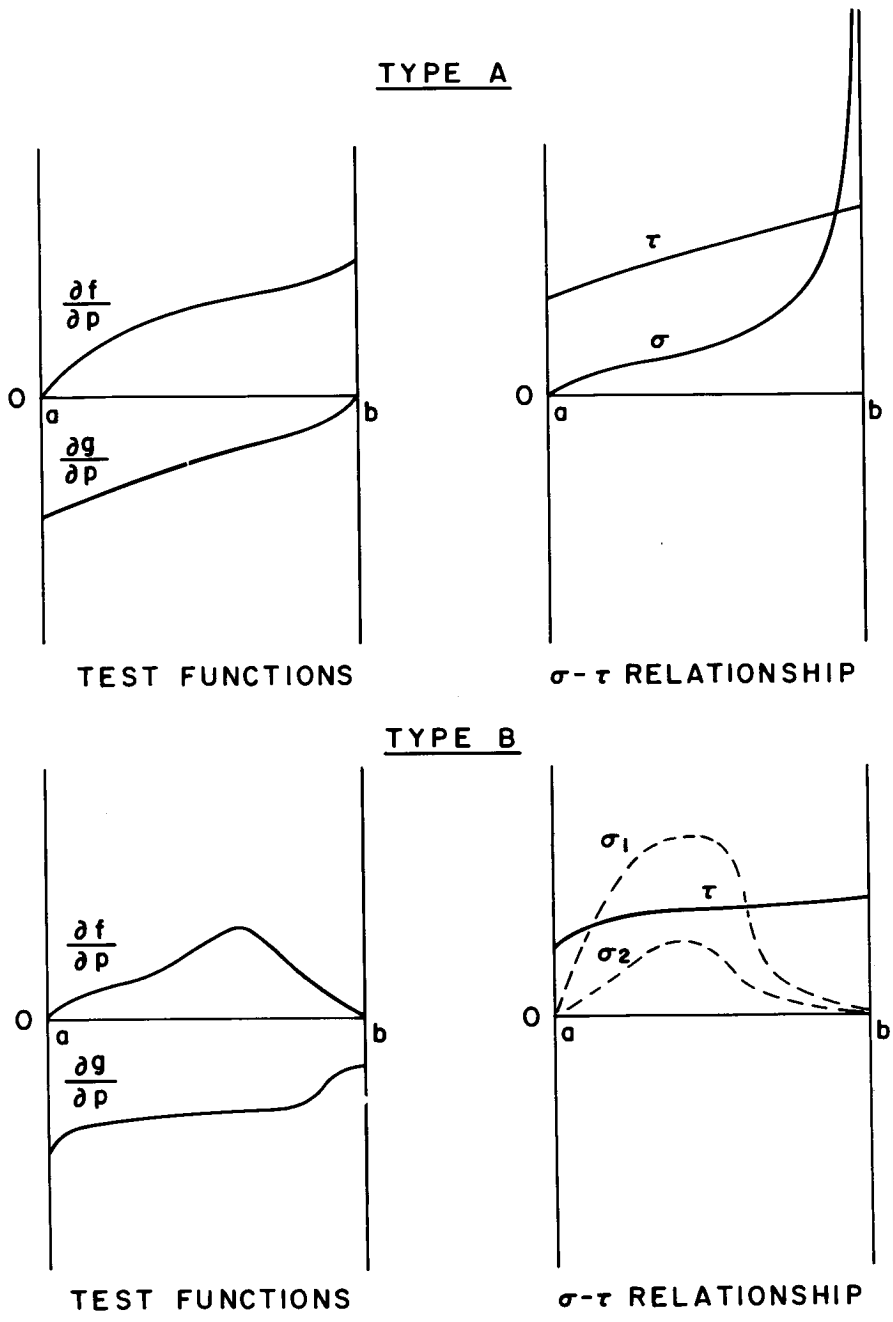

FIGURE 8. ILLUSTRATION OF INTERVAL

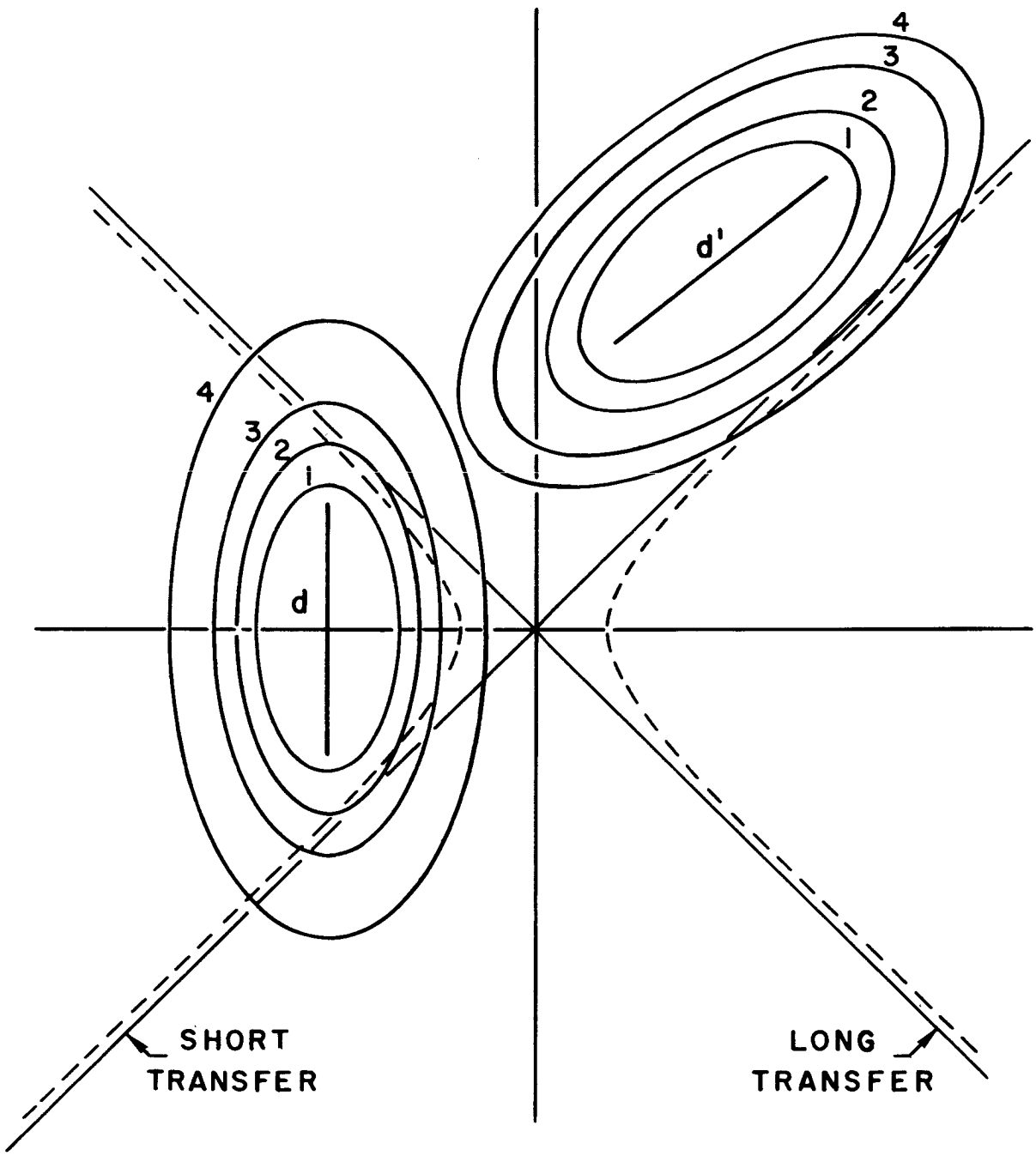

FIGURE A2-1 GEOMETRY OF DOUBLE MINIMUM IN EQUAL RADII CASE

REPUBLIC AVIATION CORPORATION

APPLICATION OF THE TWO FIXED CENTER PROBLEM TO LUNAR TRAJECTORIES

by

Mary Payne

Farmingdale, L.I., N. Y.

ACKNOWLEDGMENT

The writer wishes to express her appreciation to Dr. George Nomicos, Chief, Applied Mathematics Subdivision and Mr. Maxwell Eichenwald, Applied Mathematics Subdivision for many helpful discussions and illuminating comments in the course of the work.

REPUBLIC AVIATION CORPORATION
Farmingdale, L.I., N. Y.

APPLICATION OF THE TWO FIXED CENTER PROBLEM TO LUNAR TRAJECTORIES

by

Mary Payne

SUMMARY

Six methods for the approximation of lunar trajectories by the two fixed center problem are developed. Four of these methods arise from a formulation of the restricted problem in a rotating coordinate system. The origin of the rotating system, to be regarded as the center of rotation is to be so selected as to improve the degree of approximation. The other two are developed from a formulation in an inertial system with fictitious fixed positions of the earth and moon selected so as to improve the approximation.

The results of a numerical comparison of the six methods with a typical lunar trajectory and the Kepler predictions are presented. These results are discussed and some suggestions are made for further development of the theory.

TABLE OF CONTENTS

LIST OF SYMBOLS

R	Position vector of vehicle relative to the earth-moon barycenter
R_1	Position vector of the vehicle relative to the earth
r_1	Distance of vehicle from earth
R_2	Position vector of the vehicle relative to the moon
r_2	Distance of vehicle from moon
μ	Gravitational constant times mass of the earth
μ'	Gravitational constant times mass of the moon
L	Position vector of moon relative to the earth
ℓ	Distance of moon from earth
$\dot{L}$	Velocity vector of the moon relative to the earth
Ω	Angular velocity vector of the moon relative to the earth
ω	Magnitude of Ω
$A=\alpha L+\beta\Omega+\gamma\dot{L}$	Origin, relative to the barycenter, of the rotating coordinate system
α, β, γ	Constants relating A to L, Ω and $\dot{L}$
$A_1=A-\beta\Omega$	Projection of A on the plane of the moon's motion
R_A	Position vector of the vehicle relative to A
H_A	Hamiltonian for restricted problem in a coordinate system rotating with angular velocity Ω about A
$\bar{R}_A$	Position vector of vehicle relative to A in the rotating system
$\bar{P}_A$	Momentum vector conjugate to $\bar{R}_A$

H_E	Hamiltonian for the Euler, or two fixed center problem
H_1	Perturbation Hamiltonian
M(t)	Rotation matrix through an angle $-\omega t$ about Ω
δ	A parameter introduced to improve minimization of the effect of the non-integrable terms in the perturbation equations
H	Hamiltonian in the inertial system
P	Momentum conjugate to R in the inertial system

SUBSCRIPTS

E	Refers to Euler problem
R	Refers to restricted problem
o	Refers to initial value
F	Refers to final value

NOTE: In general, capital letters represent vectors and the corresponding small letters their magnitudes. Bars over vectors denote vectors in a rotating coordinate system.

INTRODUCTION

This report contains a detailed discussion of two general methods for treating the three dimensional restricted problem of three bodies as a perturbation of the two fixed center problem. The first method is based on a formulation of the restricted problem in a rotating coordinate system and the second on a formulation in an inertial system. In both methods perturbation equations are obtained for the initial conditions of the two fixed center problem regarded as osculating time varying parameters for the restricted problem. Both methods may be regarded as generalizations of a method developed by Arenstorf[1] and the first method using the rotating system is an extension of work described in an earlier report[2].

Arenstorf formulated the two dimensional restricted problem in a coordinate system rotating about the barycenter and obtained perturbation equations for the initial values of the canonical variables (porition relative to the barycenter in the rotating system and its conjugate momentum). The generalization treated in Reference [2] included the extension to three dimensions and was carried out in a system rotating about an arbitrary point fixed relative to the earth and the moon. This center of rotation was then selected so as to minimize the difference between the Hamiltonian functions for the restricted and two fixed center problems. The present generalization consists in an attempt to minimize the effects of the non-integrable terms in the perturbation equations, which arise from derivatives of the perturbing terms in the Hamiltonian, rather than the perturbing Hamiltonian itself. In addition another parameter is introduced which allows part of one of the integrable terms to be used to further reduce the effect of some of the non-integrable terms. Thus altogether four parameters, three of which are the coordinates of the center of rotation, are available for the minimization.

A method for the determination of these four parameters is presented, and a set of osculating initial conditions is obtained by an approximate integration of the perturbation equations. In addition to this set three other sets are obtained by variations in the values of these parameters. In all of the methods developed the

center of rotation is close to the center of the earth if the portion of the restricted orbit to be approximated has a close approach to the earth and no close approach to the moon. The center of rotation is close to the moon if the portion of the restricted orbit has a close approach to the moon and not to the earth. For mid-course portions, the center of rotation is somewhere between the earth and the moon. No attempt has so far been made to extend the theory to the approximation of portions containing close approaches to both the earth and the moon.

The formulation in the inertial system makes use of fictitious fixed portions for the earth and moon, so selected as to reduce the effect of the non-integrable terms in the perturbation equations. Two sets of formulas result which differ in the approximations used in the integration of the perturbation equations.

Altogether, then, six schemes are developed for approximating the restricted problem by the two fixed center problem. These schemes have been tested numerically for various portions of a typical lunar trajectory obtained by numerical integration. Some results of this numerical comparison are presented, following the analytical treatment.

The comparison shows clearly that the formulations in the rotating system are superior and the reasons for this are discussed in the last section.

THEORY FOR THE ROTATING SYSTEM

Derivation of the Perturbation Equations

The equations of motion of the restricted problem in an inertial system with origin at the barycenter are

$$\ddot{R} = -\mu \frac{R_1}{r_1^3} - \mu' \frac{R_2}{r_2^3} \tag{1}$$

Consider a point A defined by

$$A = \alpha L + \beta \Omega + \gamma \dot{L} \tag{2}$$

where L and $\dot{L}$ are position and velocity vectors of the moon relative to the earth, and hence are known functions of time satisfying the relation

$$\ddot{L} = -(\mu+\mu') \frac{L}{\ell^3} = \Omega x\ (\Omega x L) \qquad A_1 = \alpha L + \gamma \dot{L} \tag{3}$$

$$\dot{L} = \Omega x\ L \qquad \ddot{A} = \Omega x (\Omega x A) = -\omega^2 A_1$$

$$\Omega = \frac{L x \dot{L}}{\ell^2}$$

The point A thus rotates about the barycenter with the earth and the moon. The equations of motion for the restricted problem in an accelerated coordinate system with origin at A, but with axes always parallel to those of the inertial system, are

$$\ddot{R}_A = -\mu \frac{R_1}{r_1^3} - \mu' \frac{R_2}{r_2^3} - \ddot{A} \tag{4}$$

since

$$R = A + R_A, \quad \dot{R} = \dot{A} + \dot{R}_A, \quad \ddot{R} = \ddot{A} + \ddot{R}_A \tag{5}$$

and finally in a coordinate system rotating about A with angular velocity Ω, the equation of motion become

$$\ddot{\bar{R}}_A = -\mu \frac{\bar{R}_1}{r_1^3} - \mu' \frac{\bar{R}_2}{r_2^3} - \ddot{\bar{A}} - \Omega x (\Omega x \bar{R}_A) - 2(\Omega x \dot{\bar{R}}_A) \tag{6}$$

where bars denote vectors in the rotating system. We assume that at time $t = 0$, the axes of the rotating system are parallel to those in the inertial system, so that the constant vectors $\bar{A}$, $\dot{\bar{A}}$ and $\ddot{\bar{A}}$ satisfy the relations

$$\bar{A} = A(0) \qquad \dot{\bar{A}} = \dot{A}(0) \qquad \ddot{\bar{A}} = -\omega^2 \bar{A}_1 = -\omega^2 A_1(0) \tag{7}$$

It is readily verified that the Hamiltonian

$$H_A = \frac{1}{2} \bar{P}_A^2 - \frac{\mu}{r_1} - \frac{\mu'}{r_2} - \omega^2 \bar{R}_A \cdot A_1 - \Omega \cdot \bar{R}_A \times \bar{P}_A \tag{8}$$

is a Hamiltonian for the problem represented by Eq. (6) with

$$\dot{\bar{R}}_A = \text{grad}_{P_A} H_A = \bar{P}_A - \Omega x \bar{R}_A \tag{9}$$

and

$$\dot{\bar{P}}_A = \ddot{\bar{R}}_A + \Omega x \dot{\bar{R}}_A = -\text{grad}_{\bar{R}_A} H_A$$

$$= -\mu \frac{R_1}{r_1^3} - \mu' \frac{R_2}{r_2^3} + \omega^2 \bar{A}_1 - \Omega x \bar{P}_A$$

$$= -\mu \frac{R_1}{r_1^3} - \mu' \frac{R_2}{r_2^3} + \omega^2 \bar{A}_1 - \Omega x \dot{\bar{R}}_A - \Omega x (\Omega x \bar{R}_A) \tag{10}$$

which reduces immediately to Eq. (6). A word on the relation between position in the rotating system $\bar{R}_A$ and its conjugate momentum $\bar{P}_A$ and the position R_A and velocity $\dot{R}_A$ in the non-rotating system is necessary for the interpretation of results to be obtained later. Since the rotating and non-rotating systems are assumed coincident at $t = 0$

$$\bar{R}_{A0} = R_{A0}$$

$$\bar{P}_{A0} = \dot{\bar{R}}_{A0} + \Omega x \bar{R}_{A0} = \dot{R}_{A0} \tag{11}$$

are vector equations which are valid component by component, and since $\dot{\bar{R}}_{A0}$ is the velocity relative to A in the rotating system while $\Omega x\, \bar{R}_{A0}$ is the velocity due to the rotation of the system it is seen that the initial value of the momentum conjugate to $\bar{R}_A$ is just the velocity in the non-rotating system. The same statements hold for time t also, except that to get component agreement a rotation through ωt is necessary. That is, at time t

$$\begin{aligned} R_A &= M^{-1}(t)\, \bar{R}_A \\ \dot{R}_A &= M^{-1}(t)\, \bar{P}_A = M^{-1}(t)\, (\dot{\bar{R}}_A + \Omega x\, \bar{R}_A) \end{aligned} \tag{12}$$

where $M^{-1}(t)$ may be regarded either as a rotation of the axes of the rotating system through an angle $-\omega t$ or as a rotation of $\bar{R}_A$ and $\bar{P}_A$ relative to the rotating axes through and angle ωt, both rotations about the vector Ω which is the same in both systems.

The Hamiltonian H_A may be written as the sum of

$$H_E = \frac{1}{2} \bar{P}_A^{\,2} - \frac{\mu}{r_1} - \frac{\mu'}{r_2} \tag{13}$$

the Hamiltonian for the Euler problem with Hamilton equation

$$\begin{aligned} \dot{\bar{R}}_{AE} &= \text{grad}_{\bar{P}_{AE}}\, H_E = \bar{P}_{AE} \\ \dot{\bar{P}}_{AE} &= \ddot{\bar{R}}_{AE} = -\mu \frac{R_1}{r_1^{\,3}} - \mu' \frac{R_2}{r_2^{\,3}} \end{aligned} \tag{14}$$

and a perturbation

$$H_1 = -\omega^2\, \bar{R}_A \cdot \bar{A}_1 - \Omega \cdot \bar{R}_A x\, \bar{P}_A \tag{15}$$

where the subscript E in Eqs. (14) refers to the functional forms for $\bar{R}_A$ and $\bar{P}_A$ obtained by solving Eqs. (14).

A solution of the restricted problem with Hamiltonian given by Eq. (8) and Hamiltonian Eqs. (9) and (10) is now sought in the functional form of the solution of the Euler problem with time varying initial conditions. That is,

one seeks the solution of the restricted problem, denoted by a subscript R, in the form

$$\begin{aligned} \bar{R}_{AR}(\bar{R}_{AR0}, \bar{P}_{AR0}, t) &= \bar{R}_{AE}\left(\bar{R}_{AE0}(t), \bar{P}_{AE0}(t), t\right) \\ \bar{P}_{AR}(\bar{R}_{AR0}, \bar{P}_{AR0}, t) &= \bar{P}_{AE}\left(\bar{R}_{AE0}(t), \bar{P}_{AE0}(t), t\right) \end{aligned} \tag{16}$$

with initial conditions for the restricted and Euler problems satisfying the relations

$$\begin{aligned} \bar{R}_{AR}(\bar{R}_{AR0}, \bar{P}_{AR0}, 0) &= \bar{R}_{AR0} = \bar{R}_{AE}\left(\bar{R}_{AE0}(0), \bar{P}_{AE0}(0), 0\right) = \bar{R}_{AE}(0) \\ \bar{P}_{AR}(\bar{R}_{AR0}, \bar{P}_{AR0}, 0) &= \bar{P}_{AR0} = \bar{P}_{AE}\left(\bar{R}_{AE0}(0), \bar{P}_{AE0}(0), 0\right) = \bar{P}_{AE0}(0) \end{aligned} \tag{17}$$

It has been shown by Arenstorf[1] that the functions $\bar{R}_{AE0}(t)$ and $\bar{P}_{AE0}(t)$ necessary for the validity of Eq. (16) satisfy the differential equations

$$\begin{aligned} \frac{d}{dt}\bar{R}_{AE0}(t) &= \text{grad}_{\bar{P}_{AE0}} \bar{H}_1 \\ \frac{d}{dt}\bar{P}_{AE0}(t) &= -\text{grad}_{\bar{R}_{AE0}} \bar{H}_1 \end{aligned} \tag{18}$$

where

$$\bar{H}_1 = \bar{H}_1\left(\bar{R}_{AE0}(t), \bar{P}_{AE0}(t), t\right) \tag{19}$$

is obtained by substitution of $\bar{R}_{AE}\left(\bar{R}_{AE0}(t), \bar{P}_{AE0}(t), t\right)$ and $\bar{P}_{AE}\left(\bar{R}_{AE0}(t), \bar{P}_{AE0}(t), t\right)$ for $\bar{R}_A$ and $\bar{P}_A$ in H_1 (given by Eq. (15). To actually carry out the substitution using the solution of the Euler problem (which is known in closed form) and then compute the gradients required in Eq. (18) would be very complex because of the extreme complexity of the closed form solution. Even could this be carried out the integration of the resulting highly nonlinear equations in $\bar{R}_{AE0}(t)$ and $\bar{P}_{AE0}(t)$ would be very difficult. Further, any approximation method for integration of perturbation equations for initial conditions must be developed with great care to avoid the introduction of troublesome secular terms, which increase in order with higher order approximations.

In view of this last fundamental difficulty, only a first approximation will be attempted. This approximation will lead to some integrable terms in the perturbation equations and the point A will be selected in such a way as to reduce the effect of the non-integrable terms, which will then be ignored. The resulting expressions for the time variation in the initial conditions and hence the solution of the restricted problem represented by Eq. (16) will thus have limited validity in time. The hardest part of the problem will be in obtaining an estimate for duration of validity. Although this might appear to restrict considerably the application of the theory, it should nevertheless be noted that from the solutions of a sequence of two fixed center problems, each valid for a certain time, the solution of the restricted problem may be constructed solely in terms of closed form calculations without the use of numerical integration. Such a procedure will be outlined later.

Explicit Form of the Perturbation Equations

To proceed with the approximation $\bar{H}_1$ is written in the form

$$\bar{H}_1 = -\Omega\bar{R}_{AE0} \times \bar{P}_{AE0} - \omega^2 \delta\, \bar{R}_{AE0} \cdot \bar{A}_1 - \omega^2 (1-\delta)\, \bar{R}_{AE} \cdot \bar{A}_1$$

$$- \int \left\{ \omega^2 \delta\, \bar{P}_{AE} \cdot \bar{A} - \Omega\bar{R}_{AE} \times \left(\mu \frac{R_1}{r_1^3} - \mu' \frac{R_2}{r_2^3} \right) \right\} dt \qquad (20)$$

where the integral is obtained by time differentiation of $(-\omega^2 \delta\, \bar{R}_{AE} \cdot \bar{A}_1 - \Omega\bar{R}_{AE} \times \bar{P}_{AE})$ and use of the Hamilton Eqs. (14) for the Euler problem. The first two terms of $\bar{H}_1$ will be shown to lead to integrable terms in the perturbation equations (18) for the initial conditions. The factor δ permits part of the $R_A \cdot A_1$ term to appear with the integrable terms and part with the non-integrable terms. This second part helps to reduce the effect of the other non-integrable terms. The third term and the integral are not written explicitly in terms of initial conditions. It is these terms for which an effort at minimization will be made by proper selection of the factor δ and the point A. To see how this may be done one now takes the gradients of $\bar{H}_1$ with respect to $\bar{R}_{AE0}$ and $\bar{P}_{AE0}$ to obtain the perturbation equations. The differentiation of the triple product in the integral is facilitated by noting that

$$\bar{R}_1 = \bar{R}_A + \bar{A} + \frac{\mu'}{\mu+\mu'}\,\bar{L} \qquad \bar{R}_2 = \bar{R}_A + \bar{A} - \frac{\mu}{\mu+\mu'}\,\bar{L} \tag{21}$$

so that

$$\bar{R}_A \times \bar{R}_1 = \bar{R}_A \times \left(\bar{A} + \frac{\mu'}{\mu+\mu'}\,\bar{L}\right)$$
$$\bar{R}_A \times \bar{R}_2 = \bar{R}_A \times \left(\bar{A} - \frac{\mu}{\mu+\mu'}\,\bar{L}\right) \tag{22}$$

The perturbation equations for the time derivatives of $\bar{R}_{AE0}(t)$ and $\bar{P}_{AE0}(t)$ are readily verified to be

$$\frac{d}{dt} R_{AE0}(t) = \text{grad}_{PAE0}\bar{H}_1 = -\Omega \times R_{AE0} - \omega^2(1-\delta)\Psi_{RP} A_1$$
$$- \int\left[\omega^2 \delta \Psi_{PP} A_1 - \Psi_{RP}(\Omega \times M - \omega Q)\right] dt \tag{23}$$

and

$$\frac{d}{dt} P_{AE0}(t) = -\text{grad}_{RAE0}\bar{H}_1 = -\Omega \times P_{AE0} + \omega^2 \delta A_1 + \omega^2(1-\delta)\Psi_{RR} A_1$$
$$+ \int\left[\omega^2 \delta \Psi_{PR} A_1 - \Psi_{RR}(\Omega \times M - \omega Q)\right] dt \tag{24}$$

where the M and Q are vectors given by

$$M = \mu \frac{\bar{A} + \frac{\mu'}{\mu+\mu'}\,\bar{L}}{r_1^3} + \mu' \frac{\bar{A} - \frac{\mu}{\mu+\mu'}\,\bar{L}}{r_2^3}$$

$$Q = \frac{3}{\omega}\left\{\mu\left[\bar{\Omega}\cdot\bar{R}_{AE} \times \left(\bar{A} + \frac{\mu'}{\mu+\mu'}\,\bar{L}\right)\frac{\bar{R}_1}{r_1^5}\right]\right. \tag{25}$$
$$\left. + \mu'\left[\bar{\Omega}\cdot\bar{R}_{AE} \times \left(\bar{A} - \frac{\mu}{\mu+\mu'}\,\bar{L}\right)\frac{\bar{R}_2}{r_2^5}\right]\right\}$$

These vectors are so defined that they have the same dimension. The Ψ's are matrices given by

$$\Psi_{RR} = \left(\frac{\partial R_{AEj}}{\partial R_{AE0i}}\right) \qquad \Psi_{RP} = \left(\frac{\partial R_{AEj}}{\partial P_{AE0i}}\right)$$

$$\Psi_{PR} = \left(\frac{\partial P_{AEj}}{\partial R_{AE0i}}\right) \qquad \Psi_{PP} = \left(\frac{\partial P_{AEj}}{\partial P_{AE0i}}\right) \tag{26}$$

with the i^{th} row and j^{th} column containing the derivative of the j^{th} component of the time varying vector in the numerator with respect to the i^{th} component of the initial value vector in the denominator evaluated at $R_{AE0}(t)$ and $P_{AE0}(t)$. It may be noted that the transposes of these matrices constitute the transition matrix for the Euler problem with the transposes of the first two matrices forming the top three rows and the transposes of the last two matrices forming the bottom three rows.

Determination of the Origin A and the Parameter δ

The first term in the right hand side of Eq. (23) and the first two terms on the right side of Eq. (24) depend only on the initial values $R_{AE0}(t)$ and $P_{AE0}(t)$ and if these were the only terms present Eqs. (23) and (24) would be integrable. The remaining terms all involve components of the transition matrix for the Euler problem and no attempt will be made to include them in the integration. Instead methods will be sought for making them small, and this will be done by seeking an approximate minimization of the vectors on which the matrices operate. These vectors appear in both equations as follows:

$$N_1 = \omega^2(1-\delta)\,\bar{A}_1 \qquad \text{outside the integrals}$$

$$N_2 = \omega^2\delta\,\bar{A}_1 \qquad \text{inside the integrals} \tag{27}$$

together with M and Q defined in Eqs. (25), which appear inside the integrals. It will be noted that all these vectors have the same dimension. The vectors M and Q are functions of time. Since however, they have, effectively, the cubes of r_1 and r_2 in the denominator, it is clear that they are large only for brief periods of time at approach to the earth or the moon closer than a few earth radii.

As a first trial at minimization, δ and A were sought such that the scalar σ

$$\sigma = N_1^2 + N_2^2 + M_o^2 + M_f^2 \tag{28}$$

is minimized, where M_o and M_f are computed from initial and anticipated final conditions, respectively. The omission of Q is heuristically justified by an argument of the following type. Suppose the initial position is close to the earth and the final position close to the moon. Initially the r_2 terms are small, so that to minimize the r_1 terms $\left(\bar{A} + \frac{\mu'}{\mu + \mu'} \bar{L}\right)$ must nearly vanish in order to keep M_o small. It will then follow that Q_o is also small. Evidently, of course, such a procedure will mean that both M_f and Q_f will become more or less large depending on the final value of r_2. In effect, this will place a limitation on the duration of validity of the two fixed center approximation.

The minimization of Eq. (28) will now be carried out. Since M and, for that matter Q also, are independent of δ, partial derivatives of σ with respect to δ involve only the N_1 and N_2 terms:

$$\frac{\partial \sigma}{\partial \delta} = N_1 \cdot \frac{\partial N_1}{\partial \delta} + N_2 \cdot \frac{\partial N_2}{\partial \delta} = \omega^4 \bar{A}_1^2 \left(2\delta - 2(1-\delta)\right) \tag{29}$$

which vanishes for $\delta = \frac{1}{2}$. It now remains to minimize

$$\sigma_1 = \frac{1}{2} \omega^4 \bar{A}_1^2 + M_o^2 + M_f^2 \tag{30}$$

with respect to α, β and γ. That is the equations

$$\frac{\partial \sigma_1}{\partial x} = \omega^4 \bar{A}_1 \cdot \frac{\partial \bar{A}_1}{\partial x} + M_o \cdot \frac{\partial M_o}{\partial x} + 2M_f \cdot \frac{\partial M_f}{\partial x} = 0 \tag{31}$$

where x denotes α, β and γ must be solved for α, β and γ. Recalling that

$$\bar{A} = \alpha \bar{L} + \beta \bar{\Omega} + \gamma \dot{\bar{L}} \quad , \qquad \bar{A}_1 = \alpha \bar{L} + \gamma \dot{\bar{L}} \tag{32}$$

one obtains the following:

$$\frac{\partial \bar{A}_1}{\partial \alpha} = \frac{\partial \bar{A}}{\partial \alpha} = \bar{L}, \quad \frac{\partial \bar{A}_1}{\partial \beta} = 0, \quad \frac{\partial \bar{A}}{\partial \beta} = \bar{\Omega}, \quad \frac{\partial A_1}{\partial \gamma} = \frac{\partial \bar{A}}{\partial \gamma} = \dot{\bar{L}} \tag{33}$$

and from the first of Eqs. (25) evaluated at initial and final positions, respectively:

$$\frac{\partial M}{\partial \alpha} = \bar{L}\left(\frac{\mu}{r_1^3} + \frac{\mu'}{r_2^3}\right), \quad \frac{\partial M}{\partial \beta} = \bar{\Omega}\left(\frac{\mu}{r_1^3} + \frac{\mu'}{r_2^3}\right), \quad \frac{\partial M}{\partial \gamma} = \dot{\bar{L}}\left(\frac{\mu}{r_1^3} + \frac{\mu'}{r_2^3}\right) \tag{34}$$

so that

$$\bar{A}_1 \cdot \frac{\partial \bar{A}_1}{\partial \alpha} = \alpha \ell^2, \qquad \bar{A}_1 \cdot \frac{\partial \bar{A}_1}{\partial \beta} = 0, \qquad \bar{A}_1 \cdot \frac{\partial \bar{A}_1}{\partial \gamma} = \gamma \dot{\ell}^2 \tag{35}$$

$$M \cdot \frac{\partial M}{\partial \alpha} = \alpha \left(\frac{\mu}{r_1^3} + \frac{\mu'}{r_2^3}\right)^2 \ell^2 + \frac{\mu\mu'}{\mu+\mu'} \ell^2 \left(\frac{1}{r_1^3} - \frac{1}{r_2^3}\right)\left(\frac{\mu}{r_1^3} + \frac{\mu'}{r_2^3}\right) \tag{36}$$

$$M \cdot \frac{\partial M}{\partial \beta} = \omega^2 \left(\frac{\mu}{r_1^3} + \frac{\mu'}{r_2^3}\right)^2 \beta, \quad M \cdot \frac{\partial M}{\partial \gamma} = \dot{\ell}^2 \left(\frac{\mu}{r_1^3} + \frac{\mu'}{r_2^3}\right)^2 \gamma \tag{37}$$

Substitution in Eq. (31) for $x = \beta$ and γ lead to

$$\beta = \gamma = 0 \tag{38}$$

while for $x = \alpha$, one obtains

$$\omega^4 \alpha \ell^2 + 2\alpha \ell^2 \left[\left(\frac{\mu}{r_{10}^3} + \frac{\mu'}{r_{20}^3}\right)^2 + \left(\frac{\mu}{r_{1f}^3} + \frac{\mu'}{r_{2f}^3}\right)^2\right] \tag{39}$$

$$+ 2\mu\mu' \ell^2 \left[\left(\frac{1}{r_{10}^3} - \frac{1}{r_{20}^3}\right)\left(\frac{\mu}{r_{10}^3} + \frac{\mu'}{r_{20}^3}\right)\right.$$

$$\left. + \left(\frac{1}{r_{1f}^3} - \frac{1}{r_{2f}^3}\right)\left(\frac{\mu}{r_{1f}^3} + \frac{\mu'}{r_{2f}^3}\right)\right] = 0$$

or

$$\alpha = -\frac{\mu\mu'}{\mu+\mu'} \frac{\sum_{i=0,f} \left(\frac{1}{r_{1i}^3} - \frac{1}{r_{2i}^3}\right)\left(\frac{\mu}{r_{1i}^3} + \frac{\mu'}{r_{2i}^3}\right)}{\left[\sum_{i=0,f} \left(\frac{\mu}{r_{1i}^3} + \frac{\mu'}{r_{2i}^3}\right)^2\right] + \frac{1}{2}\omega^4} \tag{40}$$

Some comments on the value of α may be made. If a close approach only to the earth is made, that is if either r_{10} or r_{1f} is close to unity while r_{20} and r_{2f} are both large it is readily seen that

$$\alpha \sim -\frac{\mu'}{\mu+\mu'},$$

which corresponds to placing the origin at the earth, while if a close approach only to the moon is made

$$\alpha \sim \frac{\mu}{\mu+\mu'},$$

which corresponds to placing the origin at the moon. If a midcourse portion of the trajectory is to be approximated so that none of the r's is near unity α will be somewhere between these extreme values -- that is the origin will lie on the line of centers between the earth and the moon. The origin is at the barycenter for $\alpha = 0$.

Integration of the Perturbation Equations

Once the point A has been determined the non-integrable terms in the perturbation equations (23) and (24) will be ignored and the equations to be integrated are

$$\frac{d}{dt}\bar{R}_{AE0}(t) = -\bar{\Omega} \times \bar{R}_{AE0}(t) \tag{41}$$

$$\frac{d}{dt}\bar{P}_{AE0}(t) = -\bar{\Omega} \times \bar{P}_{AE0}(t) + \omega^2 \delta \bar{A} \tag{42}$$

$$= -\bar{\Omega} \times \left(\bar{P}_{AE0}(t) + \delta\, \bar{\Omega} \times \bar{A}\right)$$

where use has been made of the relation

$$\bar{\Omega} \times (\bar{\Omega} \times \bar{A}) = -\omega^2 \bar{A} \tag{43}$$

The integrals of these equations are, since $\delta\, \bar{\Omega} \times \bar{A}$ is a constant,

$$\bar{R}_{AE0}(t) = M(t)\, \bar{R}_{AE0}(0) \tag{44}$$

$$\bar{P}_{AE0}(t) = M(t)\left[\bar{P}_{AE0}(0) + \delta\, \bar{\Omega} \times \bar{A}\right] - \delta\, \bar{\Omega} \times \bar{A} \tag{45}$$

where the matrix M(t) is a rotation matrix through an angle $-\omega t$ about the $\bar{\Omega}$ direction.

Referring back, now, to Eq. (16), it is seen that, in the rotating system, a solution to the restricted problem valid from the initial time zero to some time t, determined by how long the nonintegrable terms remain negligible, is obtained by substitution of the expressions (44) and (45) for $\bar{R}_{AE0}(t)$ and $\bar{P}_{AE0}(t)$ in terms of the two fixed center problem. This means that in order to construct the solution of the restricted problem in terms of that of the two fixed center problem, it is necessary, for each time t of interest, to compute initial conditions from Eqs. (44) and (45), and then obtain the solution,evaluated at the time t, of a two fixed center problem with these initial conditions. Thus if n points on the restricted orbit are desired, n different two fixed center problems must be evaluated.

One other point should be mentioned. The initial value $\bar{P}_{AE0}(0)$ is to be thought of as given by $\bar{P}_{AR0}$, which in turn is determined by the first Hamilton equation (9) for the restricted problem evaluated at time t=0:

$$\bar{P}_{AR0} = \dot{\bar{R}}_{A0} + \Omega \times \bar{R}_{A0} = \dot{R}_{A0} \tag{46}$$

where $\dot{R}_{A0}$ is the initial velocity in the non-rotating system, since the assumption has been made that the rotating and non-rotating systems have parallel axes at the initial time. Once $\bar{P}_{AE0}(0)$ has been been determined $\bar{P}_{AE0}(t)$ is given by Eq. (45) and is to be interpreted as an initial velocity relative to $\bar{A}$ in the rotating system for the two fixed center problem, by virtue of the first of the Hamilton equations (14) for this problem. Since in the rotating system the earth and moon are fixed the initial velocity $\bar{P}_{AE0}(t)$ is the same relative to any point in this system. The two fixed center solution obtained from this initial velocity $\bar{P}_{AE0}(t)$ and the initial position $\bar{R}_{AE0}(t)$ lead to position $\bar{R}_{AE}(t)$ and velocity $\bar{P}_{AE}(t)$ for the two fixed center problem, which are to be interpreted as position $\bar{R}_{AR}(t)$ and momentum $\bar{P}_{AR}(t)$ for the restricted problem in the rotating system.

THEORY FOR THE INERTIAL SYSTEM

Derivation and Integration of the Perturbation Equations

A direct approach to an approximation of the solution of the restricted problem by the two fixed center problem in an inertial coordinate system can be developed as follows. Recalling the equations of motion for the restricted problem in the inertial system with origin at the barycenter.

$$\ddot{R} = -\mu \frac{R_1}{r_1^3} - \mu' \frac{R_2}{r_2^3} \tag{1}$$

it is easily shown that the Hamiltonian is

$$H = \frac{1}{2} \dot{P}^2 - \frac{\mu}{r_1} - \frac{\mu'}{r_2} \tag{47}$$

This Hamiltonian has an explicit time dependence since r_1 and r_2 are distances of the vehicle from the earth and moon which are assumed moving in known orbits about the barycenter. The momentum P conjugate to position R relative to the varycenter is just $\dot{R}$, the velocity relative to the barycenter. The first Hamilton equation expresses this fact, and the second, together with the first, yields the equations of motion (1).

In this formulation two fixed points are selected for a fixed earth and a fixed moon. The selection of these points is to be made so as to minimize the non-integrable portion of the perturbation equations. Thus, denoting positions relative to these fixed points by stars, the equations of motion are

$$\ddot{R} = -\mu \frac{R_1^*}{r_1^{*3}} - \mu' \frac{R_2^*}{r_2^{*3}} + \mu\left(\frac{R_1^*}{r_1^{*3}} - \frac{R_1}{r_1^3}\right) + \mu'\left(\frac{R_2^*}{r_2^{*3}} - \frac{R_2}{r_2^3}\right) \tag{48}$$

and the Hamiltonian is

$$H = \frac{1}{2} P^2 - \frac{\mu}{r^*_1} - \frac{\mu'}{r^*_2} + \mu\left(\frac{1}{r^*_1} - \frac{1}{r_1}\right) + \mu'\left(\frac{1}{r^*_2} - \frac{1}{r_2}\right) \tag{49}$$

The Hamiltonian can be expressed as the sum of two terms. The first is the Hamiltonian for the two fixed center problem

$$H_E = \frac{1}{2} P^2 - \frac{\mu}{r^*_1} - \frac{\mu'}{r^*_2} \tag{50}$$

and the second

$$H_1 = \mu\left(\frac{1}{r^*_1} - \frac{1}{r_1}\right) + \mu'\left(\frac{1}{r^*_2} - \frac{1}{r_2}\right) \tag{51}$$

is the perturbation Hamiltonian which may be written in the form

$$H_1 = \mu\left(\frac{1}{r^*_{10}} - \frac{1}{r_{10}}\right) + \mu'\left(\frac{1}{r^*_{20}} - \frac{1}{r_{20}}\right) \tag{52}$$

$$-\int\left\{\mu\left[\frac{\dot{R}^*_1 \cdot \dot{R}^*_1}{r^{*3}_1} - \frac{\dot{R}_1 \cdot \dot{R}_1}{r^3_1}\right] + \mu'\left[\frac{\dot{R}^*_2 \cdot \dot{R}^*_2}{r^{*3}_2} - \frac{\dot{R}_2 \cdot \dot{R}_2}{r^3_2}\right]\right\} dt$$

Perturbation equations for the initial conditions may now be written as

$$\frac{d}{dt} R_o(t) = \text{grad}_{Po} H_1 = 0 - \text{grad}_{Po} \int \{\cdots\}\, dt \tag{53}$$

$$\frac{d}{dt} P_o(t) = -\text{grad}_{Ro} H_1 = \mu\left(\frac{R^*_{10}}{r^{*3}_{10}} - \frac{R_{10}}{r^3_{10}}\right) + \mu'\left(\frac{R^*_{20}}{r^{*3}_{20}} - \frac{R_{20}}{r^3_{20}}\right) + \text{grad}_{Ro} \int \{\cdots\}\, dt$$

If the terms involving the integrals are ignored in the perturbation equations, one obtains

$$R_o(t) = R_o(0) \tag{54}$$

$$P_o(t) = P_o(0) + (t - t_o)\left[\mu\left(\frac{R^*_{10}}{r^{*3}_{10}} - \frac{R_{10}}{r^{*3}_{10}}\right) + \mu'\left(\frac{R^*_{20}}{r^{*3}_{20}} - \frac{R_{20}}{r^3_{20}}\right)\right]$$

since the first of these equations implies also

$$R^*_{io}(t) = R^*_{io}(o) \qquad R_{io}(t) = R_{io}(o) \qquad i = 1, 2 \tag{55}$$

Selection of Fixed Positions for Earth and Moon

It is not easy to see how the fixed positions for the earth and moon should be selected so as to minimize the contribution of the integrals to the perturbation equations (53). Examination of the equations of motion (48), however, suggests that two cases should be considered as follows:

1) Motion from earth towards moon; fix earth in its initial and moon in its final position.

2) Motion from moon towards earth; fix earth in its final and moon in its initial position.

The initial conditions for the two fixed center problem will then be determined by the condition that initial position relative to the barycenter is unmodified and initial velocity relative to the barycenter be determined from Eq. (54), with momentum identified with velocity. The solution $R_E(R_o, P_o(t), t)$ and $P_E(R_o, P_o(t), t)$ for the Euler problem will then be related to that for the restricted problem by

$$R_R(R_o, P_o, t) = R_E(R_o, P_o(t), t) \tag{56}$$

$$P_R(R_o, P_o, t) = P_E(R_o, P_o(t), t)$$

where R_R and P_R are to be interpreted as position and velocity relative to the barycenter at time t.

RESULTS OF NUMERICAL COMPARISONS

Two methods of approximating the restricted problem by the two fixed center problem have been obtained in the preceding two sections. In addition to these methods, three others based on the formulation in the rotating system have been considered. These last three methods are defined as follows:

A. The center of rotation is taken at the center of the moon if the portion of a lunar trajectory to be approximated lies in "moon reference"; that is, if all points on this portion are within about 9 earth radii of the moon. For portions of the trajectory outside moon reference the center of rotation is taken at the earth. The method has not been applied to portions of a lunar trajectory crossing the moon's sphere of influence. Thus the values of α used for method A:

$$\alpha = -\frac{\mu'}{\mu+\mu'}, \qquad \text{earth reference}$$

$$\alpha = \frac{\mu}{\mu+\mu'}, \qquad \text{moon reference}$$

are the two extreme values noted in the discussion following Eq. (40) for α.

In addition, the parameter δ is taken to be zero.

B. This method uses the value of α determined by Eq. (40). The value of δ is taken to be one.

C. This method also uses the value of α given by Eq. (40), and δ is set equal to zero.

The two methods already derived are identified by

D. The method in the rotating system.

E. The method in the inertial system.

F. Finally, a sixth method was tried in which the effect of the perturbation Hamiltonian in the inertial formulation was neglected. That is the initial conditions for the two fixed center problem are to be just the initial position and velocity relative to the barycenter.

The comparison of the effectiveness of these methods was carried out as follows. First a typical lunar trajectory was integrated with the effects of moving earth and moon included, but with all perturbations due to sun, other planets, oblateness etc. eliminated from the program. The integration was carried out by the Republic Interplanetary Program using the Encke method. In this program the earth is used as origin in earth reference and the moon is the origin in moon reference. Various points on this typical lunar trajectory were taken as initial points and the two fixed center approximation was computed at various specified later times. This necessitated the transformation of the initial conditions associated with the various methods (relative to the origin A for the rotating formulations and relative to the barycenter for the inertial formulations) into equivalent initial conditions relative to the earth or moon for portions of the trajectory in earth and moon reference respectively. These transformations are given in Appendix I for the rotating system and in Appendix II for the inertial system.

The base lunar trajectory started at time t=0 from about 6590 Km from the center of the earth, reached a perisel distance of about 4350 Km at 71 hr. and reached a perigee distance of 8174 Km at 153.9 hr. The entry and exit from moon reference occurred at about 58.7 hr. and 84.1 hr. respectively.

Tables I, II, III and IV contain some typical results for the numerical calculations. Tables I and IV are for the earth-reference portions of the trajectory on the first and last legs, respectively. Tables II and III are for moon reference portions approaching and receding from the moon, respectively. The left hand column contains the initial and final times for the portion of the trajectory to be approximated. The deviations Δx, Δy and Δz in kilometers for the various methods are entered in columns headed by the corresponding letter. These deviations represent the difference in the rectangular coordinates relative to the reference body, the values predicted by the various methods being subtracted from the values given by the base case. The column headed K, which appears in Tables I and IV, give the deviations for the Kepler problem. The last column gives the value of α determined from Eq. (40) for use in methods B, C and D.

In Table V the x, y and z coordinates of the vehicle relative to the reference body are given for the various times which appear in Tables I, II, III and IV. Also given are the distances of the vehicle from the reference body in earth radii. The distance of the earth from the moon is a little less than 60 E.R.

Some general conclusions on the relative merits of these methods may be drawn. First it may be noted that methods A and C are practically the same except for midcourse portions of the trajectory. The reason for this is that except for such portions the value of α is such that the origin is nearly at the earth for earth reference and nearly at the moon for moon reference.

To summarize the results, then, for the methods described in this report A is the best in moon reference.

A and C are best for long range on the return leg.

B and C have a slight superiority for midcourse.

D is best on the first leg and is also best for short range on the return leg.

E and F are inferior almost everywhere.

The Kepler problem is superior to all of these methods for short to medium range in the neighborhood of the earth and moon. It fails, however, for long range and midcourse portions of the trajectory.

CONCLUSIONS

The results of the numerical comparison made in the previous section show that the formulation in a rotating system is best suited to the approximation of the restricted problem by the two fixed center problem. This is not really very surprising because in a rotating system the earth and moon are automatically fixed. This is achieved by introducing terms corresponding to the centrifugal and Coriolis accelerations, which are interpreted as perturbations on the two fixed center problem. In the inertial system, on the other hand, fixed positions for the earth and moon had to be selected more or less arbitrarily. As a consequence the perturbations from the two fixed center problem so selected depends on this selection. Thus approximations have been introduced before the problem of approximating the effect of the perturbations can even be considered. It would therefore seem that a rotating system, in which only the problem of how to treat the perturbations appears, should be the proper choice.

From the numerical results shown in the last section, it is evident that the problem of treating the perturbations is far from an easy one. None of the numerical results obtained can be regarded as satisfactory, or, in fact, as fulfilling the expectations that one might have for the theory. Nevertheless, there are a number of reasons for expecting that further development of the theory should lead to useful and interesting results.

If, for example, one considers the determination of the origin for the rotating system, it is obvious that the method used is fairly crude. The sum of squares of certain vectors appearing in the perturbation equations is minimized. Evidently, if the sum were a weighted sum, different origins would be obtained depending on the weighting factors used. It should, however, be remarked that the present determination yields plausible results, e.g., in the case of motion of an earth or moon satellite, one would certainly expect the rotation of initial conditions implied by Eqs. (44) and (45) to be about the center of the primary attracting body, or at least about a point very close to its center. A large rotation about a point very far removed from the center would obviously drastically distort what should be a stable orbit. Thus, the property that the origin is closer to the earth or moon according as the portion of the restricted problem orbit under consideration is closer to the earth or moon is a reasonable one and shows that the theory is at least qualitatively correct in this respect. For midcourse portions of the trajectory, one cannot use the satellite argument to suggest the proper choice of the origin, though it might be conjectured that the origin should vary continuously with the portion of the trajectory to be approximated.

It is possible to make a few remarks on the parameter δ. Reference to the perturbation Eqs. (23) and (24) shows that if $\delta = 1$ the non-integrable terms are all integrals from initial to final time, which therefore have zero initial value. It would thus appear that for short range predictions, results for $\delta = 1$, that is for method B, would be superior to the others. This result has been observed for some midcourse runs.

It may have been noticed that the perturbation term $\Omega \cdot R_A \times P_A$ in the perturbation Hamiltonian H_1 (see Eqs. (15) and (20) could be treated in the same way as the $R_A \cdot A_1$ term. That is, a factor ϵ could be introduced in the same way as δ. This would change the rotation in the initial conditions, resulting from integration of the perturbation equations, from an angle ωt to an angle $\epsilon \omega t$. To actually introduce the ϵ and obtain a value for it in the same way as for δ would not be easy because the terms in $(1-\epsilon)$ which would appear both inside and outside the integrals would be far more complex and difficult to treat than the corresponding terms in $(1-\delta)$.

To summarize, then, the various methods so far developed for the rotating system depend on the selection of four parameters α, β, γ (determining the center of rotation A) and δ. At this stage it appears that some sort of a parameter study using variations from the values of the parameters so far used, and including also, perhaps, variations in the parameter ϵ defined in the last paragraph, might well lead to some useful approximation formulae. There are many ways in which such a study might be carried out, for example, by using weighting factors with the vectors to be minimized, by a systematic variation of the parameters, or by the development of some sort of interation procedure. From the above discussion, it would appear that β and γ should be close to zero, that ϵ should be close to one, and that α should vary approximately according to Eq. (40). Only for the parameter δ is it difficult to estimate a value except for relatively short range predictions for which one would expect δ to be close to one.

APPENDIX I

TRANSFORMATION TO EARTH AND MOON REFERENCE FOR THE ROTATING FORMULATION

In this appendix the results obtained for the formulation of the problem in the rotating system are transformed so that a numerical comparison of the various methods may be carried out using the Republic Interplanetary Program. The first step is to interpret the results in a non-rotating coordinate system. To do this one uses Eq. (12) to obtain R_{AR} and $\dot{R}_{AR}$ for the restricted problem in this system:

$$R_{AR} = M^{-1}(t)\,\bar{R}_{AR} = M^{-1}(t)\,\bar{R}_{AE}\left(\bar{R}_{AE0}(t),\ \bar{P}_{AE0}(t),\ t\right) \tag{57}$$

$$\dot{R}_{AR} = M^{-1}(t)\,\bar{P}_{AR} = M^{-1}(t)\,\bar{P}_{AE}\left(R_{AE0}(t),\ \bar{P}_{AE0}(t),\ t\right)$$

Thus $\bar{P}_{AE}$ is the velocity in the rotating system for the two fixed center problem and represents the velocity in the fixed system for the restricted problem.

It is now possible to rephrase the whole procedure in the fixed system. The procedure, so far, is as follows:

1. Obtain initial values $\bar{R}_{AE0}(o)$ and $\bar{P}_{AE0}(0)$ from Eqs.
2. Obtain $\bar{R}_{AE0}(t)$ and $\bar{P}_{AE0}(t)$ from Eqs.
3. Rotate $\bar{R}_{AE}\left(\bar{R}_{AE0}(t),\ \bar{P}_{AE0}(t),\ t\right)$ and $\bar{P}_{A}\left(\bar{R}_{AE0}(t),\ \bar{P}_{AE0}(t),\ t\right)$ by $M^{-1}(t)$ to obtain R_{AR} and $\dot{R}_{AR}$.

Suppose that instead of carrying out steps 2 and 3, the earth, moon and initial conditions are all rotated by $M^{-1}(t)$ about the origin A. None of the essential characteristics of the two fixed center problem will be changed by this rotation. The effect is that not only the final but also the initial values of the coordinates and momentum components will be given for the fixed system, and the coordinates of the earth and moon will correspond to their final positions. That is one may obtain

$$R_{AR}(R_o, P_o, t) = \bar{R}_{AE}\left(M^{-1}(t)\,\bar{R}_{AE0}(t),\ M^{-1}(t)\,\bar{P}_{AE0}(t),\ t\right) \tag{58}$$

$$P_{AR}(R_o, P_o, t) = \dot{R}_{AR} = \bar{P}_{AE}\left(M^{-1}(t)\,\bar{R}_{AE0}(t),\ M^{-1}(t)\,\bar{P}_{AE0}(t),\ t\right)$$

in terms of position $\bar{R}_{AE}$ and momentum $\bar{P}_{AE}$ of a two fixed center problem computed in the non-rotating system with origin at A, with earth and moon in their final positions relative to A, and initial conditions

$$\begin{aligned} R_{AE0}(t) &= M^{-1}(t)\,\bar{R}_{AE0}(t) \\ \dot{R}_{AE0}(t) &= M^{-1}(t)\,\bar{P}_{AE0}(t) \end{aligned} \tag{59}$$

Since all comparisons of the results obtained by the two fixed center approximation with the restricted problem are made by numerical integrations of these problems using the R.A.C. interplanetary program which operates with either earth or moon as origin, depending on which is the primary attracting center, it remains to transform both the initial conditions given by Eq. (59) into a form usable in the R.A.C. program. The transformation on the initial conditions are obtained by combination of Eqs. (59) with Eqs. (44) and (45) and then using Eqs. (12)

$$
\begin{aligned}
R_{AE0}(t) &= M^{-1}(t)\left[M(t)\,\bar{R}_{AE0}(o)\right] = \bar{R}_{AE0}(o) = R_{A0} \\
\dot{R}_{AE0}(t) &= M^{-1}(t)\left[M(t)\,(\bar{P}_{AE0}(o) + \delta\bar{\Omega}\times\bar{A}) - \delta\bar{\Omega}\times\bar{A}\right] \\
&= \bar{P}_{AE0}(o) + \delta\Omega\times A(o) - \delta\Omega\times A(t) \\
&= \dot{R}_{A0} + \delta\Omega\times A(o) - \delta\Omega\times A(t)
\end{aligned}
\tag{60}
$$

If the initial conditions are in earth reference, that is, if R_{10} and $\dot{R}_{10}$ are given, it is necessary to find the modified initial conditions R'_{10} and $\dot{R}'_{10}$ relative to the earth dictated by Eqs. (60). First, since R_{10} is given relative to the initial position of the earth, and the procedure outlined above require the earth fixed in its final position, one obtains

$$
\begin{aligned}
R_{A0} &= R_{10} - \frac{\mu'}{\mu+\mu'}\,L(o) - A(o) \\
&= R'_{10} - \frac{\mu'}{\mu+\mu'}\,L(t) - A(t)
\end{aligned}
\tag{61}
$$

or

$$
\begin{aligned}
R'_{10} &= R_{10} + \frac{\mu'}{\mu+\mu'}\left(L(t) - L(o)\right) - \left(A(t) - A(o)\right) \\
&= R_{10} + \left(\alpha + \frac{\mu'}{\mu+\mu'}\right)\left(L(t) - L(o)\right)
\end{aligned}
\tag{62}
$$

on making use of Eqs. (38) and (40) determining the point A. To obtain $\dot{R}'_{10}$ one sets

$$
\dot{R}'_{10} = \dot{R}_{AE0}(t) = \dot{R}_{A0} - \delta\,\alpha\left(\dot{L}\,(t) - \dot{L}\,(o)\right) \tag{63}
$$

since for the two fixed center problem the velocity relative to the earth is the same as that relative to A, while the time derivative of Eq. (21) gives

$$
\dot{R}_{A0} = \dot{R}_{10} - \frac{\mu'}{\mu+\mu'}\,\dot{L}\,(o) - \alpha\,\dot{L}\,(o) \tag{64}
$$

so that, finally

$$
\dot{R}'_{10} = \dot{R}_{10} - \left(\alpha + \frac{\mu'}{\mu+\mu'}\right)\dot{L}\,(o) - \alpha\,\delta\left(\dot{L}\,(t) - \dot{L}\,(o)\right) \tag{65}
$$

Thus, using R'_{10} and $\dot{R}'_{10}$, a two fixed center problem is integrated, and at time t the $R_1(t)$ and $\dot{R}_1(t)$ obtained are to be interpreted as follows. The $R_1(t)$ is supposed to give position of the vehicle relative to the earth that would have been obtained had the restricted problem been integrated. The $\dot{R}_1(t)$ is the velocity relative to a point fixed at the final position of the earth and is therefore also the velocity relative to A. It is to be compared with the velocity relative to the earth moving with respect to A in its final position obtained by integrating the restricted problem. That is

$$\dot{R}_{1RF} = \dot{R}_{1EF} + \left(\frac{\mu'}{\mu+\mu'} + \alpha\right)\dot{L}\ (t) \tag{66}$$

Similarly if the initial and final conditions are in moon reference, one obtains instead of Eq. (61)

$$\begin{aligned} R_{A0} &= R_{20} + \frac{\mu}{\mu+\mu'}\, L(o) - A(o) \\ &= R'_{20} + \frac{\mu}{\mu+\mu'}\, L(t) - A(t) \end{aligned} \tag{67}$$

or

$$R'_{20} = R_{20} + \left(\alpha - \frac{\mu}{\mu+\mu'}\right)\left(L(t) - L(o)\right) \tag{68}$$

for the modified initial position associated with time t. In similar fashion

$$\dot{R}'_{20} = \dot{R}_{20} - \left(\alpha - \frac{\mu}{\mu+\mu'}\right)\dot{L}\ (o) - \alpha\,\delta\left(\dot{L}\ (t) - \dot{L}\ (o)\right) \tag{69}$$

and

$$\dot{R}_{2RF} = \dot{R}_{2EF} + \left(\alpha - \frac{\mu}{\mu+\mu'}\right)\dot{L}\ (t) \tag{70}$$

Since the moon is at the origin in moon reference, $R_2(t)$ from the Euler problem is the same as that for the restricted problem, in the range of applicability of this approximation of the restricted problem by the two fixed center problem.

APPENDIX II

TRANSFORMATION TO EARTH AND MOON REFERENCE FOR THE INERTIAL FORMULATION

Again, to obtain a comparison from the RAC program transformations must be made to position and velocity components relative to the reference body. To explore the usefulness of this approximation the following four cases were considered, for the four portions of a circumlunar trajectory corresponding to the four combinations of earth or moon reference with motion away from or towards the earth

1) From earth up to the moon's sphere of influence
2) From entry into moon's sphere of influence up to perisel
3) From perisel up to exit from moon's sphere of influence
4) From moon's sphere of influence towards earth

For these four cases the modification of initial conditions, the fixed position of the moon relative to the earth, and the relation between the final condition for the Euler and restricted problems are summarized below, with $P_o(t)$ of Eq. (54) identified with $\dot{R}_o(t)$, velocity relative to the barycenter.

I. Earth reference - earth towards moon

relative to barycenter: earth in initial position, moon in final position

relative to earth: moon at $$\frac{\mu'}{\mu+\mu'} L(o) + \frac{\mu}{\mu+\mu'} L(t) \tag{71}$$

initial position $$R_{10}' = R_{10} \tag{72}$$

$$R_{20}' = R_{20} - \frac{\mu}{\mu+\mu'} \left(L(t) - L(o) \right) \tag{73}$$

initial velocity $$\dot{R}_{10} = \dot{R}_{10} - \frac{\mu'}{\mu+\mu'} \dot{L}(o) + (t_f - t_o)\left[\mu \left(\frac{R_{10}'}{r_{10}'^3} - \frac{R_{10}}{r_{10}^3} \right) + \mu' \left(\frac{R_{20}'}{r_{20}'^3} - \frac{R_{20}}{r_{20}^3} \right) \right]$$

The first two terms in the initial velocity arise from the relation between velocity

relative to earth and velocity relative to the barycenter (i.e. the P_o term in Eq. (54). It will be noted that the μ term in the square bracket vanishes because of Eq. (71) so that the expression for $\dot{R}'_{10}$ thus becomes

$$\dot{R}'_{10} = \dot{R}_{10} - \frac{\mu'}{\mu+\mu'} \dot{L}(o) + \mu'(t_f - t_o)\left(\frac{R_{20}'}{r_{20}'^3} - \frac{R_{20}}{r_{20}^3}\right) \tag{74}$$

and the last term is computed using Eq. (73).

The relations between the restricted and Euler solutions at time t are given by

$$R_{1R}(R_{10}, \dot{R}_{10}, t) = R_{1E}(R_{10}', \dot{R}_{10}', t)$$

$$\dot{R}_{1R}(R_{10}, \dot{R}_{10}, t) = \dot{R}_{1E}(R_{10}', \dot{R}_{10}', t) + \frac{\mu'}{\mu+\mu'} \dot{L}(t) \tag{75}$$

in which the last expression includes a second transformation of velocity relative to the barycenter $\dot{R}_{1E}$ to velocity $\dot{R}_{1R}$ relative to the real moving earth.

II. Moon reference - earth towards moon

relative to barycenter: earth in initial position, moon in final position

relative to the earth: moon at $\frac{\mu'}{\mu+\mu'} L(o) + \frac{\mu}{\mu+\mu'} L(t)$ (76)

Initial position $R_{10}' = R_{10}$ (77)

$$R_{20}' = R_{20} - \frac{\mu}{\mu+\mu'}\left(L(t) - L(o)\right) \tag{78}$$

Initial velocity $\dot{R}_{20}' = \dot{R}_{20} + \frac{\mu}{\mu+\mu'} \dot{L}(o) + \mu'(t_f - t_o)\left(\frac{R_{20}'}{r_{20}'^3} - \frac{R_{20}}{r_{20}^3}\right)$ (79)

by the same analysis as for case I, except relation between velocity relative to barycenter and moon is used. Relations among final conditions

$$R_{2R}(R_{20}, \dot{R}_{20}, t) = R_{2E}(R_{20}', \dot{R}_{20}', t)$$
$$\dot{R}_{2R}(R_{20}, \dot{R}_{20}, t) = \dot{R}_{2E}(R_{20}', \dot{R}_{20}, t) - \frac{\mu}{\mu+\mu'} \dot{L}(t) \tag{80}$$

III. Moon reference - moon towards earth

relative to barycenter: earth in final position, moon in initial position

relative to the earth: moon at $\frac{\mu'}{\mu+\mu'} L(t) + \frac{\mu}{\mu+\mu'} L(o)$ (81)

Initial position $R_{10}' = R_{10} + \frac{\mu'}{\mu+\mu'} \left(L(t) - L(o)\right)$ (82)

$R_{20}' = R_{20}$ (83)

Initial velocity $\dot{R}_{20}' = \dot{R}_{20} + \frac{\mu}{\mu+\mu'} \dot{L}(o) + (t_f - t_o)\left[\mu\left(\frac{R_{10}'}{r_{10}'^3} - \frac{R_{10}}{r_{10}^3}\right) + \mu'\left(\frac{R_{20}'}{r_{20}'^3} - \frac{R_{20}}{r_{20}^3}\right)\right]$ (84)

The first two terms in the initial velocity arise from the relation between velocity relative to the moon and velocity relative to the barycenter. In this case the μ' term of the square bracket vanishes because of Eq. (83) so that Eq. (84) becomes

$$\dot{R}_{20}' = \dot{R}_{20} + \frac{\mu}{\mu+\mu'} \dot{L}(o) + \mu(t_f - t_o)\left(\frac{R_{10}'}{r_{10}'^3} - \frac{R_{10}}{r_{10}^3}\right) \tag{85}$$

in which the last term may be evaluated using Eq. (82). The relations among the final conditions are

$$R_{2R}(R_{20}, \dot{R}_{20}, t) = R_{2E}(R_{20}', \dot{R}_{20}', t)$$
$$\dot{R}_{2R}(R_{20}, \dot{R}_{20}, t) = \dot{R}_{2E}(R_{20}', \dot{R}_{20}', t) - \frac{\mu}{\mu+\mu'} \dot{L}(t) \tag{86}$$

IV. Earth reference - from moon towards earth

relative to barycenter: earth in final position, moon in initial position

relative to earth: $\frac{\mu'}{\mu+\mu'} L(t) + \frac{\mu}{\mu+\mu'} L(o)$ (87)

Initial position $R_{10}' = R_{10} + \frac{\mu'}{\mu+\mu'}\left(L(t) - L(o)\right)$ (88)

$R_{20}' = R_{20}$ (89)

Initial velocity $\dot{R}_{10}' = \dot{R}_{10} - \frac{\mu'}{\mu+\mu'} \dot{L}(o) + \mu(t_f - t_o)\left(\frac{R_{10}'}{r_{10}'^3} - \frac{R_{10}}{r_{10}^3}\right)$ (90)

obtained as in the earlier cases. The relation among the final conditions are

$$R_{1R}(R_{10}, \dot{R}_{10}, t) = R_{1E}(R_{10}', \dot{R}_{10}', t)$$
$$\dot{R}_{1R}(R_{10}, \dot{R}_{10}, t) = \dot{R}_{1E}(R_{10}', \dot{R}_{10}', t) + \frac{\mu'}{\mu+\mu'} \dot{L}(t) \quad (91)$$

REFERENCES

1. Arenstorf, R., and Davidson, M., "Solutions of Restricted Three-Body Problem Represented by Means of Two-Fixed-Center Problem," AIAA Journal, Vol. 1, No. 1, January 1963, p. 228.

2. Payne, M., "Approximation of the Restricted Problem by the Two Fixed Center Problem," Progress Report No. 3 on Studies in the Fields of Space Flight and Guidance Theory, Marshall Space Flight Center, NASA, 1963.

Table I. Earth Reference From Earth to Moon
α = -.012116806 Corresponds to Center of Rotation at the Earth

		A	B	C	D	E	F	K	α
0-1	Δx	.195	-.170	.177	.008			-.001	-.012116746
	Δy	.1169	-.0277	.1189	.0449			-.0074	
	Δz	.0426	-.0610	.0506	-.0045			.0002	
0-10	Δx	19	-52	19	-16	1033	1025	-6	-.012116746
	Δy	20	-28	20	-4	310	308	-4.8	
	Δz	8.4	-32	8.3	-1.692	471	467	-.65	
0-30	Δx		-523	125	-198	3431	3181	-174	-.012116746
	Δy		-515	282	-115	3020	2817	-109	
	Δz		-377	101	-137	2158	2004	-13	
0-50	Δx		-1425	217	-604			-1036	-.012116746
	Δy		-1177	1524	176			-596	
	Δz		-917	478	-218			-65	
10-30	Δx	47	-32	65	17	705	669		-.010659765
	Δy	119	-21	113	46	-590	-447		
	Δz	36	-8.2	358	14	-215	-184		
30-50	Δx	97	702	64	383	900	875		.093362437
	Δy	393	977	-354	361	-592	-22		
	Δz	98	284	-107	88	-221	-72		

Table II. Moon Reference From Earth to Moon
α = .987883194 Corresponds to Center of Rotation at the Moon

		A	B	C	D	E	F	α
59-60	Δx	4.9	14	6.3	10	8.7	10	.74542049
	Δy	17.2	47	22	35	33	35	
	Δz	5.6	15	7.0	11	11	11	
59-66	Δx	205	679	225	452	182	889	.95560202
	Δy	877	2566	915	1741	1026	2378	
	Δz	286	831	296	563	444	624	
59-71	Δx	219	1029	220	641	10584	16250	.98774102
	Δy	2321	6883	2322	4560	-5049	2456	
	Δz	831	2406	831	1601	-8198	-6994	
66-71	Δx	17	89	17	54	-1849	7978	.98774026
	Δy	417	1214	417	813	-3759	-7109	
	Δz	153	440	153	295	-332	-5818	

Table III. Moon Reference Moon Towards Earth
α = .987883194 Corresponds to Center of Rotation at the Moon

		A	B	C	D	E	F	α
72-73	Δx	1.65	9.11	2.77	5.9	-3923	3923	.98746055
	Δy	17.8	53.6	17.9	35.8	154	154	
	Δz	5.86	17.5	5.88	11.7	-238	-238	
72-75	Δx	20	87	22	55	-14442	-14442	.98750712
	Δy	159	469	160	315	-165	-165	
	Δz	52	151	52	101	1545	1545	
72-84	Δx	5.72	877	66	457	-53441	-64997	.98751836
	Δy	2535	7152	2563	4854	14180	14161	
	Δz	860	2314	855	1586	17901	17879	
75-80	Δx	25	124	44		-19459	-19459	.97489278
	Δy	450	1091	453		1390	1390	
	Δz	151	441	146		1446	1446	
75-84	Δx	12	262	87	174	-36022	-36018	.97552707
	Δy	1454	4326	1458	2892	3702	3700	
	Δz	491	1432	468	950	3611	3610	
80-84	Δx	4.1	38	17	27	-15244	-15244	.84840941
	Δy	289	1032	355	693	413	413	
	Δz	97	273	105	189	682	682	

Table IV. Earth Reference Moon Towards Earth
α = -.012116806 Corresponds to Center of Rotation at the Earth

		A	B	C	D	E	F	K	α
85-86	Δx	.453	.285	.2		-.241	-.235	7.26	.63122346
	Δy	-.04	6.46	-283.		-5.02	-5.02	-2.00	
	Δz	-.199	3.81	-4.1		.138	.136	-2.52	
85-100	Δx	536	395	704	540	-321	-304	1036	.53630503
	Δy	-207	1817	-6132	-2157	221	208	-291	
	Δz	-246	530	-1020	244	274	269	-366	
85-153	Δx	2268	1486	2268	1894	-667	-309	2317	-.012113913
	Δy	-3553	-14204	-5556	-9812	19431	13105	-4320	
	Δz	430	4819	431	2210	-771	-451	-178	
100-120	Δx	167	168	342	255	-102	-55		.044721505
	Δy	-57	68	-601	-266	158	92		
	Δz	-90	-31	-260	-145	99	82		
100-153	Δx	477	520	477	501				-.012114226
	Δy	-1027	-4630	-1028	-2808				
	Δz	-26	954	-26	424				
120-153	Δx	-11	90	-11	40	40	159		-.12114239
	Δy	60	-962	60	-449	1034	1224		
	Δz	-36	169	-36	63	-206	492		

Table V. Lunar Trajectory - Position Relative to Reference Body

Time in hours	X in Km	Y in Km	Z in Km	Distance in Earth Radii	Reference Body
0	47	6300	1800	1.0	Earth
1	-19000	-8000	-10000	3.6	Earth
10	-45000	-100000	-46000	18.6	Earth
30	-53000	-210000	-82000	36.8	Earth
50	-51000	-290000	-103000	48.8	Earth
59	50000	22000	482	8.6	Moon
60	46000	20000	187	7.96	Moon
66	24000	7300	-1500	3.97	Moon
71	1300	-3700	-2100	.70	Moon
72	-5000	-3500	-681	.96	Moon
73	-10000	-2100	1080	1.62	Moon
75	-19000	1100	4450	3.0	Moon
80	-38000	9100	12000	6.4	Moon
84	-52000	15000	18000	9.0	Moon
85	-57000	-329000	-97000	54.5	Earth
86	-56000	-327000	-95000	54.2	Earth
100	-50000	-300000	-75000	48.9	Earth
120	-36000	-240000	-41000	38.4	Earth
153	2300	-13000	16000	3.3	Earth

Department of Mathematics and Astronomy

University of Kentucky

Lexington, Kentucky

The Convergence of the Series Used in Hill's Solution of the Three Body Problem

by

The Kentucky Team

T. J. Pignani, H. G. Robertson

J. B. Wells, Jr., J. C. Eaves

Special Report No. 6

17 July 1963

Contract NAS 8-1611

Prepared for

George C. Marshall Space Flight Center

Huntsville, Alabama

Department of Mathematics and Astronomy

University of Kentucky

Lexington, Kentucky

The Convergence of the Series Used in Hill's Solution of the Three Body Problem

by

The Kentucky Team

T. J. Pignani, H. G. Robertson

J. B. Wells, Jr., J. C. Eaves

SUMMARY

This report presents, by request, details of the development of the Convergence of the Series used in Hill's Solution of the Three body problem, together with suggestions for an investigation which may reveal sharper bounds on the interval of convergence. Convergence in any interval was the object of the initial investigations. The objective of future studies will be to examine other methods which may yield better bounds, and to develop some transformations which permit comparison with known results.

Introduction. The equations of motion for this problem are well known and given as,

$$(1) \qquad \ddot{x} = 2\dot{y}+x+F_x \qquad\qquad \ddot{y} = -2\dot{x}+y+F_y$$

where the "dotted" variables, here and throughout, represent derivatives of that variable with respect to time,

$$(2) \qquad F \equiv (1-\mu)[(x+\mu)^2+y^2]^{-\frac{1}{2}} +\mu[(x+\mu-1)^2+y^2]^{-\frac{1}{2}}$$

and (x, y) are the coordinates or the point of the smallest of the three bodies (with mass zero) in a rotating coordinate system with angular velocity unity. Here $(1-\mu)$ is the mass of the largest of the three bodies, while μ is the mass of the medium sized body, where $0<\mu<1$. The origin of the system of coordinates is at the center of mass of the bodies with masses μ and $(1-\mu)$.

The equations of motion (1) are rewritten as

$$(3) \qquad \ddot{u} = -2i\dot{u}+H_v \qquad\qquad \ddot{v} = 2i\dot{v}+H_u$$

1. Siegel, Carl Ludwig, Vorlesunger Über Himmelsmechanik, Springer-Verlag, Berlin (1956), pp.104.
_____ Summer Lectures on Celestial Mechanics, The Johns Hopkin Univ., Md. (195?).

when equations (1) are subjected to the transformation

$$\mu^{\frac{1}{3}}u = (x+\mu-1)+iy \qquad \mu^{\frac{1}{3}}v = (x+\mu-1)-iy$$

where

(4) $$H \equiv uv+\mu^{-\frac{1}{3}}(1-\mu)(u+v)+\frac{2}{\sqrt{uv}}+\frac{2\mu^{-\frac{2}{3}}(1-\mu)}{\sqrt{(1+\mu^{-\frac{1}{3}}u)(1+\mu^{-\frac{1}{3}}v)}}$$

Note that $u = \bar{v}$, where here and hereafter, the "bar" designates the conjugate variable. The series development of (4) in increasing powers of $\mu^{\frac{1}{3}}$ is

$$H = uv+\mu^{-\frac{1}{3}}(u+v)+2\mu^{-\frac{2}{3}}(1-\frac{1}{2}\mu^{\frac{1}{3}}u+\frac{3}{8}\mu^{\frac{2}{3}}u^2)(1-\frac{1}{2}\mu^{\frac{1}{3}}v+\frac{3}{8}\mu^{\frac{2}{3}}v^2)+2(uv)^{-\frac{1}{2}}+\cdots$$
$$= 2\mu^{-\frac{2}{3}}+\frac{3}{4}(u+v)^2+2(uv)^{-\frac{1}{2}}+\cdots$$

where the omitted terms contain only powers of $\mu^{\frac{1}{3}}$. Since μ is taken to be small, the omitted terms are disregarded, and in place of (3), a mutated system is considered, namely

(5a) $$\ddot{u} = -2i\dot{u}+\frac{3}{2}(u+v)-u(uv)^{-\frac{3}{2}}$$

(5b) $$\ddot{v} = 2i\dot{v}+\frac{3}{2}(u+v)-v(uv)^{-\frac{3}{2}}$$

Solutions of (5a) and (5b) of the form

(6) $$u = \xi^4[1+A] \qquad v = \eta^4[1+B]$$

are now to be investigated, where $\eta = \bar{\xi}$, ξ and η satisfy the auxilary conditions

(7) $$\dot{\xi} = a\xi, \qquad \dot{\eta} = -a\eta, \qquad a = \pm\frac{i}{4}(\xi\eta)^{-3}$$

and hence $\xi = \xi_0 e^{\omega t}, \eta = \eta_0 e^{-\omega t}$, where $\omega = \pm\frac{i}{4}(\xi_0\eta_0)^{-3}$, and $\eta_0 = \bar{\xi}_0$.

Futhermore,

(8) $$A = \sum_{k=1}^{\infty}\sum_{\ell=-N}^{\ell=N} a_{k\ell}\xi^{3k+4\ell}\eta^{3k-4\ell}, \quad B = \sum_{k=1}^{\infty}\sum_{\ell=-N}^{\ell=N} a_{k,-\ell}\xi^{3k+4\ell}\eta^{3k-4\ell}$$

where the coefficients $a_{k\ell}$ are assumed to be real and $N = [3k/4]$, i.e. the largest integer in $(3k/4)$. These summations are abbreviated by

(9) $$A = \sum{}' a_{k\ell}\zeta_{k\ell} \qquad B = \sum{}' a_{k,-\ell}\zeta_{k\ell}$$

where $\zeta_{k\ell} = \xi^{3k+4\ell}\eta^{3k-4\ell}$, $\sum'$ means the summation is taken over all positive integral values of k. At times not only is a summation taken over all positive integral values of k, but also when $k = 0$; in this event, these

summations do not bear primes. Also in this case a_{oo} is defined to be 1. In passing, note that the series B can also be given as $B = \sum' a_{k\ell} \mathcal{G}_{k,-\ell}$. For reference, the first of the two subscripts of $\mathcal{G}_{k\ell}$ and $a_{k\ell}$ shall be called the order of $\mathcal{G}_{k\ell}$ or $a_{k\ell}$, as the case may be.

With the use of (6), (7), (8), and the notation introduced in (9)

$$\dot{u} = \pm i \xi \eta^{-3} \sum a_{k\ell}(2\ell+1) \mathcal{G}_{k\ell} \qquad \dot{v} = \pm i \xi^{-3} \eta \sum a_{k,-\ell}(2\ell-1) \mathcal{G}_{k\ell}$$

$$\ddot{u} = -\xi^{-2} \eta^{-6} \sum a_{k\ell}(2\ell+1)^2 \mathcal{G}_{k\ell} \qquad \ddot{v} = -\xi^{-6} \eta^{-2} \sum a_{k,-\ell}(2\ell-1)^2 \mathcal{G}_{k\ell}$$

Equation (5a) contains the expression $u(uv)^{-\frac{3}{2}}$, and (5b) contains the expression $v(uv)^{-\frac{3}{2}}$. Under the suposition of (6), these take the form

$$u(uv)^{-\frac{3}{2}} = \xi^{-2} \eta^{-6} (1+A)^{-\frac{1}{2}} (1+B)^{-\frac{3}{2}}$$
$$= \xi^{-2} \eta^{-6} [1 - \tfrac{1}{2}A - \tfrac{3}{2}B + P(A,B)]$$

where $P(A,B) = (1+A)^{-\frac{1}{2}}(1+B)^{-\frac{3}{2}} - 1 + \frac{1}{2}A + \frac{3}{2}B$, and

$$v(uv)^{-\frac{3}{2}} = \xi^{-6} \eta^{-2} (1+A)^{-\frac{3}{2}} (1+B)^{-\frac{1}{2}}$$
$$= \xi^{-6} \eta^{-2} [1 - \tfrac{3}{2}A - \tfrac{1}{2}B + P^*(A,B)]$$

where $P^*(A,B) = (1+A)^{-\frac{3}{2}}(1+B)^{-\frac{1}{2}} - 1 + \frac{3}{2}A + \frac{1}{2}B$. Both $P(A,B)$ and $P^*(A,B)$ are power series in A and B starting with quadratic terms. These power series yield series in $\xi_{k\ell}$; for, products of the form $\xi_{k\ell}\xi_{gh} = \xi_{k+g,\ \ell+h}$. Furthermore, the coefficients of all such variables are polynomials in a_{rs} with rational coefficents.

With the above evaluations and some algebraic manipulations, equations (5a) and (5b) become, respectively

$$(10a)\qquad \sum{}'\left\{\left[(2\ell+1)^2+\frac{1}{2}\right]a_{k\ell}+\frac{3}{2}a_{k,-\ell}\right\}\xi_{k\ell} = \pm 2\sum(2\ell+1)a_{k\ell}\,\xi_{k+1,\ell} - \frac{3}{2}\sum a_{k\ell}\,\xi_{k+2,\ell} - \frac{3}{2}\sum a_{k,-\ell}\,\xi_{k+2,\ell-1} + P(A,B)$$

$$(10b)\qquad \sum{}'\left\{\frac{3}{2}a_{k\ell}+\left[(2\ell-1)^2+\frac{1}{2}\right]a_{k,-\ell}\right\}\xi_{k\ell} = \pm 2\sum(2\ell-1)a_{k,-\ell}\,\xi_{k+1,\ell} - \frac{3}{2}\sum a_{k,-\ell}\,\xi_{k+2,\ell} - \frac{3}{2}\sum a_{k\ell}\,\xi_{k+2,\ell+1} + P^*(A,B)$$

Before proceeding with the problems presented in the material which is to follow, a point of worthiness is to note that for all k the order of the a_{rs} in the polynomial coefficients of the variables are of the lower order in the right members of (10a) and (10b) than they are in the corresponding left members of these equations.

PROBLEM I: To show that $a_{k\ell}$ and $a_{k,-\ell}$ are rational numbers.

The major tool which is employed to give these results is mathematical induction. To begin with $a_{oo} = 1$, by definition, and of course, a rational number.

The cases when $k>0$ are now considered. Assume that all a_{pq} are known rational numbers for $p = 0, 1, 2, \cdots, k-1$ and for all permissible q corresponding to each p, i.e. $q = [3p/4]$. With this hypothesis, all polynomials in a_{pq} with rational coefficients and $p<k$ are rational numbers. A comparison of coefficients of $\xi_{k\ell}$ on both sides of (10a) and (10b) yield

$$[(2\ell+1)^2+\frac{1}{2}]a_{k\ell}+\frac{3}{2}a_{k,-\ell} = Q(a_{pq}) \tag{11a}$$

$$\frac{3}{2}a_{k\ell}+[(2\ell-1)^2+\frac{1}{2}]a_{k,-\ell} = R(a_{pq}) \tag{11b}$$

where $R(a_{pq})$ and $Q(a_{pq})$ are polynomials with rational coefficients in the a_{pq} for $p<k$ and all permissible q. Since each a_{pq} is assumed to be rational then R and Q are also rational.

Now two cases must be considered; the first of these is when $\ell = 0$. In this case, the left members of (11a) and (11b) reduce to the same quantity $3a_{k0}$. Since the right members are rational members, then by mathematical induction, each a_{k0} ($k = 1, 2, \cdots$) is a rational member.

The second of the two cases is when $\ell \neq 0$. In this case, the value of the determinant of the coefficients of (11a) and (11b) is $4\ell^2(4\ell^2-1) \neq 0$. With this, the solutions of (11a) and (11b) are

$$a_{k\ell} = \frac{1}{4\ell^2(4\ell^2-1)}\left\{[(2\ell-1)^2+\frac{1}{2}]Q(a_{pq})-\frac{3}{2}R(a_{pq})\right\} \tag{12a}$$

and

$$(12b) \qquad a_{k,-\ell} = \frac{1}{4\ell^2(4\ell^2-1)}\left\{\left[(2\ell+1)^2+\frac{1}{2}\right]R(a_{pq}) - \frac{3}{2}Q(a_{pq})\right\}$$

Since the right members of each expression is a rational number when $p = 0, 1, 2, \cdots, k-1$ and all permissable q, then $a_{k\ell}$ and $a_{k,-\ell}$ are rational numbers. Hence by mathematical induction all $a_{k\ell}$ are rational numbers for $k = 1, 2, 3, \cdots$ and all admissable ℓ.

PROBLEM II: The functions u and v of (6) are periodic.

From (6), (7), (8) and (9)

$$u = \xi^4\left[1+\sum{}' a_{k\ell}\,\xi^{3k+4\ell}\,\eta^{3k-4\ell}\right]$$
$$= \xi_o^4 e^{4\omega t} + \sum{}' a_{k\ell}\,\xi_o^{3k+4(\ell+1)}\,\eta_o^{3k-4\ell}\,(e^{4\omega t})^{2\ell+1}$$

where $\omega = \pm\frac{i}{4}(\xi_o\eta_o)^{-3}$. Hence u is a function of $e^{4\omega t}$. Since

$$e^{4\omega t} = \cos(\xi_o\eta_o)^{-3}t \pm i\sin(\xi_o\eta_o)^{-3}t$$

then u is a periodic function of period $2\pi/(\xi_o\eta_o)^{-3}$. With $\bar{\xi}_o = \eta_o$, then the period becomes $2\pi\rho^6$, where $\rho = |\xi_o|$.

An arguement entirely similar to this given for u shows that v is periodic and of the same period as u.

Since the independent variable t does not explicitly appear in the differential equations (5a) and (5b), then any real constant may be added to the variable t without effecting these differential equations, i.e. a new independent variable (t+constant) may be used instead of t. With this liberty, a suitable translation can be employed to have $\rho = \eta_o = \xi_o > 0$.

CONVERGENCE OF THE SERIES USED IN HILL'S SOLUTION OF THE THREE BODY PROBLEM

The convergence of the series

$$(8)^* \qquad A = \sum_{k=1}^{\infty} \sum_{\ell=-N}^{\ell=N} a_{k\ell} \xi^{3k+4\ell} \eta^{3k-4\ell},$$

$$B = \sum_{k=1}^{\infty} \sum_{\ell=-N}^{\ell=N} a_{k,-\ell} \xi^{3k+4\ell} \eta^{3k-4\ell}$$

is of prime importance and the establishment of this convergence is our objective.

We recall that the coefficients $a_{k\ell}$ were shown to be rational numbers. Also, symbolically N is the largest integer in $3k/4$; i.e., in standard notation, $N = [3k/4]$. These summations have been abbreviated,

$$(9) \qquad A = \sum{}' a_{k\ell} \zeta_{k\ell}, \qquad B = \sum{}' a_{k,-\ell} \zeta_{k\ell}$$

where $\zeta_{k\ell} = \xi^{3k+4\ell} \eta^{3k-4\ell}$, and $\sum'$ means that the summation is taken over all positive integral values of k.

---

* In order to avoid duplication and provide greater clarity text references refer to Report No. 5 and reference numbers continue from that report. In case of repetition the notation, nomenclature, and assumptions are identical.

We now employ the Majorant method to show the series of (9) to be absolutely convergent when $|\xi|$ and $|\eta|$ are sufficiently small. Since we already have, from (7), that $|\xi| = |\xi_o|$, $|\eta| = |\eta_o|$, and $|\eta_o| = |\xi_o|$, it follows that

$$|\xi| = |\eta| = |\eta_o| = |\xi_o|. \tag{13}$$

Thus, it is sufficient to establish convergence for sufficiently small values of $|\xi_o|$.

Referring now to (10a) and (10b), and denoting the right members of (10a) and (10b) respectively by

$$\sum{}' P_{k\ell}\zeta_{k\ell} \quad \text{and} \quad \sum{}' P_{k,-\ell}\zeta_{k\ell}, \tag{10c}$$

these become

$$\sum{}' \{[(2\ell+1)^2+\tfrac{1}{2}]a_{k\ell}+\tfrac{3}{2}a_{k,-\ell}\}\zeta_{k\ell} = \sum{}' P_{k\ell}\zeta_{k\ell} \tag{14a}$$

$$\sum{}' \{\tfrac{3}{2}a_{k\ell}+[(2\ell-1)^2+\tfrac{1}{2}]a_{k,-\ell}\}\zeta_{k\ell} = \sum{}' P_{k,-\ell}\zeta_{k\ell} \tag{14b}$$

For $\ell = o$ (14a) and (14b) each reduces to

$$\sum{}' \{3a_{ko}\}\zeta_{ko} = \sum{}' P_{ko}\zeta_{ko}, \qquad k = 1, 2, 3, \cdots$$

$k = 4p$ or $4p+1$, and for $\ell = |3p+1|$.

By using the absolute values of the members of (18a) and (18b), we have

$$(19a)\ |P_{k\ell}| \leq 2|2\ell+1| \cdot |a_{k-1,\ell}| + \frac{3}{2}|a_{k-2,\ell}| + \frac{3}{2}|a_{k-2,-\ell-1}| + |c_{k\ell}|$$

$$(19b)\ |P_{k,-\ell}| \leq 2|2\ell-1| \cdot |a_{k-1,-\ell}| + \frac{3}{2}|a_{k-2,-\ell}| + \frac{3}{2}|a_{k-2,\ell-1}| + |c^{*}_{k,-\ell}|$$

We shall see momentarily that these $|P_{k,\ell}|$, $|P_{k,-\ell}|$ are bounds for the $|a_{k\ell}|$, $|a_{k,-\ell}|$.

Under the assumption that $\xi = \eta$ it follows that the series of (8) are identical, for, under these condition, we have

$$\zeta_{k\ell} = \xi^{3k+4\ell}\xi^{3k-4\ell} = \xi^{6k}$$

and

$$\zeta_{k,-\ell} = \xi^{3k-4\ell}\xi^{3k+4\ell} = \xi^{6k}$$

and setting $\xi^6 = \zeta$, we write

$$A = \sum{}' a_{k\ell}\zeta^{k} = B$$

In this case, the required convergence is established by comparing A and B with Z, where $Z = \sum{}' |a_{k\ell}|\,|\zeta_{k\ell}|$. Since $|\zeta_{k\ell}| = \zeta^{k}$, then $Z = \sum{}' |a_{k\ell}|\zeta^{k}$.

The comparison which is used herein is now defined.

Let $a_o, a_1, a_2, \cdots, a_n, \cdots$ be arbitrary complex numbers and $q_o, q_1, q_2, \cdots, q_n, \cdots$ be nonnegative real numbers. Also let

$$A(z) = \sum_{n=o}^{\infty} a_n z^n \quad \text{and} \quad Q(z) = \sum_{n=o}^{\infty} q_n z^n$$

where $|a_o| \leq q$, $|a_1| \leq q_1$, $|a_2| \leq q_2$, $\cdots$, $|a_n| \leq q_n, \cdots$. Then $Q(z)$ is said to <u>majorize</u> $A(z)$ or $A(z)$ to <u>minorize</u> $Q(z)$. This is indicated by use of the double symbol $\gg$ to indicate "majorizes" and $\ll$ to indicate "minorizes", and we write $Q(z) \gg A(z)$, and $A(z) \ll Q(z)$, respectively. (Seigel uses the ordering symbols $\succ$ and $\prec$ in the sense that Polya and Szego use the symbols $\gg$ and $\ll$.)

With this definition of $A(z)$ and $Q(z)$ and with the restriction $\xi = \eta$, it follows that $A \ll Z$ and $B \ll Z$. A property of majorants and minorants yields $A^n \ll Z^n$.

Also, when $\xi = \eta$, $P(A, B)$ in (10a) takes the form $P(A, A) = (1+A)^{-2} - 1 + 2A$. Since $(1+A)^{-2} = \sum_{n=o}^{\infty} (-1)^n (n+1) A^n$, then $(1+A)^{-2} \ll \sum_{n=o}^{\infty} (n+1) Z^n$. But, $P(A, A) = \sum_{n=2}^{\infty} (-1)^n (n+1) A^n$, and hence

$$P(A, A) \ll \sum_{n=2}^{\infty} (n+1) Z^n = (1-Z)^{-2} - 1 - 2Z = (1-Z)^{-2}(3Z^2 - 2Z^3)$$
$$\ll 3Z^2 (1-Z)^{-2}$$

where

$$P_4 = 4\ell^2(4\ell^2-1),\ P_3 = 2|2\ell+1|\cdot\left[(2\ell-1)^2+\frac{1}{2}\right],$$

$$P_2 = \frac{3}{2}\left[(2\ell-1)^2+\frac{1}{2}\right],\ P_1 = 3|2\ell-1|.$$

For $\ell \neq 0$, we have

$$0 < \frac{P_3}{P_4} < \frac{8}{5},\ 0 < \frac{P_2}{P_4} < \frac{6}{5},\ 0 < \frac{P_1}{P_4} < \frac{3}{4},\ \text{and}$$

$$0 < \frac{9}{4P_4} < \frac{1}{5}\ .$$

And thus there exists a constant c_1 such that

(21a) $$|a_{k\ell}| \leq c_1\ \left[|a_{k-1,\ell}|+|a_{k-2,\ell}|+|a_{k-2,-\ell-1}|+\right.$$

$$\left.|a_{k-1,-\ell}|+|a_{k-2,-\ell}|+|a_{k-2,\ell-1}|+d_{k\ell}\right].$$

By the use of (16b), (19a) and (19b) it follows that there exists a constant c_2 such that

(21b) $$|a_{k,-\ell}| \leq c_2\left[|a_{k-1,-\ell}|+|a_{k-2,-\ell}|+|a_{k-2,\ell-1}|+\right.$$

$$\left.|a_{k-1,\ell}|+|a_{k-2,\ell}|+|a_{k-2,\ell-1}|+d_{k\ell}\right] \qquad (\text{for } \ell\neq 0)$$

By choosing $c = \max\{c_1, c_2\}$ and noting that $d_{k\ell} = d_{k,-\ell}$, we see that the right members of (21a) and (21b) are symmetric in $\ell, -\ell$ and furthermore, $|a_{k\ell}| = |a_{k,-\ell}|$.

Furthermore, $\frac{1}{(1-z)^2} \ll \frac{1}{1-2z}$. Hence,

$$P(A,A) \ll \frac{3z^2}{1-2z} \tag{20}$$

In a manner entirely similar to this, $P^*(A,B)$ in (10b) has the same majorant function as $P(A,B)$.

Now, both the $|c_{k\ell}|$ of (19a) and the $|c^*_{k,-\ell}|$ of (19b) are bounded by numerical coefficients, say $d_{k\ell}$, given by (20), i.e. $|c_{k\ell}| \leq d_{k\ell}$ and $|c^*_{k,-\ell}| \leq d_{k\ell}$. Whenever a property has been established for an expression envolving "ℓ" and whenever we are then confronted with the same situation envolving this expression but for which "$-\ell$" replaces "ℓ", we shall not pursue the study of the latter case. It is convenient to think of the expression in ℓ and its counterpart in $(-\ell)$ as companion expressions and, occasionally, for clarity, both of these are given.

From (16a) it follows that

$$|a_{k\ell}| \leq \frac{1}{4\ell^2(4\ell^2-1)} \left\{\left[(2\ell-1)^2+\frac{1}{2}\right]|P_{k\ell}|+\frac{3}{2}|P_{k,-\ell}|\right\}$$

and in view of (19a) and (19b)

$$|a_{k\ell}| \leq \frac{P_3}{P_4}|a_{k-1,\ell}|+\frac{P_2}{P_4}|a_{k-2,\ell}|+\frac{P_2}{P_4}|a_{k-2,-\ell-1}|+$$
$$\frac{P_1}{P_4}|a_{k-1,-\ell}|+\frac{9}{4P_4}|a_{k-2,-\ell}|+\frac{9}{4P_4}|a_{k-2,\ell-1}|+\frac{2P_2}{3P_4}d_{k\ell}$$

In the case when $\ell = 0$, (15) yields $|a_{ko}| = \frac{1}{3}|P_{ko}|$.

Furthermore, from (20) and either (19a) or (19b), we have

$$|a_{ko}| \leq \frac{1}{3}\left[2|a_{k-1,o}| + \frac{3}{2}|a_{k-2,o}| + \frac{3}{2}|a_{k-2,-1}| + d_{ko}\right].$$

Again there exists a constant c such that

$$|a_{ko}| \leq c\left[|a_{k-1,o}| + |a_{k-2,o}| + |a_{k-2,-1}| + d_{ko}\right].$$

The right member here is a special case of (21a) and (21b).

Since $\zeta = \xi^6 > 0$, then $\zeta^k > 0$ and, by using (21a) to form a majorant for Z, we have

$$\begin{aligned}(22)\quad \sum_{k=1}^{\infty}\sum_{\ell=-N}^{\ell=N}|a_{k\ell}|\zeta^k \ll c\{&\sum_{k=1}^{\infty}\sum_{\ell=-N_1}^{\ell=N_1}|a_{k-1,\ell}|\zeta^k + \\ &\sum_{k=1}^{\infty}\sum_{\ell=-N_1}^{\ell=N_1}|a_{k-1,-\ell}|\zeta^k + \sum_{k=1}^{\infty}\sum_{\ell=-N_2}^{\ell=N_2}|a_{k-2,\ell}|\zeta^k + \\ &\sum_{k=1}^{\infty}\sum_{\ell=-N_2}^{\ell=N_2}|a_{k-2,-\ell-1}|\zeta^k + \sum_{k=1}^{\infty}\sum_{\ell=-N_2}^{\ell=N_2}|a_{k-2,-\ell}|\zeta^k + \\ &\sum_{k=1}^{\infty}\sum_{\ell=-N_2}^{\ell=N_2}|a_{k-2,\ell-1}|\zeta^k + \\ &\sum_{k=1}^{\infty}\sum_{\ell=-N}^{\ell=N}d_{k\ell}\zeta^k\}\end{aligned}$$

where $N = [3k/4]$, $N_1 = [3(k-1)/4]$, $N_2 = [3(k-2)/4]$ and $a_{k\ell} = 0$ if $k < 0$.

Each of the double summations in the right member of (22) is either rewritten or bounded above and given in the order in which it appears as,

$$\sum_{k=1}^{\infty}\sum_{\ell=-N_1}^{\ell=N_1}|a_{k-1,\ell}|\zeta^k = |a_{oo}|\zeta+\zeta\sum_{k=1}^{\infty}\sum_{\ell=-N}^{\ell=N}|a_{k\ell}|\zeta^k = \zeta+\zeta Z,$$

$$\sum_{k=1}^{\infty}\sum_{\ell=-N_1}^{\ell=N_1}|a_{k-1,-\ell}|\zeta^k = |a_{oo}|\zeta+\zeta\sum_{k=1}^{\infty}\sum_{\ell=-N}^{\ell=N}|a_{k\ell}|\zeta^k = \zeta+\zeta Z,$$

$$\sum_{k=1}^{\infty}\sum_{\ell=-N_2}^{\ell=N_2}|a_{k-2,\ell}|\zeta^k = \zeta^2+\zeta^2\sum_{k=1}^{\infty}\sum_{\ell=-N}^{\ell=N}|a_{k\ell}|\zeta^k = \zeta^2+\zeta^2 Z,$$

$$\sum_{k=1}^{\infty}\sum_{\ell=-N_2}^{\ell=N_2}|a_{k-2,-\ell-1}|\zeta^k \le |a_{o,-1}|\zeta^2+\zeta^2\sum_{k=1}^{\infty}\sum_{\ell=-N}^{\ell=N}|a_{k\ell}|\zeta^k =$$

$$|a_{o,-1}|\zeta^2+\zeta^2 Z,$$

$$\sum_{k=1}^{\infty}\sum_{\ell=-N_2}^{\ell=N_2}|a_{k-2,-\ell}|\zeta^k = \zeta^k+\zeta^k Z,$$

$$\sum_{k=1}^{\infty}\sum_{\ell=-N_2}^{\ell=N_2}|a_{k-2,\ell-1}|\zeta^k \le |a_{o,-1}|\zeta^2+\zeta^2 Z,$$

$$\sum_{k=1}^{\infty}\sum_{\ell=-N}^{\ell=N}d_{k\ell}\zeta^k = \frac{3Z^2}{1-2Z}$$

with these replacements, (22) becomes

$$(23)\quad Z \ll 2z\{(1+Z)\zeta+[(1+|a_{o,-1}|)+2Z]\zeta^2+\frac{3Z^2}{2(1-2Z)}\}$$

The coefficient $|a_{o,-1}|$ was shown to be a rational number. Let $c_3 = \max\{1+|a_{o,-1}|, 2\}$. Since $1+Z \ll (1-2Z)^{-1}$, then (23) becomes

$$(24)\qquad Z \ll c_4(1-2Z)^{-1}[\zeta+\zeta^2+Z^2],$$

where $c_4 = 2c\ c_3$. Herein $\zeta>0$, then $1-2Z \gg 1-2(\zeta+Z)$ and

$$\zeta+\zeta^2+Z \ll \zeta+(\zeta+Z)^2$$

and (24) becomes

$$Z \ll c_3\frac{\zeta+(\zeta+Z)^2}{1-2(\zeta+Z)}\ .$$

Furthermore

$$(25)\qquad Z+\zeta \ll c_3\frac{\zeta+(\zeta+Z)^2}{1-2(\zeta+Z)}+\zeta\ .$$

Let $V = Z+\zeta$. Then (25) becomes

$$V \ll c_3\frac{\zeta+V^2}{1-2V}+\zeta = \frac{c_3\zeta+c_3V^2+\zeta-2\zeta V}{1-2V}$$

from which follows that

$$V \ll \frac{(1+c_3)\zeta+c_3V^2}{1-2V} .$$

With $c_5 = \max\{1+c_4, c_4, 2\}$ then

$$X \ll \frac{t+X^2}{1-X} \tag{26}$$

where $X = c_5V$ and $t = c_4\zeta$.

Suppose U is a power series in t without a constant term and with positive coefficients satisfying $U = (t+U^2)/(1-U)$ and that U converges for $|t| < r$. Then using (26) above, we see that $X \ll U$. Also, X converges for $|t| < r$. To this end $U = (t+U^2)/(1-U)$ is rewritten as $1/(1-4U)^2 = 1/(1-8t)$. Since $1+8U \ll 1/(1-4U)^2$, then, by substitution, $1+8U \ll 1/(1-8t)$ from which it follows that $U \ll t/(1-8t)$. But the series $t/(1-8t)$ converges for $|t| < 1/8$ which implies that U converges when $|t| < 1/8$. But, in turn, X also converges when $|t| < 1/8$ which leads to the convergence of c_5V when $|c_5^2\zeta| < 1/8$. But $V = \zeta+Z$, and therefore $c_5(\zeta+Z)$ converges when $|\zeta| < 1/8c_5^2$. Since $A \ll Z$, then A converges when $|\zeta_o| < 1/8c_5^2$; this, in turn, establishes the convergence of $u = \xi(1+A)$ when $|\xi_o| < 1/8c_5^2$.

Although the results presented above are sufficient to establish convergence in the neighborhood $|\xi| < \frac{1}{8c_5^2}$ some of the mathematical techniques which were used do not appear to yield the best possible refinements. In view of the possible existence of interest in further refinement it appears that additional investigations may be initiated by pursuing some of the following suggestions.

(1). Examine the c_5, above, for the particular case at hand.

(2). Examine the sequence of coefficients leading to the c_5.

(3). Explore the possibility of a sequence of bounding functions which yield a better bound for the neighborhood.

(4). Explore several summability methods applicable to certain classes of functions.

REFERENCES

1. Siegel, Carl Ludwig, Vorlesunger Uber Himmelsmechanik, Springer-Verlag, Berlin (1956), pp. 104.

2. _____ Summer Lectures on Celestial Mechanics, The Johns Hopkin University, Maryland (195?).

3. G. Polya und G. Szego, Aufgaben und Lehrsatze Aus der Analysis I.

HAYES INTERNATIONAL CORPORATION

A MATHEMATICAL MODEL FOR AN ADAPTIVE GUIDANCE MODE SYSTEM

By

R. E. Wheeler

BIRMINGHAM, ALABAMA

HAYES INTERNATIONAL CORPORATION
BIRMINGHAM, ALABAMA

A MATHEMATICAL MODEL FOR AN ADAPTIVE GUIDANCE MODE SYSTEM

By

R. E. Wheeler

SUMMARY

This report presents the development of a mathematical model for empirical steering in support of the development of the Adaptive Guidance Mode concept. The model was derived from the equations of motion and contains arbitrary constants to be evaluated by some numerical process.

INTRODUCTION

The basic requirement for ideal guidance is to obtain a method that utilizes the true current state conditions, as measured by instrumentation in charge, to provide a nearly instantaneous solution for the description of the optimum path ahead. There is no method known today that enables one to derive a closed solution for the system of equations that define in general an optimum flight path. Likewise the limitation of the computer capacity on-board prohibits finding a solution by numerical means.

At this time two statistical methods have been employed to develop the form of the equations to be mechanized in the missile-borne computer for obtaining attitude commands. The approach taken in references 3 and 4 was to use linear programming techniques to fit linear combinations of known functions or ratios of such functions to a set of tabulated values of the steering and cutoff functions. A large number of trajectories are generated with realistic initial conditions and the data points are selected from the step by step solution of the trajectory.

In references 1 and 5 and 6 multivariate polynomial approximations by the method of least squares have been employed to obtain functions of the state variables that approximate the thrust direction angle and the time of cut-off. So far, the models employed have been restricted to polynomials involving usually x, $\dot{x}$, y, $\dot{y}$, t, and $\frac{F}{m}$. Various studies have been made and are being continued in an attempt to delete the insignificant terms in this multivariate approximating function.

The approach taken in this study consists of developing a functional relationship between the state variables at any time t. This mathematical model will have three important properties. First of all its form will not be assumed in any way. Thus when the answer is obtained it will indicate the form of the mathematical model. This functional relationship will be developed from the equations that define the motion and the conditions that insure an optimum trajectory. Thus the functional relationship obtained will satisfy all equations of motion as well as the equations involving control functions. Finally the relationship will contain a number of undetermined coefficients which can be obtained by the method of least squares so as to approximate the space of optimum trajectories, obtained in advance.

THE PROBLEM CONCEPT

In order to obtain some idea of the form of a mathematical model that would define the steering function in terms of the instantaneous state variables, it is helpful to start with a simple problem. The results of this simplified study will be utilized to obtain a model for the more complicated situation. The sample problem discussed in this development was selected because closed solutions exist and thus facilitate the derivation of the model.

The powered flight problem to be considered is defined as follows:

1. Motion is assumed to occur in a vacuum.
2. Only two dimensional motion is considered.
3. Rigid body dynamics is neglected.
4. The earth is assumed to be flat and non-rotating.
5. A constant applied force (F) is considered.
6. The time rate of change of the mass ($\dot{m}$) of the vehicle is constant.

Langrangian Multipliers will be used to formulate the necessary conditions for extremizing some variable such as propellant consumption or burning time.

EQUATIONS DEFINING THE PROBLEM

The differential equations which define the motion of the vehicle may be written as

$$\begin{aligned} \dot{u} &= \frac{F}{m} \sin\chi \\ \dot{v} &= \frac{F}{m} \cos\chi - g \\ \dot{x} &= u \\ \dot{y} &= v \end{aligned} \qquad (1)$$

The coordinate system x, y is chosen so that x is parallel to the surface of the earth, and y is perpendicular to the surface. The dot represents differentiation with respect to time. F is the thrust magnitude which we assume to be constant; g is constant and represents the magnitude of the gravitational acceleration. The m and χ represent the instantaneous mass and angle measured positive from the upward vertical to the thrust vector.

As shown in reference 2 the function whose time integral is to be minimized may be defined as $G = 1 + \sum_{i=1}^{5} \lambda_i g_i$ when λ_i are the undetermined Lagrangian Multipliers, and

$$\begin{aligned} g_1 &= \dot{u} - \frac{F}{m} \sin \chi = 0 \\ g_2 &= \dot{v} - \frac{F}{m} \cos \chi + g = 0 \\ g_3 &= u - \dot{x} = 0 \\ g_4 &= v - \dot{y} = 0 \\ g_5 &= \dot{m} - k = 0 \end{aligned} \tag{2}$$

The Euler-Lagrange equations define necessary conditions for minimization, namely that

$$\frac{\partial G}{\partial q} - \frac{d}{dt}\left[\frac{\partial G}{\partial \dot{q}}\right] = 0$$

where:

$$q = u,\ v,\ x,\ y,\ m,\ \dot{m},\ \chi,\ \lambda_1,\ \lambda_2,\ \lambda_3,\ \lambda_4,\ \lambda_5 .$$

Applying the Euler-Lagrange conditions to the function G results in the following system of equations:

$$\dot{u} = \frac{F}{m} \sin \chi \text{ and } \dot{v} = \frac{F}{m} \cos \chi - g \tag{3}$$

$$u = \dot{x} \text{ and } v = \dot{y} \tag{4}$$

$$\dot{m} = k \tag{5}$$

$$\dot{\lambda}_3 = 0,\ \dot{\lambda}_4 = 0 \text{ or } \lambda_3 = a \text{ and } \lambda_4 = c \text{ (a and c constants of integration)} \tag{6}$$

$$\dot{\lambda}_1 = \lambda_3 \text{ and } \dot{\lambda}_2 = \lambda_4 \text{ or } \lambda_1 = at+b \text{ and } \lambda_2 = ct+d \text{ where b and d are constants} \tag{7}$$

$$\tan \chi = \frac{\lambda_1}{\lambda_2} \text{ or } \sin \chi = \frac{\lambda_1}{(\lambda_1^2 + \lambda_2^2)^{1/2}} \text{ or } \cos \chi = \frac{\lambda_2}{(\lambda_1^2 + \lambda_2^2)^{1/2}} \tag{8}$$

and

$$\frac{F}{m^2} (\lambda_1 \sin \chi + \lambda_2 \cos \chi) = \dot{\lambda}_5 \tag{9}$$

The first integral for this system can be shown to be

$$\lambda_1 \dot{u} + \lambda_2 \dot{v} - \lambda_3 u - \lambda_4 v + \dot{m}\lambda_5 = c_o \tag{10}$$

ELIMINATION OF λ_5 TERMS

Equation (9) can be simplified by replacing the trigonometric functions by $\dot{u}$ and $\dot{v}$ as defined in the equations of motion (3). This result can be written as

$$m\dot{\lambda}_5 = \lambda_1 \dot{u} + \lambda_2 \dot{v} + \lambda_2 g \tag{11}$$

Substituting equation (11) in the first integral equation (10) yields

$$m\dot{\lambda}_5 + \dot{m}\lambda_5 + -\lambda_2 g - \lambda_3 u - \lambda_4 v = c_o$$

Now integrating both sides with respect to t one obtains

$$m\lambda_5 = \lambda_3 x + \lambda_4 y + \frac{cgt^2}{2} + (+dg + c_o) t + k \tag{12}$$

where k is constant of integration.
Equation (12) divided by the first integral (10) and simplified by cross multiplication, can be written as

$$m (\lambda_1 \dot{u} + \lambda_2 \dot{v} - \lambda_3 u - \lambda_4 v - c_o) = -\dot{m}(\lambda_3 x + \lambda_4 y + \frac{cgt^2}{2} + (+dg + c_o) t + k) \tag{13}$$

This expression involves $\dot{u}$ and $\dot{v}$ which must be eliminated in order to obtain an expression involving only constants, λ_1, λ_2, and

the instantanteous state variables. This expression will be integrated with respect to t by using repeatedly the formula for integration by parts. Substituting results (6) and (7) this relationship can be written as

$$4\dot{m}\left[\int \lambda_3 x dt + \int \lambda_4 y dy\right] = -m\left[\lambda_1 u + \lambda_2 v - 2\lambda_3 x - 2\lambda_4 y - c_o t\right]$$
$$+ \dot{m}\left[\lambda_1 x + \lambda_2 y - cgt^3/6 - (dg + 2c_o)t^2/2 - kt + \ell\right] \quad (14)$$

where ℓ is the constant of integration. We notice that this expression contains $\int x dt$ and $\int y dt$ which must be eliminated since, most of the time, it is not easy to obtain the instantaneous values of these two variables.

SOME RESULTS FROM EQUATIONS OF MOTION

The equations of motion (3) can be combined by division and by substituting (7) to yield $\lambda_2 \dot{u} - \lambda_1 \dot{v} = \lambda_1 g$ (15)
One integration gives

$$\lambda_2 u - \lambda_1 v - \lambda_4 x + \lambda_3 y = ag\frac{t^2}{2} + (bg)t + n \quad (16)$$

A second integration leads to

$$\lambda_2 x - \lambda_1 y - 2\lambda_4 \int x dt + 2\int \lambda_3 y dt = \frac{agt^3}{6} + \frac{(bg)t^2}{2} + nt + o \quad (17)$$

where n and o are constants of integration. Solving for $\int y dt$ in equation (17) and substituting this result in (14) yields.

$$4\dot{m}(\lambda_3^2 + \lambda_4^2)\int x dt = 2\dot{m}\left[\lambda_4 \lambda_2 x - \lambda_1 \lambda_4 y\right] - m\lambda_3\left[\lambda_1 u + \lambda_2 v\right.$$
$$\left. -2\lambda_3 x - 2\lambda_4 y - c_o t\right] + \dot{m}\left[\lambda_3 \lambda_1 x + \lambda_2 \lambda_3 y - cagt^3/2\right.$$
$$\left. - (da + 2cb)gt^2/2 - 2c_o a t^2/2 - (ka + cn)t + \ell - 2c_o\right] \quad (18)$$

It should be noted that this result still involves a variable $\int x dt$ which needs to be eliminated.

ELIMINATION OF $\int x dt$

From equation (9) it follows that

$$\lambda_1 \dot{u} + \lambda_2 \dot{v} + \lambda_2 g = m\dot{\lambda}_5 .$$

Now in (10)

$$\lambda_5 = (-\lambda_1 \dot{u} - \lambda_2 \dot{v} + \lambda_3 u + \lambda_4 v + c_o)/\dot{m}$$

so

$$\dot{\lambda}_5 = -(\lambda_1 \ddot{u} + \lambda_2 \ddot{v})/\dot{m}$$

Thus

$$\lambda_1 \dot{u} + \lambda_2 \dot{v} + \lambda_2 g = (-\lambda_1 \ddot{u} - \lambda_2 \ddot{v})\, m /\dot{m}$$

Now replace $\dot{v}$ by its value given in (15)

$$(\lambda_1^2 \dot{u} + \lambda_2^2 \dot{u})/\lambda_1 = -(\lambda_1 \ddot{u} + \lambda_2 \ddot{v})m /\dot{m}$$

Multiply both sides by λ_1 and integrate

$$(\lambda_1^2 + \lambda_2^2)\, u - (2\lambda_1 \lambda_3 + 2\lambda_2 \lambda_4)\, x + (2\lambda_3^2 + 2\lambda_4^2) \int x\, dt =$$
$$(-\lambda_1 m)/\dot{m} \left[\lambda_1 \dot{u} + \lambda_2 \dot{v} - \lambda_3 u - \lambda_4 v\right] +$$
$$\int \left[(\lambda_3 m + \lambda_1 \dot{m})/\dot{m}\right] \left[\lambda_1 \dot{u} + \lambda_2 \dot{v} - \lambda_3 u - \lambda_4 v\right] dt \qquad (19)$$

Now replace $\lambda_1 \dot{u} + \lambda_2 \dot{v}$ by $\lambda_3 u + \lambda_4 v + c_o - \dot{m}\lambda_5$ in the first term on the right side of (19) and integrate the second term.

$$(\lambda_1^2 + \lambda_2^2)\, u - (2\lambda_1 \lambda_3 + 2\lambda_2 \lambda_4)\, x + (2\lambda_3^2 + 2\lambda_4^2) \int x dt =$$
$$(-\lambda_1 mc_o)/\dot{m} + m\lambda_1 \lambda_5 + \left[(\lambda_3 m + \dot{m}\lambda_1)/\dot{m}\right] \cdot$$
$$\left[\lambda_1 u + \lambda_2 v - 2\lambda_3 x - 2\lambda_4 y\right] - 2\lambda_3 (\lambda_1 x + \lambda_2 y)$$
$$+ 6\lambda_3 \int (\lambda_3 x + \lambda_4 y)\, dt$$

From (12) replace $m\lambda_5$ to obtain

$$(\lambda_1^2 + \lambda_2^2)\, u - (2\lambda_1 \lambda_3 + 2\lambda_2 \lambda_4)\, x + (2\lambda_3^2 + 2\lambda_4^2) \int x dt =$$
$$(-\lambda_1 mc_o)/\dot{m} + \lambda_1 \left[\lambda_3 x + \lambda_4 y + (cgt^2)/2 + (+dg + c_o)\, t + k\right]$$
$$+ \left[(\lambda_3 m + \dot{m}\lambda_1)/\dot{m}\right] \cdot \left[\lambda_1 u + \lambda_2 v - 2\lambda_3 x - 2\lambda_4 y\right] - 2\lambda_3 (\lambda_1 x + \lambda_2 y)$$
$$+ 6\lambda_3 \int (\lambda_3 x + \lambda_4 y) dt \qquad (20)$$

Substituting for $\int (\lambda_3 x + \lambda_4 y)\, dt$ as given in (20) in equation (14) yields

$$4\dot{m}(\lambda_3^2 + \lambda_4^2) \int x dt = \dot{m} \left[-2(\lambda_1^2 + \lambda_2^2)\, u + 4(\lambda_1 \lambda_3 + \lambda_2 \lambda_4)\, x\right.$$
$$+ (2\lambda_1) \left\{\lambda_3 x + \lambda_4 y + cgt^{2}/2 + (+dg + c_o)\, t + k\right\} - 4\lambda_3 (\lambda_1 x + \lambda_2 y)$$
$$+ 3\lambda_3 \lambda_1 x + 3\lambda_2 \lambda_3 y - \lambda_3 cgt^{3}/2 - 3\lambda_3 (dg + 2c_o) t^{2}/2 - 3\lambda_3 (k)t$$
$$\left. + 3\lambda_3 \ell\right] - 2\lambda_1 mc_o + 2(\lambda_3 m + \dot{m}\lambda_1) \left[\lambda_1 u + \lambda_2 v - 2\lambda_3 x - 2\lambda_4 y\right]$$
$$- 3\lambda_3 m \left[\lambda_1 u + \lambda_2 v - 2\lambda_3 x - 2\lambda_4 y - c_o t\right] \qquad (21)$$

Equating equations (18) and (21) yields

$$(m/\dot{m})\left[-2b\, c_o\right] - 2\lambda_2^2 u + 2\lambda_1 \lambda_2 v + 2\lambda_2 \lambda_4 x$$
$$- 2\lambda_2 \lambda_3 y + (cb - da)\, gt^2 - 2\, c_o\, at^2 + 2(cn - ka)\, t + 3\, a\ell - \ell$$
$$+ 2c_o + 2\lambda_1 \left[cgt^{2}/2 + (dg + c_o)\, t + k\right] = 0 \qquad (22)$$

Now grouping (22) as an equation in λ_1 and λ_2 it may be expressed as

$$\lambda_1 [+ 2\,ctv + 2\,dv + cgt^2 + 2\,(dg + co)\,t + k]$$
$$+ \lambda_2 [- 2\,ctu - 2\,du + 2\,cx - 2\,ay] = 2(m/\dot{m})[bc_o] - (cb-da)gt^2$$
$$+ 2\,c_o at^2 - 2\,(cn-ka)\,t - 3\,a\ell + \ell - 2c_o \qquad (23)$$

In equations (16) and (23) solve for λ_1 and λ_2 and substitute in (8). This gives

$$\tan\chi = \frac{a_o\,(m/\dot{m})u + a_1\,uyt + a_2\,ut^2 + a_2\,uy + a_4\,uxt \ \ldots}{b_o\,(m/\dot{m})v + b_1\,vyt + b_2\,vt^2 + b_3\,vy + b_4\,vxt}$$

$$\ldots \frac{+ a_5\,ux + a_6 u + a_7\,ut + a_8\,ut^3 + a_9 tx + a_{10} ty + a_{11} y \ \ldots}{+ b_5\,vx + b_6 v + b_7\,vt + b_8 vt^3 + b_9 tx + b_{10} ty + b_{11} y}$$

$$\ldots \frac{+ a_{12} x + a_{13} t^2 x + a_{14} t^2 y + a_{15} y^2 + a_{16} x^2 + a_{17} xy}{+ b_{12} x + b_{13} t^2 x + b_{14} t^2 y + b_{15} t^4 + b_{16} t^3 + b_{17} t^2 + b_{18} t + b_{19}} \qquad (24)$$

Since $At = (m/\dot{m})\,A - A\,(m_o/\dot{m})$ and

$$Bt^2 = B(m/\dot{m})^2 - 2B(m/\dot{m})\,(m_o/\dot{m}) + B(m_o/\dot{m})^2$$

where $m = \dot{m}t + m_o$. Thus equation (24) can be changed to

$$\tan\chi = \frac{(m/\dot{m})^2\,[A_o ut + A_1 u + A_2 y + A_3 x]}{(m/\dot{m})^2\,[B_o vt + B_1 v + B_2 y + B_3 x + B_{15} t^2 + B_{16} t]} \ \ldots$$

$$\ldots \frac{+ (m/\dot{m})\,[A_4 ut + A_5\,u + A_6 y + A_7\,x + A_8 uy + A_9 ux]}{+ (m/\dot{m})\,[B_4 vt + B_5\,v + B_6 y + B_7\,x + B_8 vy + B_9 vx + B_{17} t^2 + B_{18} t]} \ \ldots$$

$$\ldots \frac{+ A_{10} uy + A_{11} ux + A_{12} u + A_{13} x + A_{14} y + A_{15} x^2 + A_{16} xy + A_{17} y^2}{+ B_{10} vy + B_{11} vx + B_{12} v + B_{13} x + B_{14} y + B_{19} t^2 + B_{20} t + B_{21}}$$

This expresses the tangent of the thrust angle as a rational function of the instantaneous state variable with forty undetermined coefficients to be evaluated by some numerical process.

REFERENCES

1. Dupee, D.E.; Harmon, F.L.; Linnstaedter, J.L.; Browning, L.; Hickman, R.A., " Recursion Process for the Generation of Orthogonal Polynomials in Several Variables". Progress Report No. 3, MSFC Report No. MTP-AERO-63-12, February 6, 1963.

2. Hoelker, R.F. and Miner, W.E., "Introduction to the Concept of the Adaptive Guidance Mode". MSFC Aeroballistics Internal Note No. 21-60, December 28, 1960.

3. Hubbard, S.M. and Suzuki, S., "Linear Programming Applied to Guidance Function Fitting". Progress Report No. 2, MSFC Report No. MTP-AERO-62-52, June 26, 1962.

4. Hubbard, S.M. and Suzuki, S., "An Application of Linear Programming to Multivariate Approximation Problems." Progress Report No. 3, MSFC Report No. MTP-AERO-63-12, February 6, 1963.

5. Swartz, R.V. and Vance, R.J., "Numerical Function Fitting Studies for Application in the Adoptive Guidance Mode." Progress Report No. 2, MSFC Report No. MTP-AERO-62-52, June 26, 1962.

6. Vance, R.J., "Numerical Approximation of Multivariate Functions Applied to the Adaptive Guidance Mode". Progress Report No. 3, MSFC Report No. MTP-AERO-63-12, February 6, 1963.

COMPUTATION CENTER
UNIVERSITY OF NORTH CAROLINA
CHAPEL HILL, NORTH CAROLINA

THE APPLICATION OF LINEAR PROGRAMMING TECHNIQUES TO RATIONAL APPROXIMATION PROBLEMS

By

Shigemichi Suzuki

SUMMARY

The purpose of this paper is to formulate linear programming algorithms for approximating, in the sense of Tchebycheff, a function of many variables by a ratio of linear forms over a finite point set. The problem of obtaining the "simplest" approximating function is also considered. Both standard and mixed integer linear programs arise in the formulations.

I. INTRODUCTION

This paper describes the use of linear programming techniques to approximate the steering and cutoff functions for the implementation of the Adaptive Guidance Mode [10, 12, 14]. This approach to the approximation of the guidance functions is basically a multivariate curve-fitting problem. Values of the steering and cutoff functions on minimum fuel trajectories are tabulated by solving the system of differential equations for a space vehicle by step-wise numerical integration. The problem is then to find functions which approximate the tabulated data over a finite point set.

In a previous report, [13], this problem was formulated with a linear combination of known functions being considered as the approximating function. In this paper the approximating function is a ratio of linear combinations of known functions. The following two statements of this general problem are studied.

Problem (a)

Given a fixed form for the ratio of linear combinations of known functions, coefficients are sought such that the maximum deviation over a finite point set is a minimum.

Problem (b)

Given the class of functions which are the ratio of linear combinations of known functions, find the "simplest" function of the class such that the maximum deviation over a finite point set is less than a preassigned tolerance.

Section II of this report contains a detailed description of Problems (a) and (b).

In Section III, Problem (a) is formulated as a mathematical programming problem with quadratic constraints and a linear objective function.

In Section IV, an algorithm for the solution of Problem (a) is developed, and a brief discussion of a second algorithm is given. Both use the simplex method iteratively. The first method is essentially identical to that of L. H. Loeb [11].

Section V is concerned with a formulation of Problem (b). The problem is formulated for a restricted case as a mixed integer programming problem. This is an original approach to this problem.

Section VI, a combination of Problem (a) and Problem (b) which will result in an "optimum" approximating function is discussed.

Section VII contains the conclusions of this report.

II. STATEMENT OF THE PROBLEM

A function $f(\vec{z})$ whose value is known at n points, $\vec{z}_1, \vec{z}_2, \ldots, \vec{z}_n$, in a multi-dimensional space is to be approximated by a function $R(\vec{z})$ in the class S whose elements are ratios of linear forms,

$$R(\vec{z}) = \frac{\sum_{i=0}^{M} A_i P_i(\vec{z})}{\sum_{j=0}^{N} B_j Q_j(\vec{z})} , \tag{1}$$

where P_i and Q_j are known functions of $\vec{z}$ and the coefficients A_i and B_j are unknown. An example of the known functions P_i and Q_j would be the set of monomials,

$$\left\{ z_1^{\alpha_1} z_2^{\alpha_2} \cdots z_m^{\alpha_m} \mid \alpha_i \geq 0, \sum_{i=1}^{m} \alpha_i \leq K, K > 0, \alpha_i \text{ and } K \text{ are integers} \right\}.$$

If the distance between $f(\vec{z})$ and $R(\vec{z})$ is defined as

$$\delta(f,R) = \max_{1 \leq k \leq n} |f(\vec{z}_k) - R(\vec{z}_k)| , \tag{2}$$

then the problem is to find that function $R(\vec{z})$ in S such that

$$\delta(f,R) = \min_{S} \delta(f,R) = \min_{S} \max_{1 \leq k \leq n} |f(\vec{z}_k) - R(\vec{z}_k)| , \tag{3}$$

or such that $\delta(f,R)$ is less than a prescribed positive number ϵ_0.

The following two formulations of this problem are considered:

(a) An approximation is required in which M, N, and possibly some of the coefficients A_i, B_i, are known. Then $R(\vec{z})$ is that function of the form

$$R(\vec{z}) = \frac{\sum_{i=0}^{M} A_i P_i(\vec{z})}{\sum_{j=0}^{N} B_j Q_j(\vec{z})}$$

which minimizes $\delta(f,R)$. In this case, $\delta(f,R)$ is the problem variable which is to be minimized.

(b) An approximation is desired in which $\delta(f,R)$ does not exceed a given tolerance ϵ_0. The given accuracy of approximation is accepted even though this does not give the best possible fit. $R(\vec{z})$ is the "simplest" function of form (1) for which $\delta(f,R) < \epsilon_0$. The "simplicity" of $R(\vec{z})$ is the problem variable which is to be minimized. Clearly, the criterion for simplicity depends upon the nature of $P_i(\vec{z})$ and $Q_j(\vec{z})$. One such criterion might be the minimization of the computation time for $R(\vec{z})$.

Problem (a) is an extension of the problem considered in Progress Report No. 3.[13] An approximation of $f(\vec{z})$ is sought among the given class of rational functions such that the maximum deviation of $R(\vec{z})$ from $f(\vec{z})$ over a finite set of points, $\vec{z}_1, \vec{z}_2, \ldots \vec{z}_n$, is minimum. Let ϵ^* be the minimum of the maximum deviations. Generally, all the coefficients, A_i and B_j, are non-zero for the approximation with maximum deviation ϵ^*. However, if the error tolerance ϵ_0 of Problem (b) is greater than ϵ^*, $\delta(f,R) \leq \epsilon_0$ might be satisfied without all the coefficients A_i and B_j being non-zero. For example, suppose

$$\epsilon_0 \geq \max_{k=1, \ldots n} |f(\vec{z}_k)| .$$

Let $B_0 = 1$, $A_i = 0$ for every i, and $B_j = 0$ for $j \geq 1$; then $R(\vec{z}) = 0$. Hence, $|f(\vec{z}_k) - R(\vec{z}_k)| \leq \epsilon_0$ for every k and $\delta(f,R) \leq \epsilon_0$.

III. FORMULATION FOR APPROXIMATIONS BY FIXED FORMS, PROBLEM (a)

Given

$$(4) \qquad R(\vec{z}) = \frac{\sum_{i=0}^{M} A_i P_i(\vec{z})}{\sum_{j=0}^{N} B_j Q_j(\vec{z})} = \frac{P(\vec{z})}{Q(\vec{z})}$$

with M and N fixed and A_i and B_j unknown, the problem is to minimize

$$\delta(f,R) = \max_{1 \leq i \leq n} |f(\vec{z}_i) - R(\vec{z}_i)| .$$

The problem is formulated as:

$$(5) \qquad \left\{ \begin{array}{l} \text{Minimize } \epsilon \text{ subject to the constraints} \\ \qquad |f(\vec{z}_k) - R(\vec{z}_k)| \leq \epsilon \qquad (k = 1, 2, \ldots, n) . \end{array} \right.$$

Each constraint of (5) can be represented by a pair of inequalities

$$(6) \qquad \begin{cases} f(\vec{z}_k) - R(\vec{z}_k) \le \epsilon \\ -f(\vec{z}_k) + R(\vec{z}_k) \le \epsilon \end{cases} \qquad (k = 1, 2, \ldots, n) .$$

Assuming that $R(\vec{z})$ does not have a pole on the set of points $\{\vec{z}_k\}_{k=1}^{n}$ and that $P(\vec{z})$ and $Q(\vec{z})$ do not have a common factor, then $Q(\vec{z}_k) > 0$ or $Q(\vec{z}_k) < 0$ for each k. The assumption that $Q(\vec{z}_k) > 0$ for all k will be made. Hence, $Q(\vec{z}_k) \ge c > 0$, $(k = 1, 2, \ldots, n)$, for some positive number c. Equation (6) can then be rewritten as:

$$(7) \qquad \begin{cases} f(\vec{z}_k)Q(\vec{z}_k) - P(\vec{z}_k) \le Q(\vec{z}_k)\epsilon \\ -f(\vec{z}_k)Q(\vec{z}_k) + P(\vec{z}_k) \le Q(\vec{z}_k)\epsilon \\ -Q(\vec{z}_k) \le -c \end{cases} \qquad (k = 1, 2, \ldots, n) .$$

Substituting (4) into (7) the problem now becomes:

Minimize ϵ subject to the constraints

$$(8) \qquad \begin{cases} -\sum_{i=0}^{M} p_{ki}A_i + \sum_{j=0}^{N} y_k q_{kj}B_j - \sum_{j=0}^{N} q_{kj}B_j\epsilon \le 0 \\ \sum_{i=0}^{M} p_{ki}A_i - \sum_{j=0}^{N} y_k q_{kj}B_j - \sum_{j=0}^{N} q_{kj}B_j\epsilon \le 0 \\ -\sum_{j=0}^{N} q_{kj}B_j \le -c \end{cases} \qquad (k = 1, 2, \ldots, n) ,$$

where $p_{ki} = P_i(\vec{z}_k)$, $q_{kj} = Q_j(\vec{z}_k)$, and $y_k = f(\vec{z}_k)$. In matrix form (8) is

$$(9)\qquad \left\{ \text{Minimize } \epsilon \text{ subject to the constraints } \left(\begin{bmatrix} -P & YQ \\ P & -YQ \\ 0 & -Q \end{bmatrix} + \epsilon \begin{bmatrix} 0 & -Q \\ 0 & -Q \\ 0 & 0 \end{bmatrix} \right) \begin{bmatrix} A \\ B \end{bmatrix} \leq \begin{bmatrix} 0 \\ 0 \\ \gamma \end{bmatrix} \right. ,$$

where

$$P = (p_{ki}) \quad (k = 1, 2, \ldots, n;\ i = 0, 1, \ldots, M) ,$$

$$Q = (q_{kj}) \quad (k = 1, 2, \ldots, n;\ j = 0, 2, \ldots, N) ,$$

$$Y = \text{diag.}\ (y_1, y_2, \ldots, y_n) ,$$

$$A = \begin{bmatrix} A_0 \\ A_1 \\ \vdots \\ A_M \end{bmatrix} , \qquad B = \begin{bmatrix} B_0 \\ B_1 \\ \vdots \\ B_N \end{bmatrix} , \qquad \gamma = \begin{bmatrix} -c \\ -c \\ \vdots \\ -c \end{bmatrix} \quad \text{(n elements)} .$$

A_i, B_j, and ϵ are the problem variables and are unrestricted in sign. p_{ki}, q_{kj}, and y_k are known values. Actually, from (6), ϵ can be shown to be non-negative. This problem is a problem of mathematical programming with quadratic constraints and a linear objective function. There are no established methods such as the simplex method for linear programming for solving this type of problem.

IV. METHODS FOR APPROXIMATING BY FIXED FORMS, PROBLEM (a)

A method for approximating the solution of Problem (a) by iterating on ϵ is now discussed. If ϵ is assigned some positive value ϵ_0, the constraints become linear in the unknowns A_i and B_j. Hence the question, "Are there any approximations of the given type (4) with $\delta(f,R)$ less than ϵ_0?" can be answered by means of linear programming. This problem does not have an objective function. Although some objective function might be considered, this is not necessary. The problem is reduced to determining whether or not there are any feasible solutions satisfying the linear constraints. If a solution does not exist, the simplex method, or any version of it, will determine this. If a

solution exists, the A_i and B_j are determined by the linear programming routine as the values of the basic variables of the feasible solution.

A solution for (9) is obtained by applying the above method iteratively. If a solution exists for a value ϵ_0 of ϵ, then the problem is resolved for $\epsilon = \epsilon_1 < \epsilon_0$. If no solution exists for ϵ_0, then ϵ is increased. The solution for (9) corresponds to the minimum value of ϵ which makes (9) a feasible program.

A systematic method for iterating on ϵ follows:

(A) Set $\epsilon_0 = \max_{k=1,\ldots,n} | f(\hat{z}_k) |$, $\Delta\epsilon_0 = \epsilon_0/2$, $i = 0$. (It has been shown that $\epsilon = \epsilon_0$ yields a feasible solution.)

(B) Do the following and go to (C).
   a) If $i = 0$, or if ϵ_i is admissible (i.e., linear program (9) with $\epsilon = \epsilon_i$ is feasible) and ϵ_{i-1} is also admissible, let $\Delta\epsilon_{i+1} = \Delta\epsilon_i$ and $\epsilon_{i+1} = \epsilon_i - \Delta\epsilon_{i+1}$.
   b) If ϵ_i is admissible and ϵ_{i-1} is not admissible, let $\Delta\epsilon_{i+1} = \Delta\epsilon_i/2$ and $\epsilon_{i+1} = \epsilon_i - \Delta\epsilon_{i+1}$.
   c) If ϵ_i is not admissible and ϵ_{i-1} is admissible, let $\Delta\epsilon_{i+1} = \Delta\epsilon_i/2$ and $\epsilon_{i+1} = \epsilon_i + \Delta\epsilon_{i+1}$.
   d) If neither ϵ_i nor ϵ_{i-1} is admissible, let $\Delta\epsilon_{i+1} = \Delta\epsilon_i$ and $\epsilon_{i+1} = \epsilon_i + \Delta\epsilon_{i+1}$.

(C) Solve the linear program (9) with $\epsilon = \epsilon_{i+1}$. Increase i by 1 and go to (B).

Clearly $\lim_{i\to\infty} \Delta\epsilon_i = 0$. Hence ϵ^* can be obtained to an arbitrary accuracy.

The study of another iterative method for solving program (9) has been initiated. It is hoped that this method will provide a better rate of convergence and information about the closeness of the approximation. A brief discussion of this method is given in the sequel.

The following notation is introduced to simplify the discussion.

$$
(10)\quad \begin{cases} g_k(A, B, \epsilon) = -\sum_{i=0}^{M} p_{ki}A_i + \sum_{j=0}^{N} y_k q_{kj}B_j - \sum_{j=0}^{N} q_{kj}B_j\epsilon \\ g_{n+k}(A, B, \epsilon) = \sum_{i=0}^{M} p_{ki}A_i - \sum_{j=0}^{N} y_k q_{kj}B_j - \sum_{j=0}^{N} q_{kj}B_j\epsilon \\ g_{2n+k}(B) = \sum_{j=0}^{N} q_{kj}B_j \end{cases} .
$$

Set ϵ to some positive value ϵ_0 and consider the following problem.

$$
(11)\quad \begin{cases} \text{Minimize} \quad \max_{k=1,\ldots,n} \left[g_k(A, B, \epsilon_0), g_{n+k}(A, B, \epsilon_0) \right] \\ \text{subject to the constraints} \\ \quad \bar{c} \geq g_{2n+k}(B) \geq c > 0. \qquad (k = 1, 2, \ldots, n) \end{cases} ,
$$

where $\bar{c}$ is a real number exceeding c.

Problem (11) is written as a linear programming problem as follows:

$$
(12)\quad \begin{cases} \text{Minimize} \quad \lambda \\ \text{subject to the constraints} \\ \quad g_k(A, B, \epsilon_0) \leq \lambda \\ \quad g_{n+k}(A, B, \epsilon_0) \leq \lambda \\ \quad -g_{2n+k}(B) \leq -c \\ \quad g_{2n+k}(B) \leq \bar{c} \end{cases} \qquad (k = 1, 2, \ldots, n) .
$$

Program (12) without the fourth constraint is equivalent to program (8), and program (8) with $\epsilon = \epsilon_0$ is feasible if and only if $\lambda \leq 0$ for program (12) without the fourth constraint. The fourth constraint restricts the class of approximating functions, but if $\bar{c}$

is so chosen that the fourth constraint does not eliminate the best approximation $R^*(\vec{z})$ from the class of approximating functions, then the best approximation will be obtained by solving (12) by iterating on ϵ. This value of $\bar{c}$ will be denoted by $\bar{c}^*$. The optimum λ of program (12) is a monotonic decreasing function of ϵ. Let it be denoted by $\lambda(\epsilon)$. The optimum ϵ, ϵ^*, satisfies

$$\lambda(\epsilon^*) = 0 \quad .$$

If $\epsilon_0 < \epsilon^*$, then $\lambda(\epsilon_0) > 0$, and if $\epsilon_0 \geq \epsilon^*$, then $\lambda(\epsilon_0) \leq 0$.

In the new method, upper and lower bounds for ϵ^* in terms of $\lambda(\epsilon_0)$, c, and $\bar{c}$ are obtained. A better estimate for ϵ is then computed from these bounds. By iterating on ϵ in this manner, ϵ^* can be obtained to an arbitrary accuracy.

One point needing further study is an algorithm for computing the value of $\bar{c}^*$.

V. FORMULATION FOR APPROXIMATIONS WITH A GIVEN TOLERANCE, PROBLEM (b)

In this section discussion will be confined to functions of a single variable $f(x)$ and the approximating functions will be restricted to the class of rational functions [i.e., $P_i(x) = x^i$ $(i = 1, 2, .., M)$ and $Q_j(x) = x^j$ $(j = 1, 2, \ldots, N)$] . The following formulation of Problem (b) with these restrictions is readily extended to the general case.

Given a class of approximating functions

$$R(x) = \frac{\sum_{i=0}^{M} A_i x^i}{\sum_{j=0}^{N} B_j x^j} \tag{13}$$

and a preassigned error tolerance ϵ_0, determine the "simplest" form of the approximating function $R(x)$ satisfying

$$|f(x_k) - R(x_k)| \leq \epsilon_0 \qquad (k = 1, 2, \ldots, n) \tag{14}$$

where x is the independent variable, $(x_k, f(x_k))$, $(k = 1, 2, \ldots, n)$ are the sample data points to be fitted, and $\{A_i\}_{i=0}^{M}$ and $\{B_j\}_{j=0}^{N}$ are the unknown coefficients to be determined. If $\epsilon_0 < \epsilon^*$ there is no approximation satisfying the requirements, so we assume that $\epsilon_0 \geq \epsilon^*$.

The following two criteria for simplicity are considered:

i) An approximation is defined to be "simplest" if the sum of the number of non-zero terms in the numerator and the denominator is minimum.

ii) An approximation is defined to be "simplest" if the sum of the orders of the highest order non-zero terms in the numerator and the denominator is minimum.

When one is interested in minimizing the storage locations for coefficients, i) is a better criterion for the simplicity. On the other

hand, if one is interested in minimizing the computation time for R(x), ii) is the better criterion. In most practical applications, the situation will be more complicated and more elaborate criteria must be considered, but slight variations of the following discussions can be expected to be applicable to these more realistic situations. Therefore, the problem is formulated with i) and ii) as examples of the criteria for simplicity.

i) Minimization of the Sum of the Numbers of Non-Zero Terms in the Numerator and the Denominator.

First, the approximating rational function R(x) must satisfy the constraints,

$$|f(x_k) - R(x_k)| \leq \epsilon_0 \qquad (k = 1, 2, \ldots, n) .$$

This requirement and the requirement that $Q(x_k) \geq c$ $(k = 1, 2, \ldots, n)$ with $c > 0$ give us the following system of linear inqualities, (9),

$$(15) \qquad \left(\begin{pmatrix} -P & YQ \\ P & -YQ \\ 0 & -Q \end{pmatrix} + \epsilon_0 \begin{pmatrix} 0 & -Q \\ 0 & -Q \\ 0 & 0 \end{pmatrix} \right) \begin{pmatrix} A \\ B \end{pmatrix} \leq \begin{pmatrix} 0 \\ 0 \\ Y \end{pmatrix} ,$$

where $p_{ki} = x_k^i$, $q_{kj} = x_k^j$, and $y_k = f(x_k)$.

Let L be a positive number which is large enough that the condition $|A_i| \leq L$ and $|B_j| \leq L$ $(i = 0, 1, \ldots, M;\ j = 0, 1, \ldots, N)$, does not eliminate the simplest solution. The existence of such an L will be discussed later. Since the values of A_i and B_j are unknown, a value for L must be arbitrarily chosen. For example, let $L = 10^{10}$ when the other entries are of the order of magnitude 1.

Now set

$$A_i = A_i^+ - A_i^- , \quad A_i^+, A_i^- \geq 0 , \qquad (i = 0, 1, \ldots, M)$$

$$B_j = B_j^+ - B_j^- , \quad B_j^+, B_j^- \geq 0 , \qquad (j = 0, 1, \ldots, N) .$$

Equation (15) becomes,

$$(16)\quad \left(\begin{pmatrix} -P & P & YQ & -YQ \\ P & -P & -YQ & YQ \\ 0 & 0 & -Q & Q \end{pmatrix} + \epsilon_0 \begin{pmatrix} 0 & 0 & -Q & Q \\ 0 & 0 & -Q & Q \\ 0 & 0 & 0 & 0 \end{pmatrix}\right) \begin{pmatrix} A^+ \\ A^- \\ B^+ \\ B^- \end{pmatrix} \leq \begin{pmatrix} 0 \\ 0 \\ \nu \end{pmatrix},$$

where

$$A^+ = \begin{pmatrix} A_0^+ \\ A_1^+ \\ \vdots \\ A_M^+ \end{pmatrix}, \qquad A^- = \begin{pmatrix} A_0^- \\ A_1^- \\ \vdots \\ A_M^- \end{pmatrix}, \qquad B^+ = \begin{pmatrix} B_0^+ \\ B_1^+ \\ \vdots \\ B_N^+ \end{pmatrix}, \qquad B_0^- = \begin{pmatrix} B_0^- \\ B_1^- \\ \vdots \\ B_N^- \end{pmatrix}.$$

Introduce the non-negative variables $\alpha_i (i = 0, 1, \ldots, M)$ and $\beta_j (j = 0, 1, \ldots, N)$ and construct the following system of linear inequalities:

$$(17)\quad \begin{cases} \alpha_i L \geq A_i^+ + A_i^- , & A_i^- \geq 0 \\ \beta_j L \geq B_j^+ + B_j^- , & B_j^- \geq 0 \end{cases} \qquad \begin{matrix} (i = 0, 1, \ldots, M) \\ (j = 0, 1, \ldots, N) \end{matrix} .$$

$$(18)\quad \begin{cases} 1 \geq \alpha_i \geq 0 \\ 1 \geq \beta_j \geq 0 \end{cases}$$

Restrict each α_i and β_j to integer values. Then from (18), each α_i and β_j is either 0 or 1. Since $|A_i| \leq A_i^+ + A_i^-$ and $|B_j| \leq B_j^+ + B_j^-$, the conditions $|A_i| \leq L$ and $|B_j| \leq L$ are satisfied when $\alpha_i = 1$ and $\beta_j = 1$.

Lemma 1. $A_i \neq 0$ implies $\alpha_i = 1$, and $B_j \neq 0$ implies $\beta_j = 1$.

Proof: Suppose $\alpha_i = 0$. Then by (17), $0 \geq A_i^+ + A_i^-$. Since both A_i^+ and A_i^- are non-negative, both A_i^+ and A_i^- must be zero. Therefore, $A_i = A_i^+ - A_i^- = 0$. By the same argument, $B_j = 0$ if $\beta_j = 0$.

Now consider the following linear programming problem:

$$(19)\begin{cases} \text{Minimize } u = \sum_{i=0}^{M} \alpha_i + \sum_{j=0}^{N} \beta_j = u(\alpha_0, \alpha_1, \ldots, \alpha_M; \beta_0, \beta_1, \ldots, \beta_N) \\ \text{subject to the constraints (16), (17), (18), where each } \alpha_i \text{ and} \\ \beta_j \text{ is an integer.} \end{cases}$$

Definition. A characteristic function with respect to R(x) is an $(M + N + 2)$-tuple $(S_0, S_1, \ldots, S_M, t_0, t_1, \ldots, t_N)$, with the following properties,

$$S_i = \begin{cases} 0 & \text{if } A_i = 0 \\ 1 & \text{if } A_i \neq 0 \end{cases} \qquad (i = 0, 1, \ldots, M)$$

$$t_j = \begin{cases} 0 & \text{if } B_j = 0 \\ 1 & \text{if } B_j \neq 0 \end{cases} \qquad (j = 0, 1, \ldots, N)$$

Let $C(R(x))$ denote the characteristic function.

Let $(A^+, A^-, B^+, \vec{\alpha}, \vec{\beta})$ denote the $3(M + N + 2)$-tuple, $(A_0^+, A_1^+, \ldots, A_M^+; A_0^-, A_1^-, \ldots, A_M^-; B_0^+, B_1^+, \ldots, B_N^+; B_0^-, B_1^-, \ldots, B_N^-; \alpha_0, \alpha_1, \ldots, \alpha_M; \beta_0, \beta_1, \ldots, \beta_N)$.

Lemma 2. If $(A^+, A^-, B^+, B^-, \vec{\alpha}, \vec{\beta})$ is a feasible solution of linear program (19) associated with a rational function

$$R(x) = \frac{\sum_{i=0}^{M} (A_i^+ - A_i^-)x^i}{\sum_{j=0}^{N} (B_j^+ - B_j^-)x^j} ,$$

then $(\bar{A}^+, \bar{A}^-, \bar{B}^+, \bar{B}^-, C(R)x)))$ is also a feasible solution associated with the same rational function $R(x)$, and $u(\vec{\alpha}, \vec{\beta}) \geq u(\mathcal{C}(R(x)))$, where

$$\bar{A}^+ = \begin{pmatrix} \bar{A}_0^+ \\ \bar{A}_1^+ \\ \vdots \\ \bar{A}_M^+ \end{pmatrix}, \quad \bar{A}^- = \begin{pmatrix} \bar{A}_0^- \\ \bar{A}_1^- \\ \vdots \\ \bar{A}_M^- \end{pmatrix}, \quad \bar{B}^+ = \begin{pmatrix} \bar{B}_0^+ \\ \bar{B}^+ \\ \vdots \\ \bar{B}_N^+ \end{pmatrix}, \quad \bar{B}^- = \begin{pmatrix} \bar{B}_0^- \\ \bar{B}_1^- \\ \vdots \\ \bar{B}_N^- \end{pmatrix},$$

$$\bar{A}_i^+ = \begin{cases} A_i^+ - A_i^- & \text{if } A_i^+ - A_i^- \geq 0 \\ 0 & \text{if } A_i^+ - A_i^- < 0 \end{cases} ,$$

$$\bar{A}_i^- = \begin{cases} -(A_i^+ - A_i^-) & \text{if } A_i^+ - A_i^- < 0 \\ 0 & \text{if } A_i^+ - A_i^- \geq 0 \end{cases} ,$$

$$\bar{B}_j^+ = \begin{cases} B_j^+ - B_j^- & \text{if } B_j^+ - B_j^- \geq 0 \\ 0 & \text{if } B_j^+ - B_j^- < 0 \end{cases} ,$$

$$\bar{B}_j^- = \begin{cases} -(B_j^+ - B_j^-) & \text{if } B_j^+ - B_j^- < 0 \\ 0 & \text{if } B_j^+ - B_j^- \geq 0 \end{cases} ,$$

Proof: Note that $\bar{A}_i^+ - \bar{A}_i^- = A_i^+ - A_i^-$ and $\bar{B}_j^+ - \bar{B}_j^- = B_j^+ - B_j^-$. Since A_i^+, A_i^-, B_j^+, and B_j^- satisfy (16), $\bar{A}_i^+$, $\bar{A}_i^-$, $\bar{B}_j^+$, and $\bar{B}_j^-$, do also.

If $A_i^+ - A_i^- = 0$, then $A_i = 0$ and $\bar{A}_i^+ = \bar{A}_i^- = 0$. Similarly if $B_j^+ - B_j^- = 0$, then $B_j = 0$ and $\bar{B}_j^+ = \bar{B}_j^- = 0$. If $\bar{A}_i^+ = \bar{A}_i^- = 0$ then (17) will be satisfied with $\alpha_i = 0$. Similarly if $\bar{B}_j^+ = \bar{B}_j^- = 0$ then (17) will be satisfied with $\beta_j = 0$. Let $\bar{\alpha}_i = 0$ if $A_i = 0$ and let $\bar{\beta}_j = 0$ if $B_j = 0$, and let $\bar{\alpha}_i = \alpha_i$ if $A_i \neq 0$ and let $\bar{\beta}_j = \beta_j$ if $B_j \neq 0$. By Lemma 1, $A_i \neq 0$ $(B_j \neq 0)$ implies $\alpha_i = 1$ $(\beta_j = 1)$, and hence $\bar{\alpha}_i = 1$ $(\bar{\beta}_j = 1)$ if $A_i \neq 0$ $(B_j \neq 0)$. Clearly $(\bar{A}^+, \bar{A}^-, \bar{B}^+, \bar{B}^-, \hat{\bar{\alpha}}, \hat{\bar{\beta}})$ satisfies (16), (17), (18) and the requirement that $\bar{\alpha}_i$ and $\bar{\beta}_j$ be integers. By construction,

$$\bar{\alpha}_i = \begin{cases} 0 & \text{if } A_i = 0 \\ 1 & \text{if } A_i \neq 0 \end{cases}$$

$$\bar{\beta}_j = \begin{cases} 0 & \text{if } B_j = 0 \\ 1 & \text{if } B_j \neq 0 \end{cases}$$

Therefore $(\hat{\bar{\alpha}}, \hat{\bar{\beta}}) = C(R(x))$. Hence there exists a feasible solution of the linear program (19) with objective function $u(C(R(x)))$. Since by Lemma 1, $A_i \neq 0$ $(B_j \neq 0)$ implies $\alpha_i = 1$ $(\beta_j = 1)$, it follows that $u(\hat{\alpha}, \hat{\beta}) \geq u(C(R(x)))$.

Theorem 1. The optimum feasible solution of linear program (19) gives the coefficients A_i and B_j of the rational approximation $R(x)$ which satisfies the preassigned error requirement

$$|f(x_k) - R(x_k)| \leq \epsilon_0 \qquad (k = 1, 2, \ldots, n) \tag{20}$$

and the auxiliary conditions

$$(21) \qquad \begin{cases} Q(x_k) \geq c & (k = 1, 2, \ldots, n) \\ |A_i| \leq L & (i = 0, 1, \ldots, M) \\ |B_j| \leq L & (j = 0, 1, \ldots, N) \end{cases} ,$$

and is the simplest in the sense that sum of the number of non-zero terms in the numerator and the denominator is minimum, if such a solution exists.

Proof: Suppose A_i and B_j are coefficients of $R(x)$ which satisfy (20) and (21). Consider the set S_R of all feasible solutions of linear program (19) which correspond to the same rational function (i.e., which have $A_i^+ - A_i^- = A_i$ and $B_j^+ - B_j^- = B_j$ for $i = 0, 1, \ldots, M$ and $j = 0, 1, \ldots, N$). By Lemma 2, the value of the objective function will be minimum in S_R for that feasible solution in S_R which has $(\hat{\alpha}, \hat{\beta})$ equal to $C(R(x))$. Hence, if S_R is non-empty, there exists an element of S_R with objective function $u(C(R(x)))$. The set of all feasible solutions of (19) is $S = \{S_R \mid R(x)$ satisfies (20) and (21)$\}$. Minimizing u over S is equivalent to minimizing u over the subset of S on which $u = u(C(R(x)))$ for each $R(x)$ satisfying (20) and (21).

$$u = \sum_{i=0}^{M} \alpha_i + \sum_{j=0}^{N} \beta_j ,$$

and $u(C(R(x)))$ is the sum of the number of non-zero terms in the numerator and the denominator of $R(x)$. Hence, by computing the optimum feasible solution of linear program (19), the coefficients of the simplest rational approximation, in the stated sense, which satisfies (20) and (21) is obtained.

Linear program (19) is a mixed integer program in which some of the variables in the linear inequalities are restricted to integers. R. Gomory [9] has constructed a finite algorithm for the solution of this type of problem. It is a modification of the usual simplex method.

One of the disadvantages of formulation (19) is that it does not always give the simplest rational approximation because of the additional restrictions $|A_i| \leq L$ and $|B_j| \leq L$.

First observe that, in general, there is more than one solution which satisfies (20) and (21) and minimizes u. For example, it may be possible to change the values of the coefficients in the rational approximation obtained from an optimum feasible solution of (19) so that a smaller maximum deviation at the set of points $\{x_k\}_{k=1}^{n}$ is obtained and the objective function is unchanged. Therefore there exists a set of (M + N +2)-tuples $\{(A, B)\}$ which gives the simplest rational approximation satisfying $|f(x_k) - R(x_k)| \leq \epsilon_0$ and $Q(x_k) \geq c$ (k = 1, 2, ..., n). Some of the A_i's and B_j's might be zero. For each element (A, B), let

$$\bar{A} = \max \{|A_0|, |A_1|, \ldots, |A_M|; |B_0|, |B_1|, \ldots, |B_N|\} .$$

This gives a set of non-negative numbers $\{\bar{A}\}$. If the greatest lower bound of $\{\bar{A}\}$ exceeds L, then the restrictions, $L \geq |A_i|$ and $L \geq |B_j|$, eliminate the simplest rational approximation from the set of feasible solutions of linear program (19). In this case, the optimum feasible solution of program (19) gives us a rational approximation with more terms than the simplest approximation. Therefore it is desirable to develop some method which can be used after solving program (19) to test whether the value of the objective function decreases if L is increased by an arbitrary amount.

ii) Minimization of the Sum of the Orders of the Highest Order Non-Zero Terms in the Numerator and the Denominator.

Introduce the new variables α and β and construct the following program

$$(23)\quad \begin{cases} \text{Minimize} \quad h = \alpha + \beta = h(\alpha, \beta) \\ \text{subject to the constraints (16), (17), (18), } \alpha_i \text{ and } \beta_j \\ \text{are integers, and} \\ (22)\quad \begin{cases} i\alpha_i \leq \alpha & (i = 0, 1, \ldots, M) \\ j\beta_j \leq \beta & (j = 0, 1, \ldots, N) \end{cases} \end{cases} .$$

The differences between linear programs (19) and (23) are the forms of the objective functions and the additional constraints (22).

Following are some of the properties of program (23).

Lemma 1 holds for program (23).

Lemma 3. If $(A^+, A^-, B^+, B^-, \hat{\alpha}, \hat{\beta}; \alpha, \beta)$ is a feasible solution corresponding to a rational function $R(x)$,

$$R(x) = \frac{\sum_{i=0}^{M} (A_i^+ - A_i^-)x^i}{\sum_{j=0}^{N} (B_j^+ - B_j^-)x^j} ,$$

then $(\bar{A}^+, \bar{A}^-, \bar{B}^+, \bar{B}^-, C(R(x)); \bar{i}, \bar{j})$ is also a feasible solution corresponding to the same rational approximation $R(x)$, and

$$h(\alpha, \beta) \geq h(\bar{i}, \bar{j}) ,$$

where $\bar{A}^+, \bar{A}^-, \bar{B}^+, \bar{B}^-, \hat{\alpha}$, and $\hat{\beta}$ are as defined in Lemma 2 and $\bar{i}$ is the highest index for which $A_i \neq 0$ and $\bar{j}$ is the highest index for which $B_j \neq 0$.

Proof: As shown in the proof of Lemma 2, $\bar{A}^+, \bar{A}^-, \bar{B}^+, \bar{B}^-$, and $C(R(x))$ satisfy (16), (17), (18) and the integer requirement for α_i and β_j. The constraints (22) will be satisfied if $\alpha = \bar{i}$ and $\beta = \bar{j}$. Hence $(\bar{A}^+, \bar{A}^-, \bar{B}^+, \bar{B}^-, C(R(x)), \bar{i}, \bar{j})$ is a feasible solution of linear program (23). This solution corresponds to the rational function $R(x)$ because $A_i = A_i^+ - A_i^- = \bar{A}_i^+ - \bar{A}_i^-$ and $B_j = B_j^+ - B_j^- = \bar{B}_j^+ - \bar{B}_j^-$. If $A_i \neq 0$ and $B_j \neq 0$, then $i \leq \alpha$ and $j \leq \beta$. Hence

$$h(\alpha, \beta) \geq h(i, j) ,$$

and

$$h(\alpha, \beta) \geq h(\bar{i}, \bar{j}) .$$

Theorem 2. The optimum feasible solution of linear program (23) results in the coefficients A_i and B_j of the rational approximation $R(x)$ which satisfies the preassigned error requirement,

$$|f(x_k) - R(x_k)| \leq \epsilon_0 \qquad (k = 1, 2, \ldots, n), \tag{24}$$

the auxiliary conditions,

$$\begin{cases} Q(x_k) \geq c & (k = 1, 2, \ldots, n) \\ |A_i| \leq L & (i = 0, 1, \ldots, M) \\ |B_j| \leq L & (j = 0, 1, \ldots, N) \end{cases} \tag{25}$$

and is the simplest in the sense that the sum of the orders of the highest order non-zero terms in the numerator and the denominator is a minimum, if such a solution exists.

Proof: Suppose A_i and B_j are coefficients of $R(x)$ which satisfy conditions (24) and (25). Consider the set S_R of all feasible solutions of linear program (23) which correspond to the rational function $R(x)$ (i.e., $A_i^+ - A_i^- = A_i$ and $B_j^+ - B_j^- = B_j$ for $i = 0, 1, \ldots, M$ and $j = 0, 1, \ldots, N$). By Lemma 3, the objective function will be a minimum in S_R for that feasible solution in S_R for which $(\alpha, \beta) = (\bar{i}, \bar{j})$; moreover, if S_R is non-empty, there exists an element of S_R whose objective function is $h(\bar{i}, \bar{j})$. Therefore minimizing h over all the feasible solutions of linear program (23) is equivalent to minimizing h over a subset of the feasible solutions for which $(\alpha, \beta) = (\bar{i}, \bar{j})$. Since $h = \alpha + \beta$, $h(\bar{i}, \bar{j})$ is the sum of the orders of the highest order non-zero terms in the numerator and the denominator. Therefore by computing the optimum feasible solution of linear program (23), the coefficients of the simplest rational approximation in the stated sense satisfying (24) and (25) are obtained.

Linear program (23) is also a mixed integer program and Gomory's algorithm can be used to get an optimum feasible solution. Formulation (23) also has the disadvantage that it might not give the simplest rational approximation desired if L is not large enough to include the set of coefficients A_i and B_j of the simplest approximation in the set of all feasible solutions of linear program (23).

iii) Other Criteria for Simplicity.

a) As a variation of criterion (i), one might wish to avoid high order terms in the "simplest" approximation. This problem can be solved by multiplying the variables α_i and β_j in the objective function by appropriate weights ω_i and ρ_j, and solving linear program (19) with the new objective function

$$u = \sum_{i=0}^{M} \omega_i \alpha_i + \sum_{j=0}^{N} \rho_j \beta_j \quad .$$

For example, $\omega_i = i$ and $\rho_j = j$ are possible choices for ω_i and ρ_j.

b) When one wishes to minimize the larger of $\bar{i}$ and $\bar{j}$, a new variable δ can be introduced, the new constraints, $\alpha \leq \delta$ and $\beta \leq \delta$, added to linear program (23) and the objective function can be replaced by $h = \delta$.

VI. COMBINATION OF PROBLEM (a) AND PROBLEM (b)

As suggested in Section V of this paper, the solutions obtained from linear programs (19) and (23) might be improved and a smaller maximum deviation than ϵ_0 might be obtained. By solving linear program (19) or (23), the form of the "simplest" rational approximation is found. This defines a subset of $\{P_i(x)\}_{i=0}^{M}$ and $\{Q_j(x)\}_{j=0}^{N}$ which is sufficient to approximate $f(x)$ with the required conditions. Now use this subset instead of $\{P_i(x)\}_{i=0}^{M}$ and $\{Q_j(x)\}_{j=0}^{N}$ and solve problem (a) starting with $\epsilon = \epsilon_0$. Since ϵ_0 is admissible, $\epsilon^* \leq \epsilon_0$. The form of the approximating function is unchanged, but the coefficients A_i and B_j are refined, in general, and give a smaller maximum deviation than the rational approximation obtained from (19) or (23). The improved solution thus obtained is optimum in the sense that a simpler approximation cannot be obtained without increasing ϵ_0 and, in general, a smaller maximum deviation cannot occur without increasing the complexity of the approximating rational function.

VII. CONCLUSIONS

The problem of approximating a function of many variables in the sense of Tchebycheff by a ratio of linear forms over a finite set of points has been studied. Two problems have been posed.

Problem (a): Given a ratio of linear combinations of known functions, unknown coefficients in this ratio of linear forms are sought such that the maximum error of the approximating function is minimized over the given finite set of points.

Problem (b): Given an error tolerance, the "simplest" approximation satisfying the tolerance at the given finite set of points is sought.

Problem (a) is formulated as a problem of mathematical programming with quadratic constraints and a linear objective function. Two methods of solving this problem are being studied. In both methods the error is considered to be a parameter and the constraints are linearized. The simplex method is employed iteratively to determine the minimax error. These two methods have not been tested numerically, and a comparison of these methods with other methods [1, 11] has not been made.

Problem (b) is formulated for the case where the approximating function is a rational function of a single variable and the criterion for the simplicity is either the minimization of the number of non-zero terms in the approximation or the minimization of the sum of the orders of the highest order non-zero terms in the numerator and the denominator. For each case, the problem is reduced to a mixed integer program. R. Gomory's algorithm may be used for solving this problem. An extension of this formulation to a rational approximation of many variables is immediate if the same criteria for simplicity are used. This formulation has not been tested.

Further work should include the completion of the development of the second algorithm for solving Problem (a). The behavior of the approximating functions should also be compared with that of the guidance functions between the sample points. The selection of sample points is another important topic for consideration. The relationship between the methods described in this report and those for approximating continuous functions by rational functions over a whole interval [3, 4] should also be investigated.

REFERENCES

1. Cheney, E. W., "A Survey of Approximation by Rational Functions", Space Technology Laboratory, Technical Note No. 149, June 1, 1960.

2. Cheney, E. W. and Loeb, H. L., "Two New Algorithms for Rational Approximation", Numerishe Mathematik, 3 Band, 1 Heft, February, 1961.

3. _____ and _____, "On Rational Chebyshev Approximation", Numerishe Mathematik, 4 Band, 2 Heft, Mai, 1962.

4. Fraser, W. and Hart, J. F., "On the Computation of Rational Approximation to Continuous Functions", Communications of the A.C.M. Vol. 5, No. 7, July , 1962.

5. Gass, S. I., Linear Programming. McGraw-Hill Book Company, Inc., New York, 1958.

6. Gomory, R. E., "An Algorithm for Integer Solution to Linear Programs", Princeton-IBM Mathematical Research Project, Technical Report No. 1, November 17, 1958.

7. _____, "An Algorithm for Integer Solution to Linear Program", Bulletin of American Mathematical Society, Vol. 64, No. 5, 1958.

8. _____, "All Integer Programming Algorithm", RC-189, IBM Research Center, January 29, 1960.

9. _____, "An Algorithm for Mixed Integer Program", RM-2597, Rand Corporation, Santa Monica, July 7, 1960.

10. Hoelker, R. F. and Miner, W. E., "Introduction to the Concept of the Adaptive Guidance Mode", MSFC Aeroballistics Internal Note No. 21-60, December 28, 1960.

11. Loeb, H. L., "Algorithms for Chebyshev Approximation Using the Ratio of Linear Forms", Journal of the Society of Industrial and Applied Mathematics, Vol. 8, No. 3, September, 1960.

12. Miner, W. E. and Schmieder, D. H., "Status Report on the Adaptive Guidance Mode", MSFC Report No. MTP-AERO-61-18, March 13, 1961.

13. Suzuki, S. and Hubbard, S. M., "The Application of Linear Programming to Multivariate Approximation Problems", Progress Report No. 2, MSFC Report No. MTP-AERO-63-12, February 6, 1963.

14. Swartz, R. V. and Vance, R. J., "Adaptive Guidance Mode Studies", Chrysler Corporation Missile Division, Technical Note AAN-TN-12-61, August 30, 1961.

SINGULAR EXTREMALS IN LAWDEN'S PROBLEM OF OPTIMAL ROCKET FLIGHT

HENRY J. KELLEY

ANALYTICAL MECHANICS ASSOCIATES, INC.

FOR PRESENTATION AT

AIAA SUMMER MEETING, JUNE 17-20, 1963, LOS ANGELES, CALIFORNIA

SINGULAR EXTREMALS IN LAWDEN'S PROBLEM OF OPTIMAL ROCKET FLIGHT

Henry J. Kelley*

Analytical Mechanics Associates, Inc.

Abstract

The problem of optimal rocket flight in an inverse square law force field has been studied extensively by Lawden[1,2] and Leitmann.[3] Periods of zero thrust, intermediate thrust, and maximum thrust are possible subarcs of the solution according to analysis of the Euler-Lagrange equations and the Weierstrass necessary condition. Arcs of intermediate thrust have recently been examined by Lawden;[4,5] however, the question of whether or not such arcs may actually furnish a minimum has been left unresolved.

The present paper derives the singular extremals of Lawden's problem by means of the Legendre-Clebsch necessary condition applied in a transformed system of state and control variables. These are obtained as circular orbits along which the thrust is zero and intermediate thrust arcs as found in Lawden's analysis. Since these solutions satisfy only the weak form of the Legendre-Clebsch condition, i.e., the extremals are singular in the transformed system of variables, the question of their minimality remains unanswered.

- -

* Vice-President. This investigation was performed while the writer was employed by the Grumman Aircraft Engineering Corporation.

Introduction

The problem of optimal rocket flight in an inverse square law force field has been investigated by Lawden[1,2] and Leitmann.[3] Although considerable progress has been made in the study of properties of the solution, a question remains as to the possible appearance of subarcs of intermediate thrust.[4,5] Such arcs are among the singular extremals of the problem, in classical variational terminology, and are resistant to analytical efforts owing to the unavailability of a general theory applicable to singular cases.

In the present paper, we first present a brief development of the Euler-Lagrange equations and the Weierstrass necessary condition along the lines of previous investigations, and then proceed to an analysis of intermediate thrust arcs.

Lawden's Problem

The equations of motion for a rocket in two-dimensional flight are given by:

$$\dot{u} = \frac{T}{m} \sin \theta + Y \tag{1}$$

$$\dot{v} = \frac{T}{m} \cos \theta + X \tag{2}$$

$$\dot{y} = u \tag{3}$$

$$\dot{x} = v \tag{4}$$

$$\dot{m} = - \frac{T}{c} . \tag{5}$$

Here y and x, Cartesian coordinates in an inertial frame, u and v, the corresponding velocity components, and the mass m are the state variables of the problem. The control variables are the thrust magnitude T and the thrust direction angle θ. The former is subject to a constraint of inequality type

$$0 \leq T \leq \overline{T} , \tag{6}$$

corresponding to an assumed capability of throttling the rocket motor over a thrust range of zero to maximum thrust $\overline{T}$. The gravitational force components Y and X are functions of the position coordinates and, in the most general case, of time as well. In the present analysis we will be concerned with the case of an inverse square law gravitational field.

Stated in Mayer form, the optimal rocket flight problem is to determine a solution of Eqs. (1)-(6), subject to appropriate boundary conditions, which furnishes a minimum of a function P of the state variable terminal values and the terminal time. In terms of the generalized Hamiltonian function

$$H = \lambda_u \left(\frac{T}{m} \sin\theta + Y\right) + \lambda_v \left(\frac{T}{m} \cos\theta + X\right) + \lambda_y u + \lambda_x v + \lambda_m \left(-\frac{T}{c}\right) . \tag{7}$$

The Euler-Lagrange equations for the problem are given as:

$$\dot{\lambda}_u = -\frac{\partial H}{\partial u} = -\lambda_y \tag{8}$$

$$\dot{\lambda}_v = -\frac{\partial H}{\partial v} = -\lambda_x \tag{9}$$

$$\dot{\lambda}_y = -\frac{\partial H}{\partial y} = -\left(\lambda_u \frac{\partial Y}{\partial y} + \lambda_v \frac{\partial X}{\partial y}\right) \tag{10}$$

$$\dot{\lambda}_x = -\frac{\partial H}{\partial x} = -\left(\lambda_u \frac{\partial Y}{\partial x} + \lambda_v \frac{\partial X}{\partial x}\right) \tag{11}$$

$$\dot{\lambda}_m = -\frac{\partial H}{\partial m} = \frac{T}{m^2}(\lambda_u \sin\theta + \lambda_v \cos\theta) \ , \tag{12}$$

in which the functions λ_u, λ_v, λ_y, λ_x, and λ_m are the usual Lagrange multipliers.

The control variables T and θ must satisfy the relation

$$H(T^*, \theta^*) \geq H(T, \theta) \tag{13}$$

for all admissible T^*, θ^*; which is to say that T and θ provide a minimum of the function H, subject to Eq. (6). This is the extended form of the Weierstrass necessary condition as derived by Pontryagin et al.[6]

A minimum of H is attained for

$$\sin\theta = \frac{-\lambda_u}{\sqrt{\lambda_u^2 + \lambda_v^2}} \qquad \cos\theta = \frac{-\lambda_v}{\sqrt{\lambda_u^2 + \lambda_v^2}} \tag{14}$$

$$T = 0 \qquad \text{for} \qquad \rho \equiv -\frac{1}{m}\sqrt{\lambda_u^2 + \lambda_v^2} - \frac{\lambda_m}{c} > 0 \tag{15}$$

$$T = \overline{T} \qquad \text{for} \qquad \rho \equiv -\frac{1}{m}\sqrt{\lambda_u^2 + \lambda_v^2} - \frac{\lambda_m}{c} < 0 \ . \tag{16}$$

In the case $\rho = 0$ the function H is not explicitly dependent upon T and the thrust magnitude is not determined by the Weierstrass necessary condition.

Portions of a solution of the Euler-Lagrange equations for which ρ vanishes identically, i.e., over a finite time interval, are known as singular subarcs according to the terminology of the classical theory, the criterion being the vanishing of the determinant

$$\begin{vmatrix} \frac{\partial^2 H}{\partial T^2} & \frac{\partial^2 H}{\partial \theta \partial T} \\ \frac{\partial^2 H}{\partial T \partial \theta} & \frac{\partial^2 H}{\partial \theta^2} \end{vmatrix} \tag{17}$$

This definition applies only if the function H is stationary at its minimum,

$$\frac{\partial H}{\partial \theta} = \frac{\partial H}{\partial T} = 0 \ . \tag{18}$$

The Intermediate Thrust Subarcs

The possible appearance of singular subarcs in a problem is accompanied by considerable analytical difficulty. There is no powerful general method available for determining these subarcs, or whether they may furnish a minimum even in the local sense, i.e., over short intervals, or in what manner they form segments of the minimizing arc. Valuable insight into these questions is provided by the Green's Theorem method of Miele,[7] which, however, is severely restricted in number of variables, as regards its applicability.

For the problem presently considered, Lawden has examined arcs of intermediate thrust satisfying the Euler-Lagrange equations and the Weierstrass necessary condition.[4,5] His results

indicate the existence of a family of such intermediate thrust arcs, including a spiral corresponding to the case $H = 0$, analyzed in some detail. The question of whether or not such arcs may actually furnish a minimum, however, has been left unresolved. In the present analysis we pursue an alternate approach to the intermediate thrust arcs.

We now introduce new variables ψ, β, γ, ϕ, V replacing u, v, y, x, m according to the transformation

$$\psi = y \sin\theta + x \cos\theta + \frac{1}{\omega}(u \cos\theta - v \sin\theta) \tag{19}$$

$$\beta = c \ln m + u \sin\theta + v \cos\theta \tag{20}$$

$$\gamma = y \cos\theta - x \sin\theta \tag{21}$$

$$\phi = y \sin\theta + x \cos\theta \tag{22}$$

$$V = - c \ln m \ . \tag{23}$$

It is readily verified that this transformation is nonsingular by the nonvanishing of the Jacobian determinant

$$\Delta = \frac{\partial(\psi, \beta, \gamma, \phi, V)}{\partial(u, v, y, x, m)} = - \frac{c}{\omega m} \neq 0 \ . \tag{24}$$

By a formal process the equations of state in the new system of variables are obtained as:

$$\dot{\psi} = \gamma\omega + \frac{1}{\omega}(Y \cos\theta - X \sin\theta) - \frac{\mu}{\omega}(\psi - \phi) \tag{25}$$

$$\dot{\beta} = Y \sin\theta + X \cos\theta + \omega^2(\psi - \phi) \tag{26}$$

$$\dot{\gamma} = \omega(\psi - 2\phi) \tag{27}$$

$$\dot{\phi} = \beta + \gamma\omega + V \tag{28}$$

$$\dot{V} = \frac{T}{m} = e^{V/c_T} \tag{29}$$

$$\dot{\theta} = \omega \tag{30}$$

$$\dot{\omega} = \mu \ . \tag{31}$$

It has been tacitly assumed in the course of the manipulations leading to Eqs. (25)-(31) that the steering angle θ is twice differentiable, i.e., that the derivatives $\dot{\theta} = \omega$ and $\ddot{\theta} = \mu$ exist. Examination of Eqs. (8)-(14) indicates that such an assumption is justified if the gravitational force components Y and X possess first partial derivatives, except for a finite number of points along the trajectory, corresponding to thrust direction reversals, at which λ_u and λ_v vanish simultaneously. We exclude such reversal points from the segments of arc analyzed in the following.

It would appear upon first inspection of the Eqs. (25)-(31) governing the new variables that an unwarranted increase in complexity has been realized. Our motivation becomes clear, however, when it is observed that the variables T and V appear <u>only</u> in Eqs. (28) and (29), and that as a consequence of this, the multipliers λ_ϕ and λ_V vanish along the singular subarcs. Means of synthesizing transformations having this property will be discussed in another paper presently in preparation.

If we consider a segment of arc of intermediate thrust, i.e., over which the strict inequality in (6) holds,

$$0 < T < \bar{T} \tag{32}$$

it follows that neighboring thrust programs

$$T + \delta T = T(t) + \epsilon\eta(t) \tag{33}$$

will also satisfy Eq. (32) if the magnitude ϵ of the (otherwise arbitrary) thrust variation is taken sufficiently small.

Evidently if we restrict attention to small variations in T, V, and ϕ, we may regard the variable ϕ as a control variable over an intermediate thrust arc, as implied by the vanishing of the multipliers λ_ϕ and λ_V. We note that the coefficient of T in Eq. (29) and the coefficient of V in Eq. (28) never vanish, and accordingly, that an admissible variation in thrust δT may be found which produces an approximation as close as one wishes to an arbitrary variation $\delta\phi(t)$, provided that the magnitude of $\delta\phi$ is sufficiently small. With ϕ is the role of control variable and small variations assumed, the intermediate thrust arcs must satisfy the necessary conditions for a weak relative minimum.

The Euler-Lagrange equations for the system (25), (26), (27), (30), (31) are

$$\dot{\lambda}_\psi = -\frac{\partial H}{\partial \psi} = \lambda_\psi \frac{\mu}{\omega} - \lambda_\beta \omega^2 - \lambda_\gamma \omega \tag{34}$$

$$\dot{\lambda}_\beta = -\frac{\partial H}{\partial \beta} = 0 \tag{35}$$

$$\dot{\lambda}_\gamma = -\frac{\partial H}{\partial \gamma} = -\lambda_\psi\left[\omega + \frac{1}{\omega}\frac{\partial}{\partial \gamma}(Y\cos\theta - X\sin\theta)\right] - \lambda_\beta \frac{\partial}{\partial \gamma}(Y\sin\theta + X\cos\theta) \tag{36}$$

$$\dot{\lambda}_\theta = -\frac{\partial H}{\partial \theta} = -\lambda_\psi \frac{\partial}{\partial \theta}(Y\cos\theta - X\sin\theta) - \lambda_\beta \frac{\partial}{\partial \theta}(Y\sin\theta + X\cos\theta) \tag{37}$$

$$\lambda_\omega = -\frac{\partial H}{\partial \omega} = -\lambda_\psi\left[\gamma - \frac{1}{\omega^2}(Y\cos\theta - X\sin\theta) + \frac{\mu}{\omega^2}(\psi - \phi)\right]$$

$$- 2\lambda_\beta\omega(\psi - \phi) - \lambda_\gamma(\psi - 2\phi) - \lambda_\theta \tag{38}$$

$$\frac{\partial H}{\partial \phi} = \lambda_\psi\left[\frac{\mu}{\omega} + \frac{1}{\omega}\frac{\partial}{\partial\phi}(Y\cos\theta - X\sin\theta)\right] + \lambda_\beta\left[-\omega^2\right.$$

$$\left. + \frac{\partial}{\partial\phi}(Y\sin\theta + X\cos\theta)\right] - 2\lambda_\gamma\omega = 0 \tag{39}$$

$$\frac{\partial H}{\partial \mu} = -\lambda_\psi\frac{(\psi - \phi)}{\omega} + \lambda_\omega = 0\ . \tag{40}$$

The Legendre-Clebsch necessary condition for a weak relative minimum is

$$\frac{\partial^2 H}{\partial \phi^2}\delta\phi^2 + 2\frac{\partial^2 H}{\partial\phi\partial\mu}\delta\phi\delta\mu + \frac{\partial^2 H}{\partial\mu^2}\delta\mu^2 \geq 0 \tag{41}$$

for arbitrary $\delta\phi$, $\delta\mu$. Positive semidefiniteness of this quadratic form requires that

$$\frac{\partial^2 H}{\partial \phi^2} \geq 0 \tag{42}$$

$$\frac{\partial^2 H}{\partial \mu^2} \geq 0 \tag{43}$$

$$\left(\frac{\partial^2 H}{\partial \phi^2}\right)\left(\frac{\partial^2 H}{\partial \mu^2}\right) - \left(\frac{\partial^2 H}{\partial\phi\partial\mu}\right)^2 \geq 0\ . \tag{44}$$

We have that

$$\frac{\partial^2 H}{\partial \phi^2} = \lambda_\beta \frac{\partial^2}{\partial \phi^2}(Y \sin\theta + X \cos\theta) + \frac{\lambda_\psi}{\omega} \frac{\partial^2}{\partial \phi^2}(Y \cos\theta - X \sin\theta) \tag{45}$$

$$\frac{\partial^2 H}{\partial \mu^2} = 0 \tag{46}$$

$$\frac{\partial^2 H}{\partial \phi \partial \mu} = \frac{\lambda_\psi}{\omega} . \tag{47}$$

From Eqs. (42)-(44) and Eqs. (45)-(47) it follows that $\lambda_\psi = 0$.

With this simplification and the elimination of the multiplier variables from the Euler-Lagrange equations (34)-(40), we arrive at

$$\omega^2 + \frac{\partial Z}{\partial \phi} = 0 \tag{48}$$

$$-\mu + \frac{\partial Z}{\partial \gamma} = 0 \tag{49}$$

$$\mu\phi + \omega^2\gamma - \left(x \frac{\partial}{\partial y} - y \frac{\partial}{\partial x}\right) Z = 0 \tag{50}$$

in which

$$Z \equiv Y \sin\theta + X \cos\theta \tag{51}$$

is the component of gravitational force along the thrust direction.

In the case of an inverse square law gravitational field

$$Y = \frac{-ky}{(x^2 + y^2)^{3/2}} \quad , \quad X = \frac{-kx}{(x^2 + y^2)^{3/2}} \tag{52}$$

Eqs. (48), (49), and (50) become

$$\omega^2 + \frac{k(2\phi^2 - \gamma^2)}{(\phi^2 + \gamma^2)^{5/2}} = 0 \tag{53}$$

$$-\mu + \frac{3k\phi\gamma}{(\phi^2 + \gamma^2)^{5/2}} = 0 \tag{54}$$

$$\mu\phi + \left[\omega^2 - \frac{k}{(\phi^2 + \gamma^2)^{3/2}}\right]\gamma = 0 \ . \tag{55}$$

If ω is eliminated between Eqs. (53) and (55), we obtain

$$\phi\left[\mu - \frac{3\gamma k}{(\phi^2 + \gamma^2)^{5/2}}\right] = 0 \tag{56}$$

The vanishing of the first factor $\phi = 0$, circumferential thrust, leads to $\mu = 0$, ω = constant and

$$|\omega| = \frac{k}{r^{3/2}} \tag{57}$$

where $r = \sqrt{\phi^2 + \gamma^2}$ is the radius. This is the orbital frequency for free fall circular motion. The vanishing of the second factor indicates that Eq. (55) is satisfied identically along solutions of Eqs. (53) and (54), which are the equations of Lawden's intermediate thrust solutions (Ref. 5), although in rather different notation.

CONCLUDING REMARKS

The present analysis amounts to little more than an alternate derivation of Lawden's results on intermediate thrust subarcs, similarly inconclusive on the question of minimality. This is a result of the singular extremals of the original problem being also singular in the transformed system of variables, i.e., only the weak form of the Legendre-Clebsch condition in these variables is met. The most suggestive feature of the analysis is the vanishing of two of the multipliers associated with the new variables. This would seem to indicate a possibility of dealing with the problem in a state space of reduced dimension.

ACKNOWLEDGMENTS

The writer is indebted to Dr. John V. Breakwell of Lockheed Missiles and Space Company and Dr. Richard E. Kopp of Grumman Aircraft for invaluable assistance in correcting errors in a provisional draft of this paper. This research was supported under Contract NAS 8-1549 with NASA's Marshall Space Flight Center and Contract AF 29(600)-2671 with USAF Office of Scientific Research.

REFERENCES

1. Lawden, D.F., "Inter-Orbital Transfer of a Rocket," Journal of the British Interplanetary Society, Vol. 11, 1952.

2. Lawden, D.F., "Interplanetary Rocket Trajectories," Advances in Space Science I, Academic Press, 1959.

3. Leitmann, G., "Variational Problems with Bounded Control Variables," in Optimization Techniques, Academic Press, 1962.

4. Lawden, D.F., "Optimal Powered Arcs in an Inverse Square Law Field," ARS Journal, April 1961.

5. Lawden, D.F., "Optimal Intermediate-Thrust Arcs in a Gravitational Field," Astronautica Acta, Vol. VIII, Fasc. 2-3, 1962.

6. Pontryagin, L.S. et al., The Mathematical Theory of Optimal Processes, Interscience Publishers, 1962.

7. Miele, A., "Extremization of Linear Integrals by Green's Theorem," Optimization Techniques, Academic Press, 1962.

A TRANSFORMATION APPROACH TO SINGULAR SUBARCS IN OPTIMAL TRAJECTORY AND CONTROL PROBLEMS

Henry J. Kelley*
Analytical Mechanics Associates, Inc.

ABSTRACT

Mayer variational problems in which the control variable appears linearly are considered and a canonical form sought for the system equations which is somewhat analogous to that adopted by Wonham and Johnson for linear constant coefficient systems with cost functional quadratic in the state variables. A means of synthesizing a transformation to the canonical form in terms of the mutually independent solutions of a first order linear homogeneous partial differential equation is described. It is then shown how the Legendre-Clebsch necessary condition applied in the transformed system of variables may be employed to obtain information on the singular extremals of the problem and the possible appearance of singular subarcs in the solution.

Two examples are employed for illustration, one a simple servomechanism problem and the other Goddard's problem of optimal thrust programming for a sounding rocket.

* Vice-president

INTRODUCTION

Optimal control problems in which the control variable appears linearly yield to conventional treatment if the optimal control has a bang-bang character. Difficulties arise with the possibility of intervals during which the optimal control may be intermediate between the specified limits, such segments of the solution being singular subarcs, in classical variational terminology. The Green's Theorem technique of Miele (Ref. 1) is a powerful tool for solution of such problems, applicable, however, only if the state space is of very limited dimension. There is presently available no general theory for determining singular arcs, deciding as to whether or not they are minimizing even locally, i.e., over a short time interval, or for determining their role as subarcs of a composite solution. In the special case of systems linear in the state variables, investigated by LaSalle (Ref. 2), the appearance of singular subarcs corresponds to degeneracy in the sense of nonuniqueness of solution.

In the present paper we investigate the possibility of a canonical form for such problems which resembles that chosen by Wonham and Johnson (Ref. 3) for study of problems featuring linear constant coefficient systems and cost functional an integral quadratic form in the state variables. Initially our concern will be with synthesis of the desired form by means of an appropriate transformation. Following this, attention will be turned to the application of optimality criteria in the transformed system of variables.

TRANSFORMATION TO CANONICAL FORM

Our analysis begins with the usual Mayer problem statement. A minimum is sought of a function P of the terminal values of variables $x_1, - -, x_n$ and the terminal value of the independent variable, time t. The variables $x_1, - -, x_n$ are state variables satisfying a system of first order differential equations of the form

$$\dot{x}_i = p_i(x_1, - -, x_n, t) + q_i(x_1, - -, x_n, t)y \qquad (1)$$

$$i = 1, - -, n$$

In the class of problems of present interest, the differential equations are linear in a single control variable y, as indicated. Initial conditions numbering at most $n+1$ and terminal conditions numbering at most n may be imposed upon the variables $x_1, - -, x_n$ and t. The variable y is subject to an inequality constraint of the form

$$y_1 \leq y \leq y_2 \qquad (2)$$

We wish to consider the possibility of introducing new variables

$$z_j = f_j(x_1, - -, x_n, t) \qquad j = 1, - -, m \qquad (3)$$

satisfying equations of state whose right members are not dependent upon the variable y explicitly:

$$\dot{z}_j = \sum_{i=1}^{n} \frac{\partial f_j}{\partial x_i} p_i + \frac{\partial f_j}{\partial t} \quad , \qquad j = 1, - -, m \qquad (4)$$

Evidently $m<n$ unless all the q_i are identically zero. The vanishing of the collected coefficient of the variable y

$$\sum_{i=1}^{n} \frac{\partial f_j}{\partial x_i} q_i = 0 \qquad j = 1, - -, m \qquad (5)$$

has been assumed in (4).

For the purpose of determining functions f_j having the desired property, we seek the solutions of the linear homogeneous first order

partial differential equation (5). From the theory of characteristics (Ref. 4) we are led to consideration of the ordinary differential equations

$$\frac{dx_i}{ds} = q_i(x_1, - -, x_n, t) \qquad i = 1, - -, n \qquad (6)$$

in which s is a parameter and t is fixed. If one of the quantities x_i is adopted instead of s as independent variable, the general solution may be represented in terms of $n-1$ parameters:

$$C_k = \varphi_k(x_1, - -, x_n, t) \qquad k = 1, - -, n-1 \qquad (7)$$

The C_k are constants of integration and the φ_k are <u>mutually independent</u> integrals of the system. Each integral φ_k is a solution of the partial differential equation (5).

The first $n-1$ of the new variables z_j are then to be defined according to $f_j = \varphi_j$. The n^{th} variable z_n we define as

$$z_n = x_\ell \qquad (8)$$

choosing ℓ such that $q_\ell \neq 0$ over the domain of interest, a choice which we assume for the time being open to us. The mutual independence of the functions φ_j together with $q_\ell \neq 0$ insures that the transformation between the variables z and x is nonsingular by the nonvanishing of the Jacobian determinant

$$\Delta = \frac{\partial(z_1, - -, z_n)}{\partial(x_1, - -, x_n)} \neq 0 \qquad (9)$$

THE LEGENDRE-CLEBSCH CONDITION IN THE TRANSFORMED VARIABLES

To provide intuitive motivation for our next step, we digress momentarily, considering the possibilities offered by our transformation in (rarely occurring) problems devoid of inequality constraints on the control variable. In such cases we are led to an equivalent problem in a state space of smaller dimension, the z_j, $j = 1, - -, n-1$, becoming the state variables and $z_n = x_\ell$ the control variable. This comes about through the identical vanishing of the Lagrange multiplier associated with the n^{th} equation of state

$$\dot{z}_n = p_\ell + q_\ell y \tag{10}$$

In this equation as well as in the first $n-1$ equations of state (4), the variables x_i are presumed eliminated in favor of the z_j by use of the inverse transformation. It should be noted that jump discontinuities in the new control variable $z_n(t) = x_\ell(t)$ occurring at corner points of the solution imply impulsive behavior of $y(t)$. Such behavior would be admissible in the absence of an inequality constraint on y, which we have momentarily assumed, and the Weierstrass necessary condition would then be directly applicable.

Unless the transformed equations were linear in the new control variable $z_n = x_\ell$, the Weierstrass necessary condition could then be employed in conjunction with the Euler equations for the transformed problem to yield information not obtainable via the corresponding condition in the original problem. The extremals of the transformed problem are the singular extremals of the original, and those satisfying the strengthened version of the Weierstrass condition are minimizing, at least over short intervals. In the special case in which the transformed equations of state (4) are linear in the new control variable x_ℓ, an additional transformation to a state space of still smaller dimension is indicated.

Redirecting attention to the problem of main interest, in which the inequality constraint (2) is operative, we perceive that the course of action just described is not open to us. We may, however, examine subarcs over which the control variable y takes on values intermediate between the specified bounds

$$y_1 < y < y_2 \tag{11}$$

with similar considerations in mind. If $y = \bar{y}(t)$ is the optimal control, we must, evidently, restrict attention to small variations $\delta y(t) = \epsilon \eta(t)$, where $\eta(t)$ is an arbitrary piecewise continuous function and the magnitude of the variation, ϵ, is vanishingly small so that $y = \bar{y} + \delta y$ satisfies (11). In the literature of classical variational theory, such variations are often referred to as weak variations, and the Legendre-Clebsch condition, necessary for a weak relative minimum, plays a role loosely analogous to that of the Weierstrass condition whenever a restriction to vanishingly small variations is either assumed or imposed.

We rewrite eqs. (4) with the notation a_j for the functions appearing on the right as

$$\dot{z}_j = a_j(x_1, - -, x_n, t) \qquad j = 1, - -, n-1 \tag{12}$$

and with the variables x_i eliminated in favor of z_j, as

$$\dot{z}_j = b_j(z_1, - -, z_n, t) \qquad j = 1, - -, n-1 \tag{13}$$

Introducing the usual Lagrange multipliers λ_j, $j = 1, - -, n-1$, we form the Hamiltonian

$$H \equiv \sum_{j=1}^{n-1} \lambda_j b_j \tag{14}$$

and write the Euler-Lagrange equations corresponding to the z_j

$$\dot{\lambda}_j = -\frac{\partial H}{\partial z_j} \qquad j = 1, \text{ - -}, n-1 \tag{15}$$

and that corresponding to z_n

$$\frac{\partial H}{\partial z_n} = 0 \tag{16}$$

The Legendre-Clebsch necessary condition is

$$\frac{\partial^2 H}{\partial z_n^2} \delta z_n^2 \geq 0 \tag{17}$$

for $\delta z_n \neq 0$, or

$$\frac{\partial^2 H}{\partial z_n^2} \geq 0 \tag{18}$$

Solutions of the system (13), (15) and (16) are the extremals of the transformed problem and the condition (18) provides an additional criterion for screening these candidates. If the left member of (18) is positive, the singular subarc is locally minimizing, i.e., over short time intervals; if negative, maximizing. The vanishing of the left member of (18) corresponds to the special case, mentioned earlier, in which z_n enters the function H linearly. Thus along singular arcs of the original problem, (18) partially fills the gap created by the Weierstrass necessary condition's being trivially satisfied.

If it is not possible to choose the variable z_n according to the scheme $z_n = x_\ell$, $q_\ell \neq 0$, or if it is inconvenient to invert the transformation Z(X) analytically, one may deal with the equations of state

in the form (12), adjoining the n-1 equations (3) as constraints by means of additional Lagrange multipliers. The more complex form of the Legendre-Clebsch necessary condition as given in Ref. 5, for example, must then be applied.

EXAMPLES

1. A Servomechanism Problem

In Refs. 1 and 6, the following problem has been studied in some detail. Given the system

$$\dot{x}_1 = x_2 + y \tag{19}$$

$$\dot{x}_2 = -y \tag{20}$$

$$\dot{x}_3 = \frac{x_1^2}{2} \tag{21}$$

$$|y| \leq 1 \tag{22}$$

the control taking the system from a specified initial state to $x_1 = x_2 = 0$ and extremizing the final value of x_3 is sought. The structure of the solution of this problem is rather complex, belying its innocuous appearance. An application of the transformation scheme just described and an examination of the Legendre-Clebsch condition leads to the conclusions:

(a) the singular subarcs of Refs. 1 and 6 are locally minimizing for the case of a minimum of the final value of x_3,

(b) the singular subarcs are <u>not</u> minimizing if the function whose minimum is sought is the <u>negative</u> of the final value of x_3, and the optimal control is bang-bang.

In Ref. 1 a result stronger than (a) is obtained, and for problems which fit the linear/quadratic format of Ref. 1 this will generally be the case. Owing to an assumed restriction in the problem statement of Ref. 1, the results do not apply to case (b).

2. Goddard's Problem

The problem of determining the optimal thrust program for the vertical flight of a sounding rocket is one which has been extensively studied in the astronautical literature. The state variables are altitude, h, velocity, V, and mass, m, satisfying

$$\dot{h} = V$$

$$\dot{V} = \frac{T - D(h, V)}{m} - g(h)$$

$$\dot{m} = -\frac{T}{c}$$

in which rocket thrust T is bounded above and below according to

$$0 \leq T \leq \bar{T}$$

The function D is aerodynamic drag, g is the acceleration of gravity, and c is rocket exhaust velocity. The problem usually of interest is the minimization of propellant expenditure $m_o - m_f$ with fixed initial mass for attainment of fixed final altitude, final velocity and time unspecified.

The transformation scheme leads to $z_1 = h$, $z_2 = m e^{V/c}$ as new state variables and $z_3 = V$ as new control variable. The problem is nonsingular in the state space of reduced dimension. The version of the problem featuring drag proportional to the square of the velocity has been investigated fairly thoroughly and in this case a single intermediate thrust

subarc enters the solution, which the Legendre-Clebsch condition confirms as locally minimizing. The advantage of employing the variables z_1 and z_2 above was first recognized by Ross (Ref. 7), who established minimality of the variable thrust subarc for the square law drag case. In the case of a more general drag law, e. g., one which exhibits sharp variation in the vicinity of sonic velocity, the Legendre-Clebsch condition may rule out intermediate thrust operation over a certain velocity range.

CONCLUDING REMARKS

The transformation scheme and application of the Legendre-Clebsch condition appear to be useful for examination of singular subarcs in Mayer problems linear in a single control variable, although, of course, the information obtained is only a fragment of that needed for complete analysis of such problems. Perhaps the most interesting and suggestive feature of the approach is the idea of treating problems of this kind in a state space of reduced dimension.

ACKNOWLEDGMENT

The investigation presently reported was performed under Contract NAS 8-1549 with NASA's Marshall Space Flight Center and Contract AF 29 (600)-2671 with USAF Office of Scientific Research while the writer was employed in the Research Department of the Grumman Aircraft Engineering Corporation.

REFERENCES

1. Miele, A.; "Extremization of Linear Integrals by Green's Theorem," Chapter 3 of Optimization Techniques, G. Leitmann, editor, Academic Press, New York, 1962.

2. LaSalle, J. P.; "The Time Optimal Control Problem," Contributions to the Theory of Nonlinear Oscillations, Vol. V, Princeton University Press, Princeton, New Jersey, 1960.

3. Wonham, W. M. and Johnson, C. D.; "Optimal Bang-Bang Control with Quadratic Performance Index," Joint Automatic Control Conference, Minneapolis, Minnesota, June 19-21, 1963.

4. Courant, R. and Hilbert, D.; Methods of Mathematical Physics, Vol. II, Partial Differential Equations, Wiley, New York, 1962.

5. Bliss, G. A.; Lectures on the Calculus of Variations, University of Chicago Press, Chicago, 1946.

6. Johnson, C. D. and Gibson, J. E.; "Singular Solutions in Problems of Optimal Control," IEEE Transactions on Automatic Control, to appear.

7. Ross, S.; "Minimality for Problems in Vertical and Horizontal Rocket Flight," Jet Propulsion, January 1958.

APPROVAL

PROGRESS REPORT NO. 4
on Studies in the Fields of
SPACE FLIGHT AND GUIDANCE THEORY

Sponsored by Aero-Astrodynamics Laboratory of
Marshall Space Flight Center

The information in this report has been reviewed for security classification. Review of any information concerning Department of Defense or Atomic Energy Commission programs has been made by the MSFC Security Classification Officer. This report, in its entirety, has been determined to be unclassified.

E. D. GEISSLER
Director, Aeroballistics Div.

DISTRIBUTION LIST

INTERNAL

M-DIR, Frank Williams

M-FPO, Mr. Ruppe

M-SAT, Col. James

M-RP, Mr. King
Dr. Johnson

M-COMP, Dr. Arenstorf
Mr. Harton
Mr. Iloff
Mr. Schollard
Mr. Seely

M-ASTR, Mr. Brandner
Mr. Moore
Mr. Richard
Mr. Gassaway
Mr. Taylor
Mr. Brooks
Mr. Hosenthien
Mr. Scofield
Mr. Woods
Mr. Digesu
Mr. R. Hill
Mr. Crowe
Mrs. Neighbors
Dr. R. Decher
Mr. Thornton

M-P&VE, Mr. Swanson
Mr. Burns
Dr. Krause
Mr. T. Miller

M-MS-IP, Mr. Ziak

M-MS-IPL (8)

M-MS-H

M-PAT

M-HME-P

M-P&C-C, Mr. Hardee

M-AERO, Dr. Geissler
Dr. Hoelker
Mr. Miner (80)
Mr. Braud
Mr. Ingram
Mr. G. Herring
Mr. Schmieder
Mr. Dearman
Mr. Schwaniger
Mr. Callaway
Mr. Thomae
Mr. Baker
Mr. Hart
Mr. Lovingood
Mr. Winch
Mr. Tucker
Mr. Hooper
Mrs. Chandler
Mr. Lisle
Mr. Kurtz
Mr. deFries
Mr. Teague
Dr. Sperling
Dr. Heybey
Mr. Cummings
Mr. Jean
Mr. Felker
Mr. McDaniel
Mr. Telfer
Mr. Goldsby

DISTRIBUTION LIST (CONT'D)

EXTERNAL

Republic Aviation Corporation
Applied Mathematics Section
Applied Research and Development
Farmingdale, Long Island, New York
ATTN: Dr. George Nomicos (5)
Dr. Mary Payne

Mr. Robert Lerman
Senior Analytical Engineer
Corporate Systems Center
United Aircraft Corporation
Farmington, Connecticut

Mr. Theodore N. Edelbaum
Senior Research Engineer
Research Laboratories
United Aircraft Corporation
East Hartford, Connecticut

University of Kentucky
College of Arts and Sciences
Department of Mathematics and Astronomy
Lexington, Kentucky
ATTN: Dr. J. C. Eaves

University of North Carolina
Computation Center
Chapel Hill, North Carolina
ATTN: Mr. J. W. Hanson (20)

Vanderbilt University
Department of Mathematics
Nashville, Tennessee
ATTN: Dr. M. G. Boyce (3)

University of Alabama
Department of Mathematics
University, Alabama
ATTN: Dr. O. R. Ainsworth

Southern Illinois University
Department of Mathematics
Carbondale, Illinois
ATTN: Dr. Robert W. Hunt
Mr. Robert Silber

DISTRIBUTION LIST (CONT'D)

Mr. J. T. Van Meter
Minneapolis-Honeywell Regulator Company
Military Products Group
Aeronautical Division
2600 Ridgway Road
Minneapolis 40, Minnesota

Space Sciences Laboratory
Space and Information Systems
North American Aviation, Inc.
Downey, California
ATTN: Dr. D. F. Bender
Mr. Gary McCue

Dr. Daniel E. Dupree (15)
Department of Mathematics
Northeast Louisiana State College
Monroe, Louisiana

Dr. Steve Hu
Northrop Corporation
Box 1484
Huntsville, Alabama

Dr. William Nesline, Jr.
Raytheon Company
Missile and Space Division
Analytical Research Department
Bedford, Massachusetts

Dr. Henry Hermes
Research Institute of Advanced Study
7212 Bellona Avenue
Baltimore 12, Maryland

Mr. Samuel Pines (10)
Analytical Mechanics Associates, Inc.
941 Front Street
Uniondale, New York

Dr. W. A. Shaw (10)
Auburn University
Mechanical Engineering Department
Auburn, Alabama

DISTRIBUTION LIST (CONT'D)

Bendix Systems Division
The Bendix Corporation
3322 Memorial Parkway South
Huntsville, Alabama
ATTN: Mr. William Green
Mr. Robert Glasson

Mr. Richard Hardy
Box AB-38
The Boeing Company
P. O. Box 1680
Huntsville, Alabama

Mr. Wes Morgan
Box AB-49
The Boeing Company
P. O. Box 1680
Huntsville, Alabama

Mr. Oliver C. Collins
Mail Stop 15-12
Organization 2-5762
Flight Technology Department
The Boeing Company
Seattle 24, Washington

Chrysler Corporation Missile Division
Sixteen Mile Road and Van Dyke
P. O. Box 2628
Detroit 31, Michigan
ATTN: Mr. T. L. Campbell
Mr. R. J. Vance
Dept. 7162
Applied Mathematics

Mr. George Westrom
Astrodynamics Section
Astrosciences Department
Aeronutronic Division of Ford Motor Co.
Ford Road
Newport Beach, California

Mr. E. M. Copps, Jr.
MIT, Instrumentation Laboratories
68 Albany Street
Cambridge 39, Massachusetts

DISTRIBUTION LIST (CONT'D)

Astrodynamics Operation
Space Sciences Laboratory
Missile and Space Vehicle Department
General Electric Company
Valley Forge Space Technology Center
P. O. Box 8555
Philadelphia 1, Pennsylvania
ATTN: Mr. J. P. deVries

Dr. I. E. Perlin
Rich Computer Center
Georgia Institute of Technology
Atlanta, Georgia

Research Department
Grumman Aircraft Engineering Corporation
Bethpage, L. I., New York
ATTN: Mr. Hans K. Hinz
Mr. Gordon Pinkham

Mr. Harry Passmore
Hayes International Corporation
P. O. Box 2287
Birmingham, Alabama

Mr. J. S. Farrior
Lockheed
P. O. Box 1103
West Station
Huntsville, Alabama

Dr. Charles C. Conley
University of Wisconsin
Department of Mathematics
Madison, Wisconsin

Dr. M. L. Anthony
Space Flight Laboratory
Mail No. A-153
The Martin Company
Denver 1, Colorado

Mr. Dahlard Lukes
Minneapolis-Honeywell Regulator Company
M.P.G. - Aeronautical Division
2600 Ridgway Road
Minneapolis 40, Minnesota

DISTRIBUTION LIST (CONT'D)

Dr. Joseph F. Shea
Office of Manned Space Flight
National Aeronautics and Space Administration
801 19th Street, N. W.
Washington 25, D. C.

Mr. E. L. Harkleroad
Office of Manned Space Flight
National Aeronautics and Space Administration
Code: MI
Washington, D. C.

Mr. Charles F. Pontious
Guidance and Navigation Program
Office of Advanced Research and Technology
Code: REG
National Aeronautics and Space Administration
Washington 25, D. C.

Mr. Jules Kanter
Guidance and Navigation Program
Office of Advanced Research and Technology
Code: REG
National Aeronautics and Space Administration
Washington 25, D. C.

Dr. Joseph Natrella
Systems Engineering
Office of Manned Space Flight
Code: ME
National Aeronautics and Space Administration
801 19th Street, N. W.
Washington 25, D. C.

Mr. Ralph W. Haumacher
A2-863: Space/Guidance and Control
Douglas Aircraft Corporation
3000 Ocean Park Blvd.
Santa Monica, California

Dr. B. Paiewonsky
Aeronautical Research Associates of Princeton
50 Washington Road
Princeton, New Jersey

DISTRIBUTION LIST (CONT'D)

Dr. Cheng Ling
Principle Staff Engineer
Systems Research Section, R & A T Dept.
Electronic Systems and Products Division
Martin Company
Baltimore 3, Maryland

Mr. F. A. Hewlett
Manager of Documentation
IBM
Federal Systems Division
6702 Gulf Freeway
Houston 17, Texas

Mr. George Cherry
Massachusetts Institute of Technology
Cambridge, Massachusetts

Mr. Paul T. Cody
76 Central Street
Peabody, Massachusetts

Mr. Roger Barron
Adaptronics, Inc.
4725 Duke Street
Alexandria, Virginia

Dr. John W. Carr, III
Department of Mathematics
University of North Carolina
Chapel Hill, North Carolina

Mr. T. W. Scheuch
North American Aviation, Inc.
Holiday Office Center
Huntsville, Alabama

Mr. H. A. McCarty
North American Aviation, Inc.
Space and Information Systems Division
12214 Lakewood Blvd.
Downey, California

DISTRIBUTION LIST (CONT'D)

Mr. Frank J. Carroll
Raytheon Company
Equipment Division
Systems Requirement Department
40 Second Avenue
Waltham, Massachusetts

Dr. Ray Rishel
Physics Technical Department
Organization No. 25413, Box 2205
The Boeing Company
Box 3707
Seattle 24, Washington

Mr. T. Perkins
Chrysler Corporation
HIC Building
Huntsville, Alabama

Mr. Robert Gregoire
Program Engineer
Corporate Systems Center
United Aircraft Corporation
Windsor Locks, Connecticut

Dr. R. M. L. Baker, Jr.
Lockheed-California Company
A Division of Lockheed Aircraft Corporation
Burbank, California

Mr. William C. Marshall
Research Engineer
M.P.G. Research Dept - Station 340
Minneapolis-Honeywell Regulator Co.
2600 Ridgway Road
Minneapolis 3, Minnesota

Mr. Rigdon
VITRO Laboratory
14000 Georgia Avenue
Silver Springs, Maryland

Mr. W. G. Melbourne
Jet Propulsion Laboratory
4800 Oak Grove Drive
Pasadena 3, California

DISTRIBUTION LIST (CONT'D)

Douglas Aircraft Corporation
3000 Ocean Park Blvd.
Santa Monica, California
ATTN: R. E. Holmen A2-263
Guidance & Control Section

Dr. Byron D. Tapley
Department of Aerospace Engineering
University of Texas
Austin, Texas

Mr. Howard S. London
Bellcomm, Inc.
Rm 910-E
1100 17th Street, N. W.
Washington, D. C.

Mr. Howard Haglund
Jet Propulsion Laboratory
4800 Oak Grove Drive
Pasadena 3, California

Mr. Hewitt Phillips
Langley Research Center
Hampton, Virginia

Mr. Robert Chilton
Manned Spacecraft Center
Houston, Texas

Mr. William E. Wagner
Space Systems Division
Mail # 3072
The Martin Company
Baltimore 3, Maryland

Mr. A. H. Jazwinski
Space Systems Division
Mail # 3072
The Martin Company
Baltimore 3, Maryland

Dr. Hermann M. Dusek
A.C. Spark Plug of General Motors
950 N. Sepulbeda Blvd.
LeSegundo, California

DISTRIBUTION LIST (CONT'D)

Mr. Donald Jezewski
Guidance Analysis Branch
Spacecraft Technology Division
Manned Spacecraft Center
Houston, Texas

Mr. Fred D. Breuer
General Dynamics/Astronautics
Lunar Systems
Department 580-3
Mail Zone 530-30
San Diego, California

Mr. Robert Reck
Martin Company
3313 S. Memorial Parkway
Huntsville, Alabama

Mr. Robert E. Allen
Manager, Huntsville,Sales Office
A. C. Spark Plug
The Electronics Division of
General Motors
Holiday Office Center
Huntsville, Alabama

Mr. Myron Schall
Supervisor, Powered Trajectory
Space and Information Division
Dept. 4695-213, Bldg 1
12214 Lakewood Blvd.
Downey, California

Mr. S. E. Cooper
North American Aviation
Space and Information Division
Dept. 4695-211, Bldg. 1
12214 Lakewood Blvd.
Downey, California

Mr. M. D. Anderson, Jr.
General Dynamics Corporation
Suite 42, Holiday Office Center
South Memorial Parkway
Huntsville, Alabama

DISTRIBUTION LIST (CONT'D)

Mr. S. V. Starr
Advanced Systems Group Engineer
General Dynamics
P. O. Box 166
San Diego 12, California

Auburn Research Foundation (2)
Auburn University
Auburn, Alabama

Astrodynamics Operation
Space Sciences Laboratory
Missile and Space Vehicle Department
General Electric Company
Valley Forge Space Technology Center
P. O. Box 8555
Philadelphia 1, Pennsylvania
ATTN: Dr. V. Szebehely
Mr. Carlos Cavoti (8)

Grumman Library
Grumman Aircraft Engineering Corp.
Bethpage, L. I., New York

Research Department
Grumman Aircraft Engineering Corp.
Bethpage, L. I., New York
ATTN: Mr. Gordon Moyer

Jet Propulsion Laboratory
4800 Oak Grove Drive
Pasadena 3, California
ATTN: Library (2)
Dr. John Gates

Scientific and Technical Information Facility (2)
ATTN: NASA Representative (S-AK/RKT)
P. O. Box 5700
Bethesda, Maryland

NASA Ames Research Center (2)
Mountain View, California
ATTN: Librarian

NASA Flight Research Center (2)
Edwards Air Force Base, California
ATTN: Librarian

DISTRIBUTION LIST (CONT'D)

NASA Goddard Space Flight Center (2)
Greenbelt, Maryland
ATTN: Librarian

Office of Manned Space Flight
NASA Headquarters
Federal Office Building #6
Washington 25, D. C.
ATTN: Mr. Eldon Hall
Mr. A. J. Kelley

NASA Langley Research Center (2)
Hampton, Virginia
ATTN: Librarian

NASA Launch Operations Directorate (2)
Cape Canaveral, Florida
ATTN: Librarian

NASA Lewis Research Center (2)
Cleveland, Ohio
ATTN: Librarian

NASA Manned Spacecraft Center (2)
Houston 1, Texas
ATTN: Librarian

NASA Wallops Space Flight Station (2)
Wallops Island, Virginia
ATTN: Librarian

Space Sciences Laboratory
Space and Information Systems
North American Aviation, Inc.
Downey, California
ATTN: Mr. Paul DesJardins
Mr. Harold Bell

Mr. J. R. Bruce (2)
Northrop Corporation
3322 Memorial Parkway, S. W.
Huntsville, Alabama

Space Flight Library (4)
University of Kentucky
Lexington, Kentucky

DISTRIBUTION LIST (CONT'D)

Raytheon Company
Missile and Space Division
Analytical Research Department
Bedford, Massachusetts
ATTN: Miss Ann Muzyka

University of Kentucky Library (10)
University of Kentucky
Lexington, Kentucky

University of Kentucky
College of Arts and Sciences
Department of Mathematics and Astronomy
Lexington, Kentucky
ATTN: Dr. Wells
Dr. Krogdahl
Dr. Pignani

Dr. Kirk Brouwer
Yale University Observatory
Box 2023, Yale Station
New Haven, Connecticut

Dr. Imre Izsak
Smithsonian Institution Astrophysical Observatory
60 Garden Street
Cambridge 38, Massachusetts

Dr. Peter Musen
Goddard Space Flight Center
N. A. S. A.
Greenbelt, Maryland

Dr. Yoshihide Kozai
Smithsonian Institution Astrophysical Observatory
60 Garden Street
Cambridge 38, Massachusetts

Dr. Rudolph Kalman
Research Institute for Advanced Study
7212 Bellona Avenue
Baltimore 12, Maryland

Mr. Ken Kissel
Aeronautical Systems Division
Applied Mathematics Research Branch
Wright-Patterson Air Force Base
Dayton, Ohio

DISTRIBUTION LIST (CONT'D)

Mr. Jack Funk
Manned Spacecraft Center
Flight Dynamics Branch
N. A. S. A.
Houston, Texas

Mr. Ken Squires
Goddard Space Flight Center
National Aeronautics and Space Administration
Building #1
Greenbelt, Maryland

Dr. Paul Degrarabedian
Space Technology Laboratory, Inc.
Astro Science Laboratory
Building G
One Space Park
Redondo Beach, California

Mr. George Leitmann
Associate Professor, Engineering Science
University of California
Berkeley, California

Dr. J. B. Rosser
Department of Mathematics
Cornell University
Ithaca, New York

Dr. R. P. Agnew
Department of Mathematics
Cornell University
Ithaca, New York

Dr. Jurgen Moser
Professor of Mathematics
Graduate School of Arts and Science
New York University
New York, New York

Dr. Lu Ting
Department of Applied Mechanics
Polytechnic Institute of Brooklyn
333 Jay Street
Brooklyn 1, New York